Lysosomal dysfunction and glycosphingolipid dysregulation in rare and common neurodegenerative diseases

Mylene Huebecker, M.Sc.

A thesis submitted for the degree of
Doctor of Philosophy

Department of Pharmacology
St Cross College
University of Oxford

Hilary Term 2019

Abstract

Historically, the rare early-onset neurodegenerative lysosomal storage disorders (LSDs) have been studied as discrete metabolic diseases in their own right. However, in recent years links with more common late-onset neurodegenerative diseases, including amyotrophic lateral sclerosis (ALS) and Parkinson's disease (PD), have emerged. For example, lysosomal dysfunction, impaired autophagy, and protein aggregation are shared features in these diseases. However, altered lipid homeostasis, especially glycosphingolipid (GSL) dysregulation, is a relatively new research field of interest in PD and even more so in ALS.

In this thesis, we provide evidence that GSL metabolism is altered during denervation, in an ALS mouse model, and in ALS patients. We further show that pharmacological modulation of GSL levels, especially the ganglioside GM1a, could be a therapeutic approach for ALS.

Mutations in the Gaucher disease-linked lysosomal enzyme GBA are major genetic risk factors for developing PD. In this thesis, we observed that a subset of sporadic PD fibroblasts phenocopied characteristics of lysosomal dysfunction associated with GBA mutations. Furthermore, ageing is the major non-genetic risk factor for adult-onset neurodegenerative diseases. We show that levels of GSLs and activities of lysosomal hydrolases, relevant to PD, are altered in the ageing brain of wildtype mice. Importantly, we demonstrate, in human post-mortem substantia nigra and putamen, that levels of GSLs, especially complex gangliosides such as GM1a, and multiple lysosomal hydrolase activities are reduced during ageing and to a greater extent in sporadic PD. However, these changes were not observed in mouse models of PD, questioning their usefulness as models for PD. Finally, we demonstrate that ganglioside levels in cerebrospinal fluid and serum from PD patients are potential biomarkers for PD. Consequently, existing LSD therapies may hold promise as new therapeutic approaches for treating PD.

Publications

Henriques A, Croixmarie V, Priestman DA, Rosenbohm A, Dirrig-Grosch S, D'Ambra E, **Huebecker M**, Hussain G, Boursier-Neyret C, Echaniz-Laguna A, Ludolph AC, Platt FM, Walther B, Spedding M, Loeffler JP, Gonzalez De Aguilar JL. 'Amyotrophic lateral sclerosis and denervation alter sphingolipids and up-regulate glucosylceramide synthase.' Hum Mol Genet. 2015 Dec 20; 24(25):7390-405. doi: 10.1093/hmg/ddv439. PubMed PMID: 26483191.

Henriques A, **Huebecker M**, Blasco H, Keime C, Andres CR, Corcia P, Priestman DA, Platt FM, Spedding M, Loeffler JP. 'Inhibition of β-Glucocerebrosidase Activity Preserves Motor Unit Integrity in a Mouse Model of Amyotrophic Lateral Sclerosis'. Sci Rep. 2017 Jul 12;7(1):5235. doi: 10.1038/s41598-017-05313-0. PubMed PMID: 28701774.

Hallett PJ*, **Huebecker M***, Brekk OR, Moloney EB, Rocha EM, Priestman DA, Platt FM, Isacson O. 'Glycosphingolipid levels and glucocerebrosidase activity are altered in normal aging of the mouse brain.' Neurobiol Aging. 2018 Jul;67:189-200. doi: 10.1016/j.neurobiolaging.2018.02.028. PubMed PMID: 29735433.
*** = joint first authors**

Huebecker M, Moloney EB, van der Spoel AC, Priestman DA, Isacson O, Hallett PJ and Platt FM. 'Reduced lysosomal enzyme activities, substrate accumulation and ganglioside decline in Parkinson's disease', currently under review, 2019.

Acknowledgements

I would like to thank my supervisor and mentor Professor Fran Platt for her support and encouragement for doing this DPhil throughout the last years. Fran, you are a role model to all female students, and your enthusiasm and knowledge are as impressive as they are a life-saver. Thanks for being the supervisor you are and for appreciating cheese and gin tonic the same way I do.

I would also like to thank my co-supervisor Dr. David Priestman for his support and guidance along the way and for introducing me to the enormously complicated field of glycosphingolipids.

Of course, thanks to all the present and past members of the Platt lab, who were around while doing my DPhil: Carla, Nick, Claire, Dave, Kerri, Dawn, Maria, Ecem, Maysa, Doris, James, Allie, Stephanie, and Ralu. Thank you all for the support in the lab and the fun at conferences. You made my time as PhD student appear not as awful as it could have been without the laughing and the crying because of too much laughing.

I am very thankful to have been funded by a studentship by Parkinson's UK. The Parkinson's UK Oxford Branch is managed by inspiring people and the events were always rewarding to be part of, and I wish everyone involved all the best.

A special thanks to Prof Ole Isacson, Prof Penny Hallett and their lab in Harvard, who were so supportive and enthusiastic about our Parkinson research and allowed me to make the most out of my thesis.

Also, a special thanks to Dr. Alexandre Henriques, Dr. Michael Spedding and Prof JP Loeffler in Strasbourg, for getting us excited about glycosphingolipids in ALS and starting such a fruitful collaboration.

Ein großes Dankeschön an meine Familie, besonders meine Eltern und meine Omas, für die anhaltende Unterstützung, auch über die Distanz. Also big thanks to my friends in Germany and Oxford, you are the best!

And finally, the biggest thanks to my husband Alex, for moving to Oxford with me, for marrying me during my DPhil, and for supporting me throughout the whole journey of becoming a Doctor of Philosophy.

Table of Contents

Abbreviations

2-AA	Anthranilic acid
AAV	Adeno-associated virus
AD	Alzheimer's Disease
ALS	Amyotrophic lateral sclerosis
AMP-DNM	N-adamantane-methyloxypentyl-1-deoxynojirimycin
ANOVA	Analysis of variance
ASO	α-synuclein overexpressing
BAC	Bacterial artificial chromosome
BBB	Blood-brain barrier
BCA	Bicinchoninic acid
BSA	Bovine serum albumin
C9ORF72	Chromosome 9 open reading frame 72
Ca^{2+}	Calcium
CBE	Conduritol B epoxide
CERT	Ceramide transfer protein
CGT	Ceramide glucosyltransferase
ChAT	Choline acetyltransferase
CHO	Chinese hamster ovary
CMT	Chaperone-mediated therapy
CNS	Central nervous system
CSF	Cerebrospinal fluid
DA	Dopaminergic
ER	Endoplasmatic reticulum
ERT	Enzyme replacement therapy
FACS	Fluorescence-activated cell sorting
FBS	Foetal bovine serum
FUS	Fused in sarcoma protein
GalCer	Galactosylceramide
GalSph	Galactosylsphingosine
Gb3	Globotriaosylceramide
GBA	Glucocerebrosidase or acid β-glucosidase
GBA2	Non-lysosomal β-glucosidase 2
GCase	Glucosylceramidase, both GBA and GBA2
GCS	Glucosylceramide synthase

GD	Gaucher disease
GlcCer	Glucosylceramide
GlcSph	Glucosylsphingosine
GSLs	Glycosphingolipids
HMDB	Human metabolome database
HPLC	High-performance liquid chromatography
HPTLC	High-performance thin layer chromatography
IP	Intraperitoneal
iPSCs	Induced pluripotent stem cells
IV	Intravenous
KI	Knock-in
KO	Knock-out
L-DOPA	Levodopa
LacCer	Lactosylceramide
LAMP	Lysosome associated membrane protein
LIMP-2	Lysosomal integral membrane protein 2
LLOMe	L-leucyl-L-leucine methyl ester
LRRK2	Leucine-rich repeat kinase 2
LSDs	Lysosomal storage disorders
MAG	Myelin-associated glycoprotein
MAOB	Monoamine oxidase type B
MEFL	Molecules of equivalent fluorescence
MND	Motor neuron disease
NB-DGJ	*N*-butyl-deoxygalactonojirimycin
NB-DNJ	*N*-butyl-deoxynojirimycin
NP-HPLC	Normal-phase high-performance liquid chromatography
NPC	Niemann-Pick disease type C
NPC1	Niemann-Pick type C1 protein
NPG	Nitrophenyl-β-D-glucopyranoside
OBB	Oxford Brain Bank
OPDC	Oxford Parkinson's Disease Centre
p14	Postnatal day 14
PBS	Phosphate buffered saline
PD	Parkinson's disease
PD-GBA	PD patients with heterozygous GBA mutations
PDUK	Parkinson's UK charity

PFA	Paraformaldehyde
PNS	Peripheral nervous system
RBD	Rapid eye movement (REM) sleep behaviour disorder
rEGCase	Recombinant endoglycoceramidase, recombinant ceramide glycanase
REM	Rapid eye movement
ROI	Region of interest
ROS	Reactive oxygen species
RP-HPLC	Reverse-phase high-performance liquid chromatography
RT	Room temperature
SM	Sphingomyelin
SN	Substantia nigra
SOD1	Superoxide dismutase 1
SpC	Spinal cord
Sph	Sphingosine
SphA	Sphinganine
SRT	Substrate reduction therapy
TDP-43	TAR DNA binding protein of 43 kDa
UPLC	Ultra-performance liquid chromatography
WT	Wildtype

1 Introduction

1.1 Lysosomes

1.1.1 Biological functions of lysosomes

Lysosomes are acidic membrane-bound organelles that are the most important sites of intracellular degradation and recycling processes for cellular and extracellular-derived material. They play a central role in the clearance of cellular substrates (including carbohydrates, lipids, proteins and nucleic acids) from multiple routes within the endosomal-autophagic-lysosomal system [1, 2]. Examples for these routes are biosynthetic pathways transporting newly synthesised proteins, endocytic and phagocytic pathways contributing to signal transduction and pathogen defence, and autophagic pathways for the degradation of damaged organelles, protein aggregates, oxidized lipids and other cellular waste (**Figure 1.1**). Accordingly, the lysosomal system is a highly efficient and major metabolic network in eurkaryotic cells and is essential for the homeostasis of cell function [3].

In addition to the catabolism and recycling of macromolecules, lysosomes are nowadays recognised to be multi-functional organelles, involved in regulation of metabolic homeostasis, cellular signalling and cellular health in general [3, 4]. Indeed, lysosomes are highly complex and dynamic key cellular signalling hubs that are involved in nutrient sensing, amino acid and ion homeostasis and calcium signalling [3, 5, 6]. Lysosomes also mediate important cellular activities such as plasma membrane repair, cholesterol homeostasis, lysosomal cell death and antigen presentation (**Figure 1.1**) [4]. Furthermore, lysosomes are considered as the regulators of lipid degradation pathways, i.e. triglycerides, as they sustain cellular metabolism and energy supply via autophagy, when extracellular nutrients are not available [5]. Taken together, this places the lysosome at the centre of the regulation of cell metabolism [3, 7].

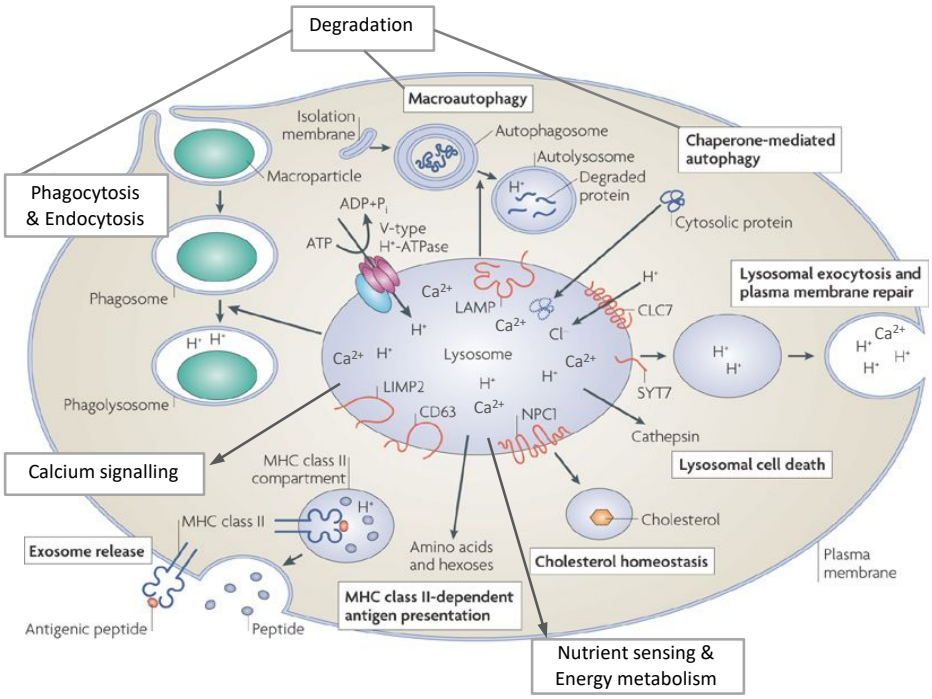

Figure 1.1: The lysosome and its functions. Lysosomes are acidic organelles that are involved in the degradation and recycling of macromolecules through the activity of more than 50 lysosomal hydrolases. The acidic pH of lysosomes is maintained through the constant action of H^+-ATPases. Lysosomes receive material for degradation through phagocytosis, endocytosis, macroautophagy and chaperone-mediated autophagy. Lysosomes are involved in cellular pathogen defence through phagocytosis and MHC class II-dependent antigen presentation. Furthermore, lysosomes are important Ca^{2+}-stores, which are implicated in intracellular calcium signalling, lysosomal exocytosis and plasma membrane repair. Lysosomes are also involved in cell death pathways (release of lysosomal cathepsins) and cholesterol homeostasis (lysosomal cholesterol efflux through NPC1). Lysosomes are nowadays also appreciated as key metabolic signalling organelles that are crucially involved in nutrient sensing and energy metabolism of the cell. Modified from [4].

Defects that impair any of these lysosomal functions can have catastrophic consequences for cells, organs and individuals. For example, defects in lysosomal enzymes can cause the accumulation (or storage) of undigested material in lysosomes, giving rise to rare neurodegenerative diseases called lysosomal storage disorders [8]. Lysosomal dysfunction also significantly contributes to the pathophysiology of common diseases, including neurodegenerative diseases (e.g. Alzheimer's, Parkinson's and Huntington's disease), cancer, obesity and infection [2, 9]. The possibility of promoting and enhancing lysosomal function with pharmacological interventions therefore holds therapeutic promise in the treatment of these diseases [2, 10].

1.1.2 Hydrolases

Lysosomes contain a variety of integral membrane proteins (e.g. ion channels, transporters, trafficking and fusion machinery proteins) and soluble proteins (e.g. hydrolases and activators) to be able to deal with the dynamics and complexity of its functions [3, 4, 11]. As a key purpose of the lysosome is the degradation of a diversity of cellular components, lysosomes contain 50-60 soluble, acidic hydrolases (e.g. proteases, nucleases, lipases) required for the degradation of macromolecules [1, 12]. The major transport pathway of newly synthesised soluble acid hydrolases to the lysosome (after biosynthesis in the ER and the Golgi) depends on mannose-6-phosphate moieties, allowing their recognition by mannose-6-phosphate receptors in the Golgi complex and ensuring their transport to the endosomal/lysosomal system [4, 13]. Transport pathways independent of mannose-6-phosphate also exist, e.g. the protein LIMP2 has been shown to escort the enzyme GBA to the lysosome and, when LIMP2 is deficient, causes Gaucher disease [14, 15].

In very simple terms, lysosomes can be regarded as storage compartments of hydrolytic enzymes that enter cycles of fusion and fission with late endosomes and autophagosomes, while the digestion of endocytosed and autophagic substrates takes place primarily in transient endolysosomes and autolysosomes [1]. For this purpose, the internal pH of lysosomes is typically maintained in the acidic range of pH 4.5-5.0 by vacuolar-type H^+-ATPases, as the hydrolases have acidic pH optima [4, 16].

In this thesis, the activities of various lysosomal enzymes (e.g. acid β-glucosidase (GBA), α-galactosidase, β-hexosaminidase, and β-galactosidase) were assayed to assess lysosomal function. Each of these enzymes has a specific role in the degradation of glycosphingolipids (GSLs). Thus, when their activity is deficient, owing to genetic mutation, accumulation of their GSL substrates occurs and results in specific lysosomal storage disorders, in this case sphingolipidoses, for each particular hydrolase (**Table 1.1**). For example, β-galactosidase catalyses the hydrolysis of terminal β-galactosidic

bonds in GM1a ganglioside, lactosylceramide and lactose [8]. Deficiencies in the enzyme result in GM1 gangliosidosis, where neuronal GM1a abnormally accumulates in ER membranes, leading to abnormal calcium flux from the ER to mitochondria and activation of mitochondria-mediated apoptosis [8, 17].

Table 1.1: Examples of lysosomal hydrolases and their related lysosomal storage disorders.

Disease (gene)	Enzyme	Substrate (or storage)
Gaucher disease (*GBA*)	acid β-glucosidase (β-glucocerebrosidase, GBA)	glucosylceramide (GlcCer) and glucosylsphingosine (GlcSph)
Fabry disease (*GLA*)	α-galactosidase	globotriaosylceramide (Gb3)
Tay-Sachs disease (*HEXA*)	β-hexosaminidase A	GM2 ganglioside
Sandhoff disease (*HEXB*)	β-hexosaminidase B	GM2 ganglioside
GM1 gangliosidosis (*GLB1*)	β-galactosidase	GM1a ganglioside

1.2 Glycosphingolipids (GSLs)

1.2.1 Structure of GSLs

Glycosphingolipids (GSLs) are common components of membranes of all eukaryotic cells. GSLs are composed of a hydrophilic glycan head group (or at least one monosaccharide residue) glycosidically linked to a hydrophobic ceramide, which consists of an N-acylated sphingosine and is imbedded in the lipid bilayer [18, 19]. For example, when either glucose or galactose is β-glycosidically linked to the primary hydroxyl group of the sphingosine moiety in the ceramide, the simplest GSLs, glucosylceramide (GlcCer) and galactosylceramide (GalCer), are formed (**Figure 1.2**). GlcCer and GalCer are called cerebrosides, the common name for monoglycosylceramides. Further addition of monosaccharides to the sugar head group

give rise to a broad range of complex GSLs, e.g. globosides or gangliosides (**Figure 1.2**) [20].

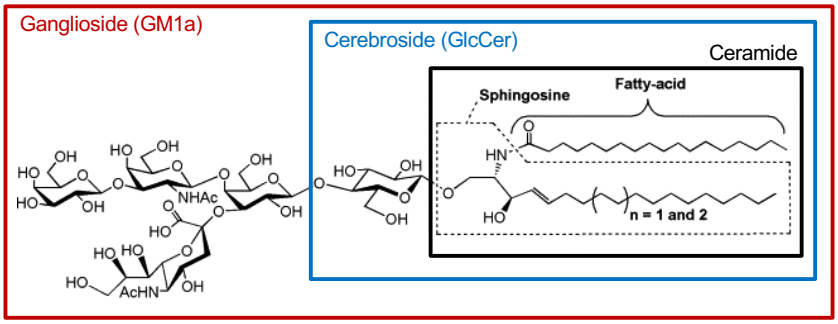

Figure 1.2: The structure of glycosphingolipids. Ceramide is composed of sphingosine and a fatty acid. Addition of either a glucose or a galactose to the primary hydroxyl group of the sphingosine moiety gives rise to a cerebroside (in the presented case GlcCer). Additions to the sugar head group convert cerebrosides into various GSLs, e.g. the complex ganglioside GM1a. Modified from [21].

The complexity of GSLs is the result of both the arrangement of sugars for the glycan head group (e.g. monosaccharide type, number, linkage) and the heterogeneity of the lipid moiety (e.g. sphingoid base type, the acyl-chain length and saturation) [19, 22]. Consequently, thousands of GSL structures exist. However, GSLs have a stable, cell-type specific expression pattern (e.g. primarily gangliosides in neurons and globo-series GSLs in fibroblasts), which indicates a tight regulation of their biosynthesis, degradation and intracellular transport in each individual cell type and is currently an active area of research [22, 23].

1.2.2 Biosynthesis of GSLs

The biosynthesis of GSLs takes place at the membranes of the endoplasmic reticulum (ER) and Golgi complex and is a multi-enzyme catalysed pathway, where the product of one enzymatic reaction typically generates the substrate for the next enzymatic reaction in the pathway [18]. The key precursor for the biosynthesis of GSLs is ceramide. Ceramide is formed *de novo* at the cytosolic leaflet of the ER through a series of enzymatic reactions, starting with L-serine and palmitoyl-CoA, leading to the generation

of 3-ketopshinganine, followed by formation of sphinganine, dihydroceramide and finally ceramide [20]. Ceramide can also be generated by acylation of sphingosine, which can only be derived from lysosomal degradation of GSLs and forms part of the salvage pathway of GSLs [19, 20]. Subsequently, ceramide can be converted into galactosylceramide in the lumen of the ER or can be transported to the Golgi complex, either via the action of the ceramide-transfer protein (CERT) to form sphingomyelin (at the luminal leaflet of the Golgi) or by vesicular transport to form glucosylceramide (at the cytosolic leaflet of the Golgi) (**Figure 1.3**) [22, 24].

Glucosylceramide (GlcCer) is generated through the action of the membrane-bound enzyme ceramide glucosyltransferase (CGT), also called GlcCer synthase (GCS), which links glucose to ceramide at the cytosolic leaflet of the cis-Golgi (**Figure 1.3**) [20, 22]. GlcCer is the core structure of most mammalian GSLs and thus occupies a key position in GSL biosynthesis, connecting 'simple' sphingolipids (including ceramide, and sphingosine, and sphingomyelin) with complex glycosylated sphingolipids (e.g. gangliosides) [20, 25]. GlcCer is translocated to the luminal side of the trans-Golgi to form complex GSLs. Interestingly, there are different pools of GlcCer, which serve as precursors for different groups of complex GSLs (**Figure 1.3**). For example, if GlcCer moves via vesicular transport through the Golgi stack, it is preferentially used to build gangliosides (starting with GM3) [22]. However, non-vesicular transport of GlcCer to the trans-Golgi mediated by the transfer protein FAPP2 leads to preferential production of globosides (starting with Gb3) [22, 26].

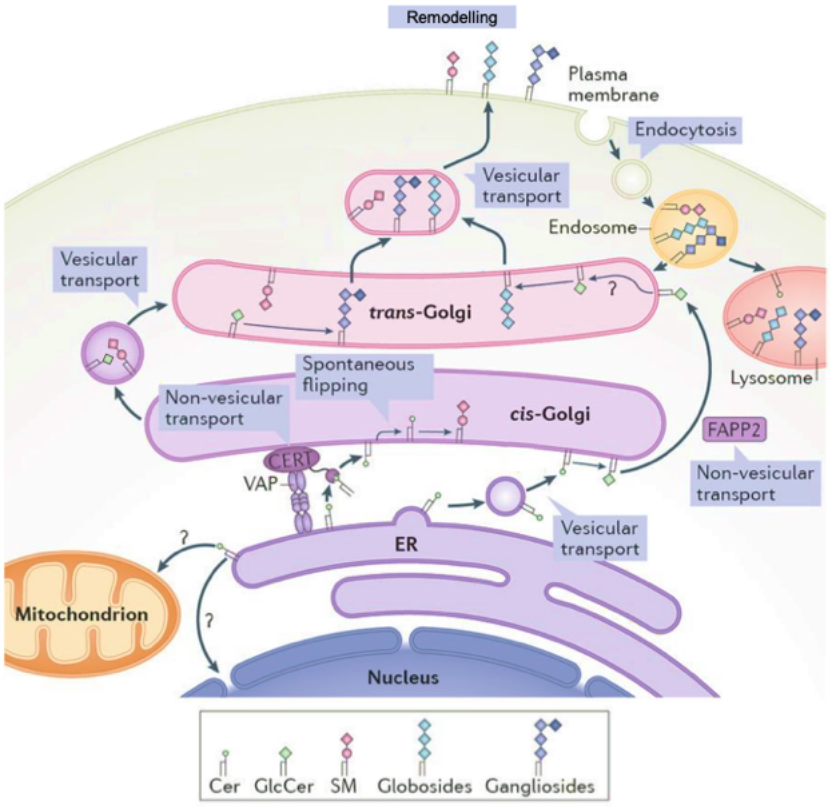

Figure 1.3: Synthesis, trafficking and degradation of GSLs. GSL synthesis starts at the ER with the generation of ceramide (Cer). Cer can reach the Golgi either by vesicular transport, where it is coupled to the synthesis of glucosylceramide (GlcCer), or by non-vesicular transport via the action of ceramide transfer protein (CERT), which couples ceramides to the synthesis of sphingomyelin (SM). GSL synthesis continues in the Golgi complex. GlcCer can reach the trans-Golgi network through vesicular transport, where it is used for the generation of anionic gangliosides, or with the help of the transfer protein FAPP2, which couples it specifically to the synthesis of neutral globosides. After synthesis, GSLs are typically transported to the lipid bilayer of the cell membrane, where they exert their biological functions and can also be remodelled until they are endocytosed and transported to lysosomes for degradation. Modified from [24].

Besides the compartmentalisation of GSL trafficking and synthesis, the complexity of GSLs is the result of sequential actions of glycosyltransferases in the Golgi complex that convert GlcCer into LacCer through the addition of a galactose and then into higher-order GSL species through stepwise glycosylation reactions (**Figure 1.4**) [23]. Once LacCer is formed, there is competition by a number of transferases to generate different types of complex mammalian GSLs [18]. The main groups of GSLs are the ganglio-series, globo-series and lacto-series (**Figure 1.4**). Gangliosides are further divided into o-series, a-series, and b-series gangliosides (**Figure 1.4**). A large number of

gangliosides exist and a useful nomenclature was introduced by Svennerholm, a pioneer in ganglioside research [20]. In this nomenclature G stands for ganglioside, A for asialo-, M for monosialo-, D for disialo-, and T for trisialo-ganglioside. For example, specific sialyl transferases can convert GM1a stepwise into GD1a and then GT1a.

In conclusion, numerous glycosyltransferases are involved in generating diverse series of mammalian GSLs [19]. After synthesis, GSLs typically undergo vesicular transport to the plasma membrane and contribute to specific biological functions. They recycle via the Golgi apparatus many times before being targeted to the lysosome for degradation. It is important to note that direct remodelling of GSLs can take place at the plasma membrane through the action of specific cell surface glycosidases, which can for example result in the formation of simpler GSLs from more complex ones and which is an especially important mechanism in neuronal development and neuronal health (**Figure 1.3**) [23, 27, 28].

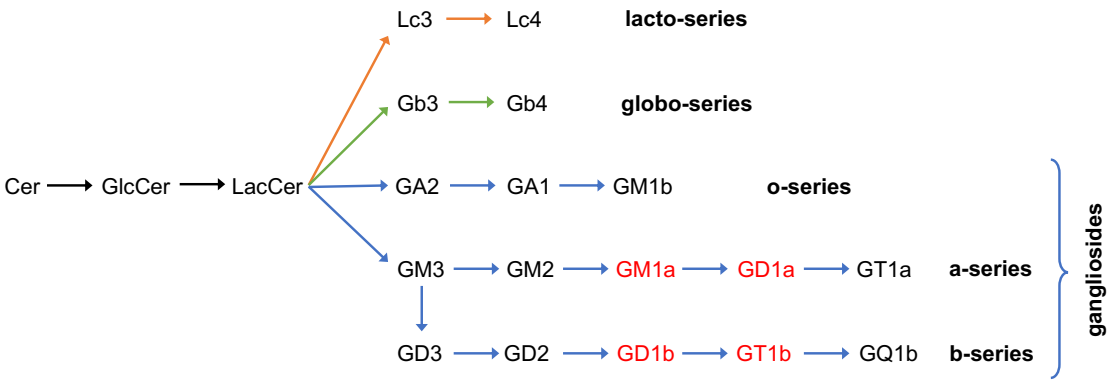

Figure 1.4: Series of complex GSLs in the biosynthetic pathway of GSLs. GSLs are classified into lacto-series, globo-series and ganglio-series GSLs. Gangliosides are further divided into o-series, a-series and b-series gangliosides. Gangliosides highlighted in red are the major GSL species in the mammalian brain. Cer: ceramide, GlcCer: glucosylceramide, LacCer: lactosylceramide.

1.2.3 Biological functions of GSLs

The importance of GSLs for cells and individuals is clearly demonstrated by the embryonic lethality of mice lacking the enzyme GlcCer synthase (GCS), which completely abolishes the biosynthesis of all GlcCer-derived GSLs [29]. GSLs are present ubiquitously in the membranes of eukaryotic cells, where they are essential for a variety of biological cell functions. For example, GSLs are involved in cell adhesion and migration, cell signalling, cell proliferation, endocytosis, intracellular transport, inflammation and apoptosis [22, 24]. Thus, GSL functions are mediated by both trans interactions (e.g. cell-cell interactions via binding to complementary molecules on opposing plasma membranes) and lateral, cis interactions (e.g. modulating activities of ion channels and receptors in the same plasma membrane) [30].

GSLs, especially ceramides and glucosylceramides, are essential components of the skin of all terrestrial animals, making it impermeable to water and thereby preventing lethal dehydration [19, 20]. GSLs have also been critically implicated in immune response, cancer cell biology, metabolic functions, bone development, neurodevelopment and neuronal health and thus are the target for therapies of diseases like HIV, diabetes, cancer and lysosomal storage disorders [24, 31-38]. Some specific physiological roles of individual GSLs or certain classes of GSLs have been revealed by genetically engineering knock-out (KO) mice lacking specific GSL biosynthetic enzymes or by analysing patients with rare mutations in these enzymes. For example, mutations in B*4GALNT1*, encoding GM2-synthase, lead to deficiency in the enzyme and thus lack of GM2 and further complex gangliosides in patients, causing a complex form of degenerative hereditary spastic paraplegia, underlining the role of gangliosides in neuronal structure and function [39].

Of particular interest for this thesis are the gangliosides. Gangliosides are complex, charged GSLs, which contain at least one capping N-acetylneuraminic acid (sialic acid) moiety [20]. Importantly, gangliosides of the a- and b-series (predominantly GM1a,

GD1a, GD1b, and GT1b) are the most abundant GSLs in the nervous system in all mammals and are essential for neuronal function (**Figure 1.4**) [23, 40, 41]. For example, ganglioside GM1a is essential for neuritogenesis and axonogenesis, modulation of calcium transport and calcium homeostasis, and signalling of several neurotrophic factors [41-43]. GM1a has also been implicated as regulator of both Aβ aggregation in Alzheimer's disease and α-synuclein aggregation in Parkinson's disease [41, 42]. As another example, the gangliosides GD1a and GT1b are essential for long-term stable myelination of axons, which is maintained through trans-interactions with myelin-associated glycoproteins (MAGs) on the innermost wrap of myelin [41, 42]. In this thesis, the levels of the main gangliosides in the mammalian central nervous system, being GM1a, GD1a, GD1b and GT1b, were analysed in detail in murine and human brain.

1.2.4 Catabolism of GSLs

Similar to the process of mammalian GSL biosynthesis, the catabolism of complex GSLs is a stepwise process, predominantly taking place in late endosomes and lysosomes (**Figure 1.3**) [20]. The sequential breakdown of GSL oligosaccharides by multiple exoglycosidases follows the reverse pathway to that of biosynthesis. Monosaccharides are cleaved from complex GSLs in a stepwise process to generate LacCer [19] (**Figure 1.5**). LacCer is processed to GlcCer by β-galactosidase. Subsequently, GlcCer is degraded to ceramide and glucose by acid β-glucosidase GBA (**Figure 1.5**). Ceramide is further catabolised by acid ceramidase to sphingosine, which is returned to the ER and recycled for GSL biosynthesis [20]. GlcCer can alternatively be processed by acid ceramidase to its deacylated form glucosylsphingosine (GlcSph), which can either be degraded by GBA to sphingosine or can exit the lysosome (**Figure 1.5**) [44-46].

As well as by GBA, GlcCer and GlcSph can also be degraded by the non-lysosomal glucocerebrosidase GBA2 (**Figure 1.5**). GBA2 was identified in 2007 and is a membrane-associated glucocerebrosidase, which is localised at the cytoplasmic face of

the ER and Golgi [47, 48]. Mutations in GBA2 cause accumulation of cytosolic GlcCer and humans carrying mutations in the *GBA2* gene are affected with a combination of cerebellar ataxia and spastic paraplegia [49, 50].

Lysosomal catabolism of GSLs is essential for maintaining lipid homeostasis of cells and failure to degrade GSLs results in a variety of rare neurodegenerative diseases called lysosomal storage diseases.

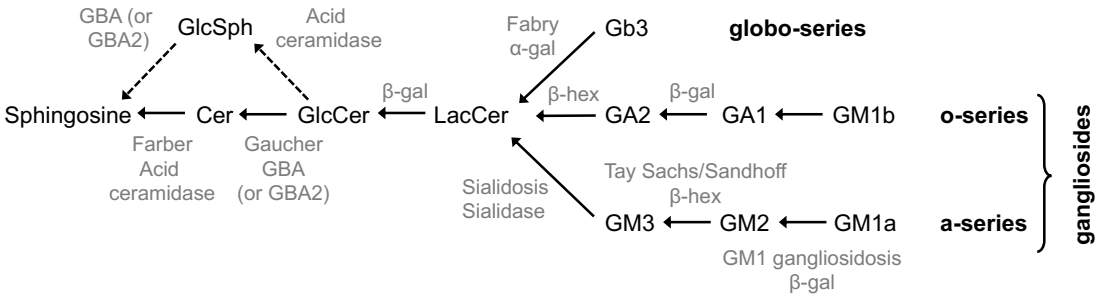

Figure 1.5: Lysosomal degradation of selected GSLs. The individual lysosomal storage diseases and their corresponding hydrolases, which are required for the respective degradation step, are indicated in grey. An alternative pathway for the degradation of GlcCer through synthesis of GlcSph is indicated with dashed arrows. GlcCer and GlcSph can also be degraded outside the lysosome through the action of GBA2. Cer: ceramide, GlcCer: glucosylceramide, LacCer: lactosylceramide, β-gal: β-galactosidase, β-hex: β-hexosaminidase, α-gal: α-galactosidase.

1.3 Neurodegenerative Diseases

1.3.1 Lysosomal storage disorders (LSDs)

Lysosomal storage disorders (LSDs) were first conceptualised by H.G. Hers as disorders resulting from deficiencies in single lysosomal hydrolases [51]. Today, LSDs are known as a group of over 70 rare inherited diseases that result from lysosomal dysfunction. They are not only caused by mutations in lysosomal hydrolases, but also in non-enzymatic lysosomal and non-lysosomal proteins critical for proper function of the lysosomal system, such as integral membrane proteins, transporters, enzyme modifiers or activators [8]. However, most LSDs result from inactive or poorly active acidic lysosomal enzymes, which arise from inherited, typically autosomal recessive gene

mutations [1, 18]. Although individually rare, with estimated incidences ranging from 1:50,000 to 1:250,000 live births, LSDs as a group are common and have a combined incidence of approximately 1:5,000 live births [52, 53].

In general, LSDs are genetically and clinically heterogeneous disorders [8]. For example, the age of onset and clinical course can vary significantly, but nearly all LSDs have a delayed non-congenital onset and progressive clinical course, ultimately leading to premature death. Symptoms and disease severity depend on the type of LSD and only loosely correlate with the type of mutation and the residual activity of the deficient protein in each individual [8, 54]. However, neurodegeneration is a common feature of these metabolic disorders and the classical clinical representation of an LSD is a paediatric neurodegenerative disease with progressive pathologies in the central nervous system (CNS) [8]. Intellectual disability, dementia, seizures, motor system deficits, visual impairment and hearing loss are common manifestations associated with several lysosomal diseases [18, 55, 56]. The progressive clinical and pathological course of LSDs highlights the vital role of lysosomes, especially in post-mitotic neurons which are predominantly affected [57]. Nevertheless, adding to the complexity of these diseases, symptoms in multiple other tissues and organ systems are also frequent [8]. Here, it is important to note that different cell types are affected differently by lysosomal dysfunction in each LSD. This divergence is probably due to numerous factors, including differential biochemistry of distinct cell types (e.g. neuronal subtypes), differential synthesis and turnover rates of substrates, differential vulnerability of different cell types (e.g. catabolic enzyme redundancy or adaptive changes to counteract the defect), differentiation status of the cell (e.g. post-mitotic) and developmental status when critical levels of storage are reached [1, 38].

The cellular pathogenesis of LSDs is complex and not fully understood. At its simplest, it is believed that at the start of disease progression, a specific threshold of enzyme activity is reached where the influx of substrate to the lysosome is greater than the rate

of lysosomal catabolism, consequently leading to substrate accumulation [18]. Thus, a common defining characteristic of all LSDs is the progressive primary accumulation (or storage) of non-metabolised macromolecules within enlarged organelles of the autophagic-lysosomal system [8, 58]. Therefore, LSDs can be subclassified according to the biochemical type of stored material (e.g. sphingolipidoses, mucopolysacharidoses and glycoproteinoses) [8]. This storage is believed to be the primary cause of disease, but the wide range of disease symptoms indicates that the storage has a broader influence on hindering the metabolic homeostasis in cells. Accordingly, substrate accumulation inside lysosomes initiates a pathogenic cascade of numerous secondary biochemical and cellular effects, which then subsequently cause irreversible cellular damage and tissue pathology (**Figure 1.6**) [1, 12, 38]. Thus, the advanced pathogenic cascade impacts not only the autophagic-lysosomal system, but also other organelles, including mitochondria, the ER and the Golgi complex (**Figure 1.6**). Relatively recently, it was found that lysosomes form contact sites with many other organelles (e.g. mitochondria, the ER, the nucleus), thus it is not surprising that secondary effects can lead to dysfunction of these organelles [59]. Accordingly, several common pathways are dysregulated in most LSDs, including deficits in cellular transport and degradation (e.g. cytoplasmic protein aggregation, endocytosis, autophagy), calcium homeostasis, ER stress, mitochondrial function and oxidative stress, and inflammatory and innate immune responses (**Figure 1.6**) [1, 8, 54]. Consequently, lysosomes become even more compromised in the pathogenic cascade, thereby exacerbating the accumulation of primary and secondary storage material, ending in a deleterious cycle of cellular dysfunctions and finally cell death (**Figure 1.6**) [8].

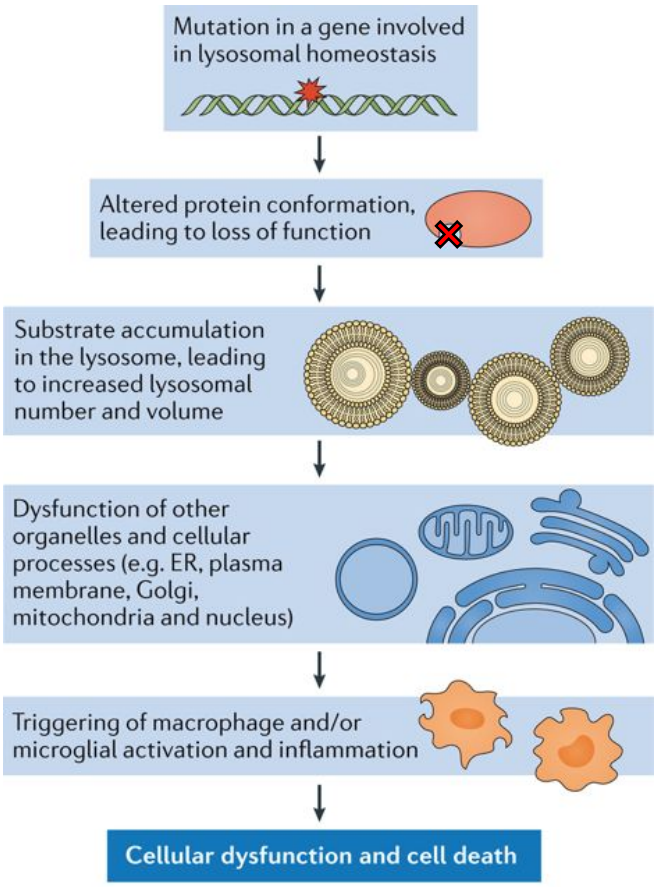

Figure 1.6: The pathogenic cascade of lysosomal storage disorders. The pathogenic cascade starts from the genetic defect, producing a mutant protein, frequently a lysosomal enzyme. The mutant protein is either not transcribed at all, misfolded and cleared via quality control mechanisms or has compromised function. The consequence of protein dysfunction is the accumulation of substrates in lysosomes, leading to an expansion of the lysosomal system. After some time, secondary effects of storage are manifested in other cellular organelles, e.g. the endoplasmic reticulum (ER) and mitochondria, leading to dysfunction in various other aspects of cell homeostasis. Then, the innate immune system is triggered, leading to inflammation in both peripheral tissues and the brain. Finally, the combination of cellular dysfunctions leads to cell death. Modified from [38].

1.3.1.1 Gaucher disease (GD)

Gaucher disease (GD) is one of the most common lysosomal storage disorders. GD is an autosomal recessive disorder, with a global incidence of GD type 1 of about 1:40,000 [60]. GD was first discovered more than a century ago in 1882 by the French physician Philippe Gaucher. In 1965, the primary defect was identified as the inability of the mutated enzyme β-glucocerebrosidase (acid β-glucosidase, GBA) to degrade its GSL substrates glucosylceramide (GlcCer) and glucosylsphingosine (GlcSph) [51]. As a

consequence, GlcCer and GlcSph accumulate in cells over time, leading to lysosomal storage primarily in cells of the monocyte-macrophage system (due to the phagocytic activity of these cells), which is the classical hallmark of this disorder [61]. In contrast to the impaired degradation of GlcCer and GlcSph, the rate of GSL biosynthesis remains unchanged. Thus, activated macrophages, or 'Gaucher cells', harbour the accumulated lipids and infiltrate into various organs, affecting the immune system, bone strength, spleen and liver function [1].

GD is divided into three clinical subtypes, based on age of onset and the absence or presence of CNS involvement. GD type 1 is classified as the chronic, non-neuronopathic form and is the most common type of GD (>90% of patients) [60]. Patients with GD type 1 typically present with hepatosplenomegaly, pancytopenia, bone disease, degenerative arthritis and elevated risk of multiple myeloma [8]. In contrast, GD types 2 and 3 are neuronopathic forms of GD. GD type 2 is an acute, infantile lethal neuronopathic form and is very rare (1% of patients). Affected children display neurological abnormalities before 6 months of age and die by the age of 2-4 years [60]. GD type 3 is known as the chronic neuronopathic form of GD and is relatively rare (5% of patients). Patients show similar symptoms to those observed in type 2 disease, but with a later onset, decreased severity and greater phenotypic heterogeneity [60].

Little is known about the molecular mechanisms by which GlcCer and GlcSph accumulation lead to the complex pathology of GD [60]. However, a number of studies have proposed a role for dysfunctional calcium stores and inflammation in GD. GlcCer was shown to directly interact with and modulate the activity of the ER ryanodine receptor, leading to increased agonist-stimulated calcium release and altered calcium homeostasis in GD neurons [62, 63]. In neuronopathic GD types 2 and 3, microglia activation, caused by neuronal GlcCer and GlcSph storage, and subsequent neuroinflammation have been associated with neuronal dysfunction and neuronal loss in the brain [60, 64].

Currently available treatments for GD include enzyme replacement therapy (ERT) and substrate reduction therapy (SRT) [61, 65-67]. Although ERT has an effect on non-neurological manifestations in GD type 1, it has no therapeutic effect on neurological symptoms in GD types 2 and 3, as the recombinant enzyme does not cross the blood-brain barrier (BBB).

1.3.1.2 Therapeutic options for LSDs

Although treatments are currently available for a number of LSDs, it is important to note that most LSDs still cannot be treated and are only managed symptomatically [8]. In general, early intervention is key for all LSDs, as the pathogenic cascade can then be prevented before the development of irreversible pathology [38]. Also, keeping the multimorbidity of LSDs in mind, that is having multiple chronic conditions at the same time, it seems very likely that only a combination of therapies will lead to successful treatment of patients [38].

Enzyme Replacement Therapy (ERT)

Since most LSDs are caused by a lysosomal enzyme deficiency, the earliest idea for a treatment of LSDs was to replace the mutant enzyme with functional wildtype enzyme. As such, enzyme replacement therapy (ERT) is a disease-specific intervention that uses direct infusion of purified soluble acid hydrolases to enhance enzyme function [57]. As the lysosome is the target organelle of this therapy, recombinant enzymes are targeted to the lysosomes on the basis of a molecular signature, the mannose-6-phosphate moiety, which serves as a lysosomal recognition signal [1].

The first and most effective ERT for an LSD was established for type 1 GD. Here, the defective enzyme (β-glucosidase GBA) was ‘replaced’ by delivering fully functional wildtype enzyme to tissues in patients, which is mainly endocytosed by macrophages

via the macrophage mannose receptor [1, 68]. In 1995, a human recombinant form of GBA, expressed in Chinese hamster ovary (CHO) cells, modified to become a mannose-terminated protein, was approved as Cerezyme (Imiglucerase; Genzyme) [61, 65]. Targeting of the modified enzyme to the affected tissue with preferential uptake by macrophages has been demonstrated in patients with GD [68, 69]. Most clinically relevant manifestations of type 1 GD can be treated or even prevented with early ERT, allowing patients to achieve stabilisation and live largely normal lives [8, 70]. Other examples of LSDs with approved ERT are Fabry disease, Pompe disease and lysosomal acid lipase deficiency [8]. However, there are known clinical limitations of ERT. Enzyme delivery is invasive and time-consuming, and recombinant lysosomal enzymes do not cross the BBB to any significant extent, so cannot effectively treat CNS disease, which is a characteristic of most LSDs [1, 71]. Nevertheless, ERT remains the major class of approved therapies for LSDs [8].

A new approach to achieve replacement of the mutant enzyme is gene therapy, which is currently in clinical trials for a number of LSDs. Gene therapy is based on introducing a normal copy of the mutant transcript into the patient DNA in the nucleus using a vector as delivery system (usually an adeno-associated virus (AAV)) [8, 72]. Gene therapy has a similar principle to ERT, but the important advantage would be that repeated dosing would not be needed [8].

Substrate Reduction Therapy (SRT)

In most sphingolipidoses the influx of GSL substrate into lysosomes is higher than the impaired lysosomal degradation, leading to lysosomal storage of the GSL substrate. Consequently, another approach for therapy of LSDs is to partially inhibit the biosynthesis of GSLs to reduce GSL substrate influx into the compromised lysosome and thus compensate for deficient enzyme activity [38, 57]. This therapeutic approach is known as substrate reduction therapy (SRT). SRT is based on selective small-

molecules, which inhibit GSL biosynthesis in its early steps to reduce lysosomal storage [73, 74]. Accordingly, the Golgi complex is the target organelle for this therapy [1]. There are currently only two approved drugs for this therapy, miglustat (Zavesca; Actelion Pharmaceuticals) and eliglustat (Cerdelga; Genzyme) [8]. Both drugs are iminosugars, which target the Golgi enzyme GlcCer synthase (GCS) and thus inhibit the first step in GSL biosynthesis [1, 61, 75]. Miglustat is able to cross the blood-brain barrier (BBB) to some extent, but eliglustat does not [76].

SRT was first successfully tested in 1998 for non-neuronopathic type 1 GD using the orally-delivered, small-molecule glucose analogue iminosugar, *N*-butyldeoxynojirimycin (miglustat) [65]. Nowadays, SRT using both miglutast and eliglustat is approved for the treatment of GD type 1 [38]. Furthermore, miglustat has been approved in 2009 for treating neurological symptoms in NPC [38, 77, 78]. Interestingly, it is speculated that the positive effect of miglustat in NPC may be due to off-target inhibition of GBA2, possibly leading to a reduction in neurotoxic sphingosine levels [79, 80].

Efficacy in treating GD-specific parameters with miglustat has a slower onset compared to ERT, as substrate turnover (which is e.g. slow in the brain) must occur before clinical benefit can be observed, but parameters improved within 6 months in clinical trials [8, 20]. Interestingly, growing evidence suggests that miglustat may be beneficial for other LSDs including Sandhoff and Tay-Sachs disease [81]. However, miglustat has side effects, mainly caused by inhibition of disaccharidases in the intestinal microvilli, which leads to gastrointestinal symptoms like diarrhoea and flatulence [1, 20].

Several BBB-penetrant drugs are currently being developed for SRT to treat the neurodegenerative phenotypes in GSL storage disorders [38]. For example, the compound ibiglustat (GZ402671; Genzyme) is currently in clinical trials for Gaucher disease (NCT02843035) [38].

Chaperone-mediated Therapy (CMT)

A relatively new and more experimental approach to treat GSL storage diseases is called chaperone-mediated therapy (CMT). CMT aims to use active site inhibitors, e.g. iminosugars, as molecular chaperones, which assist protein folding and stability of otherwise unstable mutant enzymes [38]. Here, active site inhibitors are applied at sub-inhibitory concentrations to target protein folding and trafficking and to assist correction of diminished lysosomal enzyme activity, thereby reducing storage [20, 57]. The current challenge is the discovery of new pharmacological chaperones, as they need to reversibly bind, temporarily stabilise, and then dissociate from the molecular target, while the active site of the mutant enzyme remains stable [38, 82]. As pharmacological chaperones can be designed to cross the BBB, they are good candidates for the treatment of neuropathic forms of LSDs [83]**.** The only currently approved chaperone drug is migalastat for treating Fabry disease (Amicus Therapeutics) [8, 84]. Several orally available small-molecule chaperones are currently in clinical trials for the treatment of LSDs, e.g. ambroxol for GD (NCT01463215) and pyrimethamine for Tay-Sachs and Sandhoff disease (NCT01102686) [8].

To overcome potential limiations of active-site-targeting chaperones, a new generation of chaperones that are allosteric enhancers is being developed [38]. Here, a new promising non-inhibitory compound for treating GD is called NCGC607. This compound reduced lysosomal lipid storage and α-synuclein levels in dopaminergic neurons derived from induced pluripotent stem cells from patients with GD and Parkinsonism [85].

1.3.2 Amyotrophic lateral sclerosis (ALS)

Motor neuron disease (MND) encompasses a group of diseases, whose common feature is the degeneration of motor neurons. Amyotrophic lateral sclerosis (ALS) is the most common form of motor neuron disease. ALS is a devastating adult-onset neurological disorder characterised by the selective degeneration of both upper motor

neurons in the motor cortex and lower motor neurons in the brainstem and the spinal cord [86]. Sadly, ALS is life-shortening and there is currently no cure. Clinical hallmarks of ALS are progressive muscle weakness and wasting followed by paralysis, speech and swallowing difficulties, respiratory insufficiency, altered reflexes and spasticity [86, 87]. Death typically occurs within 2-5 years of diagnosis, usually due to respiratory complications. Only two drugs have been approved for treating ALS (riluzole and edaravone), which have unknown mechanisms of action and limited therapeutic effect (e.g. riluzole increases survival by 3 months), thus ALS is mostly managed symptomatically [86].

The incidence of ALS increases dramatically with age [88]. The disease typically affects people between 40-70 years of age and has an incidence of 1.5-3.0 per 100,000 people [86, 89, 90]. Interestingly, there are several shared cellular impairments present in both ageing and ALS, e.g. impaired autophagy/lysosomal system [88]. Thus, ageing may facilitate some aspects of the disease and can be considered as one of the main non-genetic risk factors for ALS [88, 91].

About 90% of ALS cases are of unknown origin, called sporadic, and only 10% of the cases have genetically inherited causes, mainly due to autosomal dominant mutations [92, 93]. Both sporadic and familial forms of ALS are clinically heterogeneous and undistinguishable, suggesting common pathogenic mechanisms. The most common mutations associated with genetic forms of ALS are in genes encoding superoxide dismutase 1 (SOD1), TAR DNA binding protein of 43 kDa (TDP-43), fused in sarcoma protein (FUS) and chromosome 9 open reading frame 72 (C9ORF72) [94-98].

The exact pathophysiology of ALS remains unclear, but mitochondrial dysfunction and oxidative stress, impaired RNA metabolism, ER stress, and alterations in axonal transport have been shown [93, 99, 100]. A pathological hallmark of ALS is the accumulation of cytosolic protein aggregates in affected motor neurons [101]. Several studies have shown increased numbers of autophagosomes or accumulation of

autophagic vacuoles in the motor neurons of sporadic and familial ALS patients as well as ALS mouse models [102, 103]. Accordingly, dysfunctions in the autophagy-lysosome pathway have frequently been implicated in ALS [104-106]. However, it has been suggested that the autophagic dysregulation in ALS motor neurons occurs at various early steps of the autophagy process, rather than later steps involving lysosomal function [88, 107], which is in contrast to lysosomal storage disorders. Accordingly, most impairments were found in substrate sequestration/autophagosome formation and autophagosome-lysosome fusion/maturation, rather than lysosomal degradation [104, 106, 107]. For example, mutant SOD1 has been found to inhibit the initiation of autophagy (by interacting with beclin-1) as well as retrograde axonal autophagosome trafficking (by interacting with dynein), leading to abnormal autophagic flux [106]. A causative role of lysosomal dysfunction in ALS, e.g. the contribution of malfunctioning lysosomal hydrolases, has been less well studied [106]. Nevertheless, recent studies have now shown that lysosomal dysfunction is also a feature of ALS [108-111]. For example, progressive lysosomal deficits, i.e. reduced cathepsin B and D activity and reduced lysosomal density, were found as an early pathological event in spinal motor neurons of familial SOD1-mutant mice before disease-onset [112].

In summary, several pathological mechanisms have been proposed for the development of ALS. However, lysosomal dysfunction and GSL metabolism have not been studied thoroughly. With regard to the focus of this thesis, the link between GSL metabolism and ALS has only really been studied for the past 4 years or so [113-115].

1.3.3 Parkinson's disease (PD)

Parkinson's disease (PD) is the second most common, late-onset neurodegenerative disease after Alzheimer's disease. The prevalence of PD patients in the UK has been estimated to be 145,000 patients in 2018 in a recent report from Parkinson's UK (PDUK) with the lifetime risk of being diagnosed with PD in the UK in 2015 being 2.7%.

Accordingly, PD affects millions of people around the world. PD occurs most commonly in people over the age of 60 and men are more often affected than women [116]. PD is characterised by the degeneration and loss of dopaminergic (DA) neurons within the substantia nigra pars compacta of the midbrain, which is important for the control of the motor function in the basal ganglia. Thus, loss of DA neurons predominantly results in disruption of the fine-tuned motor control, causing the typical motor symptoms of tremor, rigidity, bradykinesia and gait dysfunction [116]. Further symptoms include neuropsychiatric complications like depression, sleep disturbances, and anxiety [116, 117]. A pathological hallmark of PD is the accumulation of intracellular, insoluble aggregates in DA neurons, called Lewy bodies. Lewy bodies largely consist of the synaptic protein α-synuclein [118]. With greater neuronal loss, and the occurrence of Lewy bodies beyond the substantia nigra, additional symptoms of the disease become apparent with time, including hallucinations and dementia [119]. Interestingly, lysosomal catabolism of α-synuclein is key to whether neurons can clear α-synuclein or not [120-123].

The incidence of PD increases nearly exponentially from the 5th decade of age and peaks in the 7th to 8th decade of life [117]. Consequently, ageing is the biggest non-genetic risk factor for developing several neurodegenerative diseases, including PD. The brain is especially vulnerable to age-related alterations in many biological pathways, e.g. lysosomal and mitochondrial function [124]. It is therefore conceivable that these changes may lead to dysfunction of vulnerable dopaminergic neurons with age and lower the threshold for developing PD [125].

Only 5-10% of PD cases have been linked to a monogenetic, heritable cause, whereas 90% of PD cases are sporadic [117]. Examples of genes commonly mutated and associated with PD are *SNCA* (*PARK1* or *PARK4*, encoding α-synuclein), *Parkin* (*PARK2*), *PINK1* (*PARK6*), and *LRRK2* (*PARK8*), with mutations in *SNCA* and *LRRK2* being autosomal dominant [117]. Though rare, genetic forms of PD can provide clues to

mechanisms underlying the neuropathology of PD. Some of the proteins encoded by PD-associated genes are involved in molecular pathways that have also been found to be perturbed in sporadic PD, making sporadic and genetic PD cases generally indistinguishable and suggesting common pathogenic molecular pathways. Examples of these central pathways in PD are α-synuclein protein homeostasis, mitochondrial, lysosomal and proteasomal function, oxidative stress, calcium homeostasis, axonal transport and neuroinflammation [116, 117]. Accordingly, a recent review reported that studies with post-mortem PD brains have clearly demonstrated that these cellular functions are modified at the molecular level in late-stage pathology of PD [126].

With respect to the focus of this thesis, dysfunction of the autophagic-lysosomal system has been shown to be key in the pathogenesis of PD and there are several lines of evidence supporting this. Firstly, lysosomal function is essential for the catabolism of the key pathological protein α-synuclein [120-123]. Secondly, several proteins associated with the genetic forms of PD are associated with impaired autophagic-lysosomal function, e.g. *LRRK2*, *VPS35* (encoding vacuolar protein sorting-associated protein 35), and *ATP13A2* (*PARK9*, encoding an ATPase) [117]. Thirdly, mutations in *GBA*, encoding the lysosomal hydrolase β-glucosidase GBA, have been identified as the highest genetic risk factor for developing PD (see section **1.3.3.1**) [127]. In summary, several pathological mechanisms have been implicated in the development of PD, with lysosomal dysfunction being one of the key contributors to disease pathogenesis.

Interestingly, clinical, pathological and imaging data suggest that substantia nigra lesions in PD might evolve over 10 years or more before motor symptoms appear and PD is diagnosed [116, 128, 129]. It is generally estimated that the typical motor symptoms only appear after a specific threshold of nigral dopaminergic neurons (around 50-70%) have died [125, 129-131]. Thus, it is highly likely that a prodromal phase of PD exists [128]. Indeed, numerous non-motor features, including hyposmia (olfactory dysfunction), visual disturbances (e.g. double vision), sleep disorders (e.g. rapid eye

movement sleep behaviour disorder (RBD)), dysautonomia (e.g. constipation, bladder dysfunction, cardiac arrhythmias), and neuropsychiatric features (e.g. depression, anxiety, cognitive deficits) are common symptoms in PD and some even seem to precede the typical motor symptoms of PD [128, 129]. However, some of the non-motor features appear more frequently in later disease stages of PD (after the occurrence of the typical motor phenotypes) and thus dominate the clinical presentation of the advanced disease [128, 129]. These deficits are due to dysfunction of multiple other neuronal cell types throughout the central and peripheral nervous systems and underline the existence of widespread neuronal dysfunction in PD, suggesting the existence of different thresholds for degeneration in different neuronal subtypes, with substantia nigra dopaminergic neurons being especially vulnerable [125].

Available treatments for PD consist mostly of symptomatic therapy of the motor phenotypes, focussing on replacement strategies for dopamine, and do not affect the progression of the disease [116, 128]. For example, levodopa (L-DOPA), which is an orally active dopamine precursor, remains the gold standard of oral medication for PD, despite the risk of developing motor complications [117, 128, 129]. Also, commonly used are dopamine agonists (effective, but with worse adverse effects) or monoamine oxidase type B (MAOB) inhibitors (mild symptomatic benefits) [116, 117, 128].

1.3.3.1 Links between PD and GD (and other LSDs)

Research over the past decade has led to the discovery of common mechanisms between rare, paediatric LSDs and common, adult-onset neurodegenerative diseases, including PD. One of the best-established links is the connection between GD and PD, which started to emerge at the beginning of the 21st Century. First, clinicians began to observe that an unusually high subset of GD patients and their relatives seemed to develop parkinsonism over time and shared features of PD, including tremor, rigidity and bradykinesia as symptoms and Lewy body formation and loss of dopaminergic neurons

as brain pathology [132-135]. Many of these observational studies accumulated over time and finally suggested that mutant GBA may be related to the development of parkinsonian manifestations. Accordingly, in subsequent gene mutation analysis studies, an increased number of carriers of heterozygous *GBA* mutations were found in 'sporadic' PD patients, suggesting that mutations in GBA may be a risk factor for developing late-onset neurodegenerative disease [136-138]. Importantly, in 2009, a major worldwide multi-centre genetic study reported a significant association between GBA mutations and PD, with mutations in GBA being high genetic risk factors for developing PD [127]. Further studies confirmed that around 10-30% of heterozygous and homozygous *GBA* mutation carriers develop PD, which is a 20-fold increased risk compared to non-carriers [139-142]. Furthermore, between 5-15% of 'sporadic' PD patients are estimated to carry a GBA mutation, making GBA mutations numerically the highest known genetic risk factor for PD [127, 141-144].

Subsequently, studies started to focus on common pathogenic mechanisms in PD and GD. First, α-synuclein was implicated as a plausible biological junction between GD and PD. Accumulation and impaired turnover of α-synuclein was reported in various cell and animal models of GBA deficiency and physical interactions between α-synuclein and GBA were demonstrated (**Figure 1.7**) [145-151]. Then, a major study reported a self-propagating positive feedback loop between GBA and a-synuclein [148]. GlcCer, the GSL substrate of GBA, was shown to directly influence amyloid formation of α-synuclein by stabilising soluble oligomeric intermediates in a lysosome-like environment, which in turn lead to further depletion of lysosomal GBA activity, ending in a self-propagating positive feedback loop resulting in neurodegeneration (**Figure 1.7**) [148]. Thus, this study was the first to implicate one of the substrates for GBA, namely glucosylceramide, in the pathology of PD. It had already been proposed that altered lipid metabolism and changes in lipid composition, as happens in GD, could significantly alter α-synuclein binding to lipid membranes [152]. Nowadays, further studies have supported a link

between both GSLs GlcCer and GlcSph with α-synuclein (**Figure 1.7**) [153-155]. To further underline possible dysregulation of GSLs in PD, some reports have also implicated more complex brain gangliosides, in particular a reduction in GM1a, in PD [156-158]. GM1a has been shown to act as a plasma membrane anchor for α-synuclein, which is a ganglioside-binding protein, adopting a more stable, α-helical structure when bound to membranes, but starting to form fibrils in the absence of GM1a ganglioside (**Figure 1.7**) [159-161]. Furthermore, oxidized dopamine has recently been shown to modify GBA thereby reducing its activity, leading to lysosomal dysfunction and α-synuclein aggregation specifically in dopaminergic neurons (**Figure 1.7**) [162].

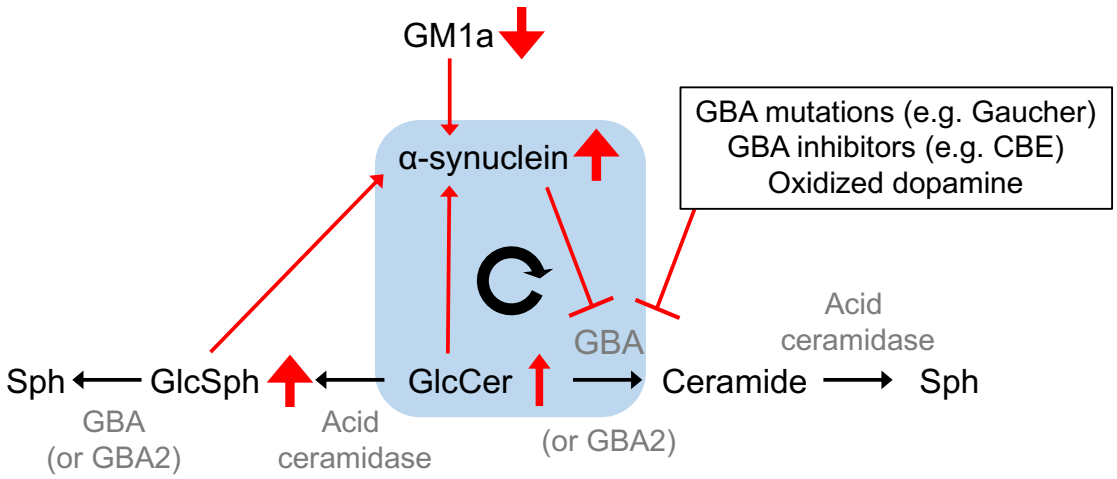

Figure 1.7: The metabolic pathways relevant for the connection between PD and GD. A hallmark of PD is the accumulation and aggregation of α-synuclein protein. α-synuclein has been shown to interact with and inhibit GBA. Consequently, glucosylceramide (GlcCer) is not properly degraded anymore and starts to accumulate. GlcCer itself has been shown to directly interact with α-synuclein and promote the formation of additional α-synuclein aggregates, which has further negative impact on GBA activity, leading to a positive feedback loop (highlighted in blue shade). The feedback-loop can also be started by primary deficiency in GBA, e.g. by GBA mutations (e.g. Gaucher), GBA inhibitors in experiments (e.g. CBE), and also oxidized dopamine in dopaminergic neurons (see black box). When GBA is dysfunctional, glucosylsphingosine (GlcSph) also accumulates and has been shown to interact with α-synuclein and promote its aggregation. Finally, the ganglioside GM1a has been shown to act as plasma membrane anchor for α-synuclein, which stabilises its α-helical structure, and consequently loss of GM1a could also promote α-synuclein aggregation.

Besides the genetic, GBA-heterozygote forms of PD, involvement of GBA in the sporadic forms of PD remains unclear. Interestingly, researchers have found that GBA activity is also reduced in several brain regions in sporadic PD patients, not carrying any GBA mutations [163-165]. Furthermore, it was reported that GBA activity progressively declines with healthy ageing in substantia nigra and putamen of controls, underlining the crucial role of ageing in the development of PD [164]. However, it remains unclear whether the GSL substrates of GBA, GlcCer and GlcSph, accumulate in PD brain tissue. For example, accumulation of GlcSph was reported in several brain regions, e.g. substantia nigra, from sporadic PD patients [164]. However, there were also reports stating that levels of GlcCer and GlcSph do not increase in either GBA-associated PD or sporadic PD in putamen, cerebellum and temporal cortex [166, 167]. Consequently, further studies are needed to determine if these GSLs accumulate in PD brain.

Based on new findings that GBA is involved in PD pathogenesis, GBA began to be viewed as an attractive target for PD therapy. Consequently, the first *in vivo* proof-of-concept studies for increasing GBA activity as a new therapeutic strategy for PD were swiftly provided [168, 169]. Several studies followed and showed beneficial effects of GBA gene therapy as well as pharmacological modulation of GBA activity in several cellular and animal models of PD [85, 170-174]. Importantly, the small-molecule GBA chaperone ambroxol is currently in clinical trials for GBA-associated and sporadic PD (NCT02941822). Furthermore, as GSLs have been implicated in PD pathology, modulation of GSL metabolism has also been recognised as a putatively viable therapeutic approach for PD [175]. Accordingly, treatment with brain-penetrant glucosylceramide synthase (GCS) inhibitors with the aim to reduce the lipid load in neurons (substrate reduction therapy, SRT) has shown beneficial effects in PD models [176, 177]. Interestingly, the compound ibiglustat (GZ402671; Genzyme/Sanofi), which is a GSL biosynthesis inhibtor, is currently in clinical trial for GBA-associated PD (NCT02906020).

Finally, it has begun to emerge that additional LSDs might also be associated with PD. An extensive literature review identified case reports about the appearance of parkinsonism symptoms, α-synuclein deposits and substantia nigra pathology in multiple LSDs, e.g. GM1 gangliosidosis, Tay-Sachs disease and Sandhoff disease [178]. For example, Parkinsonism syndrome was found in heterozygotes for Niemann-Pick disease type C, thus mutations in the *NPC1* gene could also be a risk factor for PD [179]. Most importantly, a major study in 2017 reinforced this notion, reporting an excessive burden of mutant lysosomal storage disorder gene variants in PD [180]. Robak *et al.* found that the majority of cases (56%) in their PD patient cohort had at least one putatively damaging variant in a lysosomal storage disorder gene, and 21% carried multiple damaged alleles [180].

1.4 Relevance and Aims

Historically, rare, paediatric lysosomal storage diseases and common, adult-onset neurodegenerative diseases have been viewed as clinically and mechanistically distinct disease groups [181]. However, research over the past decades has led to the discovery of common mechanisms between rare LSDs and ALS and PD. Lysosomal dysfunction, impaired autophagy, and cytoplasmic protein aggregation are recurrent themes in rare and common neurodegenerative disorders, such as PD, AD, and ALS [104, 105, 181-185]. However, altered lipid homeostasis, especially GSL dysregulation, is a relatively new focus in PD research and even more so in ALS. Furthermore, ageing seems to be the common risk factor for all adult-onset neurodegenerative diseases, including ALS and PD. Thus, the focus of this thesis was to investigate lysosomal dysfunction and glycosphingolipid dysregulation in ALS, in ageing and in PD.

The specific aims of this thesis are:

- To assess if levels of GSLs are altered in an ALS mouse model and ALS patients, to determine the role of GSLs in the pathology of ALS and during denervation, and to pharmacologically modulate levels of GSLs in an ALS mouse model as a therapeutic approach for ALS (**Chapter 2**).
- To analyse if sporadic PD fibroblasts phenocopy characteristics of lysosomal dysfunction and GSL dysregulation associated with heterozygous and homozygous GBA mutations (**Chapter 3**).
- To explore if levels of GSLs and activities of lysosomal hydrolases are altered in the ageing brain of wildtype mice of different strains and if these changes are comparable to the reported PD- and ageing-induced changes in GSL homeostasis and GBA activity in the human brain (**Chapter 4**).
- To investigate whether changes in GSL homeostasis and lysosomal hydrolase activities occur in various PD mouse models (**Chapter 5**).
- To explore if levels of GSLs and lysosomal hydrolase activities are altered in substantia nigra, putamen or spinal cord of control subjects during ageing and sporadic PD patients (**Chapter 6**).
- To investigate if GSLs in cerebrospinal fluid and serum samples from PD patients could serve as possible biomarkers for PD (**Chapter 7**).

2 Glycosphingolipids in ALS

2.1 Introduction

2.1.1 Amyotrophic lateral sclerosis (ALS)

Amyotrophic lateral sclerosis (ALS) is a devastating adult-onset neurological disorder characterized by the selective degeneration of upper motor neurons in the motor cortex and lower motor neurons in the brainstem and the spinal cord. Clinical hallmarks of ALS are progressive muscle weakness and wasting followed by paralysis, speech and swallowing difficulties, altered reflexes and spasticity. About 90% of the ALS cases are sporadic and only 10% of the cases have genetically inherited causes [92, 93].

Mutations in the *SOD1* gene are the most common genetic cause of familial ALS and account for 20% of familial ALS cases [93, 94]. Superoxide dismutase 1 (SOD1) is an abundant, ubiquitously expressed cytosolic enzyme. It converts harmful reactive oxygen species (ROS) to molecular oxygen and hydrogen peroxide, preventing oxidative stress in cells [93]. Interestingly, mutations in SOD1 do not result in a loss of dismutase activity, but rather induce toxic gain-of-function effects through which the protein acquires one or more toxic properties. The exact pathophysiology remains unclear, but mitochondrial defects, ER stress, and alterations in axonal transport have been shown [93].

2.1.2 Lipids and energy metabolism in ALS

A classical view of ALS is that the pathology of the disease is restricted to motor neurons. However, it has become clear that ALS has wider effects throughout the body, especially concerning energy metabolism [186, 187]. ALS patients display several defects in energy metabolism, including progressive body weight loss and high incidence of hypermetabolism and dyslipidaemia [186]. For example, patients with familial as well as sporadic ALS frequently display hypermetabolism, which is defined as increased higher resting energy expenditure compared to energy intake via glucose and lipids [188-190].

Interestingly, hyperlipidaemia, defined as a high LDL/HDL cholesterol ratio or elevated total cholesterol and triglycerides, and a high body mass index are positively correlated with better prognosis and slower disease progression in patients [191-195]. Accordingly, clinical trials suggest lipid-enriched diets are beneficial for ALS patients [196-198].

In summary, muscle hypermetabolism and energy deficits are part of the ALS pathogenesis and suggest a direct link between changes in lipid metabolism and ALS.

2.1.3 SOD1(G86R) mouse model of ALS

The discovery of mutations in the *SOD1* gene causing familial ALS lead to the development of several transgenic mouse models overexpressing mutant isoforms of the protein, based on commonly reported human mutations. Working with SOD1 mouse models, it is important to recognise that characteristic neuropathological findings commonly described in ALS patients, namely cytoplasmic inclusions of proteins in affected motor neurons, especially TDP-43 positive inclusions, are missing in SOD1 mouse models. In addition, it is a common and valid critique that SOD1 mutations only comprise 1-2% of sporadic ALS cases and are thus numerically rare [94].

One well-characterised ALS mouse model is the SOD1(G86R) mouse. This mouse model was first described by Ripps *et al.* in 1995 and displays a rapid, progressive decline of motor function accompanied by degeneration of motor neurons [199]. Alterations in energy metabolism, as previously described for ALS patients, are similarly found in this mouse model. SOD1(G86R) mice are thinner than wildtype mice with reduced fat mass and body weight, display hypermetabolism and present increased fatty acid uptake in muscles, already weeks before disease onset [200, 201]. Feeding SOD1(G86R) mice with a high-fat diet delayed disease onset, increased lifespan and reduced motor neuron degeneration [200].

2.1.4 Glycosphingolipids in ALS

Lipids have further roles in the pathophysiology of ALS beyond energy metabolism. Lipids, especially glycosphingolipids (GSLs), play a critical role in the structure and function of the central and peripheral nervous system [42, 202]. Glucosylceramide (GlcCer) is the precursor of all more-complex GSLs and occupies a key position in the biosynthesis of GSLs. De-novo-synthesis of GlcCer takes place in the cytoplasmic leaflet of the Golgi and is performed by the enzyme glucosylceramide synthase (GCS) [18]. Further additions of oligosaccharides and N-acetylneuraminic acids give rise to a broad range of very complex GSLs, including gangliosides [20]. Gangliosides are the predominant GSLs in the CNS of all mammals and are highly enriched in cell membranes of neurons [23, 40, 41]. GSLs form 'microdomains' or 'rafts' within cell membranes, which serve as platforms for lateral functions, e.g. the attachment of membrane proteins or ion channels during signal transduction, and for extracellular functions, e.g. cell adhesion [40]. Specific gangliosides interact with transmembrane receptors or signal transducers involved in cell adhesion and signalling to regulate cell growth, proliferation, and differentiation. Gangliosides, particularly GM1a, are essential for myelination, neuritogenesis, synaptogenesis, transmission of nervous impulses and stability of synapses [42, 43]. Consequently, gangliosides are vital for neuromuscular junctions between motor neurons and muscles fibres, which are responsible for the control of muscle contraction [203]. The destruction of neuromuscular junctions represents the first detectable event in ALS, followed by axonal degeneration and subsequent degeneration of the motor neuron cell body [204].

In 2002, lipids in the spinal cord of both ALS patients and SOD1 mice were studied and higher amounts of sphingolipids, ceramides and cholesterol were reported [205]. This report was the first hint that sphingolipids, which modulate vital CNS functions, may be involved in ALS pathophysiology. Recently, several metabolomic studies with cerebrospinal fluid (CSF) and serum of ALS patients were performed and identified sets

of metabolites as being involved in ALS, e.g. amino acids (glutamine, lysine, serine) and energy metabolites (acetate, citrate, pyruvate) [206-210]. However, the lipidome of the disease had not been studied in detail so far.

The aims of this experimental chapter are therefore:

- To perform a lipidomics analysis with murine SOD1(G86R) tissues to determine changes in the ALS lipidome.
- To analyse levels of GSLs in murine SOD1(G86R) tissues and CSF of ALS patients and try to determine their role in the pathology of ALS and during denervation.
- To pharmacologically modulate levels of GSLs in the SOD1(G86R) mouse model as a therapeutic approach or ALS.

Most of the data of this experimental chapter have been published in [115] and [211].

2.2 Materials and Methods

2.2.1 Animals

All animal experiments were performed by Dr. Alexandre Henriques in Strasbourg. Experiments were performed after approval by the ethics committee of the University of Strasbourg (license No. AL/01/20/09/12, AL/02/21/09/12 and AL/15/44/12/12). FVB/N male and female mice, overexpressing the murine SOD1(G86R) protein [199], were maintained in the INSERM animal facility at the University of Strasbourg at 23°C with a 12h light/dark cycle. Mice had access to water and regular A04 rodent chow *ad libitum*. The mouse model overexpresses the murine SOD1(G86R) missense protein under the control of the endogenous promoter. The missense mutation is a point mutation in exon 4 resulting in a glycine-86 to arginine substitution, which corresponds to amino acid position 85 in the human SOD1 protein. At 75 days of age (referred to as the pre-symptomatic age), mice are without signs of motor impairment, as determined by the absence of electromyographic abnormalities and with a comparable number of spinal cord motor neurons to wildtype mice. The early-symptomatic phase of the disease starts at 95 days of age. Symptoms include muscle weakness, mild locomotor impairments and muscle fibrillation detectable by electromyography. At around 100 days of age (referred to as the symptomatic age), mice show apparent signs of paresis, or partial paralysis, in at least one limb [212]. Symptoms progress towards skeletal muscle paralysis and atrophy, leading to death at around 105 days of age. Age-matched wildtype male and female FVB/N littermates served as controls.

Mice were sacrificed by intraperitoneal injection of sodium pentobarbital (120 mg/kg) and intracardially perfused with PBS at 4 °C. Lumbar spinal cord and muscles were rapidly dissected, frozen in liquid nitrogen and stored at −80°C. For immunohistochemistry, dissected tissue samples were fixed with 4% paraformaldehyde for 24 hours and then stored in PBS at 4°C.

2.2.1.1 Nerve crush injury

Peripheral nerve crush injury was performed to induce muscle denervation and subsequent axonal regeneration. For this, mice were anaesthetized with ketamine (100 mg/kg) and xylazine (5 mg/kg). The sciatic nerve was exposed at mid-thigh level and crushed with fine forceps for 30s. The skin incision was sutured, and mice were allowed to recover. The hind limb, contralateral to the lesion, served as control.

2.2.1.2 Treatments

To inhibit glucosylceramide synthase activity, mice subjected to sciatic nerve crush were treated with intraperitoneal injections of AMP-DNM (N-adamantane-methyloxypentyl-1-deoxynojirimycin, Cayman Chemicals, MI). AMP-DNM was given at 25 mg/kg in 0.9% NaCl containing 5% DMSO [213]. AMP-DNM was injected daily for 10 days, the typical time frame required for recovery of motor function. To inhibit glucocerebrosidase activities, mice were treated with conduritol B epoxide (CBE, 10 mg/kg/day, Cayman chemical, Ann Arbor, USA) or the vehicle (4% NaCl) as negative control with daily intraperitoneal injections. The treatment started at 75 days of age and ended at 95 days of age.

2.2.2 Behaviourals

2.2.2.1 Toe reflex spreading test

Toe spreading was manually assessed for each hind limb as an indicator of motor recovery after sciatic nerve lesion. Mice were scruffed and spacing between toes was measured. Onset of toe spreading was defined by a distance of at least one millimetre between two consecutive toes on the ipsilateral side of the injury.

2.2.2.2 Muscle grip strength

Muscle strength was determined with the grip test (Bioseb, Chaville, France). Mice were placed over a metallic grid, which they instinctively grab to stop the involuntary backward movement carried out by the manipulator, until the pulling force overcomes their grip strength. After the animal loses its grip, the strength-meter scores the peak pull force. After sciatic nerve crush, strength was measured independently in hind limbs ipsilateral and contralateral to the nerve lesion, and the mean of three assays was scored for each animal. For CBE treatment, the mean of three tests was used and onset of muscle strength loss was defined as a drop of more than 10% of the mouse's maximal strength.

2.2.2.3 Electromyography

Electromyography recordings were obtained with a standard electromyography apparatus (Dantec, Les Ulis, France). Mice were anesthetized and kept under a heating lamp to maintain physiological muscle temperature. A concentric needle electrode (diameter 0.3 mm; Medtronic, Minneapolis, MN) was inserted into the gastrocnemius muscle, and a monopolar needle electrode (diameter 0.3 mm; Medtronic) was inserted into the tail of the animal to ground the system. Each muscle was monitored in three different regions, and the degree of denervation was scored as the number of regions with spontaneous activity expressed as a percentage. Only spontaneous activity with peak-to-peak amplitude of at least 50 µV was considered to be significant.

2.2.2.4 Locomotor profile with Catwalk

The locomotor profiles of the mice were recorded with a catwalk device (Noldus) and were recorded at least three times per mouse. The software CatWalk XT (version 10.5, Noldus) was used to analyse the video recordings and to determine the run speed (average speed during the whole run), stride length (distance between successive

placements of the same paw) and paw swing (duration in seconds of the step corresponding to the absence of contact between a paw and the runway) of each mouse.

2.2.3 Patients

A case-control study was performed to study the levels of GSLs in the cerebrospinal fluid (CSF) samples of 14 ALS patients and 20 control subjects. Individuals were recruited at the ALS centre in Tours, France. CSF was collected during routine lumbar puncture at the time of diagnosis from individuals with ALS, or from individuals showing motor dysfunctions. Controls were patients diagnosed with various non-demyelinating neurological disorders e.g. Parkinson's disease, cerebellar ataxia, dementia, epilepsy, or motor dysfunctions of unclear origin but unrelated to ALS. CSF samples from age- and gender-matched healthy controls were inaccessible at the time of the study. All patients gave informed consent and the protocol was approved by the ethical committee of Tours. An ALSFRS-R score was provided for all ALS patients (score of 0-48, with 0 being the worst). The ALSFRS-R score provides a physician-generated estimate of the patient's degree of functional impairment, which can be evaluated over time to objectively assess any response to treatment or progression of disease [214]. Information about ALSFRS-R score decline over a month, equivalent to severity of disease progression, was available for 11 ALS patients. All human-related experiments were performed in accordance with the relevant guidelines and regulations. Standard biochemical tests were performed, including bacteriology tests, and glucose and protein quantifications (**Table 2.1**).

Table 2.1: Case information of ALS patients and control subjects with non-demyelinating neurological disorders. Data summarised as mean ± SD.

	Control subjects	ALS
Cohort size	20	14
Female (%)	45	36
Male (%)	55	64
Age (years)	68.3 ± 1.4	70.3 ± 0.6
ALSFRS-R	N/A	39.9 ± 0.3
Site of onset (Bulbar/spinal)	N/A	5 / 9
CSF glucose (mmol/L)	3.8 ± 0	4.1 ± 0
CSF protein (g/L)	0.44 ± 0.01	0.51 ± 0.02

2.2.4 Cell culture

Cell culture was performed by Dr. Alexandre Henriques in Strasbourg. PC12 cells (Sigma-Aldrich) were cultured in DMEM, supplemented with 10% horse serum, 5% FCS, 1% Pen/Strep, and 1% Fungizone. At 70% of confluence, differentiation was initiated in DMEM, 1% horse serum, 1% FBS, 1% Pen/Strep, 1% fungizone and nerve growth factor (100 ng/ml). CBE treatment started on the first day of differentiation. Twelve days after differentiation, cells were collected, pelleted by centrifugation and stored at -80 °C until further analysis.

Co-cultures of rat spinal cord explants and human myoblasts were performed as described previously [215, 216]. Briefly, human myoblasts were grown in F14 medium (Invitrogen, Cergy-Pontoise, France), supplemented with 2mM glutamine, insulin, epidermal growth factor, basic fibroblast growth factor, 10% FBS and an antibiotic-antimycotic mixture (Gibco). Spinal cord explants of 14-day-old Wistar rat embryos (Janvier, Le Genest-St-Isle, France) were placed on the muscle cell monolayer. The co-cultures were maintained in MEM (Gibco) supplemented with 25% medium 199 (Gibco), 5% FBS, 1 pg/ml insulin and antibiotic-antimycotic mixture. CBE treatment was initiated when the spinal cord explants were added to the muscle monolayer and was renewed twice a week for 3 weeks, until the end of the experiments. Innervation areas were

identified by the presence of contracting muscle fibres, as observed under microscopy and analysed with ImageJ.

2.2.5 Lipidomics (UPLC/TOF-MS)

2.2.5.1 UPLC/TOF-MS

Tissue samples (25 mg for lumbar spinal cord, and 25–50 mg for soleus muscle) were homogenised in methanol, mixed with chloroform and centrifuged at 2000 rpm for 5 min at 4°C. The organic phase was transferred into a conical glass tube and dried at 30°C under nitrogen. Residues were reconstituted with acetonitrile/isopropanol (1:1) and further diluted with solvent mixture before injection for chromatography. Ultra-performance liquid chromatography (UPLC) was performed with an Acquity UPLC system using an Acquity BEH C18 column (100mm×2.1mm, 1.7µm, Waters Corporation, Milford, MA) maintained at 50°C [217]. Chromatographic flow rate was 0.5 ml/min, and run time was 18 min. Mobile phases consisted of isopropanol (solvent A) and acetonitrile (solvent B). The starting condition was 100% solvent B, followed by a gradual increase of solvent A from 0 to 75% over the first 15 min. Then, 100% solvent B was used from 15.1 to 17 min. The chromatographic system was coupled to a Micromass LCT Premier TOF/W mass spectrometer (Waters Corporation), equipped with an electrospray source operating in positive ion mode with a lockspray interface for accurate mass measurements. Mass spectral data were acquired over the mass range m/z 200–1200.

2.2.5.2 Data mining and analysis

For lipidomics data, chromatogram alignment, blank and chemical noise subtraction and subsequent peak selection were achieved with Refiner MS 6.0 (Genedata, Basel, Switzerland), to obtain a list of molecular features common to each set of mice [217]. Data with retention times between 0.5 and 15 min and peak intensity distinct from zero

were normalized to fresh tissue mass and mean-centred according to wildtype samples. To define differences between SOD1(G86R) and wildtype mice, score plots were generated by unsupervised multivariate principal component analysis (PCA), using SIMCA-P 12.0 (Umetrics, Umea, Sweden). Next, an SOD1(G86R)-to-wildtype ratio was calculated for each molecular feature. The ratio was considered significant if the corresponding variable correlation coefficient was between −0.7 and +0.7. Molecular features with significant changes were associated with theoretically identified metabolites based on their atomic mass (m/z) using the online human metabolome database (HMDB) [218]. Over-represented pathways were identified with ConsensusPathDB [219], and joint enrichment analysis of transcriptomics and lipidomics data was performed using IMPaLA [220]. Lipidomics data was provided by Dr. Alexandre Henriques.

2.2.6 Glycosphingolipids (NP-HPLC)

GlcCer and downstream GSLs were analysed essentially as described by Neville and coworkers [221]. Lumbar spinal cord and soleus muscle were homogenised in water using an Ultraturax T25 probe homogenizer (IKA, Germany). Lipids from tissue homogenates were extracted with chloroform and methanol overnight at 4°C. The GSLs were then further purified using solid-phase C18 columns (Telos, Kinesis, UK). After elution, the GSL fractions were split in half, dried down under a stream of nitrogen at 42°C and treated with either Cerezyme (Genzyme, Cambridge, MA) to obtain glucose from GlcCer or ceramide glycanase (prepared in house from the medicinal leech *Hirudo medicinalis/verbena*) to obtain oligosaccharides from other GSLs. The liberated glucose and free glycans were then fluorescently-labelled with anthranillic acid (2AA). To remove excess free 2AA label, samples were purified using DPA-6S SPE columns (Supelco, PA, USA). Purified 2AA-labelled glucose and 2AA-labelled oligosaccharides were separated and quantified by normal-phase high-performance liquid chromatography (NP-HPLC) as

previously described [221]. The NP-HPLC system consisted of a Waters Alliance 2695 separations module and an in-line Waters 2475 multi λ-fluorescence detector set at excitation λ360 nm and emission λ425 nm. The solid phase used was a 4.6 × 250 mm TSK gel-Amide 80 column maintained at 30°C (Anachem, Luton, UK). Chromatographic flow rate was 0.8 ml/min, and run time was 60 min. Mobile phases consisted of acetonitrile (solvent A), Milli-Q water (solvent B), and 100mM ammonium acetate hydroxide pH 3.85 (solvent C). The starting condition was 71.6% solvent A, 8.4% solvent B and 20% solvent C, followed by a gradual increase of solvent B from 8.4% to 57% over the first 40 min. Then, 71.6% solvent A was used from 41 to 60 min. A schematic summary of the NP-HPLC method can be found in **Figure 2.1**. A standard 2AA-labelled glucose homopolymer ladder (Ludger, UK) was included in each NP-HPLC data set to determine the glucose units (GUs) of each individual HPLC peak, by which the GSL species were identified (**Figure 2.2**). Results were normalised to wet weight of tissue or protein content, determined by bicinchoninic acid (BCA) assay.

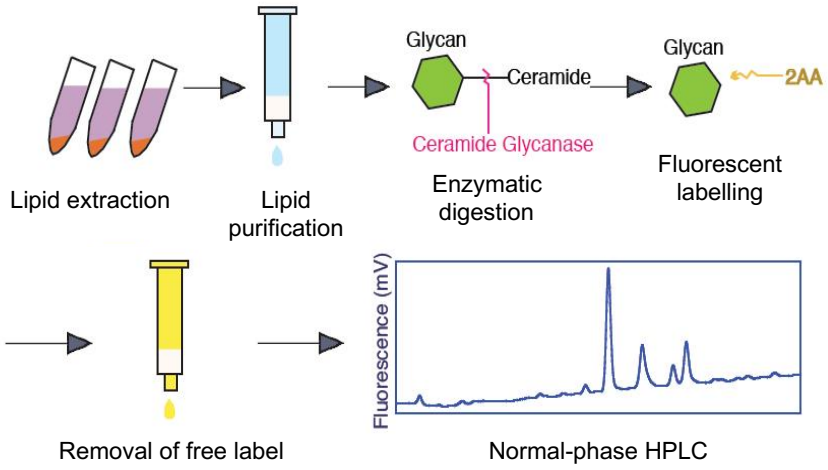

Figure 2.1: Schematic showing the various steps for quantification of glycosphingolipids with NP-HPLC. Biological material was first homogenised and lipids extracted with chloroform/methanol overnight. Free oligosaccharides (or free glucose) were removed by C18 chromatography. Purified lipids were then digested by ceramide glycanase (or Cerezyme). The cleaved off, liberated oligosaccharides (or released glucose molecules) were fluorescently labelled with anthranilic acid (2AA). Free 2AA label was removed with amide column chromatography. Finally, fluorescently labelled sugars were detected and quantified by NP-HPLC. Modified from Dr. Celeste Chuang.

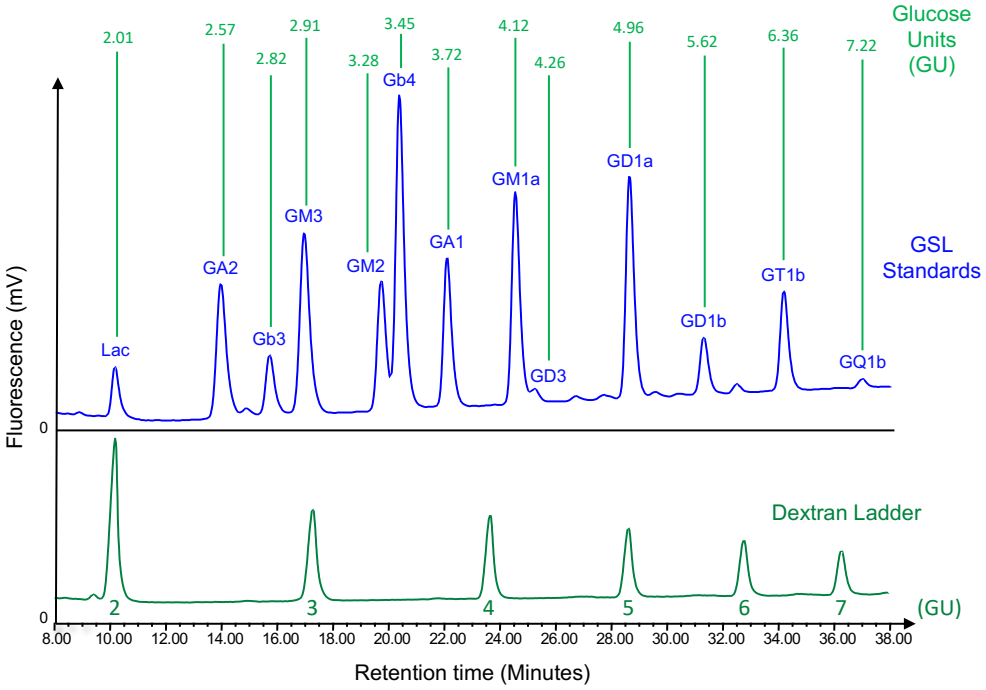

Figure 2.2: Identification of individual GSLs by their glucose unit (GU) values with NP-HPLC. Glucose unit values of GSLs are determined by comparison with a 2AA-labelled glucose oligomer ladder, derived from a partial hydrolysate of dextran. Figure provided by Dr David Priestman.

2.2.7 Histology

Histology experiments were performed by Dr. Alexandre Henriques, Strasbourg. For neuromuscular junction labelling, fixed tibialis anterior muscle samples were dissected into thin bundles under a binocular microscope. Bundles were collected from at least three different parts of the muscle. Acetylcholine receptors in the postsynaptic apparatus of neuromuscular junctions were labelled with rhodamine-conjugated α-bungarotoxin (Sigma–Aldrich). Immunofluorescent labelling of nerve terminals was performed with a rabbit polyclonal anti-synaptophysin antibody (1:200, Abcam, Cambridge, UK), and Alexa-conjugated goat anti-rabbit IgG (1:500, Jackson ImmunoResearch, Suffolk, UK). Muscle bundles were mounted onto slides, prior to fluorescence microscopy. Neuromuscular junctions were considered as denervated when the presynaptic nerve terminal was absent from the postsynaptic region. Images were taken with an ApoTom 2 Zeiss microscope and analysed with ZEN 2 (Zeiss).

For detecting motor neurons in the spinal cord innervating the tibialis anterior muscle, fixed lumbar spinal cord segments L2-L3 were used [222]. 40 µm thick coronal sections from L2-L3 spinal segment were stained with anti-choline acetyltransferase (ChAT) (1:100, Millipore, France) and Alexa594-conjugated goat (1:200, Jackson) antibodies. All neurons located in the ventral horn, that were larger than 400 μm^2 in size and ChAT positive were considered as α-motor neurons. Six sections of spinal cord that were apart over a length of 0.24 mm were counted. Photomicrographs were taken with a Nikon microscope and cell area of motor neurons was measured with NIS Element 4.0 (Nikon).

2.2.8 β-glucosidase activity assay

β-glucosidase activity was assayed using a β-glucosidase activity assay kit (MAK129, Sigma). Cell pellets or tissues were lysed with a TissueLyser (Qiagen, CA) in ice-cold PBS. After centrifugation (14000g, 10min, 4°C), the supernatants were stored at -80°C. Enzymatic reactions were carried out in phosphate buffer (60 mM, pH 5.5) with the substrate β-NPG (nitrophenyl-β-D-glucopyranoside) for 20 minutes at 37°C. Final absorbance was measured at 405 nm.

2.2.9 Statistical analysis

Experiments were performed by experimenters blinded for genotype and treatment, and patient diagnosis. Data were expressed as the mean ± SEM, unless otherwise indicated, and were analysed with PRISM 7.0 (GraphPad, San Diego, CA). Student's t-test was used to compare two groups, and one-way or two-way ANOVA followed by Fisher's LSD test was used to compare more than two groups. Grip strength curves were analysed with two-way ANOVA, and survival curves were analysed with Log-rank test.

2.3 Results

2.3.1 Lipid composition is altered in spinal cord and muscle of pre-symptomatic and symptomatic SOD1(G86R) mice

To study the lipidome of mutant SOD1(G86R) mice, lipids from lumbar spinal cord and soleus muscle of SOD1(G86R) mice at pre-symptomatic and symptomatic ages (75 days and 100 days old, respectively) were extracted and ultra-performance liquid chromatography coupled to time-of-flight mass spectrometry (UPLC/TOF-MS) was performed. The lipidomes of SOD1(G86R) mice at pre-symptomatic and symptomatic ages were then compared to those of age-matched wildtype (WT) mice. Unsupervised principal component analysis (PCA) of detected lipids of spinal cord and muscle samples revealed two clustered groups of individuals, corresponding to wildtype and SOD1(G86R) mice (**Figure 2.3**, n=9 per group). Interestingly, mutant SOD1(G86R) mice were already distinguishable from their wildtype littermates by their lipidome at the pre-symptomatic stage of the disease (**Figure 2.3**).

To further elucidate alterations in the lipidome of SOD1(G86R) mice, hypothesis-based identification of the lipid species with significantly altered levels was performed, according to their atomic masses in the human metabolome database (HMDB) [218]. Through this identification, major changes in three lipid families were found in the SOD1(G86R) lipidome of muscle and spinal cord tissues (**Figures 2.4 and 2.5**). In the spinal cord of pre-symptomatic SOD1(G86R) mice, levels of most phospholipids (67% of identified lipid species) and sphingolipids (55% of identified lipid species) were decreased compared to age-matched wildtype mice (**Figure 2.4A and B**). In spinal cord of symptomatic SOD1(G86R), less lipids were significantly changed anymore, but around a third of the phospholipid species (26%) and sphingolipid species (30%) were still decreased compared to age-matched wildtype mice. Also, levels of most triglyceride species (62%) were decreased in spinal cord of symptomatic SOD1(G86R) mice (**Figure**

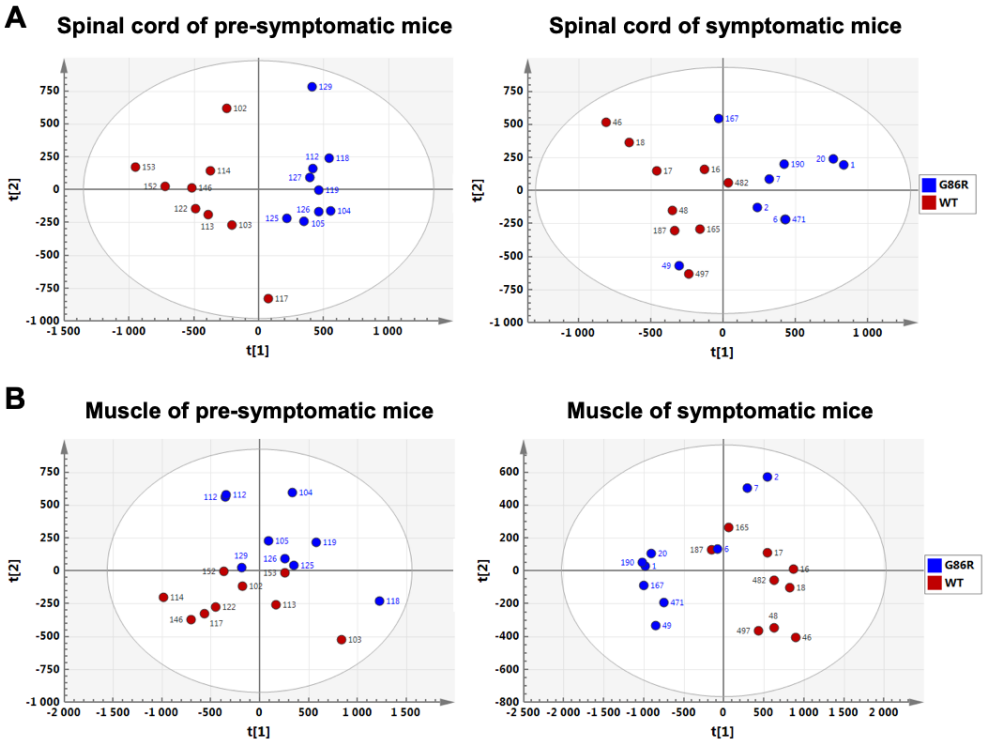

Figure 2.3: Lipidomic signatures of lumbar spinal cord and soleus muscle of pre-symptomatic and symptomatic SOD1(G86R) mice. Principal component analysis (PCA) score plots show the spatial distribution of individual SOD1(G86R) mice (blue circles, n=9) and age-matched wildtype mice (red circles, n=9) based on the lipidomic profiles of spinal cord (A) and muscle (B). Numbers close to symbols are individual identification codes. Data provided by Dr. Alexandre Henriques.

2.4C). In contrast, levels of most of these lipids were increased in soleus muscle at both pre-symptomatic and symptomatic disease stages (**Figure 2.5**). Most phospholipid species were increased in soleus muscle of pre-symptomatic (63%) and symptomatic (55%) SOD1(G86R) mice compared to age-matched wildtype mice (**Figure 2.5A**). Furthermore, 56% of the identified sphingolipid species were upregulated in muscle of pre-symptomatic SOD1(G86R) mice. However, in muscle of symptomatic SOD1(G86R), only 21% of the identified sphingolipid species were upregulated and 32% of the identified sphingolipid species were downregulated (**Figure 2.5B**). Interestingly, levels of most triglyceride species (69%) were decreased in muscle of symptomatic SOD1(G86R) mice (**Figure 2.5C**), similar to the spinal cord, with some species even being entirely depleted. Triglycerides were also depleted in plasma samples of symptomatic SOD1(G86R) mice (personal communication, Dr. Alexandre Henriques,

Strasbourg), which may indicate considerable lipid mobilization during the course of the disease.

In summary, in the spinal cord of pre-symptomatic and symptomatic SOD1(G86R) mice, most lipids which were affected, were decreased. However, most lipids with significant changes in muscle of SOD1(G86R) mice were increased.

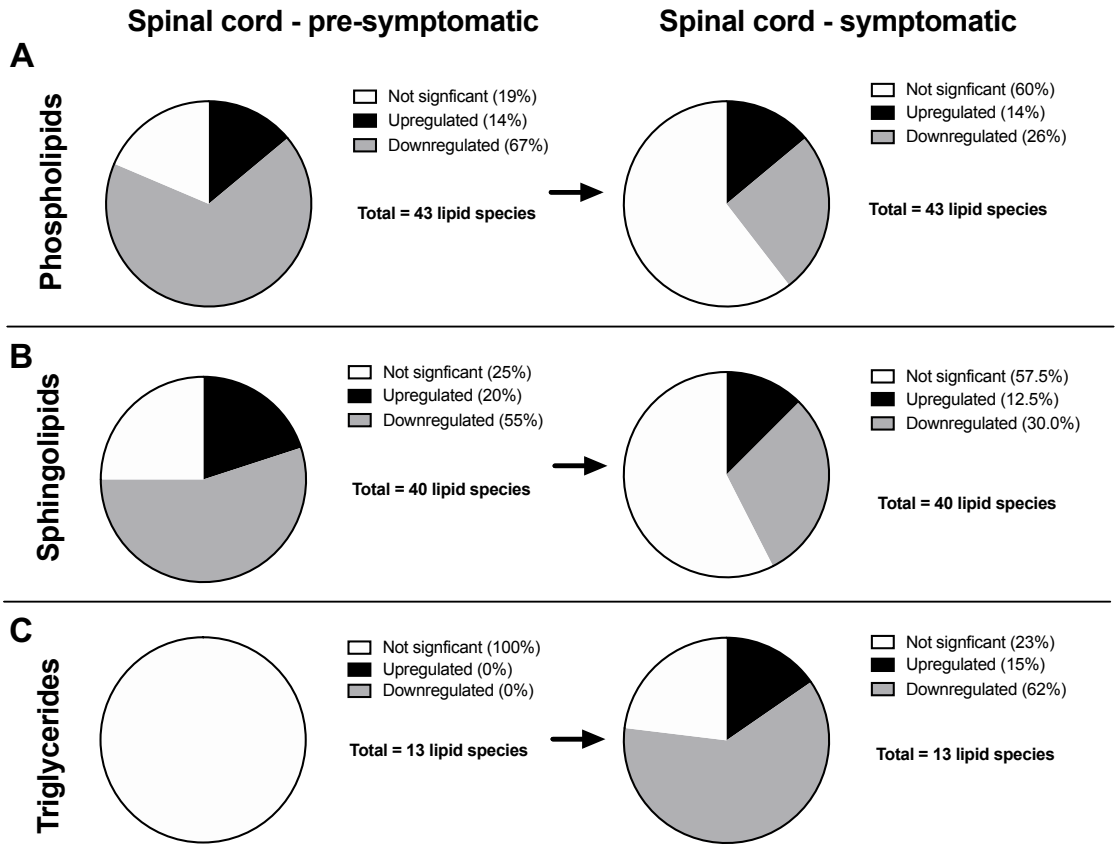

Figure 2.4: Changes in phospholipids, sphingolipids and triglycerides in lumbar spinal cord of SOD1(G86R) mice at pre-symptomatic and symptomatic age. Distribution of differentially expressed phospholipids (A), sphingolipids (B) and triglycerides (C) in spinal cord of pre-symptomatic (n=9) and symptomatic (n=9) SOD1(G86R) mice compared to age-matched wildtype littermates (n=9). Data provided by Dr. Alexandre Henriques.

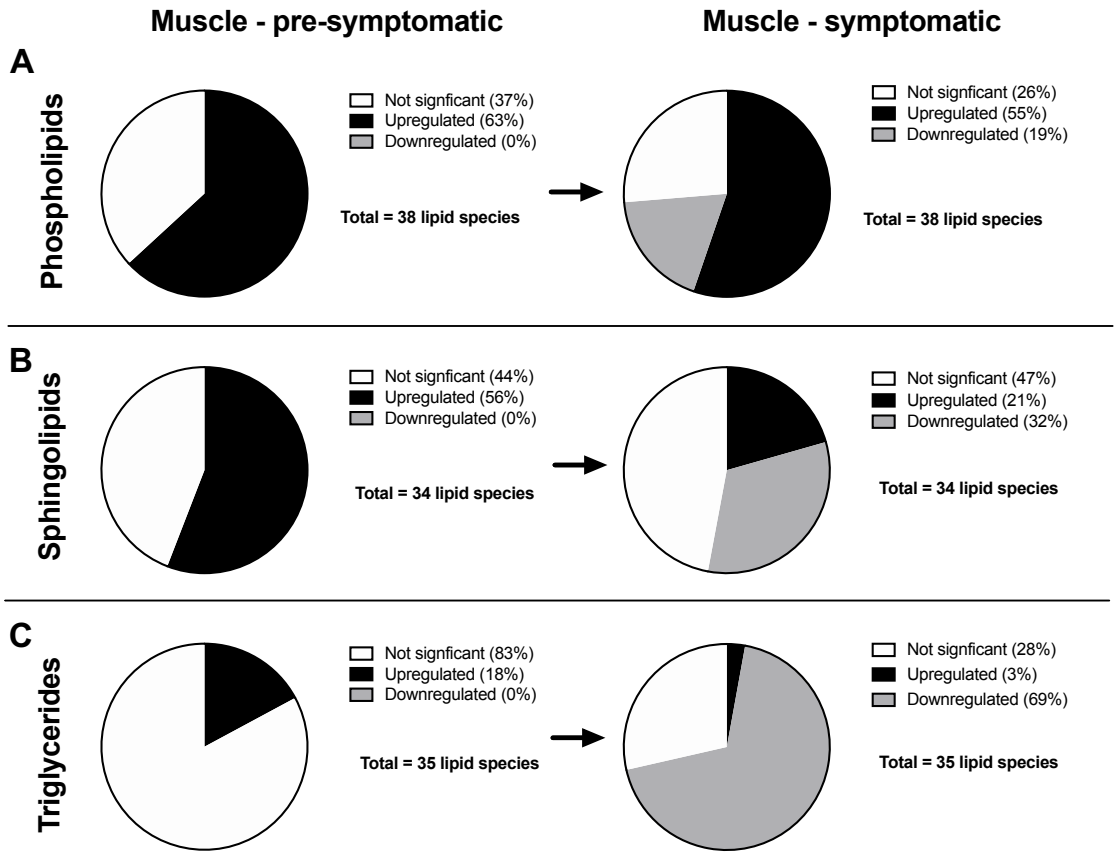

Figure 2.5: Changes in phospholipids, sphingolipids and triglycerides in soleus muscle of SOD1(G86R) mice at pre-symptomatic and symptomatic age. Distribution of differentially expressed phospholipids (A), sphingolipids (B) and triglycerides (C) in muscle of pre-symptomatic (n=9) and symptomatic (n=9) SOD1(G86R) mice compared to age-matched wildtype littermates (n=9). Data provided by Dr. Alexandre Henriques.

Next, the data was analysed with ConsensusPathDB to be able to interpret which metabolic pathways are of potential interest for further analysis [219]. The following pathways, amongst others, were highlighted by the ConsensusPathDB analysis: sphingolipid metabolism, fat digestion and absorption, glycerophospholipid metabolism, retrograde endocannabinoid signalling, steroid biosynthesis and vitamin digestion/absorption (data not shown, [115]). Interestingly, alterations in sphingolipid metabolism were of highest statistical significance of all affected lipids in both spinal cord and muscle of SOD1(G86R) mice. Some of the significantly altered lipids in the sphingolipid metabolism pathway were ceramide, dihydroceramide, sphingosine, sphingomyelin and glucosylceramide (GlcCer) (data not shown, [115]).

2.3.2 Levels of GSLs in spinal cord and muscle of pre-symptomatic and symptomatic SOD1(G86R) mice

Following the discovery of significantly altered sphingolipid metabolism in spinal cord and muscle of SOD1(G86R) mice, our collaborators combined previously published transcriptome data of muscles of SOD1(G86R) mice with the present lipidomics data of muscles of SOD1(G86R) and performed a joint enrichment analysis of both datasets (data not shown, [115]). This analysis revealed that sphingolipid metabolism, especially ceramide and glucosylceramide (GlcCer), was one of the most significantly represented pathways linked to altered expression of glucosylceramide synthase (GCS). Based on these findings, the focus of further experiments was concentrated on GlcCer, which is the precursor for more complex GSLs with important functions in neurons and muscles [40, 223, 224].

Consequently, levels of GlcCer and more complex GSLs in soleus muscle and lumbar spinal cord of pre-symptomatic (75 days-old) and symptomatic (105 days-old) SOD1(G86R) mice and age-matched wildtype mice were analysed using normal phase high-performance liquid chromatography (NP-HPLC) (**Figure 2.6**, n=6 per group). GlcCer levels were significantly increased in soleus muscle of symptomatic SOD1(G86R) mice compared to age-matched controls (**Figure 2.6A**, p=0.0345) Furthermore, levels of lactosylceramide (LacCer) and several gangliosides of the a-series, including GM3 and GM2, were significantly increased in soleus muscle at symptomatic age in SOD1(G86R) mice (**Figure 2.6B**, LacCer: p=0.036, GM3: p=0.0142, GM2: p=0.0381). In lumbar spinal cord, GlcCer levels in both SOD1(G86R) mice and WT mice showed a comparable decline with age, but were not different to each other (**Figure 2.6C**). However, levels of LacCer as well as GM1a, a major ganglioside in the CNS, were significantly increased in spinal cord of symptomatic SOD1(G86R) mice (**Figure 2.6D**, LacCer: p<0.01, GM1: p=0.0337). To investigate the mechanism for increased levels of GlcCer, our collaborators measured GCS mRNA and protein levels

in muscle of SOD1(G86R) mice. GCS mRNA and protein levels were significantly increased in muscle at both pre-symptomatic and symptomatic disease stages compared to age-matched wildtypes (data not shown, [115]), but there were no differences in spinal cord. GCS expression in soleus muscle at an earlier pre-symptomatic age (60 days) was similar in SOD1(G86R) and wildtype mice (data not shown, [115]). Thus, the upregulation of GCS may be considered as an early event preceding the onset of overt motor symptoms. Interestingly, increased GCS mRNA and protein levels were also evident in human vastus lateralis muscle of ALS patients compared to control subjects (data not shown, [115]).

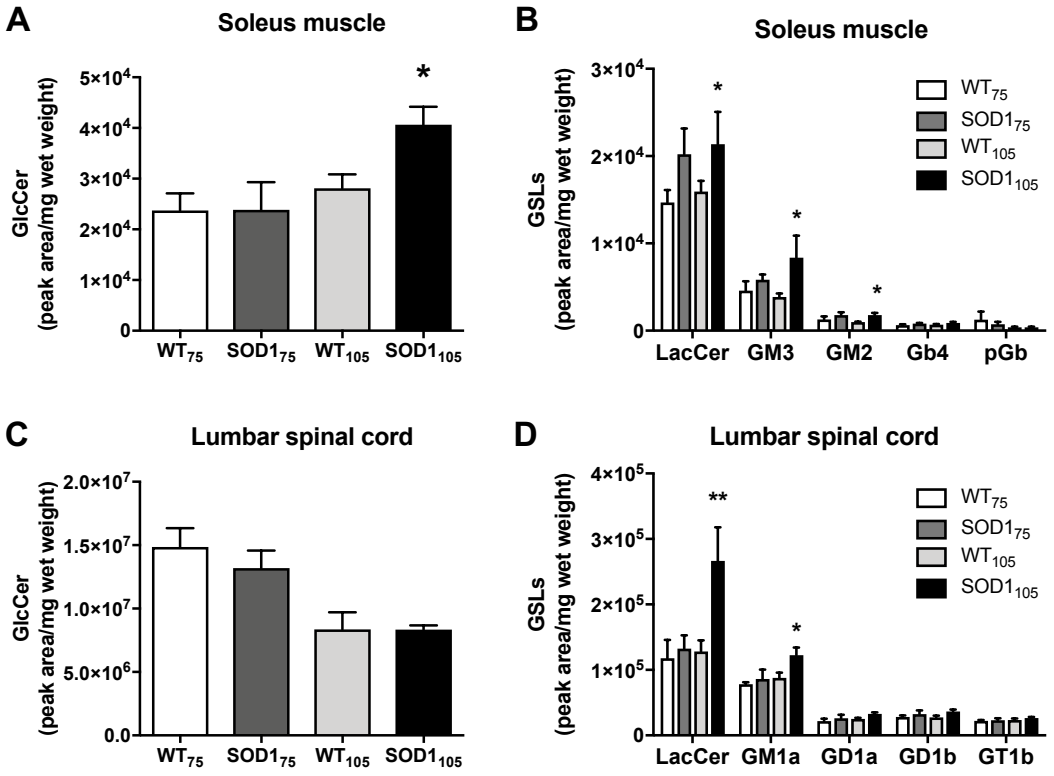

Figure 2.6: Glycosphingolipids in soleus muscle and lumbar spinal cord of SOD1(G86R) mice at pre-symptomatic and symptomatic age. Muscle and spinal cord homogenates were used to quantify levels of GlcCer (A, C) and more complex GSLs (B, D) using NP-HPLC. Data were analyzed using one-way ANOVA (A, C) or two-way ANOVA (B, D) (n=6 per group; * = $p<0.05$, ** = $p<0.01$ versus age-matched wildtype). Data shown as mean ± SEM.

2.3.3 GSL levels in muscle after nerve crush injury in wildtype mice

To further understand the upregulation of GCS and sphingolipids in muscle during the course of ALS, the response of GCS and sphingolipid levels in wildtype mice subjected to peripheral nerve injury was investigated. Crushing the sciatic nerve for several seconds is used as a model of hind limb denervation (ipsilateral hind limb) and was here used to mimic ALS-like muscle denervation. The crush injury is followed by subsequent recovery with reinnervation in about 10 days and signs of motor function recovery after 15 days. The other hind limb, which is contralateral to the lesion, served as control.

Levels of glucosylceramide and more complex GSLs in ipsilateral and contralateral soleus muscles of wildtype mice subjected to crush injury were analysed with NP-HPLC. NP-HPLC analysis showed a significant increase in GlcCer levels in ipsilateral muscle 10 days following crush injury compared to contralateral muscle (**Figure 2.7A**, n=7 per group, p=0.0229). Furthermore, levels of several gangliosides of the a-series, including GM3 and GM2, were significantly increased in ipsilateral muscle in wildtype mice subjected to sciatic nerve crush (**Figure 2.7B**, GM3: p<0.0001, GM2: p=0.0028). Furthermore, GCS mRNA and GCS protein levels were increased in denervated muscle 3 days following crush injury (data not shown, [115]).

These results mirror the observations made in soleus muscle of symptomatic SOD1(G86R) mice and provide evidence of a stimulatory effect of denervation on levels of GlcCer and more complex GSLs in muscle.

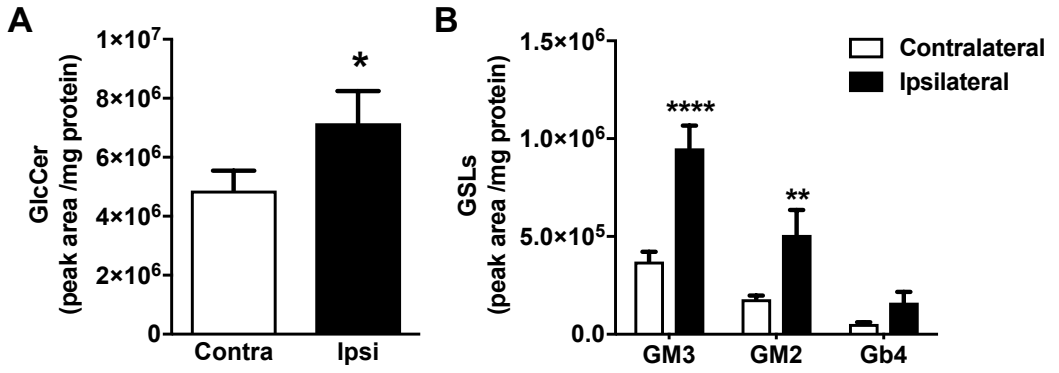

Figure 2.7: Glycosphingolipids in denervated soleus muscle of wildtype mice subjected to sciatic nerve crush injury. Muscle homogenates were used to quantify levels of GlcCer (A) and more complex GSLs (B) using NP-HPLC. Ipsilateral muscles were compared to contralateral muscles in the same animal. Data were analyzed using paired t-test (A) and two-way ANOVA (B) (n=7 per group; * = p<0.05, ** = p<0.01, **** = p<0.0001 versus corresponding contralateral muscle). Data shown as mean ± SEM.

2.3.4 Effect of GCS inhibition after nerve crush injury in wildtype mice

Until now, the purpose of GCS upregulation in muscles subjected to denervation and muscles of symptomatic SOD1(G86R) mice remained unknown. One hypothesis was that increased GlcCer levels might be a compensatory, but unfortunately detrimental, mechanism. To investigate this further, we were interested in the effects of inhibition of GCS enzyme activity during muscle denervation, leading to a decrease in GlcCer levels. For this, a specific GCS inhibitor, called AMP-DNM, was used [213].

First, the effectiveness of the treatment in soleus muscles of wildtype mice, treated with daily intraperitoneal injections of AMP-DNM for 10 days (25mg/kg/day), was assessed by measuring GlcCer levels with NP-HPLC. As expected, treatment with AMP-DNM significantly decreased GlcCer levels in soleus muscle by 33% (**Figure 2.8A**, n=6 per group, p=0.0119).

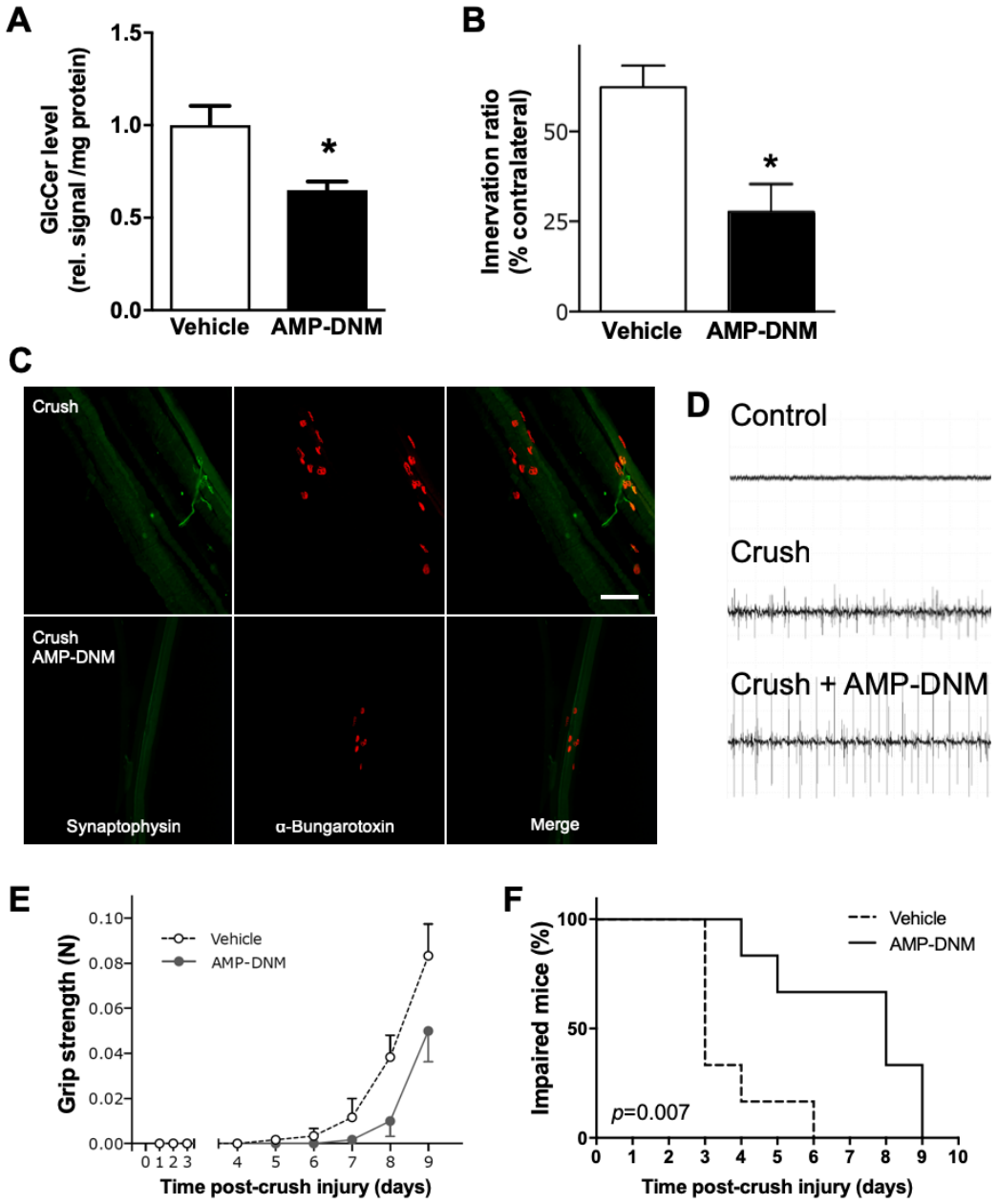

Figure 2.8: Effect of GCS inhibition with AMP-DNM on denervated muscle after nerve crush injury in wildtype mice. (A) Levels of GlcCer were quantified in soleus muscle of AMP-DNM-treated and vehicle-treated wildtype mice using NP-HPLC (n=6 per group, * = p<0.05, unpaired t-test). (B) The quantity of innervated neuromuscular junctions was determined by co-labelling with anti-synaptophysin antibody (green) and rhodamine-conjugated α-bungarotoxin (red) after 10 days of sciatic nerve crush injury (n=5-6, * = p<0.05, unpaired t-test). (C) Examples of labelled neuromuscular junctions. Scale bar, 500 µm. (D) Representative electromyographic recordings of non-denervated, control muscle and muscle of wildtype mice submitted to sciatic nerve crush treated with vehicle (Crush, middle panel) or treated with GCS inhibitor AMP-DNM (Crush + AMP-DNM, lower panel). (E) Restoration of hind limb muscle grip strength in vehicle- or AMP-DNM-treated wildtype mice over time following sciatic nerve crush injury (n=5-6). (F) Percentage of wildtype mice with vehicle or AMP-DNM treatment unable to exhibit toe spreading over time following sciatic nerve crush injury (n=6, log-rank test, ** = p<0.001).

Next, wildtype mice, which were subjected to sciatic nerve crush, were immediately treated with daily intraperitoneal injections of AMP-DNM for 10 days, the typical time frame required for recovery of motor function. The treatment did not influence the extent of muscle fibre atrophy 10 days following crush injury, but blocked the expression of several genes critical for promoting oxidative metabolism following degeneration, e.g. master activators of mitochondriogenesis and lipid catabolism (data not shown, [115]). The effect of GCS inhibition on neuromuscular junction after sciatic nerve crush was investigated next. The proportion of properly innervated neuromuscular junctions after 10 days of sciatic nerve crush was determined by co-labelling with anti-synaptophysin antibody and α-bungarotoxin and analysis of 100-150 neuromuscular junctions per animal. Treatment with AMP-DNM significantly reduced the number of innervated synapses in the ipsilateral muscle compared to the contralateral muscle, which can be interpreted as a delay in the process of axonal regeneration after nerve crush injury (**Figure 2.8B, C**, n=5-6 per group, $p<0.05$). Consequently, abnormal electromyographic episodes reflecting denervation were more frequent and severe in AMP-DNM-treated wildtype mice submitted to sciatic nerve injury compared to non-denervated control as well as untreated crush control (**Figure 2.8D**). To further assess motor function recovery during reinnervation, hind limb grip strength was measured. Restoration of hind limb grip strength was delayed in AMP-DNM treated wildtype mice compared to untreated wildtype mice (**Figure 2.8E**, $p<0.05$). In addition, the time of onset of toe spreading, considered as a sign of successful reinnervation, was delayed in AMP-DNM-treated wildtype mice (median: 8 days) compared to untreated wildtype mice (median: 3 days) (**Figure 2.8F**, n=6 per group, $p=0.007$).

Finally, the effect of GCS inhibition in SOD1(G86R) mice was examined, with the hypothesis now being that loss of GCS activity might predispose SOD1(G86R) mice to develop signs of the disease earlier. SOD1(G86R) mice were treated with daily intraperitoneal injections of AMP-DNM for 10 days, starting at pre-symptomatic age.

AMP-DNM-treated SOD1(G86R) mice showed reduced hind limb grip strength and disturbed neuromuscular junction integrity compared to untreated SOD1(G86R) mice (data not shown, [115]).

In summary, treatment with AMP-DNM reduced glucosylceramide levels and delayed the regeneration of motor function in denervated muscles, which suggests a critical role for GCS and glucosylceramide in the muscular response to denervation.

2.3.5 Effect of GCase inhibition in the SOD1(G86R) mouse model

It has already been shown that inhibition of GlcCer synthesis caused delayed motor recovery after peripheral nerve injury in wildtype mice, altered neuromuscular junction integrity in SOD1(G86R) mice and accelerated the disease course in SOD1(G93A) mice [114, 115]. Thus, our next hypothesis was that inhibition of GlcCer degradation, through inhibition of β-glucocerebrosidase (GCase) activities, leading to an increase in GlcCer levels, might be beneficial for motor function regeneration after nerve injury and in SOD1(G86R) mice. To inhibit GCase function, a well-characterised and covalent inhibitor, called conduritol B epoxide (CBE), was used [225]. It is of note that high doses of CBE (e.g. 100mg/kg/day) are used to fully inhibit lysosomal GCase (GBA) activity in neonatal mice to induce a chemical model of Gaucher's disease with neuronal toxicity [226, 227]. However, low doses of CBE (10mg/kg/day) trigger only partial inhibition of GCase activity, allowing vital residual activity and rapid wash-out without toxicity in adult mice [225, 227]. CBE is known to bind to and inhibit both the lysosomal and non-lysosomal forms of GCase (GBA and GBA2) [228].

First, we tested for toxicity of low-dose CBE treatment in FVB/N wildtype mice. CBE treatment (10mg/kg/day) for 10 days did not alter body mass and muscle strength of wildtype mice (data not shown, [211]). The treatment successfully inhibited GCase activity, slightly increased GlcCer levels and significantly increased total ganglioside levels, mainly levels of ganglioside GM1a, in spinal cord of CBE-treated wildtype mice

(**Figure 2.9A-C**, GCase inhibition: $p<0.05$, total GSLs: $p=0.0054$, GM1a: $p=0.0159$, n=5 per group).

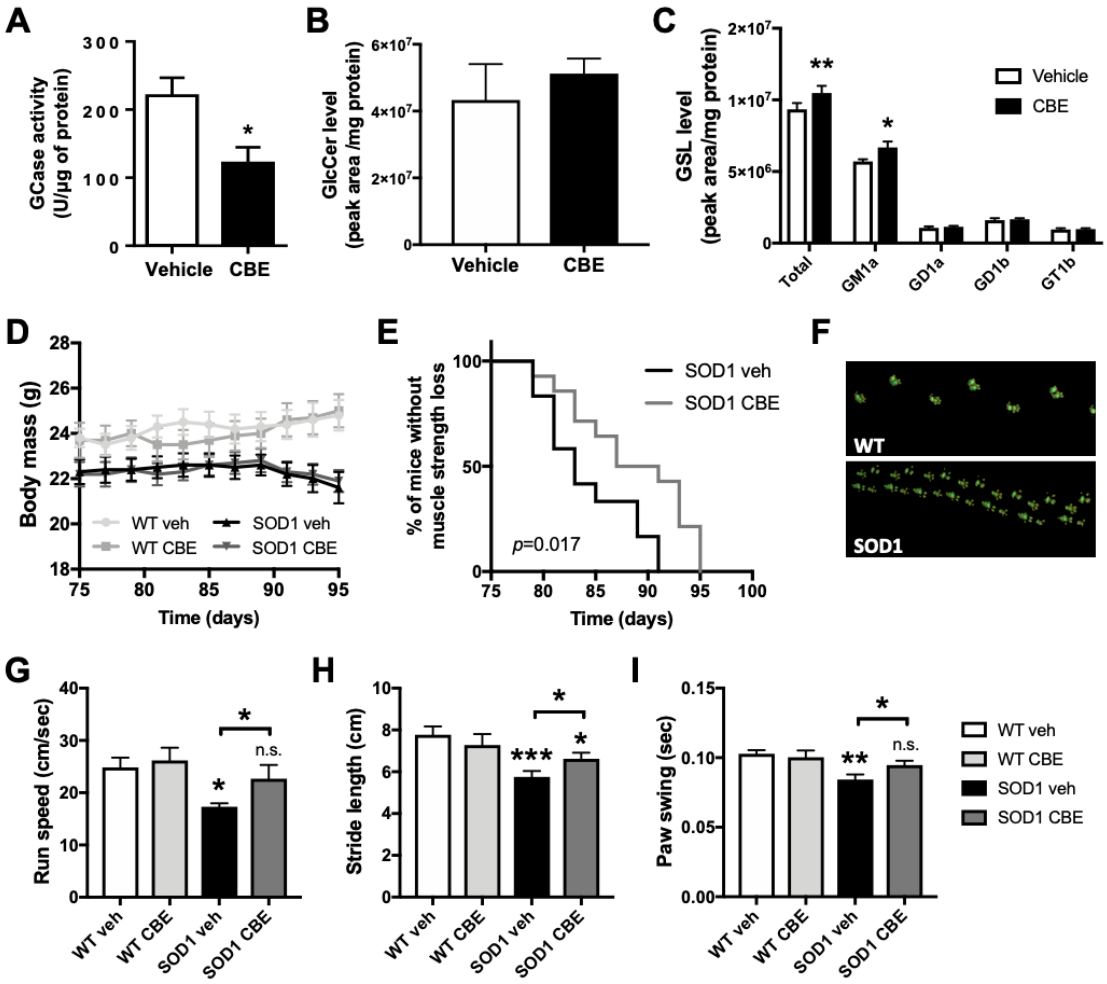

Figure 2.9: Effect of GCase inhibition with CBE on motor function in wildtype and early-symptomatic SOD1(G86R) mice. (A) GCase activity was measured in spinal cord lysates of vehicle-treated and CBE-treated wildtype mice (n=5 per group, unpaired t-test, * = $p<0.05$). Levels of GlcCer (B) and more complex GSLs (C) were quantified in spinal cord of CBE-treated and vehicle-treated wildtype mice using NP-HPLC (n=5 per group, * = $p<0.05$, ** = $p<0.01$, 2-way ANOVA). (D) Body weights of wildtype and SOD1(G86R) mice during CBE treatment (n=7 for wildtype groups, n=12-14 for SOD1 groups). (E) Onset of muscle strength loss over time in vehicle-treated and CBE-treated SOD1(G86R) mice (n=12-14 per group, log-rank test, * = $p<0.05$). (F) Representative walking patterns of wildtype and symptomatic SOD1(G86R) mice from catwalk analysis. (G-I) Gait analysis with catwalk apparatus showing run speed (G), stride length (H), and paw swing (I) in 95-days old wildtype and SOD1(G86R) mice. Data were analyzed using one-way ANOVA (n=4-5 for WT groups, n=10 for SOD1 groups, * = $p<0.05$, ** = $p<0.01$, *** = $p<0.001$). Data shown as mean ± SEM.

Pre-symptomatic SOD1(G86R) mice and age-matched wildtype mice were then treated with 10mg/kg/day CBE for 20 days. The treatment started at 75 days of age and was terminated at the early disease stage, at 95 days of age, when SOD1(G86R) mice usually start to present muscle weakness and denervation. No change in body weight was observed over the course of the treatment in SOD1(G86R) mice and wildtype mice (**Figure 2.9D**, n=7 for WT groups, n=12-14 for SOD1 groups). Interestingly, the onset of muscle strength loss was significantly delayed by 6 days in CBE-treated SOD1(G68R) mice compared to vehicle-treated SOD1(G68R) mice (**Figure 2.9E**, p=0.017). During the course of the treatment locomotor profiles of the mice were recorded using gait analysis. Typical footprint patterns of wildtype and symptomatic SOD1(G86R) mice, recorded with a catwalk device, can be seen in **Figure 2.9F**. As expected, the locomotor profile of 95-day-old early-symptomatic SOD1(G68R) mice presented significantly reduced average speed, reduced stride length and reduced paw swing when compared to age-matched wildtype mice (**Figure 2.9G-I**, n=4-5 for WT groups, n=10 for SOD1 groups, G: p=0.0226, H: p=0.0005, and I: p=0.0025). Interestingly, early-symptomatic SOD1(G68R) mice treated with low-dose CBE showed less locomotor impairments and displayed significantly improved average speed, stride length and paw swing compared to untreated SOD1(G68R) mice (**Figure 2.9G-I**, G: p=0.0440, H: p=0.0443, and I: p=0.0297). Furthermore, EMG recordings showed that muscle fibrillation, a sign of muscle denervation, was reduced from 80% of events in vehicle-treated SOD1(G86R) mice to 40% of events in the gastrocnemius muscle of CBE-treated SOD1(G86R) mice (**Figure 2.10A**, n=12-13 per group). Accordingly, in vehicle-treated early-symptomatic SOD1(G86R) mice, neurodegeneration was detected in the lumbar spinal cord with a 60% loss of large motor neurons compared to age-matched wildtype mice (**Figure 2.10B**, n=4 per WT group, n=10 per SOD1 group, p=0.0002). However, loss of α-motor neurons in the spinal cord of SOD1(G86R) mice was significantly reduced with low-dose CBE treatment, but still significantly different to wildtype mice (**Figure 2.10B**, p=0.0138).

Representative images of motor neurons in the ventral horn of the spinal cord, stained with choline acetyltransferase (ChAT), are shown in **Figure 2.10C**. These results suggest that CBE treatment, started before disease-onset, may delay muscle denervation in SOD1(G86R) mice. Furthermore, CBE-treatment improved neuromuscular junction integrity in tibialis anterior muscle and prevented the loss of cholera toxin B-positive structures at neuromuscular junctions of early-symptomatic SOD1(G86R) mice (data not shown, [211]). This potentially hints at a role for lipid rafts containing GM1a and other gangliosides in this process.

In summary, inhibition of GCase activity with low-dose CBE treatment delays disease onset and improves motor function in early-symptomatic SOD1(G86R) mice.

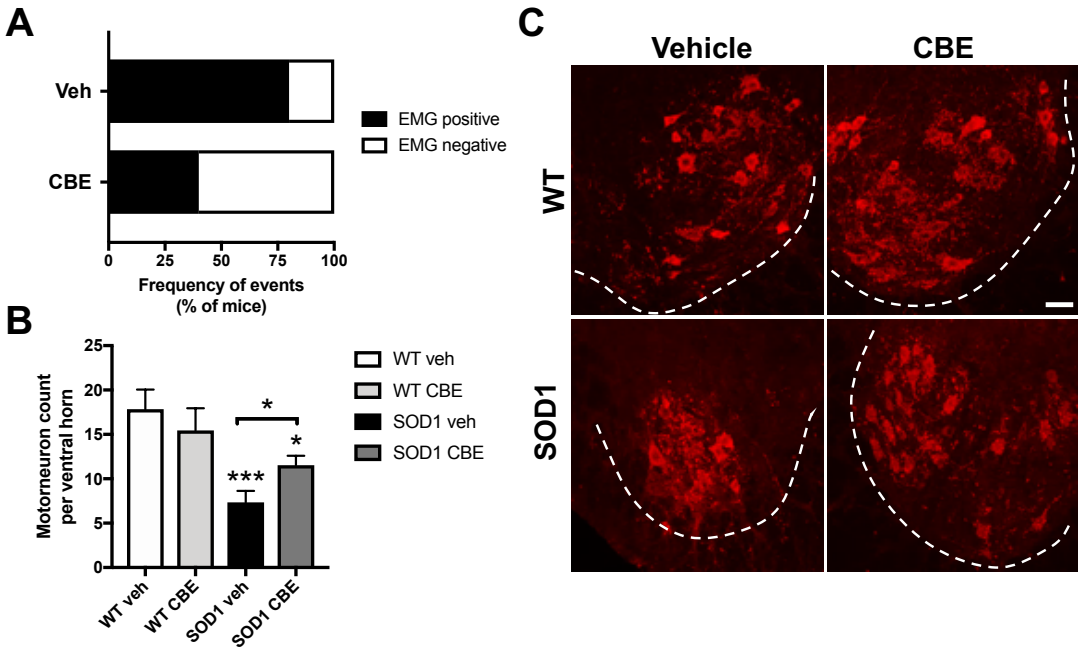

Figure 2.10: Effect of GCase inhibition with CBE on motor neurons in spinal cord of wildtype and early-symptomatic SOD1(G86R) mice. (A) Frequency of muscle fibrillation in gastrocnemius muscle of 95-days old vehicle-treated or CBE-treated SOD1(G86R) mice logged by electromyography (n=12-13 per group). (B) Counts of motor neurons located in the ventral horn of the spinal cord with a size larger than 400µm^2. Data were analyzed using one-way ANOVA (n=4 per wildtype group, n=10 per SOD1 group, * = p<0.05, *** = p<0.001). Data shown as mean ± SEM. (C) Representative images of motor neurons in the ventral horn of the spinal cord, stained with choline acetyltransferase (ChAT, red). Scale bar = 50µm. Data provided by Dr. Alexandre Henriques.

2.3.6 Effect of GCase inhibition on *in vitro* axonal plasticity

As described previously, inhibition of GlcCer synthesis delayed axonal regeneration after peripheral nerve injury [115]. This suggests that GlcCer might be involved in the regenerative process of motor axons and the maturation of neuromuscular junctions. Thus, our hypothesis was that increasing levels of GlcCer by inhibiting GCase activities with CBE might have a direct beneficial effect on neuromuscular junctions. To test this hypothesis, we used an *in vitro* model of motor units [215, 216]. This model consists of a co-culture of rat embryo spinal cord explants and human myoblast cells. First, human myoblast cells were cultured to form a muscle monolayer. Then, rat spinal cord explants were added and incubated for 3 weeks, to allow innervation. Finally, innervated areas were identified by the presence of contraction of muscle fibres. Treatment with CBE was started upon addition of spinal cord explants to the muscle monolayer.

First, the effect of different concentrations of CBE (1µM, 10µM and 100µM) in PC12 cells was tested. As expected, GCase activity significantly decreased with increasing concentrations of CBE (**Figure 2.11A**, n=3 per group, $p<0.01$ and $p<0.001$). For further experiments, a concentration of 10µM and 100µM CBE was used. As expected, glucosylceramide levels increased in a dose-dependent manner with CBE treatment in the *in vitro* models of motor units (**Figure 2.11B**, n=4 per group, 10µM: $p=0.007$, 100µM: $p<0.0001$). Furthermore, levels of the more complex neuron-derived GSLs, including LacCer, GM1a and GD1a, were significantly increased upon CBE treatment (**Figure 2.11C**, n=4 per group, LacCer: $p=0.004$, GM1a and GD1a: $p<0.0001$). Interestingly, only a modest effect of CBE was observed on the predominantly in muscle expressed ganglioside GM3 (**Figure 2.11C**, n=4 per group, $p=0.0462$). Furthermore, a higher incidence of functional spinal cord explants (**Figure 2.11D**, n=6 per group, $p<0.05$) and also a greater innervation area per functional spinal cord explant (**Figure 2.11E**, n=8 per group, $p<0.05$) was observed after maturation in the presence of 10µM CBE. However, the higher dose of CBE (100µM) had only a modest, non-significant effect on these

parameters compared to the vehicle-treated control group. The high dose of CBE led to an almost complete inhibition of GCase activity, which might lead to adverse effects in the treated *in vitro* cultures.

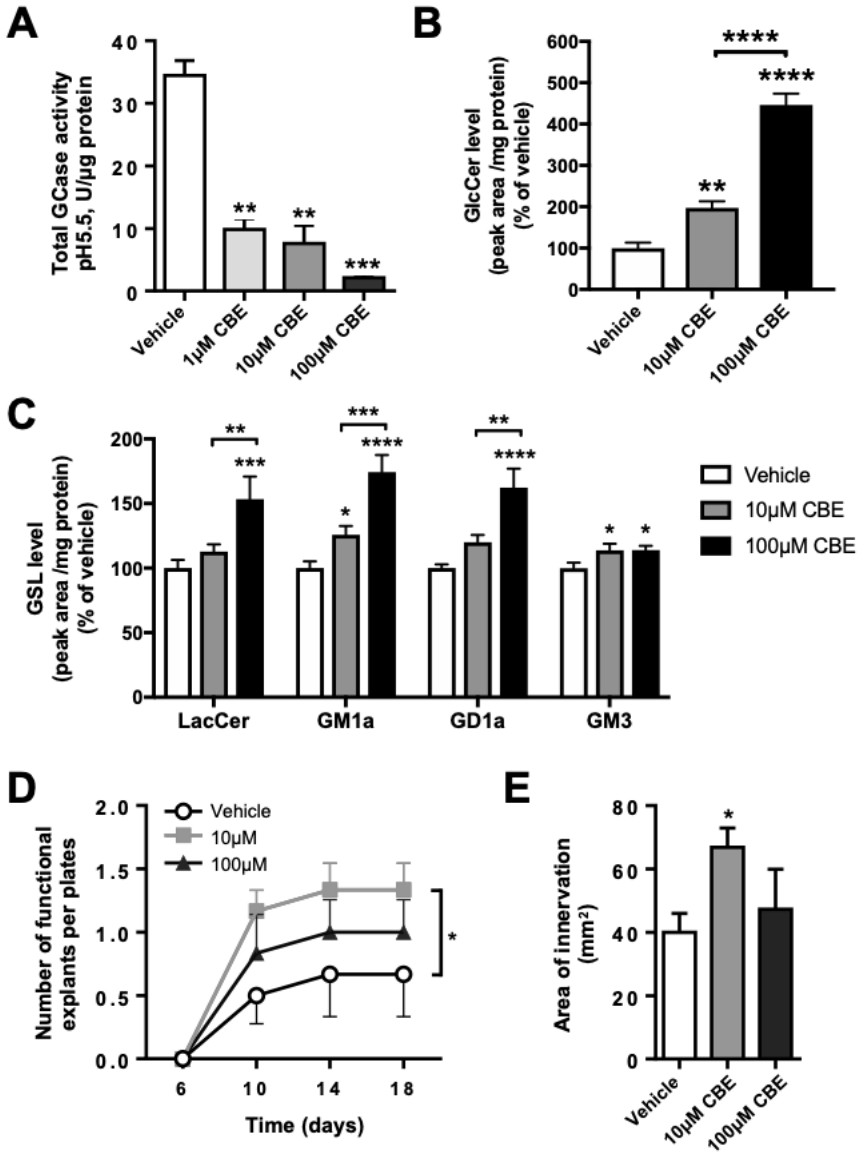

Figure 2.11: Effect of GCase inhibition with CBE on *in vitro* axonal plasticity. (A) GCase activity at pH 5.5 in PC12 cells after treatment with various concentrations of CBE (n=3 per group, ** = $p<0.01$, *** = $p<0.001$, one-way ANOVA). Levels of GlcCer (B) and more complex GSLs (C) were quantified in co-cultures of muscle cells and spinal cord explants after treatment with 10µM and 100µM CBE using NP-HPLC. Data were analyzed using one-way or two-way ANOVA, respectively (n=4 per group, * = $p<0.05$, ** = $p<0.01$, *** = $p<0.001$, **** = $p<0.0001$). (D) Count of functional spinal cord explants per culture plate as identified by the presence of contracting muscle fibers (n=6 per group, * = $p<0.05$). (E) Area of innervation of functional spinal cord explants as determined by microscopy (n=8 per group, * = $p<0.05$, one-way ANOVA). Data shown as mean ± SEM.

In summary, the *in vitro* results suggest a role for GSLs in mediating axonal plasticity and regeneration, which might explain the positive effect of CBE treatment on muscle innervation in the SOD1(G86R) mouse model.

2.3.7 Levels of GSLs in CSF of ALS patients

We have shown that denervation and ALS pathology alter spinal cord and muscle GSL levels, which are important for motor unit integrity and which can be modulated to preserve motor unit integrity and improve motor functions in an ALS mouse model. To strengthen the clinical relevance of GSL dysregulation in ALS, we investigated whether alterations in GSL levels, especially GlcCer and gangliosides like GM1a, can be detected in cerebrospinal fluid (CSF) of ALS patients.

CSF plays a major role in the clearance of neuronal and axonal debris and waste [229-231]. Accordingly, individuals suffering from demyelinating diseases or from severe neuronal loss have increased levels of sphingolipids (e.g. sphingomyelin and GSLs) in their CSF [232-234]. In an attempt to detect neuronal or axonal loss of gangliosides, the levels of GSLs in the CSF of ALS patients at diagnosis (n=14) and of age- and gender-matched individuals diagnosed with non-demyelinating neurological disorders (n=20), serving as control subjects, were analysed. GlcCer and the 4 major gangliosides in the CNS, GM1a and GD1a from the a-series and GD1b and GT1b from the b-series, were quantified using NP-HPLC. Levels of GlcCer were significantly increased in the CSF of ALS patients compared to control subjects (**Figure 2.12A**, p=0.0062). Furthermore, GM1a levels were significantly increased in the CSF of ALS patients compared to control subjects (**Figure 2.12B**, p=0.0310) and a trend for increased GD1b was evident as well (**Figure 2.12B**, p=0.0673). Levels of GSLs did not correlate with age at disease onset or BMI (data not shown). The severity of ALS disease progression can be clinically determined by the loss of ALSFRS-R score per month and was available for 11 of the 14 ALS patients. Interestingly, disease severity was positively correlated with levels of

the main gangliosides GM1a, GD1a, GD1b and GT1b in the CSF, which was significant for GM1a (p=0.0213) and showed a trend for GT1b (p=0.0630) (**Figure 2.12C-F**).

In summary, this data might indicate neuronal loss of GlcCer and GM1a, which could be detrimental for the prognosis of ALS, and shows that GSL homeostasis is dysregulated early on in ALS.

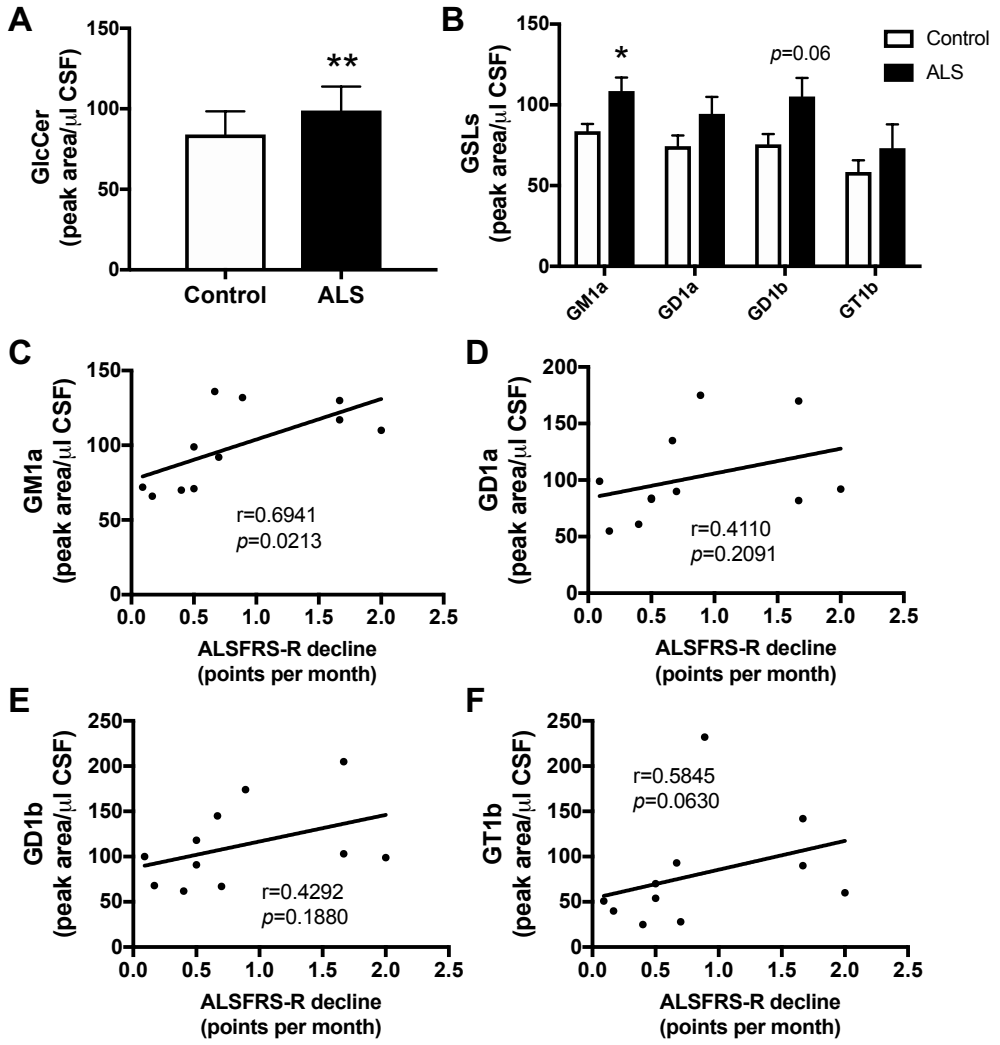

Figure 2.12: Glycosphingolipids in CSF of ALS patients at diagnosis. Cerebrospinal fluid of ALS patients and control subjects with non-demyelinating neurological disorders was used to quantify levels of GlcCer (A) and more complex GSLs (B) using NP-HPLC. Data were analyzed using unpaired t-test (A) and two-way ANOVA (B) (n=20 control subjects, n=14 ALS patients; * = p<0.05, ** = p<0.01). Data shown as mean ± SEM. (C-F) Correlation of GM1a, GD1a, GD1b and GT1b levels with severity of disease progression (decrease of ALSFRS-R score) in ALS patients (n=11). Data were analysed using Pearson correlation analysis.

2.4 Discussion

Significantly altered lipidome in ALS: Focus on GSLs

Using UPLC/TOF-MS, we found significant alterations in the lipidome of spinal cord and muscle of pre-symptomatic and symptomatic SOD1(G86R) mice compared to age-matched wildtype mice (**Figure 2.1**). Further analysis revealed significant changes in three main lipid families, namely triglycerides, phospholipids and sphingolipids (**Figures 2.2 and 2.3**). The loss of triglycerides in muscle and spinal cord of symptomatic SOD1(G86R) can be interpreted as a sign of hypermetabolism and dyslipidaemia, which has already been reported for the SOD1(G86R) mouse model as well as for ALS patients [200, 201]. Healthy adults have fairly stable energy stores, mostly in the form of triglycerides in adipocytes, which are severely decreased in ALS patients [186]. Interestingly, several phospholipid and sphingolipid species were decreased in the spinal cord of pre-symptomatic and symptomatic SOD1(G86R) mice (**Figure 2.2**). However, most phospholipids and sphingolipids were increased in muscle of SOD1(G86R) mice (**Figure 2.3**). This suggests differential responses in muscle and nervous tissues in ALS, requiring further investigation.

We concentrated on sphingolipid metabolism as changes showed the highest statistical significance of all affected lipids in both spinal cord and muscle of SOD1(G86R) mice [115]. A major limitation of mass spectrometry is that it is not possible to distinguish GlcCer species from galactosylceramide (GalCer) species, as they have the same mass. To specifically measure levels of total GlcCer species and more complex GSLs, we thus used NP-HPLC for the reliable identification and quantification of GlcCer and GSLs. In the spinal cord, GlcCer levels were the same in pre-symptomatic and symptomatic SOD1(G86R) mice compared to age-matched wildtype mice. Interestingly, levels of LacCer and GM1a, a major ganglioside in the CNS, were increased at symptomatic disease stage (**Figure 2.4**). GM1a has been shown to exhibit neurotrophic properties *in vitro* and *in vivo* [43, 157, 235, 236]. Therefore, the increase in GM1a may serve to

counteract pathological processes during the symptomatic disease stage. Concerning soleus muscle, our main findings were increased levels of GlcCer and downstream GSLs, including LacCer, GM3 and GM2, in muscle of symptomatic SOD1(G86R) mice compared to age-matched wildtype littermates (**Figure 2.4**). GM3, the main ganglioside in muscle, has been shown to be important for the regulation of skeletal muscle biology, i.e. myogenesis and insulin signalling [224]. In addition, GCS expression was upregulated in soleus muscle of SOD1(G86R) mice, and importantly also in vastus lateralis muscle of ALS patients, underlining the clinical relevance of findings in the mouse model [115].

While this data was in final preparation for publication, Dodge *et al.* reported similar alterations in GSL metabolism in ALS in mouse and man, complementary to our data [114]. Dodge *et al.* used the SOD1(G93R) mouse model of familial ALS to analyse GSLs in spinal cord. In agreement with our data, increased ceramide, GlcCer and GM3 levels were found in spinal cord of severely symptomatic SOD1(G93A) mice [114]. Importantly, Dodge *et al.* reported that levels of ceramide, GlcCer, LacCer, Gb3, and the gangliosides GM3 and GM1a were significantly elevated in spinal cords of ALS patients. Thus, both studies independently confirm the involvement of GSLs in ALS.

In summary, these results demonstrate that changes in the expression of glucosylceramide synthase and subsequent changes in levels of GSLs do take place in muscle and spinal cord in ALS and might be involved in the pathogenesis of ALS.

Changes in GSLs in response to denervation and with GCS inhibition

Next, we determined if changes in levels of GSLs also take place as a response to denervation. For this we used the sciatic nerve crush injury model in wildtype mice. Similar to muscle of symptomatic SOD1(G86R) mice, crush injury in wildtype mice resulted in increased muscle GCS expression together with significant increases in

levels of GlcCer and downstream GSLs (GM3 and GM2) (**Figure 2.5**). Thus, changes in muscular sphingolipids in ALS may be directly attributed to neuronal injury.

To determine if the observed increase in sphingolipids in muscle is a protective or detrimental response to denervation, wildtype mice submitted to sciatic nerve crush injury were treated with AMP-DNM to inhibit GCS activity to decrease GlcCer levels in the tissues (**Figure 2.6**). Clear evidence of hindered regeneration of motor units and delayed recovery of motor function with AMP-DNM treatment after nerve crush injury was found (**Figure 2.6**), suggesting that GCS and GSLs are indeed part of a vital, physiological and protective, but late, response to neurodegeneration. Further supporting this hypothesis, pre-symptomatic SOD1(G86R) mice treated with AMP-DNM showed premature reduced grip strength and disturbed neuromuscular junction integrity [115]. However, in exactly which cells/tissue, namely muscles or neurons, GCS and GSLs are essential to maintain neuromuscular function remains unknown. Previous studies reported that a deletion of GCS activity in neuronal cells led to demyelination of peripheral nerves [32] and mice lacking complex gangliosides develop Wallerian degeneration and myelination defects in both the central and peripheral nervous systems [237]. Thus, the negative effect of AMP-DNM may be the consequence of its action in neurons.

Dodge *et al.* reported similar effects of GCS inhibition in the SOD1(G93R) mouse model of familial ALS [114]. Dodge *et al.* used the orally-available GCS-inhibitor GENZ-667161 (Genzyme, MA), which is BBB permeant and led to shortened survival of mutant SOD1(G93R) mice [114]. Therefore, both studies independently reveal a detrimental effect of GCS inhibitors in ALS. In summary, the data provides evidence for the importance of lipid metabolism in denervation, as well as a novel role for GCS and GSLs in ALS pathology, but the precise mechanism needs further investigation.

GCase inhibition in ALS

Henriques *et al.* and Dodge *et al.* reported deleterious effects after administration of inhibitors of GlcCer biosynthesis in SOD1 mouse models [114, 115]. Consequently, our next hypothesis was that inhibition of GlcCer degradation, through inhibition of β-glucocerebrosidase (GCase) activities, leading to an increase in GlcCer levels, might be beneficial in early-symptomatic SOD1(G86R) mice. To inhibit GCase function, a well-characterised covalent inhibitor, conduritol B epoxide (CBE), was used. We reported for the first time a beneficial effect of an inhibitor of GCase in an animal model of ALS [211]. Partial inhibition of GCase activity in early-symptomatic SOD1(G86R) mice resulted in increased levels of GlcCer and more complex GSLs, and subsequently preserved motor functions, a higher number of motor neurons and neuromuscular junction integrity (**Figures 2.7 and 2.8**). In addition, CBE treatment was able to improve *in vitro* axonal plasticity and innervation in a co-culture of muscle cells and spinal cord explants, confirming that partial inhibition of GCase activity, associated with an increase in GlcCer and more complex GSLs, is beneficial for motor units (**Figure 2.9**). Interestingly, CBE treatment *in vitro* had major effects on neuronal GSLs (GM1a, GD1a), but to a lesser extent on predominantly muscular GSLs (GM3), suggesting the positive effect of CBE may be the consequence of action at the neuronal level.

Role of gangliosides in ALS

CBE might lead to an increased flux into the GSL biosynthetic pathway by leakage of accumulated GlcCer molecules out of the lysosome and conversion into LacCer in the early Golgi, which can then be sialyated to GM3, a precursor of GM1a. This may initiate the synthesis of more complex GSLs, like GM1a, which may have beneficial effects in ALS for several reasons. Firstly, the ganglioside GM1a is a neurotrophic factor that promotes neurite outgrowth, axonal function, regeneration and neuronal survival [43, 235]. Secondly, complex lipids, like GM1a, reside at neuromuscular junctions in lipid

rafts, which are key for the stability of cell-cell interactions in neuromuscular junctions and are important for the clustering of signalling receptors e.g. the acetylcholine receptor [238-240]. To support this notion, loss of cholera toxin B-positive structures at neuromuscular junctions of early-symptomatic SOD1(G86R) mice has previously been shown, which hints to a loss of lipid rafts containing GM1a and other gangliosides [211]. Furthermore, several case reports showed the presence of anti-ganglioside antibodies, particularly against GM1a, in the serum of ALS patients [241-244]. Interestingly, intracerebroventricular infusion of exogenous GM3, a precursor of GM1a, significantly slowed the onset of paralysis and increased survival of mutant SOD1(G93R) mice [114]. However, intramuscular administration of a ganglioside mixture, purified from the bovine brain, has already been clinically tested in ALS patients with mostly inconclusive effects, possibly because these studies were underpowered [245-247]. Loss of GM1a was also reported in dopaminergic neurons in Parkinson's disease and subcutaneous administration of purified GM1a stabilised disease progression and reduced motor symptoms in patients [156, 248, 249]. Thus, administration of GM1a may also be a treatment option for ALS. Importantly, we show that altered ganglioside expression is also evident in the CSF of ALS patients (**Figure 2.10**). Levels of GlcCer and GM1a were significantly elevated in the CSF of ALS patients (**Figure 2.10**). Furthermore, the severity of the disease was positively correlated with increasing levels of GM1a in the CSF (**Figure 2.10**). The increase in GM1a in CSF might indicate neuronal or axonal loss of gangliosides, as CSF plays a major role in the clearance of axonal debris [229-231]. However, the increase in GM1a, could also indicate an elevated basal level of GM1a in neurons of ALS patients, as was shown in spinal cord of ALS patients [114]. Shortly after our publication, Blasco *et al.* reported a lipidomics analysis of CSF of ALS patients by mass spectrometry (n=40, recruited in the same ALS centre but different from the patients included in our study) [250]. Blasco *et al.* show extensive lipid remodelling in the CSF of ALS patients and confirm increased levels of GlcCer in ALS patients

compared to controls [250]. Furthermore, analysis of CSF lipidomes at diagnosis was able to predict the clinical evolution of ALS patients [250]. Thus, sphingolipid levels may also be important clinical biomarkers of the disease, with the possibility to evaluate disease progression.

Clinical relevance for ALS

Pharmacological manipulation of GSL levels could be a novel therapeutic strategy for ALS. For this, the aim should be to induce 'healthy' levels of GSLs, with neither excess nor insufficiency of specific GSL species. Indeed, there is a large spectrum of drugs available, which selectively target GSLs and are well characterized in terms of safety and bioavailability [20, 38]. Once clear targets are identified in further studies, these compounds could be suitable therapeutic candidates for ALS patients.

As has been shown in our experiments, one of these targets could be lysosomal GBA or non-lysosomal GBA2, as their inhibition with CBE led to an increase in GlcCer levels, followed by an increase in complex, neurotrophic gangliosides. Nevertheless, the *in vitro* model of neuromuscular junctions also demonstrated a clear caveat for the compound CBE: The covalent binding of CBE to GCase may easily lead to full inhibition of total GCase activity if given in high dose. The highest dose of CBE (100µM) led to an almost complete inhibition of GCase activity, which probably caused slight adverse effects in the *in vitro* cultures, as the high concentration had less of a positive effect on innervation than the lower dosed group (10µM) (**Figure 2.9**). Following this notion, CBE is often used to induce a chemical model of Gaucher disease in neonatal mice [225]. Optimal dosage for long-term administration of GCase inhibitors should therefore be carefully determined. However, the possible toxicity of CBE does exclude it as a candidate for clinical trials in patients. Nevertheless, CBE was useful for our proof-of-concept study in SOD1(G86R) mice.

3 Lysosomal function in human PD fibroblasts

3.1 Introduction

3.1.1 Cellular mechanisms in PD

Parkinson's disease (PD) is the second most common, late-onset neurodegenerative disease. Only 5-10% of PD cases have been linked to a genetic cause, whereas 90% of PD cases are sporadic [117]. Though rare, genetic forms of PD can provide clues to mechanisms underlying the neuropathology of PD. Examples of these mechanisms are: α-synuclein protein homeostasis, mitochondrial function, lysosomal function, oxidative stress, calcium homeostasis, axonal transport and neuroinflammation [117]. Interestingly, most familial genes in PD point to both mitochondrial and lysosomal mechanisms as contributors to PD pathology [116]. However, these mechanisms are not only involved in the genetic forms of PD, but also play a major role in sporadic PD cases. For example, mitochondrial dysfunction has been reported in both sporadic and familial forms of PD and mitochondrial abnormalities were observed in disease models as well as post-mortem tissue from PD patients [162, 251-255]. Mitochondrial and lysosomal dysfunction are tightly interconnected in neurodegeneration [256, 257]. For example, a defect in lysosomal clearance can lead to the build-up of dysfunctional mitochondria, caused by e.g. impaired autophagy, alterations in lipid metabolism, neuroinflammation or perturbed calcium homeostasis [258]. In summary, lysosomal dysfunction has been consistently linked to several common neurodegenerative diseases, including AD and PD. Importantly, lysosomal dysfunction in PD is not only seen as a contributor to α-synuclein protein aggregation any more, but is regarded a key event in PD pathogenesis [104, 120, 121].

3.1.2 Risk factor for PD: Lysosomal dysfunction

There are several lines of evidence supporting lysosomal dysfunction as a major risk factor for developing PD. Firstly, in the last two decades, more than 600 papers have been published mentioning the lysosome in PD-related papers. Most of these publications report that markers of lysosomal function, e.g. lysosomal volume, lysosomal hydrolase activities, calcium homeostasis and/or autophagic flux, were found to be altered in PD cell models, PD mouse models as well as post-mortem parkinsonian brain (some examples are [126, 147, 185, 259-262]). Secondly, in the last decade, mutations in *GBA*, causing haploinsufficiency of the lysosomal enzyme glucocerebrosidase (GBA), have been identified as the most common genetic risk factors of PD [127]. GBA is a lysosomal hydrolase, which is responsible for the degradation of the GSLs glucosylceramide (GlcCer) and glucosylsphingosine (GlcSph) in the lysosome. Outside the lysosome, GlcCer and GlcSph are degraded by the non-lysosomal glucocerebrosidase GBA2. A significant reduction in lysosomal GBA activity, as occurs in the lysosomal storage disorder (LSD) Gaucher disease, causes accumulation of its glycosphingolipid substrates. GBA activity has been reported to be reduced in several brain regions of PD patients carrying a *GBA* mutation [163]. In addition, brain GBA activity has also been reported to be reduced in sporadic PD patients (without *GBA* mutation) compared to healthy controls, together with an increase in GlcSph levels [164]. Thirdly, to underscore the role of lysosomes in PD even further, a major study published in 2017 reported an excessive burden of more than 50 LSD gene variants in PD [180]. According to this report, the majority of patients with sporadic PD (around 60%) might carry at least one putative damaging variant in an LSD gene, and some (around 20%) even carry multiple damaged alleles [180].

All these points are consistent with lysosomal dysfunction representing a major risk factor for PD.

3.1.3 Cellular models of PD

An essential step in research and drug discovery is the generation of suitable models of the disease and the subsequent testing of research hypotheses or drug candidates in these models. In this chapter, we used human skin fibroblasts from PD patients as an *in vitro* disease model for PD. The advantage of skin fibroblasts is their easy availability and robustness in culture. One of the main advantages is that they have defined mutations and recapitulate the cumulative cellular damage of individual patients, based on the biological ageing of the patients, including their genetic predisposition and environmental etiopathology [263]. This is especially important when studying idiopathic PD cases. However, the use of fibroblasts also has disadvantages. Fibroblasts from aged individuals have a slow growth rate, thus they need weeks in culture to generate sufficient material for several experiments, particularly biochemical assays [263]. Finally, their main disadvantage is that they are non-neuronal cells, and their gene expression profile and signalling differ from neurons [263]. However, a recent review on skin phenotypes associated with PD suggests that skin disorders in PD are common, but are frequently overlooked [264]. Furthermore, several mechanistic insights into PD pathogenesis have already been gained by studies using skin fibroblasts (see below). This suggests that fibroblasts can be a powerful tool to investigate basic PD pathogenic mechanisms. As such, altered cell biology may not be restricted to vulnerable dopaminergic neurons, but could also be evident systemically in other cell types.

Published studies of sporadic and genetic (*LRRK2*, *PINK1*, *GBA*) PD fibroblasts have reported increased α-synuclein expression, oxidative stress, altered calcium homeostasis, mitochondrial dysfunction and lysosomal dysfunction [259, 265-271]. Regarding fibroblasts from PD patients, who are carriers of heterozygous GBA mutations (PD-GBA), it has been reported that besides GBA enzyme activity being significantly reduced, oxidative stress, ER stress, lysosomal and ER calcium defects, cholesterol accumulation and lysosomal dysfunction are also present [172, 259, 270,

272]. However, no study so far has focused on dysfunctional lysosomal phenotypes in sporadic PD fibroblasts.

In the last decade, reprogramming technologies have been developed and allowed the generation of induced pluripotent stem cells (iPSCs) from somatic cells i.e. fibroblasts. After generating iPSCs, these can be differentiated into e.g. neurons to study their biochemistry *in vitro*. Such techniques have been exploited to study midbrain dopaminergic neurons differentiated from PD patient fibroblasts. Importantly, similar to findings in fibroblasts, it has been found that dopaminergic neurons derived from PD-GBA patient cells displayed lysosomal dysfunction, autophagic disturbances, and impaired calcium homeostasis [147, 273].

Several links between PD and LSDs have been reported, e.g. lysosomal dysfunction and altered GSL homeostasis. Thus, in this chapter, we performed an exploratory study on lysosomal function and GSLs in human PD skin fibroblasts. We concentrated on identifying cellular biochemical changes associated with GBA using sporadic PD patient fibroblasts, as well as fibroblasts generated from PD patients with heterozygous GBA mutations and homozygous GBA mutations (GD). This could be important for investigating and understanding processes involved in PD pathology.

The aims of this experimental chapter are therefore:

- To assess lysosomal function, e.g. lysosomal volume, lysosomal membrane permeability, lysosomal hydrolase activities and lysosomal pH, in human CTRL, PD, PD-GBA and PD-GD fibroblasts.
- To determine levels of GlcCer, GlcSph and more-complex GSLs in human CTRL, PD, PD-GBA and PD-GD fibroblasts.
- To analyse levels of cholesterol in human CTRL, PD, PD-GBA and PD-GD fibroblasts.

3.2 Materials and Methods

3.2.1 Human fibroblasts

Fibroblasts from healthy controls (n=5), sporadic PD patients (n=6), haploinsufficient PD-GBA patients (heterozygous N370S *GBA* mutation, n=4, and heterozygous L29P *GBA* mutation, n=1) and PD-Gaucher disease (GD) patients (homozygous N370S *GBA* mutation, n=2) were kindly provided by Prof Penelope Hallett (Neuroregeneration Research Institute, McLean Hospital/Harvard Medical School, Harvard, USA). The point mutations L444P and N370S represent the most frequent GD-causing alleles that have been linked to PD [127, 274]. Additionally, as positive control for several assays, Niemann-Pick disease type C (NPC) fibroblasts were used (GM17912 Corriell, compound heterozygote with P1007A and T1036M *NPC1* mutations, diagnosed at 11 years and deceased at 19 years). All cell lines were tested negative for Mycoplasma (LookOut® Mycoplasma PCR Detection Kit, Sigma-Aldrich). Details of the fibroblast lines are summarised in **Table 3.1**. Fibroblasts were closely age-matched. Fibroblasts were cultured in high-glucose DMEM (Life Tech), supplemented with 10% FBS, 1% Pen/Strep, 1% Non-essential amino acids (Life Tech) and 0.5% L-Glutamine at 37°C with 5% CO_2. Medium was replaced every 2-4 days. As the number of passages can affect cell phenotypes, utilised passage numbers were kept consistent within groups and passage 15 was not exceeded. Cells were used at ~85% confluence. The different fibroblast lines were grown in parallel and assessed in triplicate for all experiments. For biochemistry experiments, cells were washed twice in PBS, pelleted and stored at -80°C.

Table 3.1: Details of human fibroblasts. PD: Parkinson's disease, GD: Gaucher disease.

ID	Corriell number	Mutation	PD status	Gender	Age at biopsy	Average age
CTRL1	ND34769	None	Control	F	68	66.6
CTRL2	ND34791	None	Control	M	60	
CTRL4	ND36091	None	Control	F	63	
CTRL5	AG11743	None	Control	F	76	
CTRL8	AG13220	None	Control	M	66	
PD1	AG20439	Unknown	PD	M	55	66.7
PD2	AG20445	Unknown	PD	M	60	
PD3	ND32462	Unknown	PD	M	75	
PD4	ND35302	Unknown	PD	M	69	
PD5	ND30159	Unknown	PD	F	76	
PD9	ND34106	Unknown	PD	M	65	
PD-GBA1	ND29756	*GBA* N370S Het	PD-GBA	F	55	66.4
PD-GBA2	ND34982	*GBA* N370S Het	PD-GBA	F	82	
PD-GBA3	ND34263	*GBA* N370S Het	PD-GBA	M	65	
PD-GBA6	ND31630	*GBA* N370S Het	PD-GBA	M	69	
PD-GBA8	ND35322	*GBA* L29P Het	PD-GBA	M	61	
PD-GD1	ND35843	*GBA* N370S Hom	PD-GD	M	61	63
PD-GD2	ND34263	*GBA* N370S Hom	PD-GD	M	65	

3.2.2 Flow cytometry with LysoTracker Green

Human fibroblasts were seeded in 6-well plates (0.1×10^6, in triplicate) and incubated in supplemented DMEM for 48h at 37°C with 5% CO_2. As a positive control, at least one fibroblast cell line per assay was treated with 5µM U18666A (referred to as U-Drug) for 48h at 37°C with 5% CO_2. U-Drug inhibits lysosomal cholesterol export and, therefore, is commonly used to mimic NPC defects in cell culture models, resulting in lysosomal cholesterol accumulation and increased lysosomal volume [275]. Fibroblasts were trypsinised, washed twice in PBS and stained with 200nM LysoTracker Green DND-26 (Invitrogen) in PBS for 10 minutes in the dark at room temperature (RT). Cells were spun (3000rpm, 5 min, 4°C) and resuspended in FACS buffer (0.1% BSA, 0.02M NaN_3 in PBS). Cells were kept on ice and propidium iodide (PI) staining (20nM) was added to

the cells just before FACS analysis with BD Biosciences FACSCanto II. Samples were acquired with gating on singlets (FSC-H versus FSC-A) and PI negative events. In total, 10,000 singlet events were collected. The mean fluorescence of the LysoTracker Green events was calculated using FACSDiva software (BD). Mean equivalent fluorescein (MEFL) values were calculated using 8-peak Rainbow calibration beads (BD) with the MEFL values provided by the manufacturer.

3.2.3 Confocal microscopy with LysoTracker Red

Human fibroblasts were seeded in glass bottom 8-well plates (ibidi, 5000 cells/well) and incubated in supplemented DMEM overnight at 37°C with 5% CO_2. Fibroblasts were washed in PBS and stained with 75nM LysoTracker Red DND-99 (Invitrogen) in supplemented DMEM for 30 minutes in the dark at 37°C. Fibroblasts were washed in PBS and kept in Live Cell Imaging Buffer (20mM HEPES, 115mM NaCl, 1.8mM $CaCl_2$, 1.2mM $MgCl_2$, 1.2mM K_2HPO_4 and 0.2% (w/v) glucose) for microscopy. Microscopy images were captured at RT using a confocal laser scanning microscope (Leica SP8) with a 63x oil objective by Doris Höglinger. Red channel settings were as follows: 561nm excitation, 569-655nm emission. Images were further processed and analysed using Fiji software (W. Rasband, NIH, USA) with the FluoQ macro [276]. Cells were automatically segmented without user interaction using the particle analyser plug-in with minimum particle size of 250 to define regions of interest (ROIs) and the mean pixel intensity (mean fluorescence) of each ROI was measured.

3.2.4 LAMP1 staining

Human fibroblasts were seeded onto 13mm coverslips placed in wells of 24-well plates (8000 cells/well) and incubated in supplemented DMEM overnight at 37°C with 5% CO_2. Cells were washed twice with PBS and fixed with 4% paraformaldehyde for 15min at RT. Cells were washed with PBS and incubated with 50mM ammonium chloride for

10min at RT to quench autofluorescence. Cells were then permeabilised and unspecific binding was blocked in PBS/0.3% Triton-X100/1% BSA with 5% goat serum for 30 min at RT. Cells were then incubated with primary antibody against LAMP1 (anti-LAMP1, mouse monoclonal, abcam, 1:200 in PBS/0.3% Triton/1% BSA) overnight at 4°C. Coverslips were washed three times in PBS and incubated with secondary antibody (anti-mouse Alexa Fluor 488, goat, invitrogen, 1:1,000 in PBS/0.1% Triton-X100/0.25% BSA with 5% goat serum) for 1hr at RT in the dark. Cells were washed three times in PBS and cell nuclei were visualised using Hoechst 33342 staining (25 mg/ml, 1:5,000, 10min, RT). Finally, cells were washed three times in PBS, cover slips were mounted with ProLong Gold mounting medium (Thermo Fisher) and were left to dry in the dark for 2 days. Microscopy images were captured at RT using a confocal laser scanning microscope (Leica SP8) with a 63x oil objective. Channel settings were as follows: Hoechst-channel: 405nm excitation, 409-475nm emission; green channel: 488nm excitation, 489-550nm emission. Images were further processed and analysed using Fiji software (W. Rasband, NIH, USA) with the FluoQ macro [276]. Cells were manually segmented to define regions of interest (ROIs) and the mean pixel intensity (mean fluorescence) of each ROI was measured.

3.2.5 Lysosomal membrane permeability (LMP)

Human fibroblasts were seeded on sterile cover slips in 24-well plates (20,000 cells/well, in triplicate) and incubated in supplemented DMEM for 48h at 37°C with 5% CO_2. As a positive control, fibroblasts from each cell line were treated for 6h with 2mM LLOMe. LLOMe (L-leucyl-L-leucine methyl ester) is a lysosomotrophic agent, which induces lysosome-specific membrane damage [277]. Fibroblasts were fixed in 4% paraformaldehyde in PBS for 10 minutes at 37°C. Fibroblasts were washed 3x with PBS and incubated in 0.3% TritonX-100 and 1% BSA with 5% goat serum in PBS for 20 minutes at RT for permeabilization and blocking. After washing with PBS, fibroblasts

were incubated at 4°C overnight with the primary antibody rat anti-Mac2 (galectin-3) antibody (1:500, BioLegend, cat. no. 125401). After washing with PBS, fibroblasts were incubated for 1h shaking at RT with the secondary antibody AlexaFluor 594 goat anti-mouse (Life technologies) (1:1,000). Fibroblasts were washed and stained with Hoechst 33342 (Sigma-Aldrich) at 1:5,000 in PBS for 30min shaking at RT in the dark. Coverslips were mounted onto Superfrost slides with ProLong Gold mounting medium. Images were captured using a Zeiss fluorescence microscope Axio Imager 2 and Zeiss AxioVision camera and software. Images were further processed and analysed using Fiji software (W. Rasband, NIH, USA). Cells were regarded as positive for increased LMP when punctate galectin staining was visible.

3.2.6 Lysosomal hydrolase activity assays

Lysosomal hydrolase activities were assayed fluorometrically using artificial sugar-substrates containing the fluorophore 4-methylumbelliferone (4-MU). For measuring β-glucosidase activities, samples were incubated in the presence or absence of 0.3mM *N*B-DGJ for 30min on ice prior to the assay. The substrate for GBA β-glucosidase activity was 4.5mM 4-MU β-D-glucoside in 200mM citrate/phosphate buffer, pH 5.2, 0.25% TritonX-100, 0.25% sodium taurocholate, 1.25mM EDTA and 4mM 2-mercaptoethanol. GBA activity was defined as the *N*B-DGJ non-sensitive activity at pH 5.2. The substrate for GBA2 β-glucosidase activity was 4.5mM 4-MU β-D-glucoside in 200mM citrate/phosphate buffer, pH 5.5, 0.1% TritonX-100. GBA2 activity was defined as the *N*B-DGJ sensitive activity at pH 5.5. For α-galactosidase activity, 5mM 4-MU α-D-galactoside in 100mM sodium citrate buffer, pH 4.0, 0.1% TritonX-100 was used as substrate. For β-hexosaminidase activity, 3mM 4-MU N-acetyl-β-D-glucosaminide in 200mM sodium citrate buffer, pH 4.5, 0.1% TritonX-100 was used as substrate. For β-galactosidase activity, 1mM 4-MU β-D-galactopyranoside in 200mM sodium acetate buffer, pH 4.3, 100mM NaCl, 0.1% TritonX-100 was used as substrate. The substrate

for neuraminidase activity was 0.8mM 4-MU N-acetylneuraminic acid in 0.1M acetate buffer, pH 4.6, 0.1% TritonX-100. The digests (in triplicate) containing tissue homogenate in PBS with 0.1% TritonX-100 and artificial 4-MU substrate were incubated at 37°C for 30min (or 2h for neuraminidases). The reaction was stopped by adding cold 0.5M Na_2CO_3, pH 10.7. The released fluorescent 4-MU was measured in a FLUOstar OPTIMA plate reader (BMG Labtech, Ortenberg, Germany) with an excitation at 360 nm and emission at 460 nm. A standard curve of free 4-MU was used to calculate the enzyme activity. Results were normalised to protein content.

3.2.7 Glycosphingolipids (NP-HPLC)

GlcCer and downstream GSLs were analysed as previously described in **Chapter 2.2.6** with slight modifications. GSLs extracted and purified from cell homogenates were treated with recombinant ceramide glycanase (rEGCase, prepared by Genscript and provided by Orphazyme, Denmark) to obtain oligosaccharides from more complex GSLs. Furthermore, individual GSL species were quantified by comparison of integrated peak areas with a known amount of 2AA-labelled BioQuant chitotriose standard (Ludger, UK).

3.2.8 Sphingosine and glucosylsphingosine (RP-HPLC)

Sphingosine (Sph), sphinganine (SphA) and glucosylsphingosine (GlcSph) from cell homogenates were extracted in chloroform:methanol (1:2, v/v) with sonication for 10 min at room temperature. Lipids were purified using SPE NH2 columns (Biotage, #470-0010-A). After elution, Sph, SphA and GlcSph were labelled with o-Phthalaldehyde (OPA) for 20 min at room temperature in the dark and OPA-labelled lipids were taken for analysis by reverse phase high-performance liquid chromatography (RP-HPLC). The RP-HPLC system consisted of a VWR Hitachi Elite LaChrom HPLC system with a L-2485

fluorescence detector set at Ex λ340nm and Em λ455nm. The solid phase used was a Chromolith Performance RP-18e 100-4.6 HPLC column (Merck, Darmstadt, Germany). Individual sphingosine species were identified by their retention time and quantified by comparison of integrated peak areas with a known amount of OPA-labelled C20-sphingosine standard (Avanti Polar Lipids, Alabama, USA) or OPA-labelled C20-glucosylsphingosine standard (Avanti Polar Lipids, Alabama, USA), respectively. Results were normalized to protein content.

3.2.9 Filipin staining (Cholesterol)

Free cholesterol was visualised in human fibroblasts using Filipin complex from *Streptomyces filipinensis* (Sigma-Aldrich), a cytochemical probe specific for cholesterol. Human fibroblasts were seeded onto 13mm coverslips placed in wells of 24-well plates (8000 cells/well) and incubated in supplemented DMEM overnight at 37°C with 5% CO_2. Cells were washed twice with PBS and fixed with 4% paraformaldehyde for 15min at RT. Cells were washed with PBS and incubated with 50mM ammonium chloride for 10min at RT to quench autofluorescence. Cells were then permeabilised and incubated with Filipin (0.05mg/ml in PBS/1% BSA/0.3% Triton-X100) for 2 hours at RT. Cells were washed three times in PBS and cell nuclei were visualised using Nuclear mask Deep Red Stain (1:250, 30min, RT, Invitrogen). Finally, cover slips were mounted with ProLong Gold mounting medium (Thermo Fisher) and were left to dry in the dark for 2 days. Microscopy images were captured at RT using a confocal laser scanning microscope (Leica SP8) with a 63x oil objective. Channel settings were as follows: DAPI-channel: 405nm excitation, 409-475nm emission; red channel: 561nm excitation, 569-655nm emission. Images were further processed and analysed using Fiji software (W. Rasband, NIH, USA) with the FluoQ macro [276]. Cells were manually segmented to define regions of interest (ROIs) and the mean pixel intensity (mean fluorescence) of each ROI was measured.

3.2.10 Lysosomal pH with LysoSensor

Lysosomal pH in human fibroblasts was assessed using LysoSensor Green DND-189 (molecular probes, Invitrogen), as acidotrophic LysoSensor reagents accumulate in acidic organelles and exhibit a pH-dependent increase in fluorescence intensity upon acidification. Human fibroblasts were seeded in 6-well plates (0.1×10^6, in triplicate) and incubated in supplemented DMEM for 48h at 37°C with 5% CO_2. Fibroblasts were trypsinised, washed twice in PBS and stained with 250 nM LysoSensor Green DND-189 (molecular probes, Invitrogen) in PBS for 10 minutes in the dark at room temperature (RT). Cells were spun (3000rpm, 5 min, 4°C) and resuspended in PBS. Cells were kept on ice and equal dye loading was quickly checked using the FACS. Then, to obtain a pH standard curve for each cell line, the lysosomal pH was equalized by incubating cells for 30 min at RT in extracellular medium (ECM, 145mM KCl, 5mM NaCl, 1mM $CaCl_2$, 1mM $MgCl_2$) containing the ionophore nigericin (10µM) with the pH adjusted to either 4.0, 4.5, 5.0, 5.5, 6.0, 6.5, or 7.0 using acetate, MES or HEPES, respectively. Sample cells for measuring the actual lysosomal pH were incubated for 30 min at RT either in PBS or ECM. After equilibration, samples were analysed with flow cytometry using BD Biosciences FACSCanto II. Samples were acquired with gating on singlets (FSC-H versus FSC-A). In total, 3,000-5,000 singlet events were collected. The mean fluorescence of the LysoSensor was calculated using FACSDiva software (BD).

3.2.11 Statistical analysis

All statistical analyses were performed with GraphPad Prism 7.0 (GraphPad, San Diego, CA). Unpaired student's *t*-test was used to compare two groups, one-way ANOVA or two-way ANOVA was used to compare more than two groups.

3.3 Results

Fibroblasts from healthy controls (n=5), sporadic PD patients (n=6), haploinsufficient PD-GBA patients (n=5) and PD-Gaucher disease (GD) patients (n=2) were used to perform an explorative biochemical characterisation to investigate if phenotypes of GBA haploinsufficiency, as the highest genetic risk factor for developing PD, are phenocopied in fibroblasts from sporadic PD patients.

3.3.1 Lysosomal volume

To start characterising the cellular phenotypes of the patient fibroblast cell lines, we examined the morphology of lysosomes using three independent methods.

First, relative acidic compartment volume was measured using the fluorescent, acidotrophic probe LysoTracker Green with flow cytometry. This probe can be used to infer lysosome volume and has been validated as a novel biomarker for lysosomal storage disorders [278]. Both sporadic PD and PD-GD cell lines showed similar lysosomal volumes compared to controls (**Figure 3.1A, B**). PD-GBA fibroblasts showed a decreased lysosomal volume compared to control fibroblasts, however this difference was not statistically significant (**Figure 3.1A, B**). Fibroblasts treated with U18666A served as positive control and showed the predicted increase in LysoTracker staining (**Figure 3.1A**). U18666A (referred to as U-Drug) inhibits lysosomal cholesterol export and, therefore, is commonly used to mimic NPC1 defects in cell culture models, resulting in lysosomal cholesterol accumulation and increased lysosomal volume [275].

Second, to further characterise the observed differences in the acidic compartment volume in the fibroblast cell lines, live cells were stained with LysoTracker Red and analysed by confocal microscopy. The sporadic PD cell lines showed similar lysosomal volume compared to control fibroblasts (**Figure 3.2A, B**). The PD-GBA fibroblasts showed a significant decrease in lysosomal volume compared to controls and sporadic

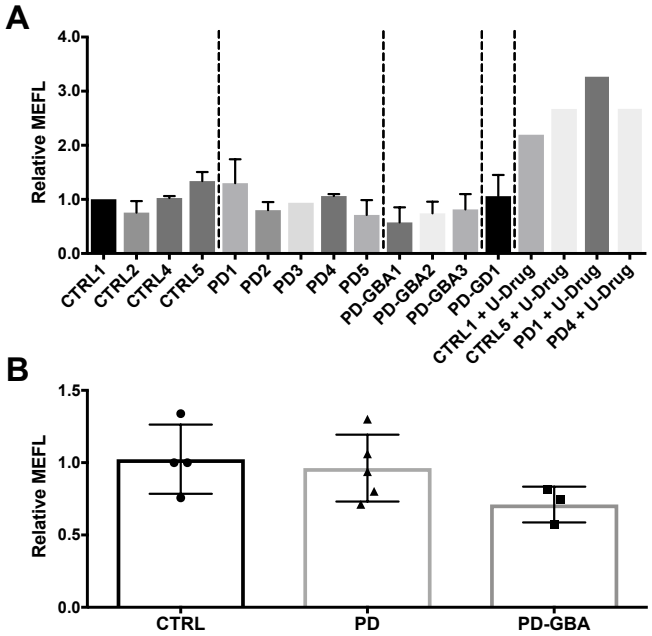

Figure 3.1: LysoTracker staining of human CTRL, PD and PD-GBA fibroblasts analysed by flow cytometry. (A) Intensity of LysoTracker® staining was expressed as molecules of equivalent fluorescein (MEFL) relative to CTRL1 (n=2, each in triplicate). CTRL1, CTRL5, PD1, and PD4 fibroblasts were treated with 5μM U-Drug. (B) Mean of LysoTracker staining of CTRL, PD and PD-GBA fibroblasts was expressed as MEFL relative to CTRL1 (n=3-5 per group, one-way ANOVA). Data are presented as mean ± SD.

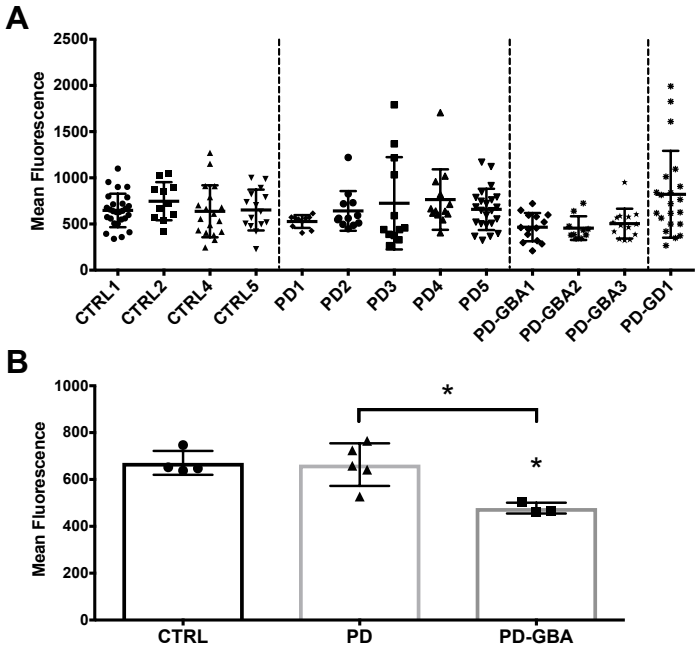

Figure 3.2: LysoTracker staining of human CTRL, PD-GBA and PD fibroblasts analysed by confocal microscopy. (A) Mean fluorescence intensity of LysoTracker staining per single cell (minimum of 15 cells per cell line). (B) Mean of LysoTracker fluorescence of CTRL, PD and PD-GBA fibroblasts (n=3-5 per group, * = p<0.05, one-way ANOVA). Data are presented as mean ± SD.

PD fibroblasts (**Figure 3.2A, B**, p=0.0123 and p=0.0119, respectively). Interestingly, some Gaucher-PD fibroblasts (PD-GD1) showed a higher acidic compartment volume compared to control fibroblasts, causing high variation in measured fluorescence in single cells (**Figure 3.2A**). Comparable to the Gaucher-PD fibroblasts, fibroblasts of the sporadic PD3 cell line also showed a high variance in measured fluorescence in single cells, with some cells presenting an increase in lysosomal volume compared to controls (**Figure 3.2A**). Representative microscopy images are shown in **Figure 3.3**.

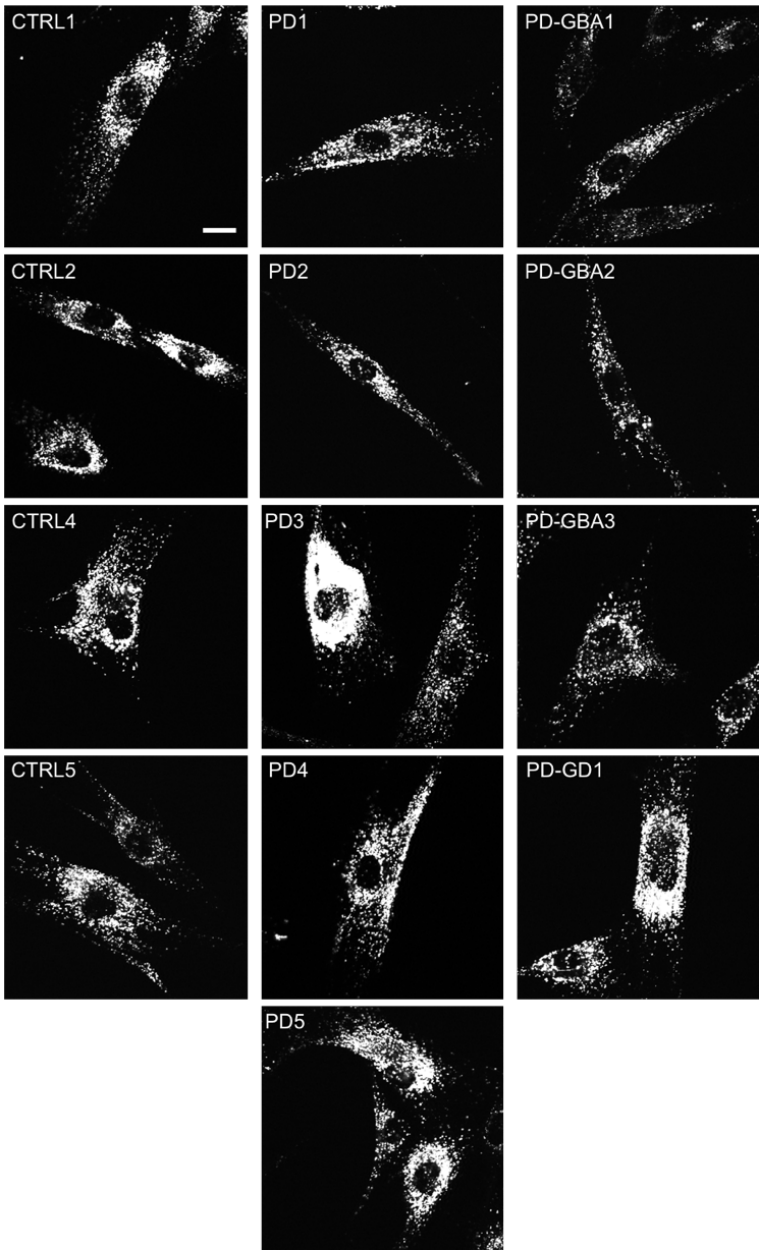

Figure 3.3: Confocal microscopy images of LysoTracker staining of CTRL, PD and PD-GBA fibroblasts. LysoTracker staining shown in grey. Scale bar = 20µm.

In a third approach, lysosomal morphology was assessed in fixed cells by immunocytochemistry using a primary antibody against LAMP1, a late endosome and lysosome marker. In healthy control fibroblasts, lysosomes were well resolved as punctate staining throughout the cell, with a concentration in the perinuclear space (**Figure 3.4A**). In contrast, lysosomes appeared slightly enlarged or clustered in some age-matched PD and PD-GBA fibroblasts, and more so in PD-GD and NPC fibroblasts (**Figure 3.4A**). By analysing the mean fluorescence intensity per cell, an increase in LAMP1 intensity of around 10% was detected in PD and PD-GBA patient fibroblasts relative to control fibroblasts, trending towards statistical significance (**Figure 3.4B, C**, p=0.0601 and p=0.0588, respectively). As expected, a higher increase in mean LAMP1 fluorescence (around 20%) was found in NPC fibroblasts compared to control fibroblasts (**Figure 3.4B, C**, p=0.0091).

3.3.2 Lysosomal membrane permeability

The decrease in the acidic compartment volume observed with LysoTracker in PD-GBA fibroblasts compared to control and sporadic PD fibroblasts may be due to an increase in lysosomal membrane permeability (LMP). Therefore, LMP of fibroblast cell lines was measured using a sensitive lysosomal galectin puncta assay described by Aits and co-workers [279]. Galectins are soluble carbohydrate-binding proteins, which specifically bind β-galactoside sugars. As the endo-lysosomal glycocalyx is especially rich in β-galactosides, galectins are quickly recruited to sites of endo-lysosomal leakage and initiate a signalling cascade for the degradation of these damaged organelles [59, 279]. Cells were regarded as positive for increased LMP when punctate galectin staining was visible. Representative images of control, sporadic PD and PD-GBA fibroblasts are shown in **Figure 3.5A**. Furthermore, representative images of sporadic PD1 fibroblasts are shown (**Figure 3.5A**). Untreated PD1 fibroblasts showed a significant increase in lysosomal membrane permeability, which was also confirmed by quantification of cells

with punctate galectin staining (50% positive cells, **Figure 3.5B**). No other untreated control, PD or PD-GBA fibroblast cell line showed significant punctate galectin staining (**Figure 3.5B**). LLOMe (L-leucyl-L-leucine methyl ester) is a lysosomotrophic agent, which induces lysosome-specific membrane damage [277]. As expected, all LLOMe-treated fibroblasts (positive control) showed punctate galectin staining (80-100% positive cells, **Figure 3.5A, B**).

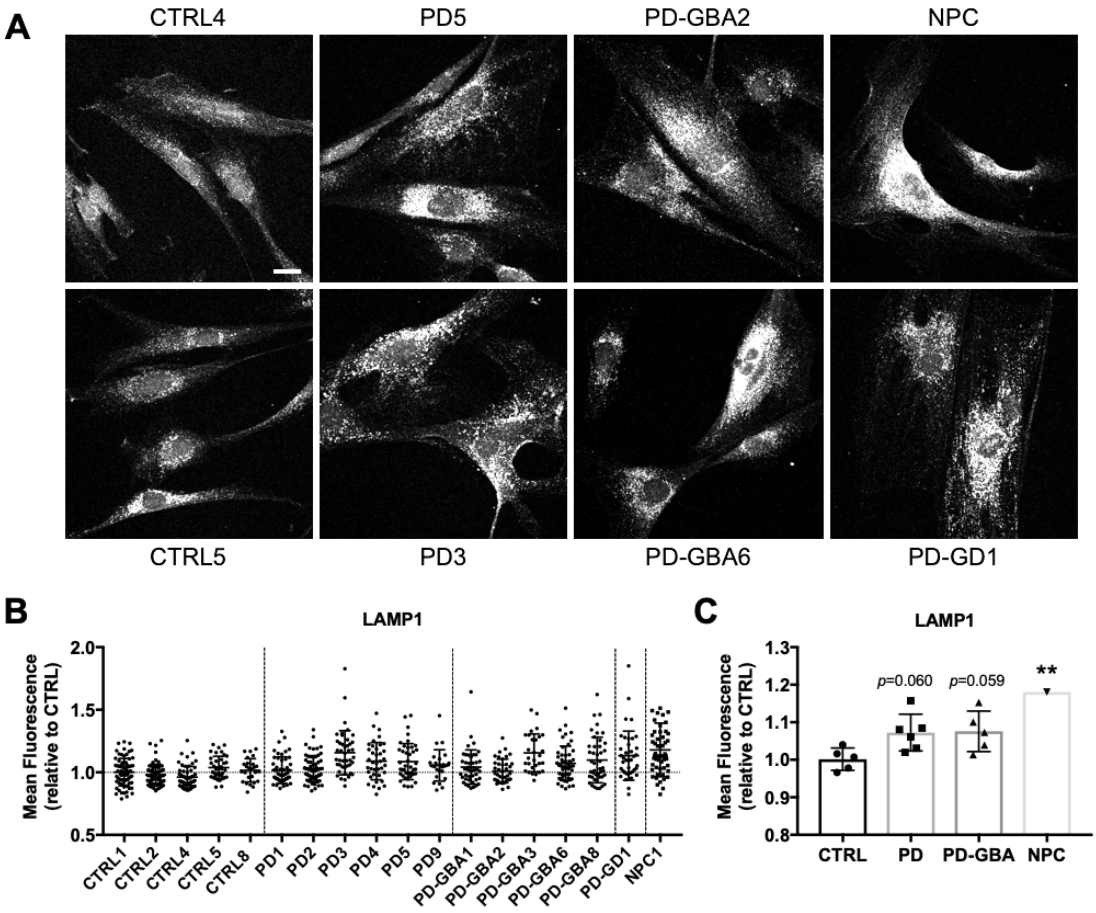

Figure 3.4: LAMP1 staining of human CTRL, PD-GBA and PD fibroblasts analysed by confocal microscopy. (A) Exemplary confocal microscopy images of LAMP1 staining of CTRL, PD, PD-GBA, PD-GD, and NPC fibroblasts. LAMP1 staining shown in grey. Scale bar = 20µm. (B) Mean fluorescence intensity of LAMP1 staining per single cell (minimum of 25 cells per cell line). (C) Summary of mean intensity of LAMP1 fluorescence in CTRL, PD, PD-GBA, and NPC fibroblasts (n=5-6 per group, except for NPC with n=1, ** = p<0.01, one-way ANOVA). Data are presented as mean ± SD.

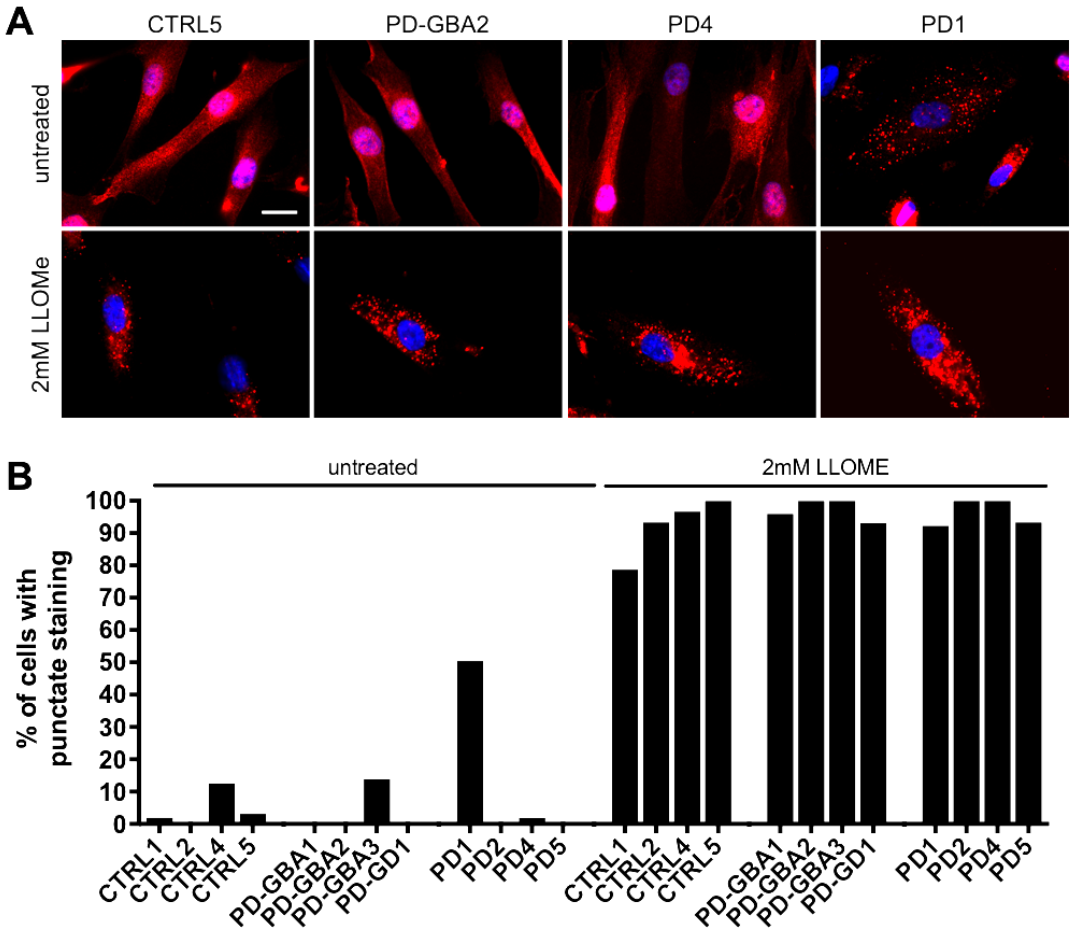

Figure 3.5: Galectin staining in untreated and LLOMe-treated CTRL, PD-GBA and PD fibroblasts. Cells were treated with 2mM LLOMe for 6h. (A) Galectin staining is shown in red, nucleus staining with Hoechst is shown in blue. Scale bar = 20µm. (B) Quantification of punctate Galectin staining in untreated and LLOMe-treated CTRL, PD-GBA and PD fibroblasts. A minimum of 30 cells were analysed per cell line per treatment.

3.3.3 Hydrolase activities

To further characterise the cellular phenotypes of the fibroblast cell lines, lysosomal hydrolase assays were performed to assess their activity. However, beforehand, an assay was developed to reliably distinguish lysosomal GBA and non-lysosomal GBA2 β-glucosidase activities. For this, the inhibitor *N*B-DGJ was used in combination with specific assay buffers at different pH values [228]. GBA was shown to be most active in the presence of detergents [47, 228], thus the assays were performed in 200mM citrate/phosphate buffer containing 0.25% Triton X-100, 0.25% sodium taurocholate, 1.25mM EDTA and 4mM 2-mercaptoethanol. First, to determine the optimal pH

conditions, hydrolase activities were measured in murine whole-brain homogenates (n=3, BALB/c wildtypes, 5-weeks old) using artificial 4-MU-substrate and assay buffer at varying pH (**Figure 3.6A**). Through this pH titration, it was determined that pH 5.5 is best for measuring GBA2 activity and pH 5.2 is best for measuring GBA activity in our assay conditions (**Figure 3.6A**). GBA activity was defined as the *N*B-DGJ non-sensitive activity at pH 5.2 using 200mM citrate/phosphate buffer containing 0.25% Triton X-100, 0.25% sodium taurocholate, 1.25mM EDTA and 4mM 2-mercaptoethanol. However, GBA2 is more active in buffer with low amount of detergents [47]. Thus, GBA2 activity was defined as the *N*B-DGJ sensitive activity at pH 5.5 using 200mM citrate/phosphate buffer with 0.1% Triton X-100.

To confirm accurate assay conditions, GBA and GBA2 activities were measured in brains of wildtype and end-stage Gaucher disease (GD) mice (n=2 per group, P14, CD1 background). As expected, no GBA activity was measured in brains from end-stage GD mice (**Figure 3.6B***, p*=0.0001). Interestingly, a slight increase in GBA2 activity was observed in brains from GD mice (**Figure 3.6B**, *p*=0.0316). This experiment confirms that we can reliably distinguish lysosomal GBA and non-lysosomal GBA2 β-glucosidase activities with the developed assay.

Finally, we wanted to know the proportion of GBA and GBA2 activities in human control fibroblasts, compared to murine wildtype brain tissue. Hardly any activity of GBA2 was found in control fibroblast lines (n=4), in contrast to high activity in brains of 3-months-old WT FVB mice (n=4) (**Figure 3.6C**). This is supported by the very low gene expression of GBA2 in the skin, but high gene expression in the CNS (The Human Protein Atlas, www.proteinatlas.org). As the activity of GBA2 is only around 1% of total β-glucosidase activity in fibroblasts, GBA2 activity was negligible for further fibroblast β-glucosidase assays.

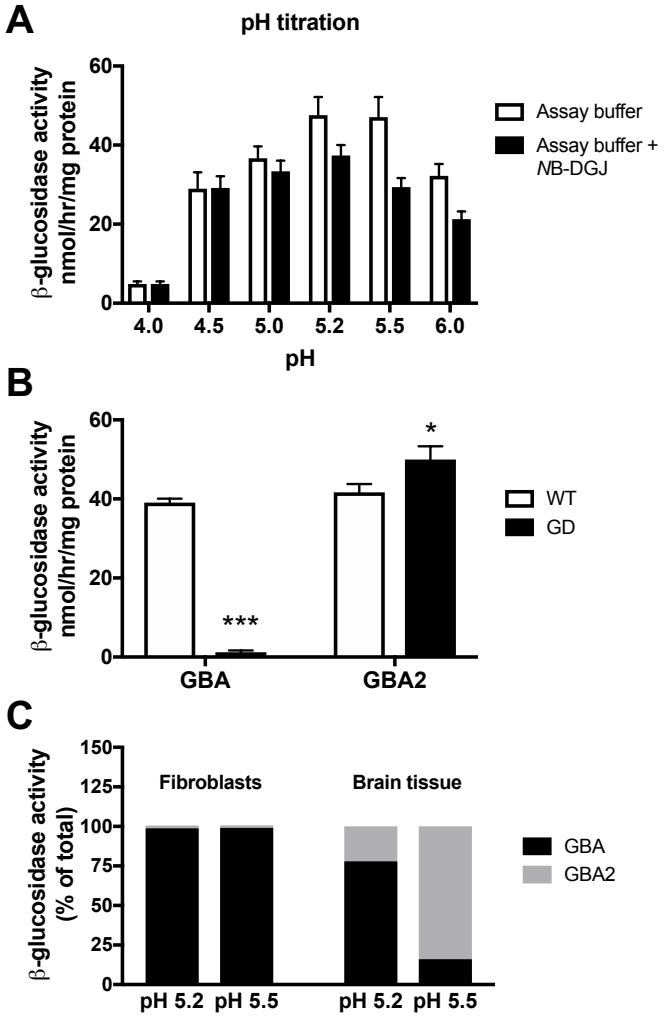

Figure 3.6: Assay development to distinguish lysosomal GBA and non-lysosomal GBA2 β-glucosidase activities. (A) Hydrolase activities were measured in whole-brain homogenates of 5-weeks-old WT BALB/c mice (n=3) using artificial 4-MU-substrate and assay buffer at varying pH. (B) GBA and GBA2 activities in WT and Gaucher disease (GD) mice (n=2 per group, P14). Lysosomal β-glucosidase activity is defined as GBA, and non-lysosomal β-glucosidase as GBA2. (C) Comparison of GBA and GBA2 activities in human control fibroblasts (n=4) and brains of 3-months-old WT FVB mice (n=4). Data are presented as mean ± SD (* = p<0.05, *** = p<0.001, two-way ANOVA).

Consequently, lysosomal GBA β-glucosidase activity was measured in CTRL, PD-GBA, PD-GD and PD fibroblasts using artificial 4-MU-substrate at pH 5.2 with detergents. A significant decrease in GBA activity of around 50% was observed in PD-GBA fibroblasts in comparison to control fibroblasts (**Figure 3.7A, B**, p=0.0018). This is in accordance with PD-GBA fibroblasts being heterozygote carriers for the N370S *GBA* mutation. Furthermore, as expected, the PD-GD fibroblasts (PD-GD1 and PD-GD2), carrying homozygous N370S *GBA* mutations, showed minimal GBA activity (**Figure 3.7A, B,**

p<0.0001). Importantly, a subset of sporadic PD patient fibroblasts (PD1, PD3 and PD4, n=3 out of 5 (60%)) displayed low levels of GBA activity under basal conditions (around 50% activity of controls), reflecting the levels observed in PD-GBA patient fibroblasts carrying a *GBA* mutation (**Figure 3.7A, B**, *p*=0.0011). On the other hand, sporadic PD cell lines PD2 and PD5 showed GBA activities comparable to control fibroblasts **(Figure 3.7A, B**).

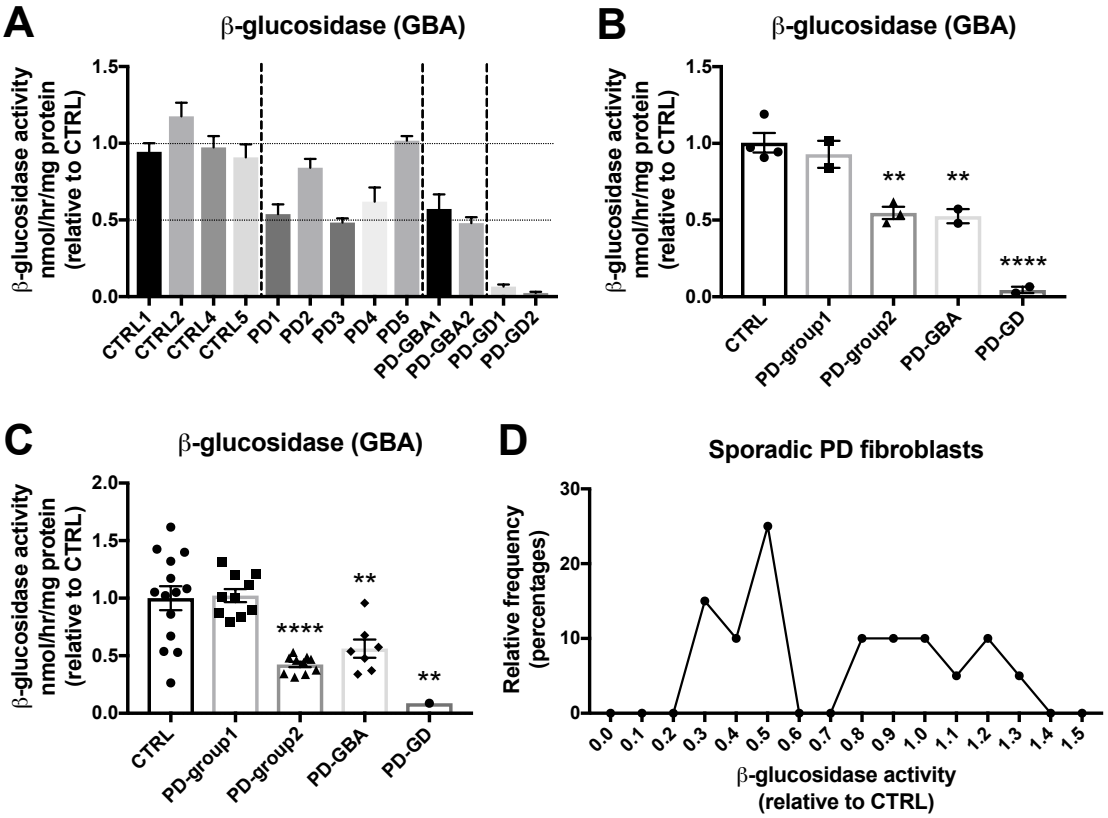

Figure 3.7: Reduced GBA activity is phenocopied in a subset of human sporadic PD fibroblasts. (A, B) Lysosomal GBA β-glucosidase activity was measured in CTRL, PD, PD-GBA, and PD-GD fibroblasts using artificial 4-MU-substrate (n=2-5 cell lines per group, each in triplicate). (C) GBA activity in CTRL (n=14), PD (n=20), PD-GBA (n=7), and PD-GD (n=1) fibroblasts was measured by Dr. Elizabeth B. Moloney. (D) Histogram of the relative frequency of GBA activity documented for sporadic PD fibroblasts (n=20) shows two sub-populations. Bar graphs are presented as mean ± SEM (** = *p*<0.01, **** = *p*<0.0001, one-way ANOVA).

To confirm these results, GBA activity was assayed in larger cohorts of human patient fibroblast cell lines by Dr. Elizabeth Moloney (Neuroregeneration Research Institute, McLean Hospital/Harvard Medical School, Harvard, US). GBA activity was measured in

CTRL (n=14), PD (n=20), PD-GBA (n=7), and PD-GD (n=1) fibroblasts. Indeed, reduced GBA activity was again phenocopied in a subset of sporadic PD fibroblasts (n=10 out of 20 (50%)) and was comparable to activity in PD-GBA fibroblasts (**Figure 3.7C**, $p<0.0001$). Plotting the data as a histogram of the relative frequency of GBA activity documented for sporadic PD fibroblasts (n=20) confirmed the existence of two sub-populations in the PD group, further called PD-group1 and PD-group2 (**Figure 3.7D**).

To further assess lysosomal function in the fibroblast lines, we measured additional hydrolase activities. No significant changes in α-galactosidase, β-hexosaminidase, β-galactosidase and neuraminidase activities were found in sporadic PD, PD-GBA and PD-GD fibroblasts compared to control fibroblasts (**Figure 3.8**). However, there was a slight increase in α-galactosidase activity in sporadic PD1 and PD4 fibroblasts (PD-group2) (**Figure 3.8A, B**). Furthermore, there was a slight increase in neuraminidase activity in PD-GBA1 and PD-GD fibroblasts (**Figure 3.8A, B and G, H**). Analysis of more fibroblast cell lines is needed to reliably determine if there are significant changes in lysosomal hydrolases other than GBA β-glucosidase.

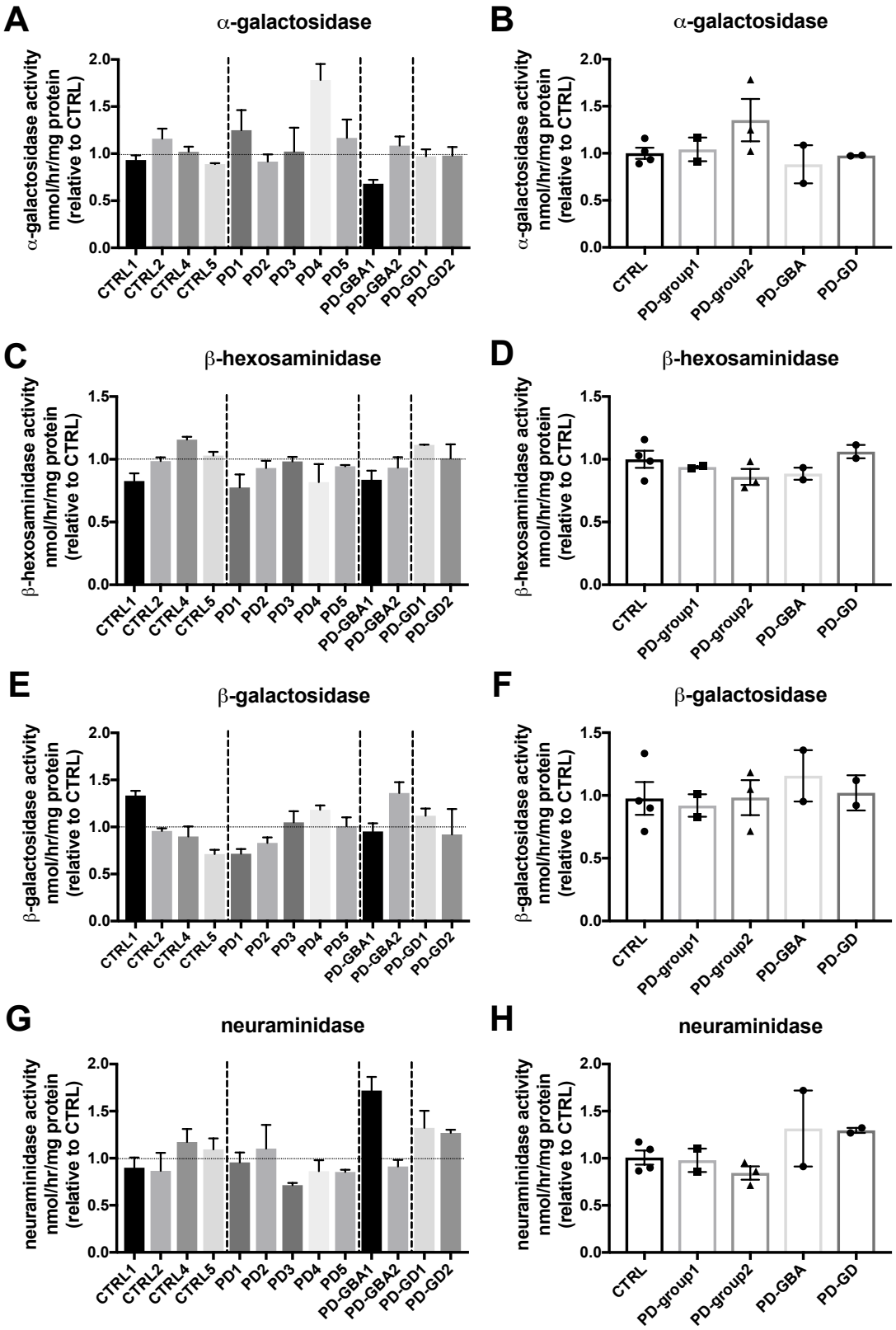

Figure 3.8: No difference in hydrolase activities in human CTRL, PD, PD-GBA and PD-GD fibroblasts. Lysosomal α-galactosidase (A, B), β-hexosaminidase (C, D), β-galactosidase (E, F) and neuraminidase (G, H) activities were measured in CTRL, PD, PD-GBA, and PD-GD fibroblasts using artificial 4-MU-substrates (n=2-5 cell lines per group, each in triplicate). Data are presented as mean ± SEM (n.s., one-way ANOVA).

3.3.4 Glycosphingolipids

Levels of GSLs can be modulated by the activity of multiple lysosomal hydrolases. For example, the observed decrease in GBA activity in the subset of sporadic PD fibroblasts could lead to an increase in the levels of its GSL substrates, GlcCer and GlcSph. Consequently, the levels of GlcCer and more-complex downstream GSLs in fibroblasts were quantified using normal phase high-performance liquid chromatography (NP-HPLC).

First, control fibroblasts were used to determine a typical GSL profile of human dermal fibroblasts using NP-HPLC. Representative GSL profiles of CTRL4 fibroblasts are shown in **Figure 3.9A**. The GSLs Gb3 and GM3 are the major expressed GSLs in fibroblasts, followed by LacCer, GM2 and Gb4 (**Figure 3.9A, B**). The GSLs pGb, GA1, GM1a, GD3, SpGb and GD1a are all expressed in very low amounts (less than 0.5% of total GSLs) and thus could not be reasonably quantified. Importantly, analysis of three independent cell pellets, collected at different times and different passages, gave the same GSL ratio (CTRL4 as example, **Figure 3.9B**). However, when comparing GSLs in multiple control fibroblast lines (n=3 independent cell pellets per cell line), GSL ratios were not comparable (**Figure 3.9C**). It appeared that each human fibroblast cell line (aka human being) had its own, individual GSL profile: Gb3 and GM3 are the predominant peaks, but ratios of both GSLs are variable in-between cell lines (**Figure 3.9C**). Some cell lines express preferably the a-series (from LacCer → GM3 → GM2), other cell lines express preferably the globo-series (from LacCer → Gb3 → Gb4) (**Figure 3.9D**). Consequently, the percentage amount of Gb3+GM3 in human CTRL, PD, PD-GBA, and PD-GD fibroblasts is constant (**Figure 3.9E**), making up around 80% of total GSLs. This analysis showed that comparison of levels of individual GSLs is not meaningful in fibroblasts due to different GSL expression preferences in individual fibroblast lines and that comparison of combined GSLs is more meaningful and should be performed.

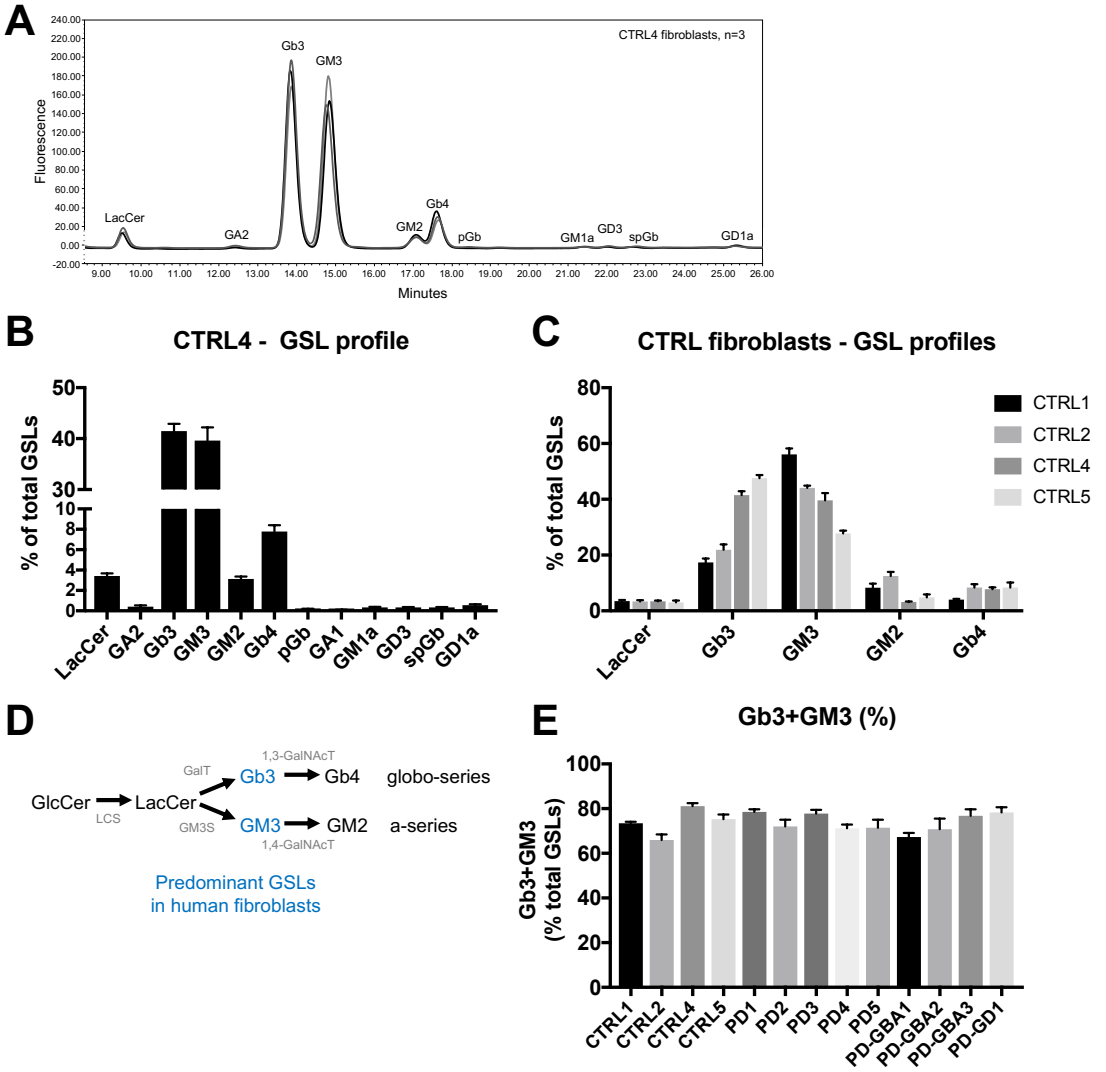

Figure 3.9: GSL profiles of human fibroblasts. (A, B) Control fibroblasts were used to determine a typical GSL profile of human dermal fibroblasts using NP-HPLC (CTRL4, in triplicate). Gb3 and GM3 are the major peaks, followed by peaks of LacCer, GM2 and Gb4. (C) Each control fibroblast cell line has its own, individual GSL profile (n=4, in triplicate). Gb3 and GM3 are dominant peaks, but ratios are variable in-between cell lines. (D) Biosynthetic pathway of GSLs. Abbreviations: LCS, lactosylceramide synthase; GM3S, GM3 synthase; GalT, galactosyl transferase; GalNAcT, N-acetylgalactosamine transferase. (E) Percentage of Gb3+GM3 levels was determined in human CTRL, PD, PD-GBA, and PD-GD fibroblasts using NP-HPLC. Data are presented as mean ± SEM.

Next, we assessed if GSL levels are changed in sporadic PD or PD-GBA fibroblasts compared to control fibroblasts. First, we summed Gb3 and GM3 levels to asses overall GSL load in fibroblast cell lines (**Figure 3.10A, B**). No changes in GSL load were found in most PD and all PD-GBA fibroblasts. Interestingly, sporadic PD fibroblast cell line PD3 showed significantly increased GSL levels (around 77%) compared to controls (**Figure**

3.10B, *p*=0.0044). Furthermore, PD-Gaucher cell line PD-GD1 also showed elevated GSL levels compared to controls (**Figure 3.10A, B**, 40% increase).

Next, we were interested in studying the levels of glucosylceramide (GlcCer) and lactosylceramide (LacCer), both precursors in the GSL biosynthetic pathway. There was no difference in GlcCer and LacCer levels in PD-GBA and PD-GD fibroblasts compared to control fibroblasts (**Figure 3.10C-F**). However, significantly increased GlcCer levels were seen in a subset of human sporadic PD fibroblasts (PD3 and PD4, PD-group2) compared to control fibroblasts (**Figure 3.10C, D**, *p*=0.0018). Furthermore, LacCer levels were significantly increased in sporadic PD fibroblast cell line PD3 (**Figure 3.10E, F**, *p*=0.0132). Interestingly, the sporadic PD fibroblast lines PD3 and PD4 also showed reduced GBA activity (PD-group 2).

3.3.5 Sphingosine and GlcSph

Next, we investigated the levels of sphingosine (Sph), sphinganine (SphA) and glucosylsphingosine (GlcSph) in the fibroblast cell lines, especially with GlcSph being a substrate for GBA. No differences in C18-Sph or SphA levels were found in fibroblasts from sporadic PD, PD-GBA and PD-GD patients compared to control fibroblasts using RP-HPLC (**Figure 3.11A-D**). However, human Niemann-Pick disease type C (NPC) fibroblasts, which served as positive control, showed significantly elevated levels of C18-Sph and SphA compared to control fibroblasts (**Figure 3.11B**, *p*=0.0005 and **Figure 3.11D**, *p*=0.0329). In addition, a significant increase in C18-GlcSph levels was seen in PD-GD fibroblast lines compared to controls (**Figure 3.11E, F**, *p*=0.0001). C18-GlcSph levels in sporadic PD and PD-GBA fibroblasts were comparable to control fibroblasts, however there was some variation in the PD-GBA fibroblasts lines (**Figure 3.11E, F**).

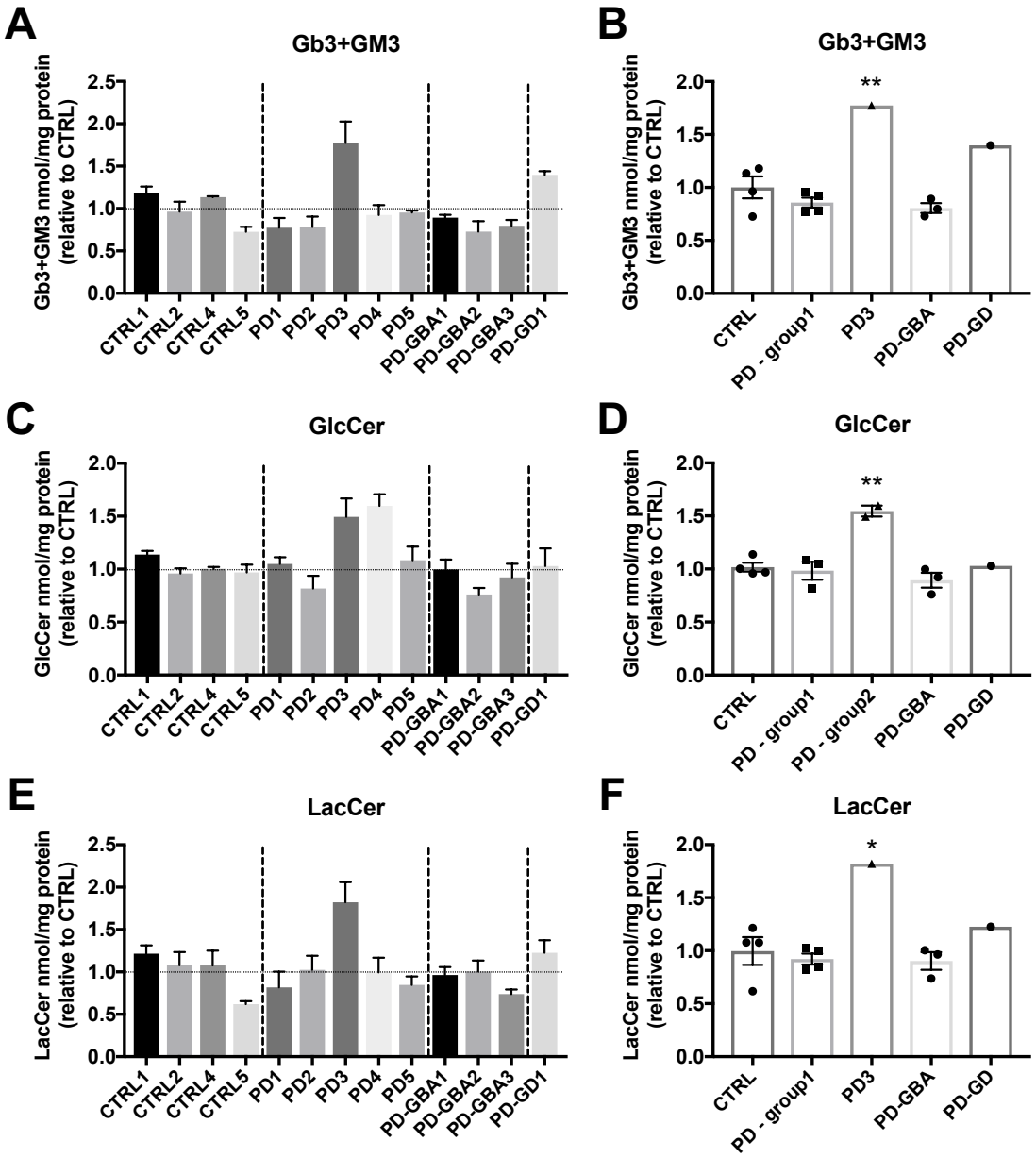

Figure 3.10: Increased GlcCer levels in a subset of human sporadic PD fibroblasts. Human CTRL, PD, PD-GBA, and PD-GD fibroblasts were used to determine levels of Gb3+GM3 (A, B), GlcCer (C, D) and LacCer (E, F) using NP-HPLC (each in triplicate). Gb3 and GM3 are the major GSLs in fibroblast GSL profiles. Data are presented as mean ± SEM (* = $p<0.05$, ** = $p<0.01$, one-way ANOVA).

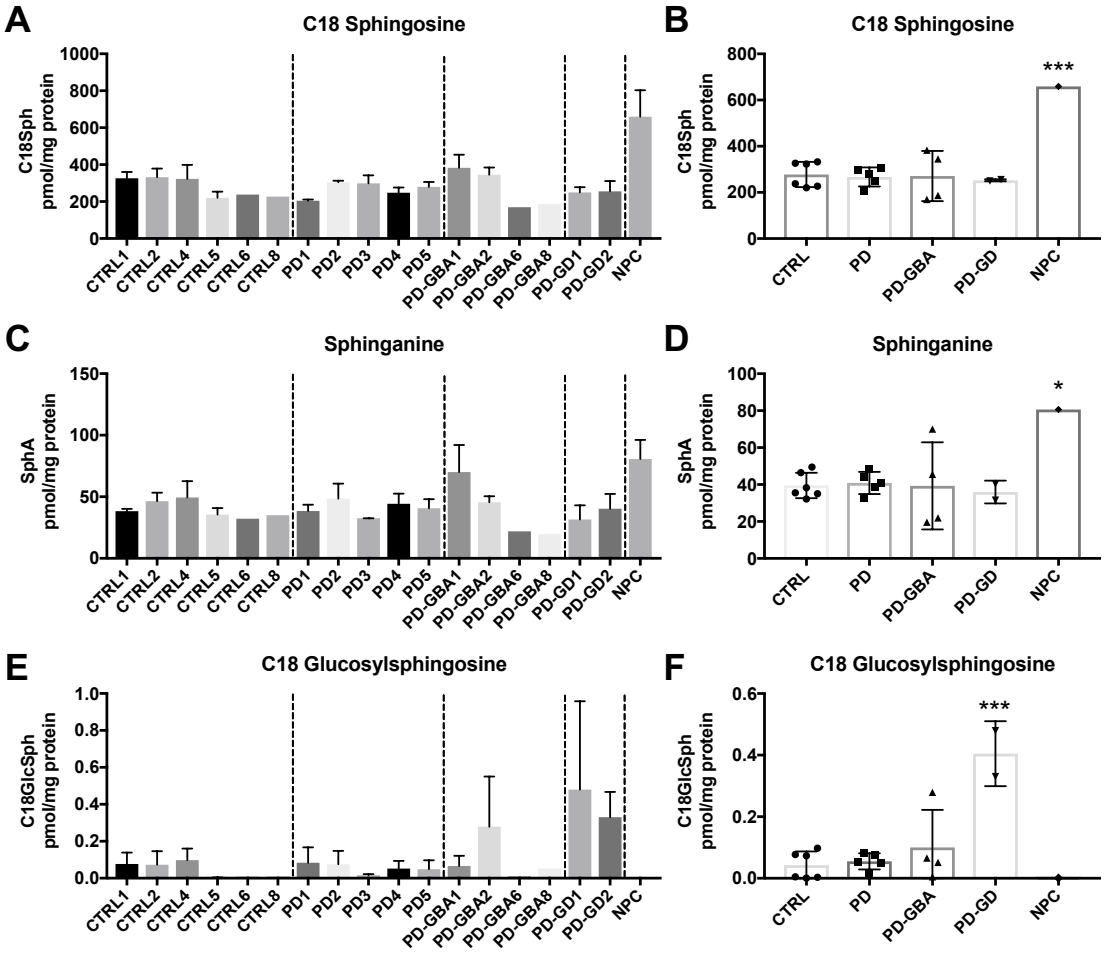

Figure 3.11: Sphingosine, sphinganine and glucosylsphingosine levels in human CTRL PD-GBA, PD-GD and PD fibroblasts. C18-sphingosine (A, B), sphinganine (C, D) and C18-glucosylsphingosine (E, F) levels in CTRL (n=6), PD (n=5), PD-GBA (n=4), PD-GD (n=2), and NPC (n=1) fibroblasts were analysed using RP-HPLC (in triplicate, * = p<0.05, *** = p<0.001, one-way ANOVA). Data are presented as mean ± SD.

3.3.6 Cholesterol

To explore whether cholesterol is involved in PD, cholesterol levels were assessed in sporadic PD, PD-GBA, PD-Gaucher and control fibroblasts using Filipin staining. In healthy control fibroblasts, cholesterol staining with Filipin was diffuse throughout the cell (**Figure 3.12A**). In contrast, Filipin staining was punctate and clustered in NPC fibroblasts (**Figure 3.12A**), suggestive of lysosomal storage of cholesterol, which is a hallmark of Niemann-Pick type C disease. Interestingly, Filipin staining was also punctate in some PD and PD-GBA fibroblast cell lines, as well as PD-GD fibroblasts (**Figure 3.12A**).

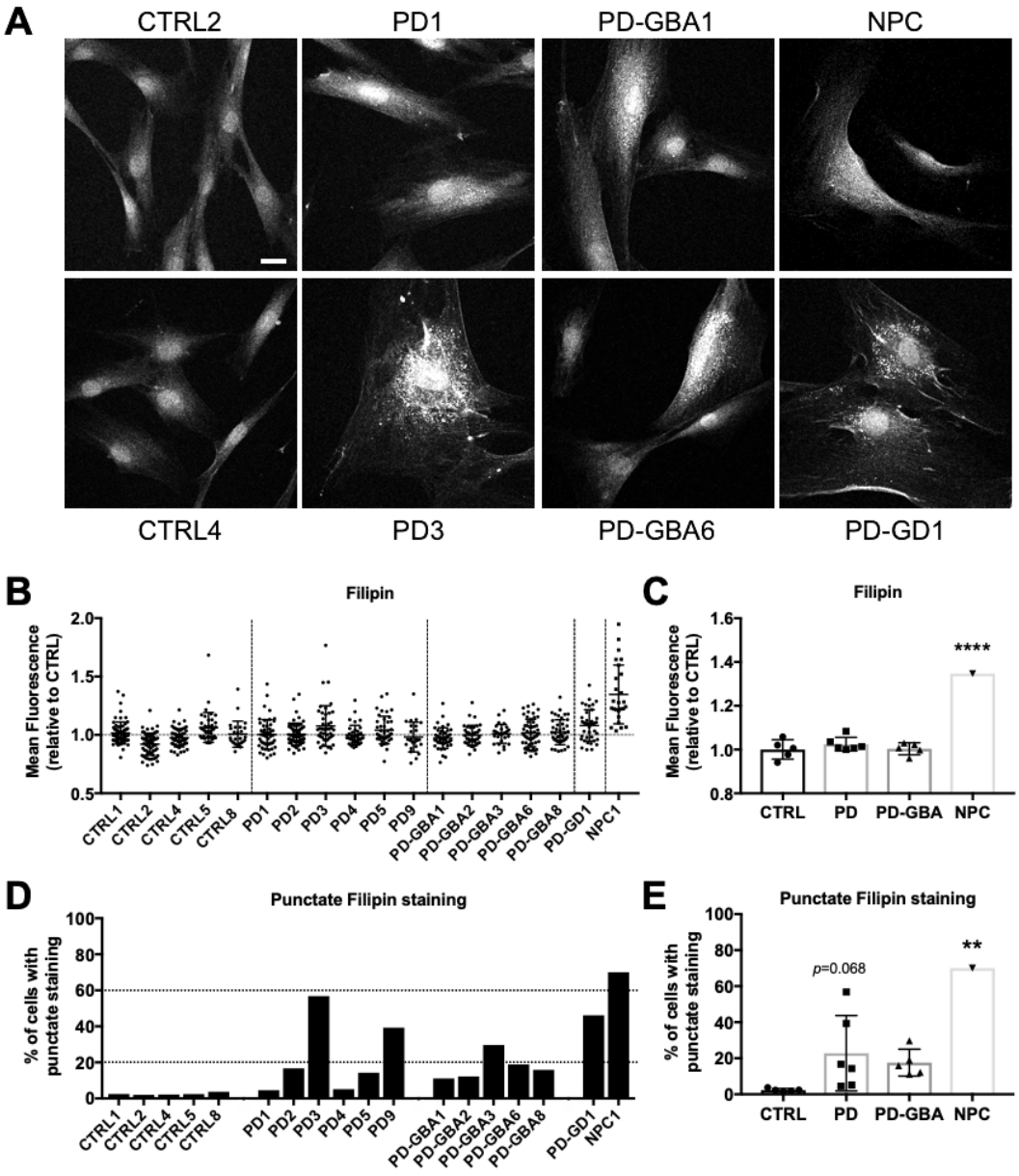

Figure 3.12: Filipin staining of human CTRL, PD-GBA and PD fibroblasts analysed by confocal microscopy. (A) Exemplary confocal microscopy images of Filipin staining of CTRL, PD, PD-GBA, PD-GD, and NPC fibroblasts. Filipin staining shown in grey. Scale bar = 20µm. (B) Mean fluorescence intensity of Filipin staining per single cell (minimum of 25 cells per cell line). (C) Summary of mean intensity of Filipin fluorescence in CTRL, PD, PD-GBA, and NPC fibroblasts (n=5-6 per group, except for NPC with n=1, **** = p<0.0001, one-way ANOVA). (D, E) Quantification of punctate Filipin staining in CTRL, PD, PD-GBA, PD-GD and NPC fibroblasts (n=5-6 per group, except for NPC with n=1, ** = p<0.01, one-way ANOVA). Data are presented as mean ± SD.

By analysing the mean fluorescence intensity per cell, no change in Filipin intensity was detected in PD and PD-GBA patient fibroblasts relative to control fibroblasts (**Figure 3.12B, C**). As expected, a significant increase in Filipin mean fluorescence (around 35%) was found in NPC fibroblasts compared to control fibroblasts (**Figure 3.12B, C**, $p<0.0001$). The mean fluorescence value is the sum of all pixel values in the selection area divided by the number of pixels in the selection area, thus it averages out dim and bright pixels. If a cell has brighter pixel, but these are more clustered, the difference compared to an evenly distributed fluorescence throughout the cell would most likely not be picked out in the mean fluorescence. To try and get a better measure of the observed phenotype, we counted the percentage of fibroblasts with punctate Filipin staining per cell line, indicative of lysosomal storage of cholesterol. Sporadic PD3 and PD9 fibroblasts showed a significant increase in punctate Filipin staining (**Figure 3.12D**, PD3: 57% positive cells, PD9: 39% positive cells). Furthermore, PD-GBA fibroblasts showed in average around 15-20% cells with punctate Filipin staining (**Figure 3.12D, E**). Interestingly, PD-GD fibroblasts showed 46% positive cells with punctate staining (**Figure 3.12D**). As expected, NPC fibroblasts showed significant punctate Filipin staining (70% positive cells, **Figure 3.12D, E,** $p=0.0015$).

3.3.7 Lysosomal pH

LysoTracker fluorescence was decreased in PD-GBA fibroblasts compared to control and sporadic PD fibroblasts, indicative of a decreased acidic compartment volume. However, LAMP1 fluorescence was not decreased in PD-GBA fibroblasts. LysoTracker is pH dependent, thus a decrease in fluorescence may be due to an increase in lysosomal pH. Consequently, lysosomal pH was investigated next.

Lysosomal pH was analysed broadly based on a method described by Zhang and co-workers [280]. Briefly, fibroblasts were stained with LysoSensor Green DND-189, incubated for 30min in PBS to obtain sample values or in calibration buffers to obtain

standard curve values (extracellular medium with nigericin adjusted to pH values ranging from 4.0–7.0) and analysed by flow cytometry. Nigericin was used to permeabilise the cells.

Exemplary calibration curves for CTRL, PD, PD-GBA and PD-GD fibroblasts can be found in **Figures 3.13A-F**. We found that the LysoSensor Green DND-189 fluorescence was not linear over the investigated pH range, but rather followed a second order polynomial (quadratic) equation with the centre roughly around pH 5.5. However, the pH values ranging from 5.5-7.0 could be disregarded for further analysis, as their meaning is biologically irrelevant.

The lysosomal pH in control fibroblasts was around pH 4.4, a reasonable pH for the lysosomes in healthy control cells (**Figure 3.13G, H**). There was no difference in the lysosomal pH in PD-GBA fibroblasts compared to control fibroblasts (**Figure 3.13G, H**). However, a significantly increased lysosomal pH was seen in a subset of human sporadic PD fibroblasts (PD3 and PD4, PD-group2) compared to control fibroblasts (**Figure 3.13G, H**, average of pH 4.8, p=0.0002). Furthermore, the lysosomal pH was significantly increased in PD-GD fibroblasts compared to controls (**Figure 3.13G, H,** average of pH 4.6, p=0.0060). Interestingly, the sporadic PD fibroblast lines PD3 and PD4 also showed reduced GBA activity and increased GlcCer levels (PD-group 2).

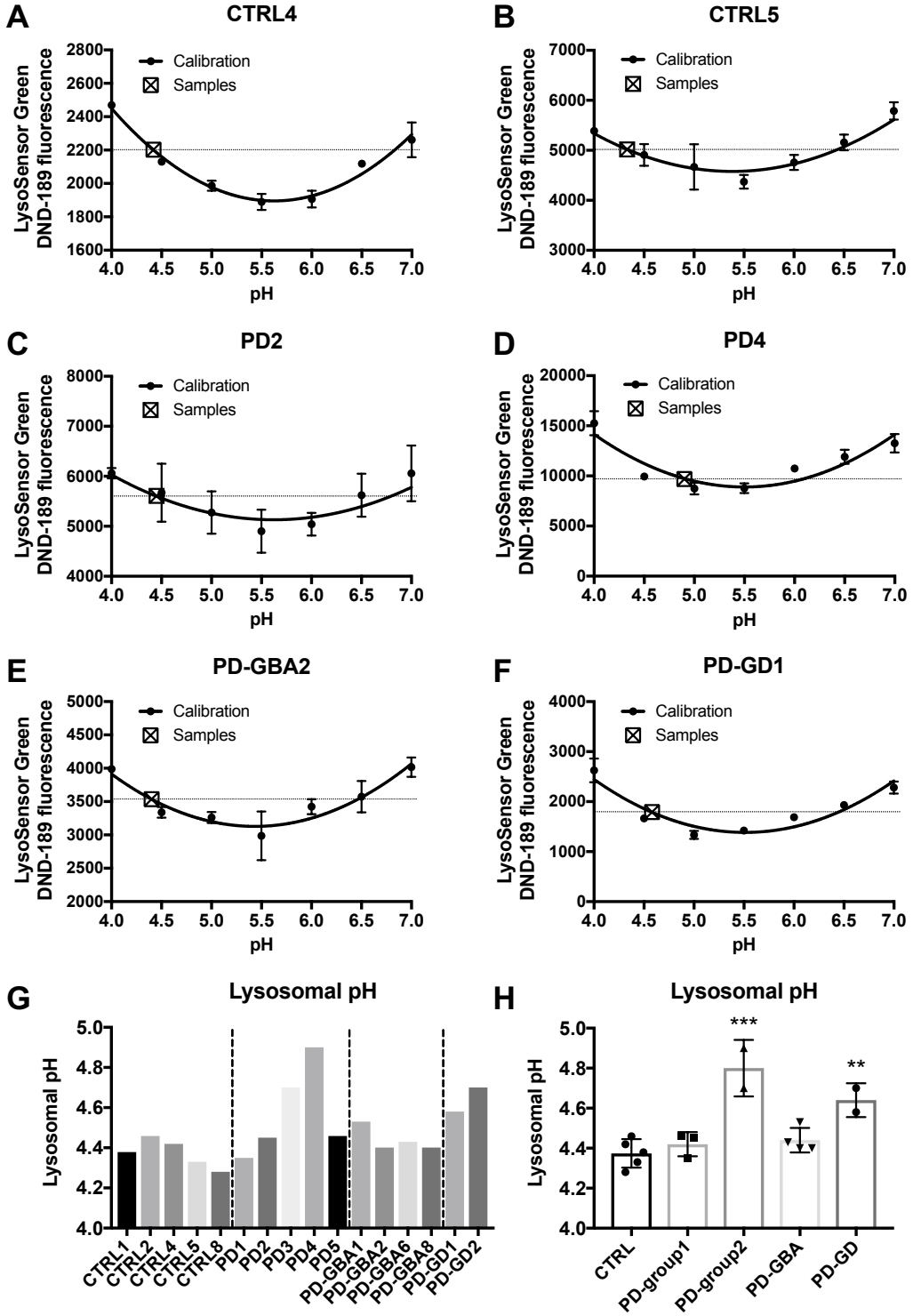

Figure 3.13: Increased lysosomal pH in a subset of human sporadic PD fibroblasts. CTRL (n=5), PD (n=5), PD-GBA (n=4), and PD-GD (n=2) fibroblasts were stained with LysoSensor Green DND-189, incubated in PBS or in extracellular medium adjusted to pH values ranging from 4.0–7.0 for 30min and analysed by flow cytometry. Calibration curves of CTRL4 (A), CTRL5 (B), PD2 (C), PD4 (D), PD-GBA2 (E) and PD-GD1 (F) are shown (n=2-3 per pH value and per sample, presented as mean ± SD). (G) Individual lysosomal pH values for each fibroblast cell line (average of 2-3 samples). (H) Grouped lysosomal pH values are presented as mean ± SD (** = p<0.01, *** = p<0.001, one-way ANOVA).

3.4 Discussion

In this chapter, we performed an explorative study on lysosomal function, activities of various lysosomal hydrolases and levels of GSLs in human PD skin fibroblasts. No study so far focused on lysosomal phenotypes in sporadic PD fibroblasts, thus we focused on identifying cellular biochemical changes associated with GBA mutations that might predispose to neurodegeneration using fibroblasts generated from a series of sporadic PD patients, as well as PD patients with GD and heterozygous GBA mutation carriers. We observed several phenotypic differences in individual sporadic PD fibroblast cell lines compared to age-matched control fibroblasts. A summary of our findings in sporadic PD fibroblasts, as well as PD-GBA and PD-GD fibroblasts, compared to control fibroblasts can be found in **Table 3.2** and distinct findings are further discussed below.

Table 3.2: Summary of findings in sporadic PD fibroblasts, as well as PD-GBA and PD-GD fibroblasts, compared to controls. LMP: lysosomal membrane permeability, GlcCer: glucosylceramide, GSLs: glycosphingolipids, GlcSph: glucosylsphingosine, Chol: cholesterol, Lys: lysosomal.

	GBA activity	Other enzyme activities	Lyso-Tracker	LAMP1	LMP	GlcCer	GSLs	GlcSph	Chol	Lys. pH
PD1	↓ 50%	↑ α-gal			↑					
PD2										
PD3	↓ 50%		(↑)	(↑)		↑	↑		↑	↑
PD4	↓ 50%	↑ α-gal				↑				↑
PD5										
PD-GBA	↓ (50%, het)		↓	(↑)					↑	
PD-GD	↓ (5%, hom)	↑ neu	(↑)	(↑)			(↑)	↑	↑	↑

GBA and GlcCer: Phenotype in sporadic PD fibroblasts

It has been unclear until now whether disease-relevant phenotypes can be seen in sporadic PD patient-derived fibroblasts, as there may be an excess of various underlying pathological mechanisms in these PD patients. Here, our major finding was that a subset of sporadic PD cell lines phenocopied PD-GBA patient-derived cells in their GBA activity and showed an approximately 50% reduction in GBA activity compared to controls

(**Figure 3.7**). Importantly, these results were verified in a larger cohort of sporadic PD patients by our collaborators at the Neuroregeneration Institute in Harvard (**Figure 3.7**). In our sporadic PD patient fibroblasts cohort, around half of the fibroblast lines showed deficits in GBA enzyme activity, which were comparable to PD-GBA fibroblasts (**Figure 3.7**). Furthermore, two of the three sporadic PD cell lines with low GBA activity showed increased levels of the GSL substrate GlcCer (**Figure 3.10**) and one of the three sporadic PD cell lines showed increased overall GSL load (Gb3+GM3 and LacCer, **Figure 3.10**). However, no changes in the levels of the GBA substrate GlcSph were observed in these sporadic PD cell lines (**Figure 3.11**).

Previously published reports showed no change in GBA activity in sporadic PD cases compared to control fibroblasts [172, 281]. However, these studies did not intensely focus on sporadic PD fibroblasts, analysing only a small number of patients. It is therefore possible that these studies missed the here observed GBA haploinsufficiency phenotype by chance. Interestingly, supporting our data, reduced GBA activity has been reported in studies with iPSC-derived dopaminergic neurons from sporadic PD patients [162, 282]. Increased GlcCer levels were not reported for sporadic PD fibroblasts until now. An accumulation of several GlcCer species was reported in GBA knock-out and GBA heterozygote mouse embryonic fibroblasts [283], suggesting that haploinsufficiency in GBA enzyme activity can indeed lead to an accumulation of its GSL substrate GlcCer. Supporting this view, significantly increased GlcCer levels were found in PD-GBA iPSC-derived dopaminergic neurons compared to control dopaminergic neurons [147]. A different study reported no accumulation of GlcCer in dopaminergic neurons derived from PD-GBA patients, but found an altered distribution of GlcCer species, resulting in an abnormal lipid profile [273]. Interestingly, decreased lysosomal GBA activity and increased hexosylceramide and hexosylsphingosine species have also been reported for iPSC-derived neurons carrying a triplication mutation for *SNCA* [282].

In general, these reports indicate that significantly reduced GBA activity can lead to GlcCer accumulation in numerous PD cell models.

We did not observe increased levels of GlcCer in the PD-Gaucher fibroblasts. This finding has previously been reported and it seems that GlcCer accumulation does not occur in Gaucher fibroblasts, although this phenomenon is still unexplained [284-287]. There are several possible explanations for the missing storage phenotype in GD fibroblasts: Firstly, the amount of GlcCer in fibroblasts is minor compared to the amount of GlcCer that is present in neuronal tissue. Secondly, the GSL metabolism and turnover rate is completely different between fibroblasts and neurons and it is very slow in fibroblasts, thus it is possible that no obvious storage occurs. Thirdly, there are 3 sub-types of Gaucher disease and our PD-GD cell lines are from the mildest version of Gaucher disease (type 1, non-neuronopathic). Thus, it is actually surprising that we see significantly increased GlcCer levels in two sporadic PD cell lines (PD3 and PD4), which also have decreased GBA activity.

In summary, the underlying cause for the observed GBA haploinsufficiency phenotype and the accumulation of GlcCer in these sporadic PD cell lines remains to be further investigated. A sub-classification of sporadic PD cell lines has previously only been attempted once, with the focus on mitochondrial dysfunction in a subset of sporadic PD fibroblasts, which resembled the mitochondrial dysfunction phenotype of LRRK2 mutant fibroblasts [269]. Here, focussing on GBA enzyme activity, a sub-classification of sporadic PD patients was also possible, underling common mechanisms in sporadic PD cases, but also demonstrating the heterogeneity of sporadic PD patients. This data may have potential implications as biomarkers for recruiting patients for clinical trials, as not all sporadic PD cases may respond the same way to novel treatments aiming at improving GBA activity (e.g. Ambroxol).

Lysosomal function in sporadic PD and PD-GBA fibroblasts

In this chapter, lysosomal volume was measured with two different methods based on LAMP1 immunocytochemistry or LysoTracker staining. LAMP1 immunocytochemistry revealed clustered and enlarged lysosomes with slightly increased mean fluorescence intensity in sporadic PD and PD-GBA patients in comparison to age-matched control patients (**Figure 3.4**). In contrast, LysoTracker fluorescence was found to be decreased in PD-GBA fibroblasts compared to control and sporadic PD fibroblasts (**Figures 3.1 and 3.2**), indicative of a decreased acidic compartment volume. Published studies have shown conflicting results with either no alteration in lysosomal mass in GD and PD-GBA fibroblasts (LysoID fluorescent probe and LAMP1 western botting) [270] or significant increase in lysosomal mass in PD-GBA fibroblasts (LysoTracker or LAMP1 microscopy and LAMP1 western blotting) [259, 272]. However, alterations in lysosomal morphology, e.g. enlargement and clustering, as we observed for both PD-GBA and sporadic PD fibroblasts, were already reported for PD-GBA fibroblasts [259, 272]. Interestingly, the lysosomal morphology defects were found to be age-dependent as they were not seen in older cohorts of PD-GBA fibroblasts (around 75-80 years old) anymore compared to a younger cohort of PD-GBA fibroblasts (55 years old) [259]. Our PD-GBA cohort had the average age of 66.4 years, thus it might be possible that alterations in lysosomal morphology and increases in lysosomal mass are not substantial anymore. To further support the presence of a lysosomal dysfunction phenotype in PD, an accumulation of lysosomes has been reported in iPSC-derived dopaminergic neurons from PD-GBA patients [147, 273].

LysoTracker probes consists of a fluorophore linked to a weak base, which makes them cell-permeant fluorescent acidotrophic probes for the selective labelling of acidic organelles. Upon entry into an acidic organelle, LysoTracker is protonated and the protonated form is less likely to cross the membrane again, leading to its sequestration in acidic organelles. It is important to note that LysoTracker fluorescence can be

influenced by other cellular parameters and a decrease in fluorescence could e.g. be due to increased lysosomal membrane permeability (LMP) or increased lysosomal pH. Pathogenic lysosomal depletion, which was found to be secondary to the abnormal permeabilisation of lysosomal membranes, has already been reported in PD mouse models and human PD substantia nigra tissue [260]. An investigation into LMP in our fibroblasts, based on staining of sugar-binding galectins, did not show increased LMP in the PD-GBA fibroblast lines compared to control fibroblasts (**Figure 3.5**). Interestingly, the sporadic PD1 cell line showed significantly increased LMP, which could be an underlying mechanism for neurodegeneration in this specific patient (**Figure 3.5**).

As LMP was not altered in PD-GBA cell lines, the lysosomal pH was investigated as another parameter with the ability to influence LysoTracker fluorescence. To measure the lysosomal pH we used LysoSensor Green DND-189. Similar to LysoTracker probes, the LysoSensor dyes are acidotrophic probes that accumulate in acidic organelles as the result of protonation. However, in the case of LysoSensor probes, this protonation also relieves a fluorescence quenching of the dye by its weakly basic side chain. Thus, the LysoSensor dyes exhibit a pH-dependent increase in fluorescence intensity upon acidification. However, in our fibroblast assays, we found that the LysoSensor fluorescence was not linear over the investigated pH range, but rather followed a second order (quadratic) equation with the lowest fluorescence intensity roughly around pH 5.5. This observation can only be explained by a chemical characteristic of the LysoSensor dye and/or the experimental set-up, rather than a true biological read-out.

As an example for severe lysosomal dysfunction, inhibition of the vacuolar proton pump (H^+-ATPase) by 100nM bafilomycin has been reported to increase the lysosomal pH from around 4.5 to around 6.5 in human and murine epithelial cells [288]. An example of a severe disorder affecting the lysosomal pH is the LSD Salla disease. The lysosomal pH in patient fibroblasts of this LSD has been observed to be around pH 6.0 [289]. Such altered pH values were not reasonably expected in our PD fibroblasts. Thus, standard

curve pH values ranging from 5.5-7.0 were disregarded for further analysis of the data, as their meaning was biologically irrelevant.

Following the observation of unchanged LMP in PD-GBA fibroblasts, we found that the lysosomal pH was also not altered in PD-GBA fibroblasts compared to control fibroblasts (**Figure 3.13**). However, the sporadic PD3 and PD4 fibroblast lines, which previously already showed a reduction in GBA activity and an accumulation of GlcCer, showed significantly increased lysosomal pH values (**Figure 3.13**). Interestingly, also PD-GD fibroblasts demonstrated a significant increase in the lysosomal pH (**Figure 3.13**). For future experiments, it would be advisable to confirm the results using a different assay for measuring lysosomal pH, e.g. based on LysoSensor Yellow/Blue dextran fluorescence. It exhibits blue fluorescence in neutral environments, but changes to predominantly yellow fluorescence in acidic organelles, thus dual-emission measurements could facilitate the ratio imaging of the pH in acidic organelles. Furthermore, the dextran conjugate is taken up by the cells through endocytosis and is very unlikely to exit the lysosomes.

It is important to note that LysoTracker fluorescence can also be influenced by lysosomal calcium levels. Calcium dysregulation has been strongly implicated in PD, with dopaminergic neurons being especially vulnerable to alterations in calcium homeostasis [147, 267, 290-295]. As examples, disruptions in calcium signalling have been shown in human mutant LRRK2 fibroblasts [267] and impaired calcium homeostasis has been demonstrated in PD-GBA iPSC-derived dopaminergic neurons [147]. Thus, it is crucial to investigate lysosomal, ER and global cytosolic calcium levels in our fibroblast cohort in future experiments. Interestingly, alterations in ER calcium release and reduced lysosomal calcium content have already been observed in PD patient fibroblasts carrying *GBA* mutations [259]. It would be interesting to investigate the role of calcium in sporadic PD fibroblasts and determine if there are again sub-populations in the sporadic PD cohort based on calcium alterations.

Finally, we explored whether cholesterol plays a role in PD by analysing cholesterol levels in our fibroblast cohort using Filipin. In healthy control fibroblasts, cholesterol staining with Filipin was diffuse throughout the cell (**Figure 3.12**). In contrast, Filipin staining was punctate and clustered in NPC fibroblasts (**Figure 3.12**), indicating lysosomal storage of cholesterol, which is a hallmark of Niemann-Pick type C disease. Interestingly, Filipin staining was also found to be punctate in some sporadic PD and PD-GBA fibroblast cell lines, as well as PD-GD fibroblasts, suggesting lysosomal accumulation of cholesterol in these cell lines (**Figure 3.12**). An increase in cholesterol has previously been shown in GBA knock-out and GBA heterozygote mouse embryonic fibroblasts [283]. Importantly, increased levels of cholesterol were also found in lysosomes of human PD-GBA fibroblasts, but not in sporadic PD fibroblasts [272]. However, our data suggests that cholesterol also accumulates in a subset of sporadic PD fibroblasts. Increased cholesterol can be regarded as a marker for dysfunctional lysosomes and/or impaired lysosomal maturation [285, 296]. Lysosomal cholesterol accumulation has also been shown to lead to retrograde transport of lysosomes, which could be an explanation for the observed clustered lysosomal phenotype in fibroblasts from sporadic PD and PD-GBA patients [59, 297]. It is possible that GBA deficiency might contribute to this phenotype through downstream effects of lysosomal dysfunction, impaired autophagy and alterations in GlcCer and other lipid species. Importantly, it has recently been shown that GBA also has a glucosyltransferase activity, which catalyses the formation of glucosylated cholesterol (cholesteryl-β-glucoside), supporting a possible link between GBA function and cholesterol metabolism [298]. Nevertheless, the exact reason for the cholesterol accumulation remains unknown, but it would be interesting to analyse NPC1 expression in these fibroblasts.

Having discovered several characteristics of lysosomal dysfunction in sporadic PD fibroblasts, it would be interesting to perform whole genome sequencing of the sporadic

PD fibroblast lines, with a focus on lysosomal genes, as a significantly increased burden of LSD gene variants was found in association with increased risk for PD [180].

Fibroblasts: A useful model?

In this chapter, we used human skin fibroblasts from PD patients as *in vitro* disease models for PD. It still is an essential step in pre-clinical research to test research hypotheses and therapeutics in easily accessible tissues, such as fibroblasts, to be able to determine the underlying pathological mechanisms of the disease and to test if and how patients will respond to new treatments. Here, we found disease relevant biomarker phenotypes in sporadic PD patient-derived fibroblasts, e.g. haploinsuffiency in GBA, accumulation of GSLs and increased lysosomal pH. This highlights the importance of the truthful representation of the cumulative cellular damage in sporadic PD patient fibroblasts in order to be able to perform valuable research [263]. In contrast, despite the significant contribution of PD animal models to our understanding of PD, none of these models truthfully reproduce the human condition [299].

However, the main disadvantage of fibroblasts is that they are non-neuronal cells, and their gene expression profile and signalling differ strongly from neurons [263]. Thus, dopaminergic neurons derived from iPSCs might be more useful to investigate the lysosomal system in PD: Besides GBA, we did not observe significant changes in four other lysosomal hydrolases in sporadic PD or PD-GBA fibroblasts compared to control fibroblasts (**Figure 3.8**). Published studies report conflicting results regarding alterations in β-galactosidase and β-hexosaminidase activity in PD-GBA fibroblasts [270, 272]. Besides inconclusive results in fibroblasts, it is likely that the metabolism of these enzymes and their GSL substrates is completely different in a neuronal setting. Accordingly, it has been shown that iPSC-derived dopaminergic neurons showed significantly higher enzyme activities compared with their originating iPSCs and fibroblasts, suggesting a key role of these enzymes in the differentiation and

maintenance of GSL expression in neurons [147]. Furthermore, a recent study highlighted the fundamental involvement of dopamine oxidation in the pathogenic cascade in PD leading to mitochondrial and lysosomal dysfunction and resulting in degeneration of dopaminergic neurons [162]. Thus, to investigate the involvement of lysosomes and GSLs in PD, iPSC-derived dopaminergic neurons may have several advantages. Nevertheless, fibroblasts are more robust, easier to handle and readily available compared to iPSC-derived neurons.

In summary, skin fibroblasts can be an important model for investigating and understanding basic processes involved in PD pathology and, as fibroblasts hardly express α-synuclein, this could potentially challenge the popular view that proteinopathy is the only trigger for neuronal death in PD. Furthermore, skin fibroblasts could play a significant role in future PD diagnosis and therapy and stratification for clinical trials.

4 Glycosphingolipids in the ageing mouse brain

4.1 Introduction

4.1.1 Ageing

Ageing is the biggest non-genetic risk factor for developing several neurodegenerative diseases, including Parkinson's disease (PD). Ageing is defined as the progressive and irreversible loss of function together with increasing mortality with advancing age [300]. It is believed that common cellular stresses (e.g. proteotoxic stress, oxidative stress, DNA damage) cause damaged or senescent cells to accumulate in various tissues over time, which may contribute to tissue dysfunction even within healthy ageing [300]. The brain is especially vulnerable to age-related changes, as alterations in multiple biological pathways may impair dopaminergic and other vulnerable terminally differentiated neurons, rendering it susceptible to Alzheimer's disease, Parkinson's disease and stroke [124]. For example, during normal ageing, the brain exhibits signs of impaired adaptive neuroplasticity and resilience, dysregulation of neuronal Ca^{2+} homeostasis, the accumulation of oxidatively modified molecules and organelles, and inflammation [124]. Importantly, cellular and molecular hallmarks of brain ageing, especially mitochondrial dysfunction and intracellular accumulation of oxidatively damaged proteins and lipids, clearly demonstrate the importance of effective cellular waste disposal mechanisms, i.e. autophagy-lysosome and proteasome functionality [124]. Oxidatively modified proteins are mostly targeted for proteasomal degradation by ubiquitination, while damaged membranes and mitochondria are targeted to lysosomes by the process of autophagy [104]. For example, ageing is associated with the accumulation of damaged mitochondria in dopaminergic neurons in the substantia nigra [301]. Several PD-associated gene mutations have been shown to impair mitochondrial function, including *PINK1* and *parkin*, which are involved in mitochondrial quality control and mitophagy [302]. It is therefore conceivable that with age, changes in multiple cell biological

pathways, such as those associated with lysosomal function and subsequently GSL homeostasis, may lead to cell dysfunction in vulnerable neurons and lower the threshold for developing PD [125].

When using the mouse as a model for ageing, it is important to think about the age relation between mice and humans [303]. Mice have a very short lifespan compared to humans, thus it is critical to compare and correlate the lifespan of mice versus humans. A mature adult mouse is 3-6 months old and compares to 20-30 years in humans, whereas a senescent mouse is 18-24 months old, which compares to 70-80 years in humans (The Jackson Laboratory) [303].

4.1.2 Genetic risk factor for PD: GBA

Genetic links to PD are well-described. For example, monogenic forms of the disease are caused by mutations in *SNCA*, *parkin*, and *LRRK2*. To date, one of the most common genetic risk factors of PD identified are mutations in *GBA*, causing haploinsufficiency of the enzyme glucocerebrosidase (GBA) [127]. GBA is a lysosomal hydrolase, which is responsible for the degradation of the GSLs glucosylceramide (GlcCer) and glucosylsphingosine (GlcSph). Outside the lysosome, GlcCer and GlcSph are degraded by the non-lysosomal glucocerebrosidase GBA2. Many studies combine lysosomal GBA and non-lysosomal GBA2 activities and therefore refer to a combined glucocerebrosidase (GCase) activity. Such combined GCase activity has been reported to be reduced in several brain regions of PD patients carrying a *GBA* mutation [163]. In addition, brain GCase activity has also been reported to be reduced in sporadic PD patients (without GBA mutation) compared to healthy controls, together with an increase in GlcSph levels [164]. This demonstrates an interesting biological resemblance to sporadic PD cases with GBA loss-of-function mutations-PD cases. A loss of GCase activity in PD has also been shown in the blood and CSF of PD patients [304, 305]. Importantly, an age-dependent reduction of GCase activity in several brain regions of

healthy subjects has also been reported [164]. By the time healthy individuals have reached the 7th to 8th decade of life, GCase activity in the substantia nigra and putamen was reduced to the same extent as in subjects with sporadic PD [164]. The potential implication of these findings is that haploinsufficiency of GBA is not only phenocopied in sporadic forms of PD, but also in the process of normal ageing.

GlcCer is the simplest GSL and the precursor of all more-complex GSLs. Increased GlcCer levels have been shown in primary cultured cortical neurons with GBA knockdown (approximately 50% GCase activity loss) and in dopaminergic neurons differentiated from induced pluripotent stem cells carrying heterozygote *GBA* mutations [147, 148]. It has been proposed that intracellular GlcCer levels control the formation of toxic α-synuclein assemblies in cultured neurons and mouse and human brain, leading to neurodegeneration [148]. GlcSph is the deacylated form of GlcCer. GlcSph levels have been shown to be directly neurotoxic, have been correlated with CNS involvement in GD patients and have been shown to promote α-synuclein pathology in GBA-associated PD [153, 306, 307].

4.1.3 Complex GSLs in PD

Addition of oligosaccharides and N-acetylneuraminic acid to GlcCer give rise to a broad range of very complex GSLs, including the gangliosides. Gangliosides are the pre-dominant GSLs in the CNS of all mammals and are highly enriched in cell membranes of neurons [40, 202]. Gangliosides, particularly GM1a, are essential for myelination, neuritogenesis, synaptogenesis, transmission of nervous impulses and stability of synapses [42, 43]. With respect to changes in complex GSLs in the human brain during normal ageing, previous reports have indicated alterations to several complex gangliosides in multiple brain regions, including reduced GM1a and GD1a [308, 309]. Concerning GSLs in normal ageing in wildtype mice, or murine models of accelerated

senescence, two reports have indicated increased GM1a brain ganglioside content, whereas levels of GD1a, GD1b and GT1b were reduced [310, 311].

We were interested whether PD- and ageing-induced changes to GSL homeostasis and changes in either, or both, lysosomal GBA and non-lysosomal GBA2 activity in the brain could be reflected in other non-human mammalian systems. This is important for investigating and understanding processes involved in normal brain ageing and could potentially also challenge the popular view that proteinopathy is the only trigger for neuronal death in PD. Furthermore, besides investigating GlcCer and GlcSph levels, we focused on more complex gangliosides, because of their important biological, neurotrophic functions in the CNS.

The aims of this experimental chapter are therefore:

- To determine levels of GlcCer and GlcSph in the ageing brain of wildtype mice of three different strains.
- To analyse levels of gangliosides in the ageing brain of wildtype mice of three different strains.
- To assess various lysosomal hydrolase activities in the ageing brain of wildtype mice of three different strains.
- To evaluate proteolytic impairments and levels of α-synuclein in the ageing brain of wildtype FVB/N mice.
- To assess the number of dopaminergic neurons and microglia in BALB/c mouse brain with ageing.

Most of the data of this experimental chapter have been published in [312].

4.2 Materials and Methods

4.2.1 Animals

All animal procedures in Harvard were performed in accordance with the guidelines of the National Institute of Health and were approved by the Institutional Animal Care and Use Committee at McLean Hospital, Harvard Medical School. All procedures conducted in Oxford were performed according to the Animals (scientific Procedures) Act 1986 under a project licence from the UK Home Office (PPL No. P8088558D). Animals were housed according to standard conditions, in a dark/light cycle of 12 hours, with ad-libitum access to food and water.

For LC-MS/MS analysis, male BDF1 (mixed C57/BL/6-DBA-2 background; Charles River, MA, USA) wildtype mice at 2 months (n=4) and 12 months (n=6) of age were used. Male (n=20) and female (n=36) FVB/N wildtype mice between 1.5-24 months of age (The Jackson Laboratory, ME, USA) were used for NP-HPLC and biochemistry analysis. Furthermore, a cohort of BDF1 male wildtype mice aged 3-4 months (n=6) and 17-18 months (n=7) was used for NP-HPLC and biochemistry analysis. Finally, male and female BALB/c wildtype mice at 1-2 months (n=13) and 20-21 months (n=9) (The Jackson Laboratory, Charles River, UK) were used. Mice were terminally anesthetised by intraperitoneal injection of sodium pentobarbital (130 mg/kg) and intracardially perfused with heparinised saline. Brains were rapidly dissected and stored at -80°C or immediately homogenised in water using a handheld Ultraturax T25 probe homogeniser (IKA, Germany) and aliquoted before being stored at -80°C.

4.2.2 LC-MS/MS analysis for GlcCer and GlcSph

Quantification of GlcCer and GlcSph levels in brain homogenates of BDF1 mice using liquid chromatography/tandem mass spectrometry (LC-MS/MS) was performed as

previously described [313]. Data provided by Prof. Penelope Hallett, Neuroregeneration Institute, McLean Hospital/Harvard Medical School, MA, USA.

4.2.3 Glycosphingolipids (NP-HPLC)

GlcCer and downstream GSLs were analysed as previously described in **Chapters 2.2.6 and 3.2.7**.

4.2.4 Sphingosine and glucosylsphingosine (RP-HPLC)

As detailed in **Chapter 3.2.8**.

4.2.5 Cholesterol

Total cholesterol (free cholesterol and cholesteryl esters) in murine whole-brain homogenates was quantified using the Amplex Red Cholesterol Assay Kit (Thermo Fisher Scientific, UK), according to manufacturer's instructions. Results were normalized to protein content.

4.2.6 Lysosomal hydrolase activity assays

As detailed in **Chapter 3.2.6**.

4.2.7 Western blotting

Western blot experiments were performed by Dr. Oeystein Brekk, Neuroregeneration Institute, McLean Hospital/Harvard Medical School, MA, USA. Whole-brain homogenates of mice were thawed on ice with protease and phosphatase inhibitors added (Halt Protease & Phosphatase Inhibitor Cocktail (100X), Thermo Fisher Scientific). Lysis was carried out for 30min on ice in lysis buffer (150mM NaCl, 50mM

Tris pH 7.6, 1% TritonX-100, 2mM EDTA), and the lysates sonicated for 30 seconds (5 second pulses, on ice). Membrane-enriched fractions were pelleted in 1% Triton-X by ultracentrifugation (100,000g, 1h, 4°C), and reconstituted in lysis buffer supplemented 2% SDS. Further insoluble materials were pelleted at 100,000g (1h, room temperature), and the supernatant utilized in subsequent experiments. Equal amounts of protein were separated using polyacrylamide gel electrophoresis. Primary antibodies were antibodies to LAMP2A (1:1000, ab18528, abcam), LC3 (1:1000, PM036, MBL Life Science), p62/SQSTM1 (1:1000, PM045, MBL Life Science), ubiquitin (1:5000, Z0458, DAKO), SNCA/syn-1/α-synuclein (1:1000, 619787, BD Biosciences) and GAPDH (1:2000, AB2302, Milipore Sigma). The intensities of the immunoreactive bands were analysed using the gel analyser suite in ImageJ (v1.7).

4.2.8 Immunohistochemistry

BALB/c wildtype mice at 2-months and 21-months of age were euthanised and immediately transcardially perfused with 4% paraformaldehyde (PFA) in PBS. The brains were dissected, post-fixed for 24h in 4% PFA, and transferred to 30% sucrose until the tissues lost buoyancy. Sectioning and immunohistochemistry was performed by Dr. Elena-Raluca Nicoli (NIH, Bethesda, US). The brains were cut with a cryostat (30 µm sagittal sections) and sections were collected in PBS with 0.25% Triton-X100. Sections were incubated with rabbit anti-tyrosine hydroxylase (TH) (1:500, Novus, NB300-109) and rat anti-CD68 (1:500, BioRad, MCA1957) primary antibodies, detected using DyLight 594 goat anti-rabbit IgG (1:1000, Thermo Fisher, 35560) and Alexa-488 conjugated donkey anti-rat IgG (1:1000, Thermo Fisher, A-21208) secondary antibodies respectively, and counterstained with Hoechst. Incubation with primary antibodies was performed overnight at 4 °C in PBS with 1.5% serum and 0.25% Triton X-100. After washing, the sections were incubated for 1h at room temperature with secondary antibodies. After washing, the stained sections were mounted on microscope slides with

Tris–glycerol supplemented with 10% Mowiol (Calbiochem, La Jolla, CA) to reduce fading of fluorescence. Images were captured using a confocal laser scanning microscope (Zeiss LSM 780 AxioObserver). Channel settings were as follows: Hoechst-channel: 405nm excitation, 447nm emission; green channel: 488nm excitation, 522nm emission; red channel: 561nm excitation, 640nm emission. One plane tile scan (10x) was used for imaging the whole brain and z-stack tile scan (20x) was used for imaging a close-up of the substantia nigra region.

4.2.9 Statistical analysis

All statistical analyses were performed with GraphPad Prism 7.0 (GraphPad, San Diego, CA). Unpaired student's *t*-test was used to compare two groups and correlations were analysed with Pearson correlation analysis.

4.3 Results

4.3.1 Accumulation of GlcCer and GlcSph in the brain of wildtype mice during normal ageing

We were interested in studying the levels of glucosylceramide (GlcCer) and glucosylsphingosine (GlcSph) in the brain of wildtype mice during ageing. For this, whole-brain homogenates from wildtype (WT) BDF1 mice were collected at 2 and 12 months of age, and liquid chromatography/tandem mass spectrometry (LC-MS/MS) was used to measure levels of GlcCer and GlcSph (**Figure 4.1A, B and C**). A significant increase in both GlcCer (147.3%, $p<0.01$) and GlcSph (175.4%, $p<0.01$) was observed in the brains of 12-month-old mice compared to 2-month-old mice (**Figure 4.1B and C**). Next, to establish whether the ageing-induced increase in GlcCer was also observed in a different inbred mouse strain, whole-brain homogenates from FVB/N mice between 1.5 and 24 months of age were used for normal-phase high-performance liquid chromatography (NP-HPLC) analysis of GlcCer. Increasing age was significantly correlated with GlcCer levels (**Figure 4.1D**, r=0.8095, $p<0.0001$). In mice at 17-24 months of age, GlcCer levels were increased to 163.8% of young mice aged 1.5-3 months (**Figure 4.1E**, $p<0.0001$). Interestingly, levels of LacCer were also significantly correlated with age (**Figure 4.1F**, r=0.6832, $p<0.0001$) in brains of FVB/N mice. At 17-24 months of age, levels of LacCer were increased to 148.7% of levels detected in wildtype brain at 1.5-3 months of age (**Figure 4.1G**, $p<0.0001$).

To confirm the LC-MS/MS results, GlcSph levels were measured in whole-brain homogenates from young (3 months) and old (24 months) FVB/N mice using RP-HPLC (**Figure 4.2**). Furthermore, sphingosine and sphinganine levels were measured with this method. There was no difference in C18-sphingosine levels in brains of young and old FVB/N mice (**Figure 4.2A**), but a significant decrease in sphinganine levels in brains of 24-month-old animals in comparison to 3-month-old animals was detected (**Figure 4.2B**,

64.0%, p<0.01). Importantly, a significant increase in C18-GlcSph was observed in the brains of 24-month-old mice compared to 3-month-old mice, confirming LC-MS/MS results (**Figure 4.2C**, 182.6%, p<0.01).

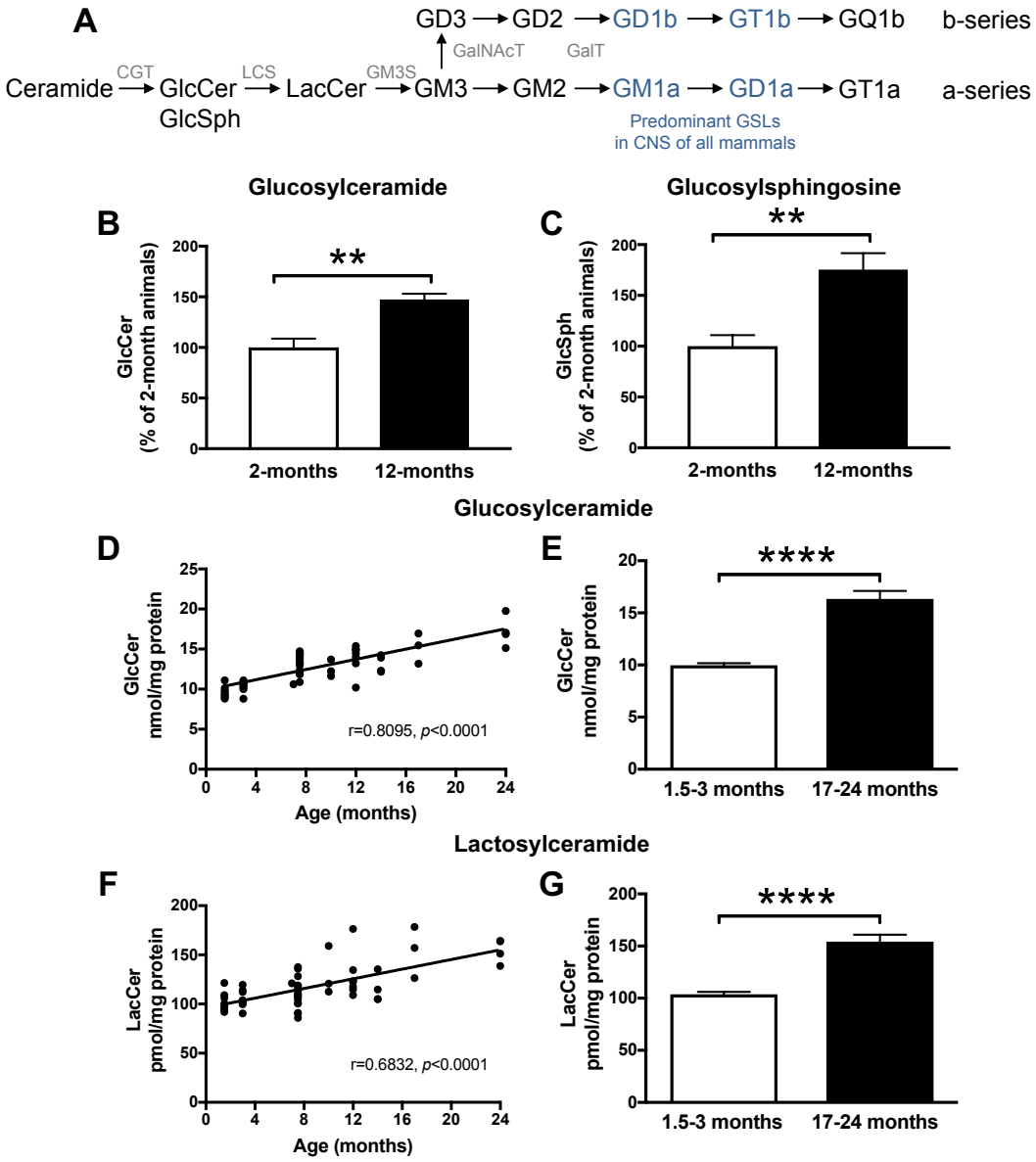

Figure 4.1: GlcCer, GlcSph, and LacCer levels are increased with age in brains of WT FVB and BDF1 mice. (A) Biosynthetic pathway of GSLs. Abbreviations: CGT, ceramide glucosyl transferase; LCS, lactosylceramide synthase; GM3S, GM3 synthase; GalNAcT, N-acetylgalactosamine transferase; GalT, galactosyl transferase (B, C) Whole-brain homogenates from WT BDF1 mice at 2 (n=4) and 12 (n=6) months of age were used to determine GlcCer (B) and GlcSph (C) levels using LC-MS/MS (** = p<0.01, unpaired t-test). (D, F) Whole-brain homogenates from WT FVB mice between 1.5-24 months of age (n=56) were used to determine GlcCer (D) and LacCer (F) levels using NP-HPLC. Data were analysed using Pearson correlation analysis. (E, G) Comparison of GlcCer (E) and LacCer (G) levels in brains of young (1.5-3 months, n=16) and aged (17-24 months, n=7) WT FVB mice (**** = p<0.0001, unpaired t-test). Data are presented as mean ± SEM.

To test whether cholesterol changes with ageing, cholesterol levels were measured in brain homogenates from young (3 months) and old (24 months) FVB/N mice using the Amplex Red kit. No difference in cholesterol was detected (**Figure 4.3**).

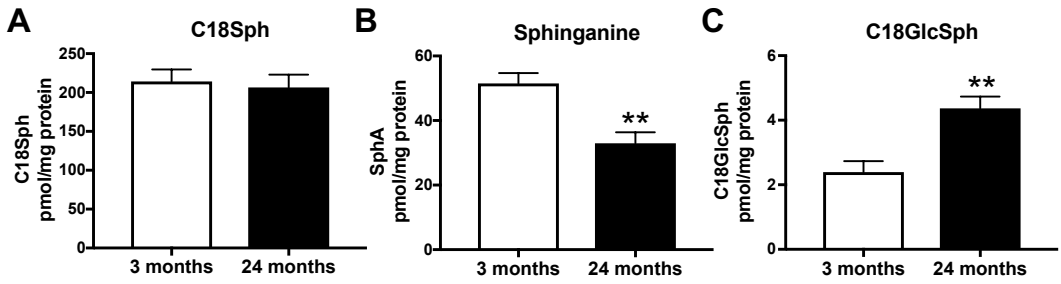

Figure 4.2: Sphingosine, sphinganine and glucosylsphingosine levels in brains of aged FVB WT mice. C18-sphingosine (A), sphinganine (B) and C18-glucosylsphingosine (C) levels in whole-brain homogenates of young (3 months, n=6) vs. old (24 months, n=4) mice were analysed using RP-HPLC (** = p<0.01, unpaired t-test). Data are presented as mean ± SEM.

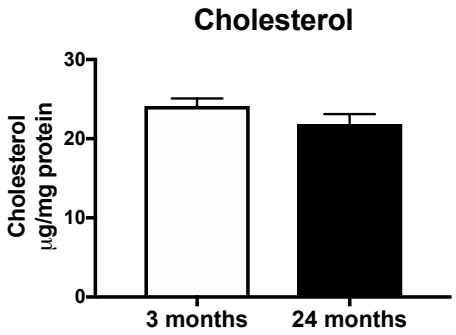

Figure 4.3: Brain cholesterol levels are not changed with normal ageing in WT FVB mice. Comparison of total cholesterol levels in whole-brain homogenates of young (3 months, n=6) vs. old (24 months, n=4) mice (not significant, unpaired t-test). Cholesterol levels were analysed with Amplex Red kit. Data are presented as mean ± SEM.

4.3.2 Changes in levels of complex gangliosides are associated with normal ageing of the FVB/N mouse brain

To evaluate whether ageing induced a selective increase in levels of brain GlcCer, GlcSph and LacCer, levels of complex gangliosides were measured with NP-HPLC. The major GSLs found in the mammalian nervous system are GM1a, GD1a, GD1b and GT1b. Levels of GM1a were significantly increased with age in mouse brain (**Figure 4.4A**, r=0.8566, p<0.0001). At 17-24 months, GM1a levels were increased to 134.0% of levels at 1.5-3 months of age (**Figure 4.4B**, p<0.0001). Conversely, GD1a, GD1b and

GT1b levels were all negatively correlated with age (**Figure 4.4C, E, G**; GD1a: r=0.6494, p<0.0001; GD1b: r=-0.3624, p<0.01; GT1b: r=-0.7519, p<0.0001). In brains of mice at 17-24 months of age, GD1a, GD1b and GT1b were all significantly reduced compared to ganglioside levels in mice at 1.5-3 months of age (**Figure 4.4D, F, H**; GD1a: 74.9%, p<0.0001; GD1b: 86.5%, p<0.001; GT1b: 55.6%, p<0.0001). Exemplary NP-HPLC traces of GlcCer and ganglioside levels in brain homogenates of 3-month and 24-month old WT FVB mice are shown in **Figure 4.5**.

In summary, levels of GM1a increase, whereas levels of GD1a, GD1b and GT1b decrease concomitantly in brains of FVB/N wildtype mice with normal ageing.

4.3.3 Total brain GSL load is increased with age in wildtype FVB/N mice

To evaluate whether total brain GSL load changes with age, GlcCer, LacCer and ganglioside levels were summed (**Figure 4.6**). The level of total GSLs was significantly correlated with age (**Figure 4.6A**, r=0.7887, p<0.0001), and total GSL levels in 17-24 months old FVB/N mice were increased to 136.8% of those measured in 1.5-3 months old mice (**Figure 4.6B,** p<0.0001).

4.3.4 Age-dependent alterations in GSL levels are conserved across different strains of wildtype mice

To assess whether the alterations in glycosphingolipid levels (e.g. increase in GlcCer, GlcSph and GM1a) in brain during normal ageing is a phenomenon specific for wildtype FVB/N mice, we performed the same lipidomic analyses of whole-brain homogenates of wildtype BALB/c mice at 1-2 months and 20-21 months of age and wildtype C57BL/6-DBA/2-BDF1 mice at 3-4 months and 17-18 months of age.

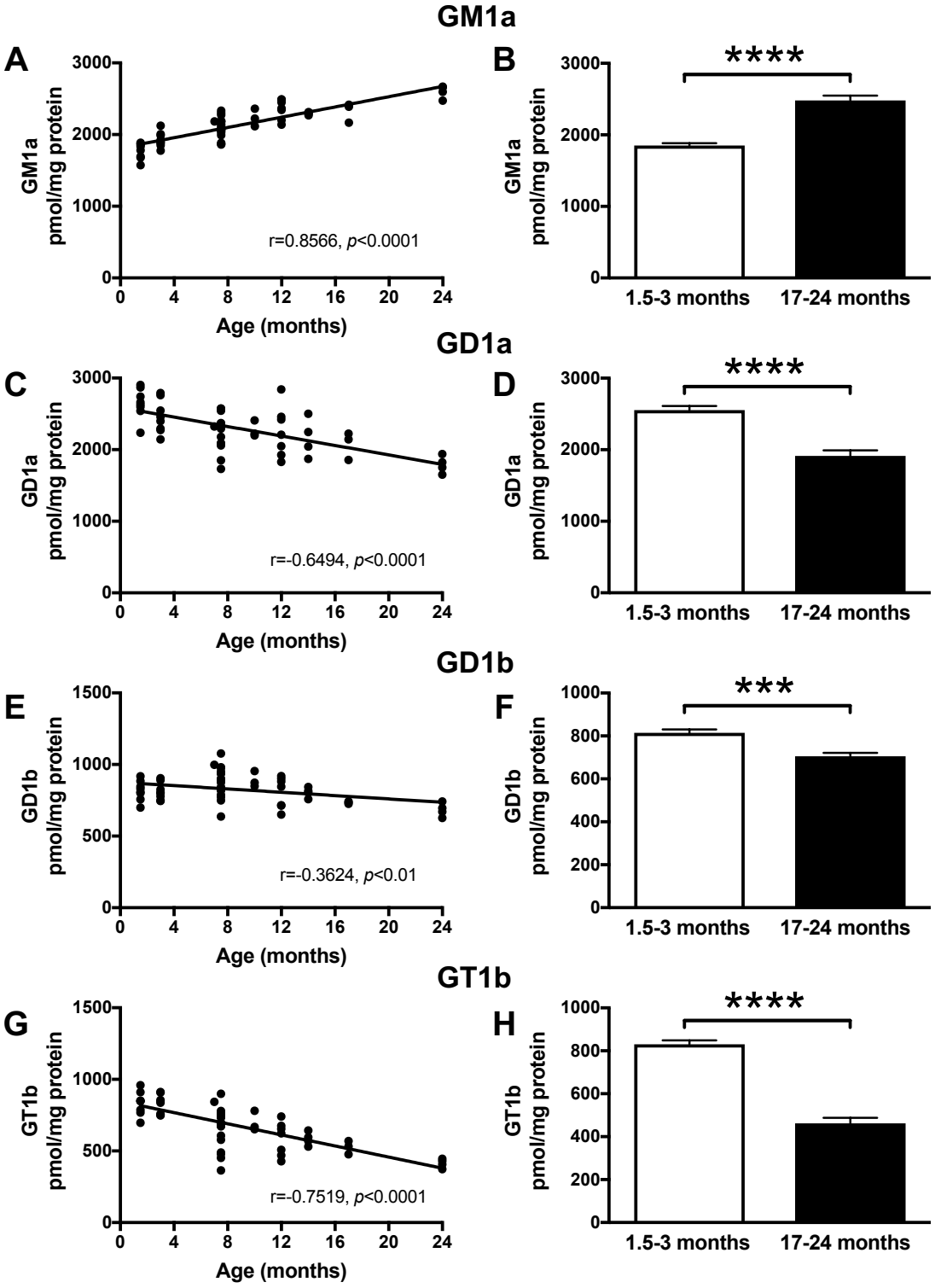

Figure 4.4: Altered levels of gangliosides with normal ageing in WT FVB mice. Whole-brain homogenates from WT FVB mice between 1.5-24 months of age were used to determine levels of GM1a (A, B), GD1a (C, D), GD1b (E, F), and GT1b (G, H) with NP-HPLC. Data were analysed using Pearson correlation analysis (A, C, E, G) (n=56) and unpaired t-test (B, D, F, H) (n=16, 1.5-3 months; n=7, 17-24 months; *** = $p<0.001$; **** = $p<0.0001$).

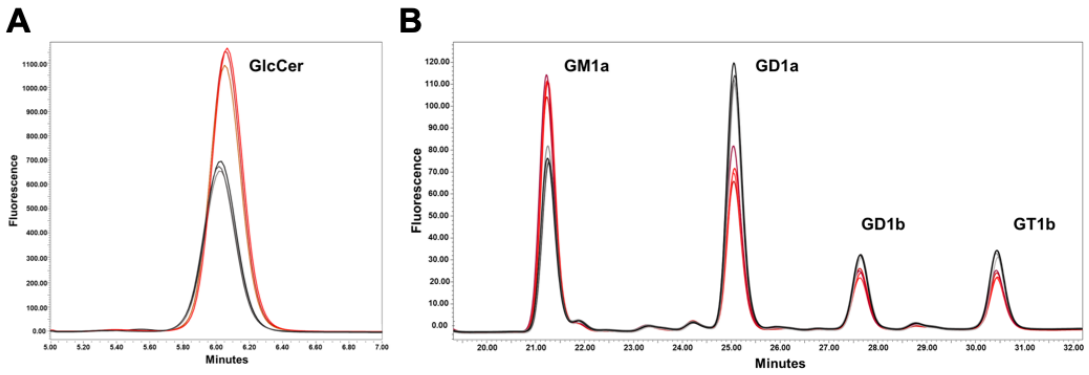

Figure 4.5: HPLC traces of GlcCer and gangliosides GM1a, GD1a, GD1b and GT1b extracted from brain homogenates of 3-month and 24-month old WT FVB mice. Exemplary HPLC traces of (A) GlcCer and (B) gangliosides of 3 months old WT FVB mice are shown in grey and 24 months old WT FVB mice are shown in red (n=3-4).

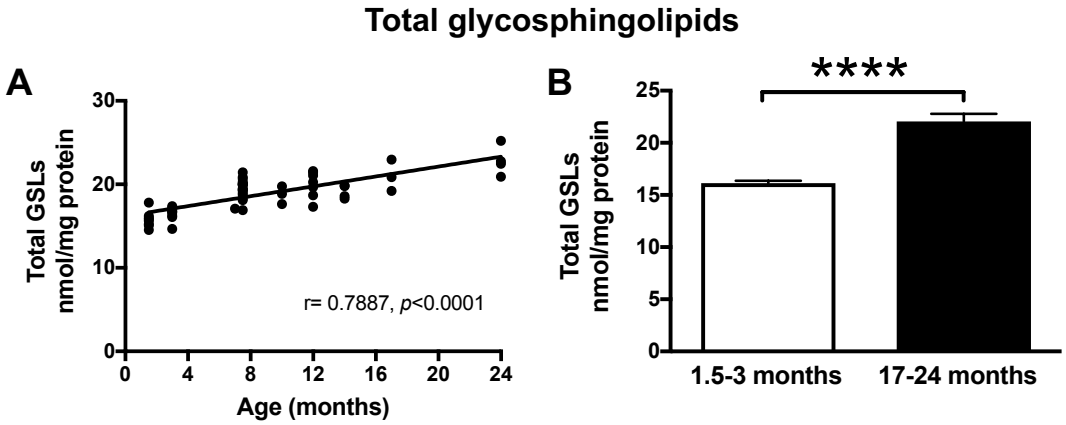

Figure 4.6: Normal ageing increases total levels of GSLs in the brain. (A) Pearson correlation analysis of total GSL levels in whole-brain homogenates from WT FVB mice at 1.5-24 months of age (n=56) shows that normal ageing in mice is associated with increased load of GSLs with age. (B) Comparison of total GSL levels in young (1.5-3 months, n=16) vs. old mice (17-24 months, n=7) (**** = p<0.0001, unpaired t-test).

In accordance with previous results, a significant increase in GlcCer and LacCer in wildtype BALB/c mice was observed in the brains of old mice compared to young mice (**Figure 4.7A, B**, GlcCer: p<0.0001, LacCer: p<0.0001). Levels of GM1a were significantly increased with age in wildtype BALB/c mouse brains (**Figure 4.7C**, p<0.0001). Conversely, in old BALB/c mice, GD1a, GD1b and GT1b were all significantly reduced compared to young mice (**Figure 4.7D-F**, GD1a: p<0.0001, GD1b: p=0.0005, GT1b: p<0.0001). The level of total GSLs in 20-21 months old BALB/c mice was increased to 163% of those measured in 1-2 months old animals (**Figure 4.7G**,

p<0.0001). Further supporting previous results, no difference in C18-sphingosine levels in brains of young and old BALB/c mice was observed (**Figure 4.8A**), but a significant decrease in sphinganine levels and a significant increase in C18-GlcSph levels was detected in brains of 21-month-old mice in comparison to 2-month-old BALB/c mice using RP-HPLC (**Figure 4.8B, C**, *p*=0.0010 and *p*=0.0076, respectively). No difference in cholesterol in brain homogenates of young and old BALB/c wildtype mice was detected (**Figure 4.8D**).

Next, confirming previous results, a significant increase in GlcCer and LacCer was observed in the brains of old wildtype C57BL/6-DBA/2-BDF1 mice compared to young mice (**Figure 4.9A, B**, GlcCer: *p*=0.0021, LacCer: *p*=0.0059). Levels of GM1a were significantly increased with age in mouse brain of the C57BL/6-DBA/2-BDF1 strain (**Figure 4.9C**, *p*<0.0001). In contrast, in old C57BL/6-DBA/2-BDF1 mice, GD1a, GD1b and GT1b were significantly reduced compared to young mice (**Figure 4.9D-F**, GD1a: *p*=0.0237, GD1b: *p*=0.1011, GT1b: *p*=0.0176). Total GSL levels in 17-18 months old C57BL/6-DBA/2-BDF1 mice were increased to 127.6% of those measured in 3-4 months old animals (**Figure 4.9G**, *p*=0.0017). Again, supporting previous results, no difference in C18-sphingosine levels in brains of young and old C57BL/6-DBA/2-BDF1 mice was observed (**Figure 4.10A**). However, a significant decrease in sphinganine levels and a significant increase in C18-GlcSph levels was detected in brains of 17-18-month-old mice in comparison to 3-4-month-old C57BL/6-DBA/2-BDF1 mice using RP-HPLC (**Figure 4.10B-C**, *p*=0.0114 and *p*=0.0060, respectively). No difference in cholesterol in brain homogenates of young and old C57BL/6-DBA/2-BDF1 wildtype mice was detected (**Figure 4.10D**).

To summarise, age-dependent changes in levels of specific GSLs are conserved across different strains of wildtype mice.

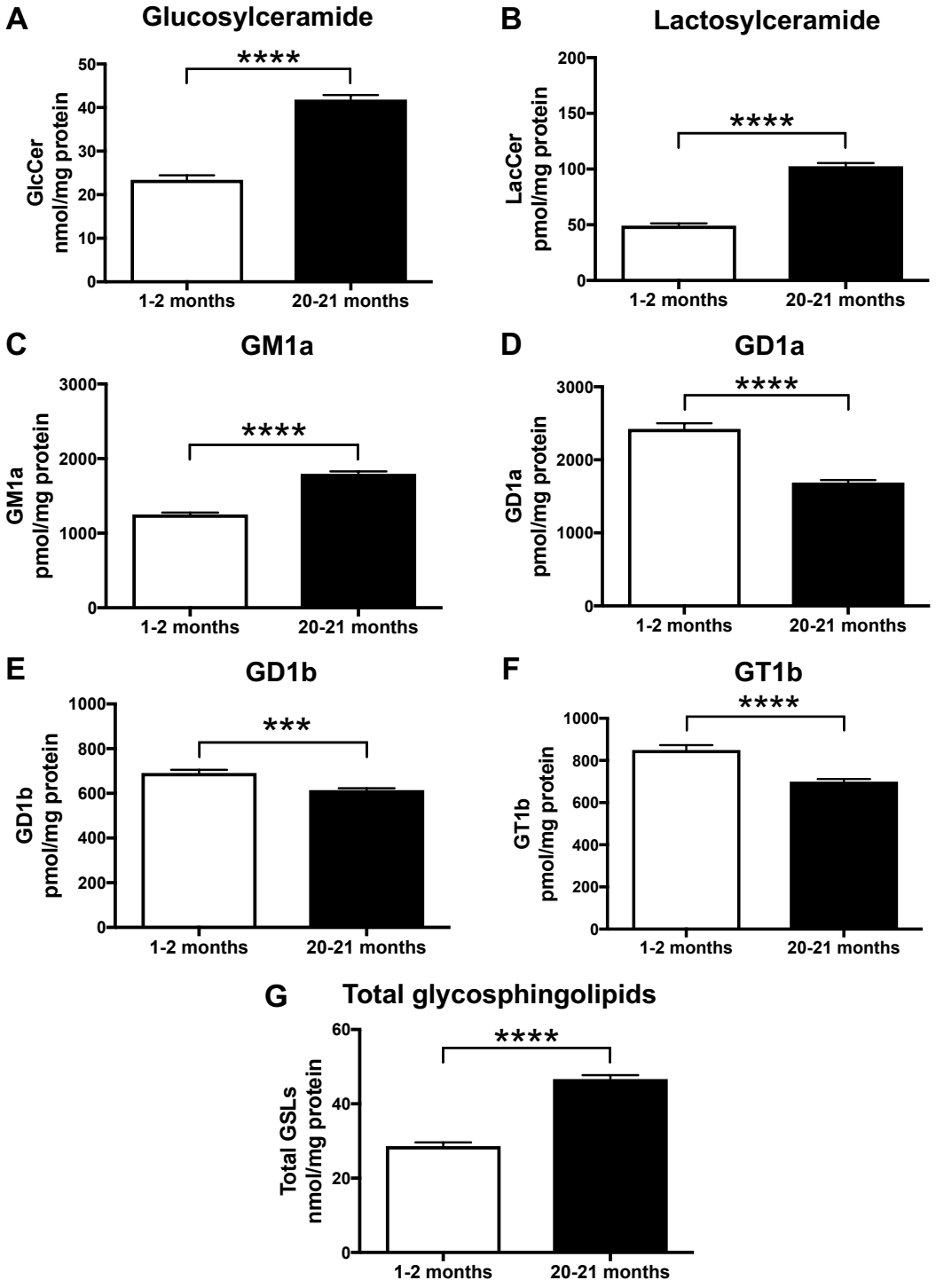

Figure 4.7: GlcCer, LacCer, and GM1a levels are increased in brains of old WT BALB/c mice, whereas levels of GD1a, GD1b, and GT1b are decreased with age. Whole-brain homogenates of WT BALB/c mice at 1-2 months and 20-21 months of age were used to determine levels of GlcCer (A), LacCer (B), GM1a (C), GD1a (D), GD1b (E), GT1b (F) and total GSLs (G) using NP-HPLC. Data were analysed using unpaired t-test (n=13, 1-2 months; n=9, 20-21 months; *** = $p<0.001$, **** = $p<0.0001$). Data are presented as mean ± SEM.

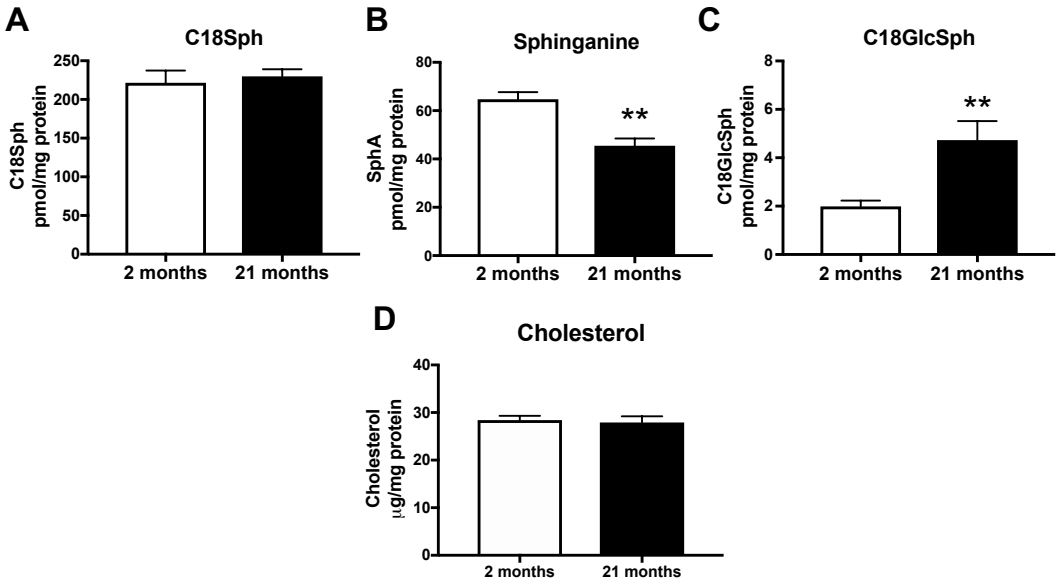

Figure 4.8: Sphingosine, sphinganine, glucosylsphingosine and cholesterol levels in brains of aged BALB/c WT mice. (A-C) C18-sphingosine (A), sphinganine (B) and C18-glucosylsphingosine (C) levels in whole-brain homogenates of young (2 months, n=6) vs. old mice (21 months, n=6) were analysed using RP-HPLC (** = $p<0.01$, unpaired t-test). (D) Total cholesterol levels in whole-brain homogenates of young (2 months, n=6) vs. old mice (21 months, n=6) were determined with Amplex Red kit (not significant, unpaired t-test). Data are presented as mean ± SEM.

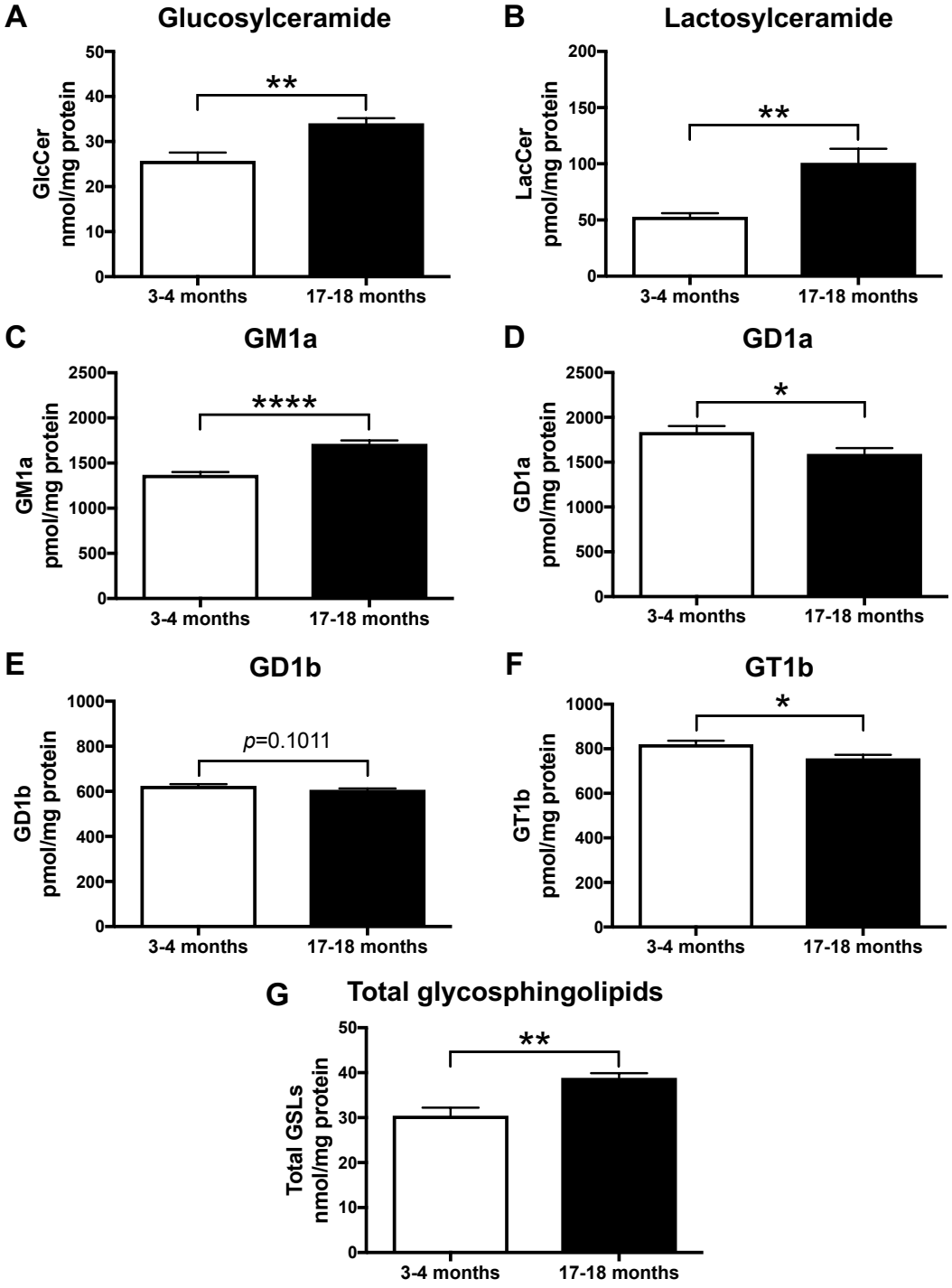

Figure 4.9: GlcCer, LacCer, and GM1a levels are increased in brains of old WT BDF1 mice, whereas levels of GD1a, GD1b, and GT1b are decreased with age. Whole-brain homogenates of WT C57BL/6-DBA/2-BDF1 mice at 3-4 months and 17-18 months of age were used to determine levels of GlcCer (A), LacCer (B), GM1a (C), GD1a (D), GD1b (E), GT1b (F)and total GSLs (G) using NP-HPLC. Data were analysed using unpaired t-test (n=6, 3-4 months; n=7, 17-18 months; * = p<0.05, ** = p<0.01, **** = p<0.0001). Data are presented as mean ± SEM.

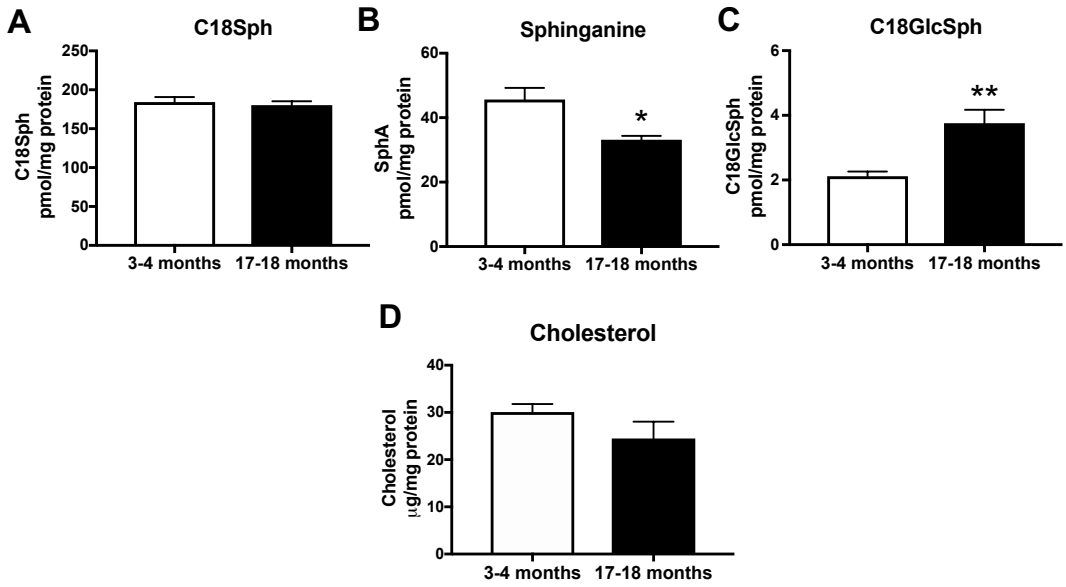

Figure 4.10: Sphingosine, sphinganine, glucosylsphingosine and cholesterol levels in brains of aged BDF1 WT mice. (A-C) C18-sphingosine (A), sphinganine (B) and C18-glucosylsphingosine (C) levels in whole-brain homogenates of young (3-4 months, n=5) vs. old (17-18 months, n=5) C57BL/6-DBA/2-BDF1 mice were analysed using RP-HPLC (* = $p<0.05$, ** = $p<0.01$, unpaired t-test). (D) Total cholesterol levels in whole-brain homogenates of young (3-4 months, n=5) vs. old mice (17-18 months, n=5) were determined with Amplex Red kit (not significant, unpaired t-test). Data are presented as mean ± SEM.

4.3.5 Reduced glucocerebrosidase and increased neuraminidase activities in brains of aged wildtype mice

The observed increase in GlcCer and GlcSph levels in the ageing mouse brain could be due to a decrease in the activity of their degrading enzymes, β-glucosidases GBA and GBA2. In addition, not all GSLs are necessarily exclusively formed from *de novo* biosynthesis as they can be recycled as well as remodelled by neuraminidases. It is interesting to note that the increase in GM1a may likely be a result of sequential removal of sialic acid residues from GD1a, GD1b and GT1b by neuraminidases, explaining their selective concomitant reduction with ageing. Consequently, the activities of various lysosomal hydrolases were assayed in whole-brain homogenates of 3-month and 24-month old WT FVB mice (n=4 per age). Activities of lysosomal β-glucosidase (GBA) and non-lysosomal β-glucosidase (GBA2) were measured independently. A significant decrease in GBA β-glucosidase activity was observed in brain homogenates of 24-

month old WT FVB/N mice compared to 3-month old WT FVB/N mice (**Figure 4.11A**, *p*=0.0007, 17% reduction). In addition, a significant decrease in GBA2 β-glucosidase activity was observed in brain homogenates of aged WT FVB/N mice compared to young WT FVB/N mice (**Figure 4.11B**, *p*=0.0292, 13% reduction). There was no difference in α-galactosidase or β-hexosaminidase activity in brain homogenates of 3-month and 24-month old WT FVB/N mice (**Figure 4.11C, D**). However, a significant decrease in β-galactosidase activity was observed in brain homogenates of 24-month old WT FVB/N mice compared to 3-month old WT FVB/N mice (**Figure 4.11E**, *p*=0.0103, 12% reduction). Furthermore, a significant increase in neuraminidase activity was observed in brain homogenates of old WT FVB/N mice compared to young WT FVB/N mice (**Figure 4.11F**, *p*=0.0247, 38% increase).

Next, we measured the activity of these hydrolases in two independent mouse strains, BALB/c and C57BL/6-DBA/2-BDF1. Confirming previous results, a significant decrease in GBA β-glucosidase activity in both strains was observed in brains of old animals compared to young animals (**Figures 4.12A and 4.13A**, *p*=0.0008 and *p*=0.0011, respectively). Additionally, a significant decrease in GBA2 β-glucosidase activity was observed in brain homogenates of aged mice compared to young mice of both strains (**Figures 4.12B and 4.13B**, *p*=0.0035 and *p*=0.0497, respectively). There was no difference in α-galactosidase or β-hexosaminidase activity in brain homogenates of young and old mice of both strains (**Figures 4.12C, D and 4.13C, D**). However, in accordance with previous results, a significant decrease in β-galactosidase activity in brain homogenates of old BALB/c mice was observed compared to young mice (**Figure 4.12E**, *p*=0.0165). Furthermore, supporting results from FVB/N mice, a significant increase in neuraminidase activity was observed with age in the mouse brain of both BALB/c and C57BL/6-DBA/2-BDF1 strains (**Figures 4.12F and 4.13F**, *p*=0.0028 and *p*=0.0074, respectively).

To summarise, a decrease in both GBA and GBA2 β-glucosidase activities and a decrease in β-galactosidase activity, together with an increase in neuraminidase activity take place in the murine FVB/N brain with normal ageing. Importantly, we confirm these age-dependent changes in two independent mouse strains, BALB/c and BDF1.

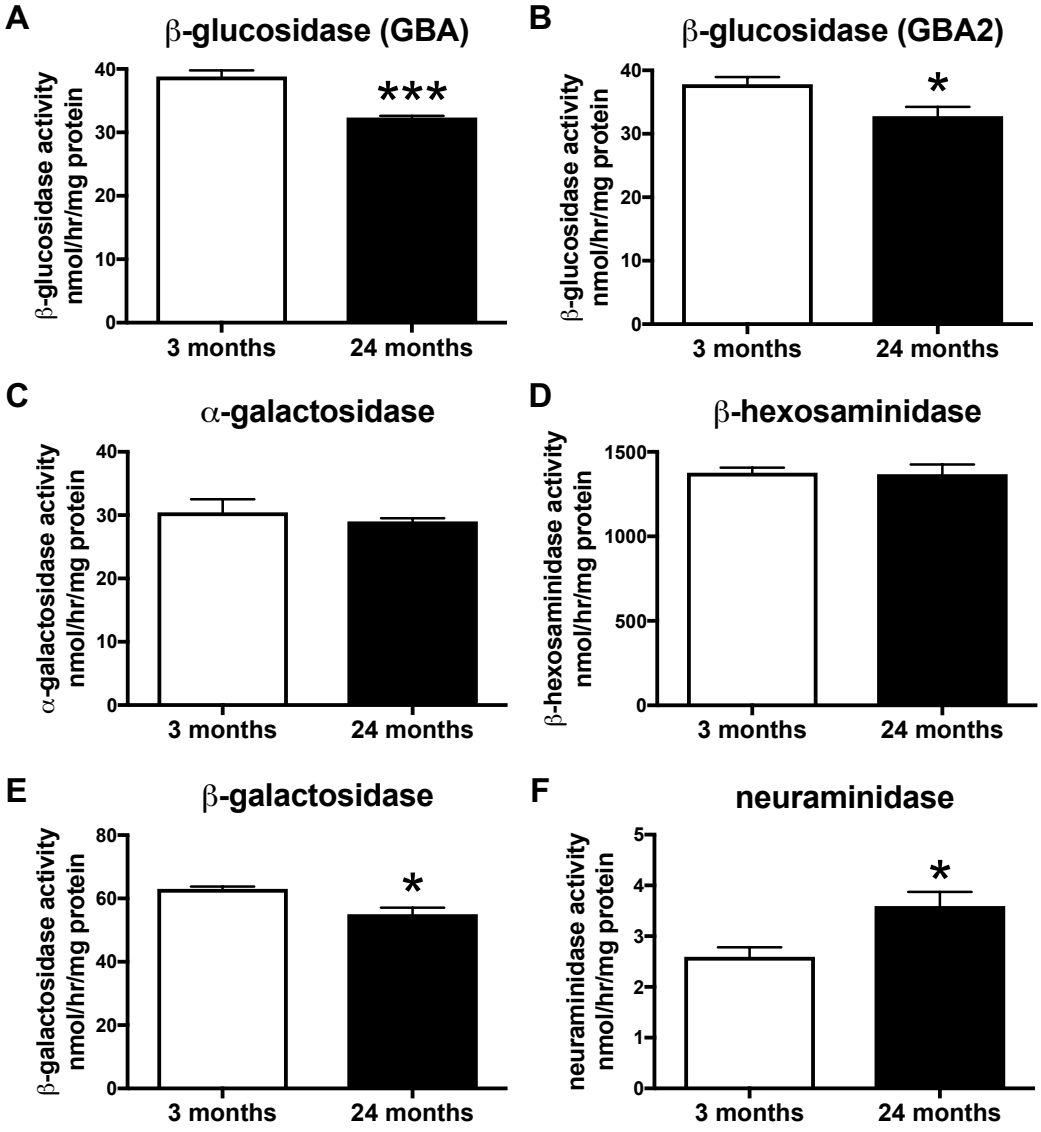

Figure 4.11: Reduced GBA, GBA2 and β-galactosidase activities and increased neuraminidase activity in the brain of aged WT FVB mice. Lysosomal hydrolase activities were measured in whole-brain homogenates of 3- and 24-month-old WT FVB mice using artificial 4-MU-substrates. Lysosomal β-glucosidase activity is defined as GBA, and non-lysosomal β-glucosidase as GBA2. Data are presented as mean ± SEM (n=4 per age, * = $p<0.05$, *** = $p<0.001$, unpaired t-test).

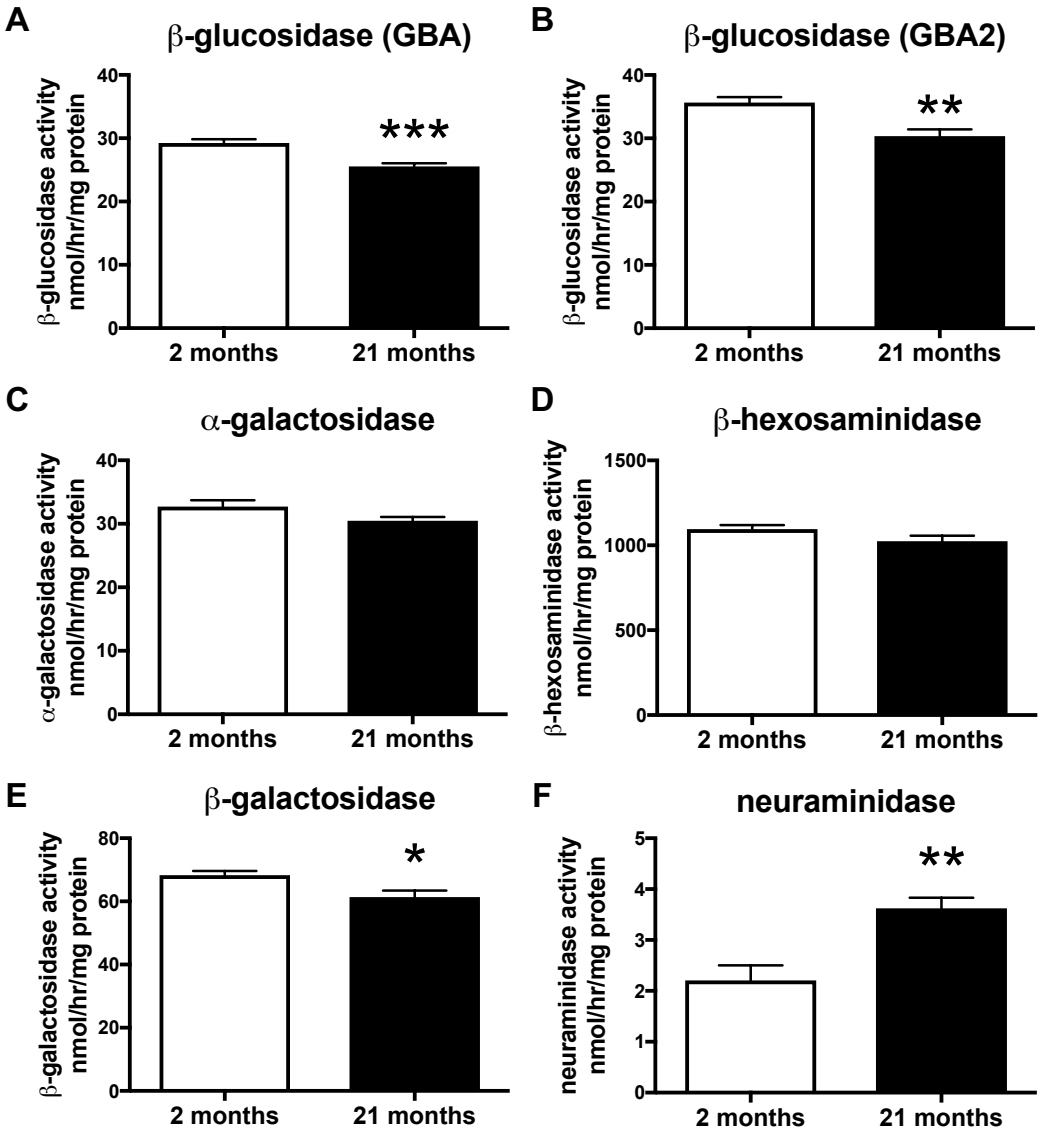

Figure 4.12.: Various hydrolase activities in the brain of aged WT BALB/c mice. Lysosomal hydrolase activities were measured in whole-brain homogenates of 2- and 21-month-old WT BALB/c mice using artificial 4-MU-substrates. Lysosomal β-glucosidase activity is defined as GBA, and non-lysosomal β-glucosidase as GBA2. Data are presented as mean ± SEM (n=6 per age, * = $p<0.05$, ** = $p<0.01$, *** = $p<0.001$, unpaired t-test).

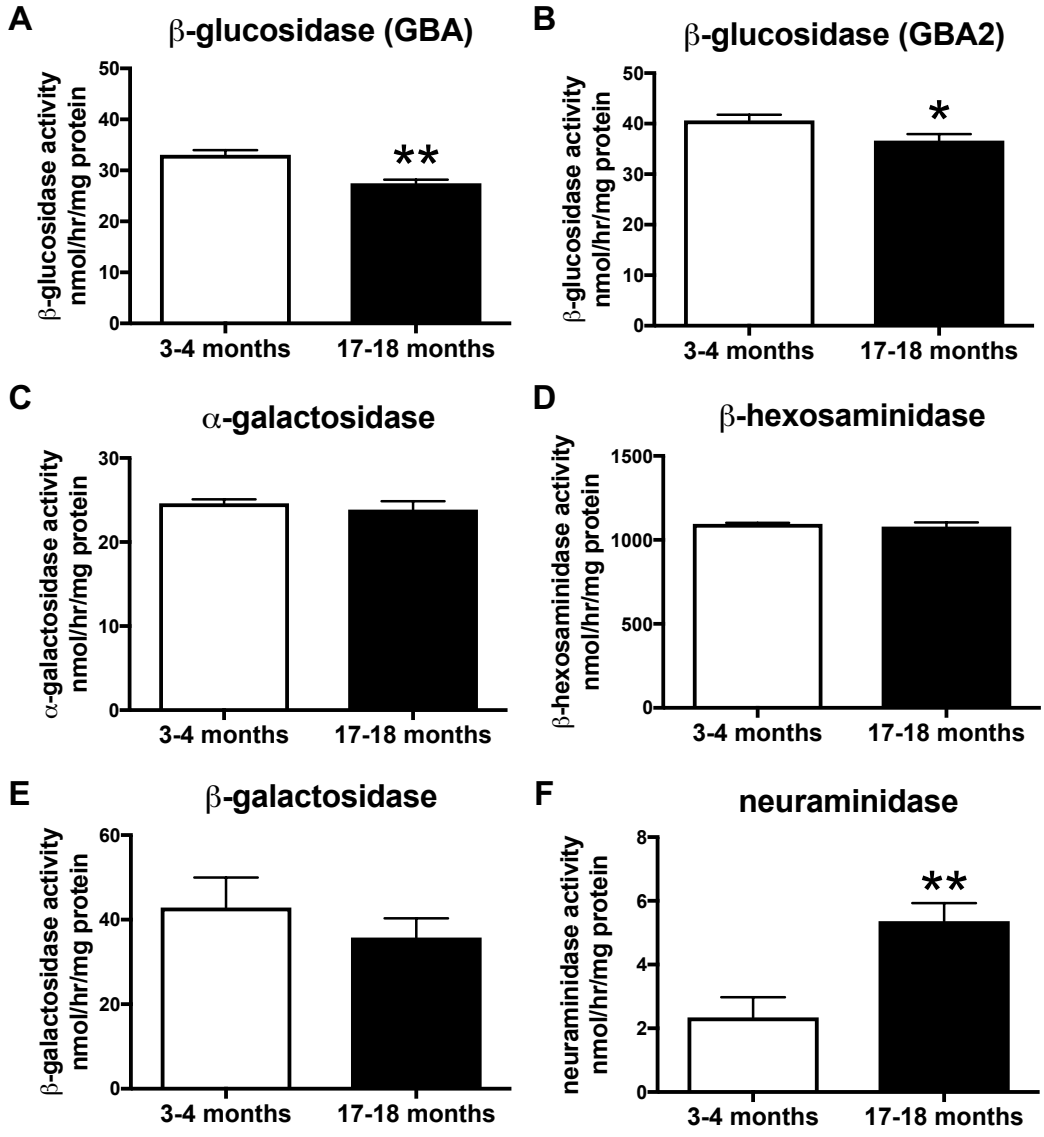

Figure 4.13: Reduced GBA and GBA2 activities and increased neuraminidase activity in the brain of aged WT BDF1 mice. Lysosomal hydrolase activities were measured in whole-brain homogenates of WT C57BL/6-DBA/2-BDF1 mice at 3-4 months and 17-18 months of age using artificial 4-MU-substrates. Lysosomal β-glucosidase activity is defined as GBA, and non-lysosomal β-glucosidase as GBA2. Data are presented as mean ± SEM (n=5 per age, * = $p<0.05$, ** = $p<0.01$, unpaired t-test).

4.3.6 Brains of aged FVB/N wildtype mice display markers of impaired protein degradation and lysosomal dysfunction

To correlate age-dependent changes in lipid homeostasis with levels of protein homeostasis, young and aged FVB/N mouse whole-brain homogenates were lysed and probed for a variety of protein degradation and lysosomal markers (**Figure 4.14**).

Interestingly, a significant increase in the levels of polyubiquitin in the brains of 24-months old wildtype mice in comparison to 1.5-months old wildtype animals was found (**Figure 4.14A, B**, 74.7%, p=0.0014). Further supporting this finding, we report significantly increased levels of LAMP2A in brains of old mice (**Figure 4.14A, C**, 30.6%, p=0.0376). However, the steady-state markers of autophagy, LC3 and p62, were unchanged in the brains of young and aged FVB/N wildtype mice (**Figure 4.14A, D, E**).

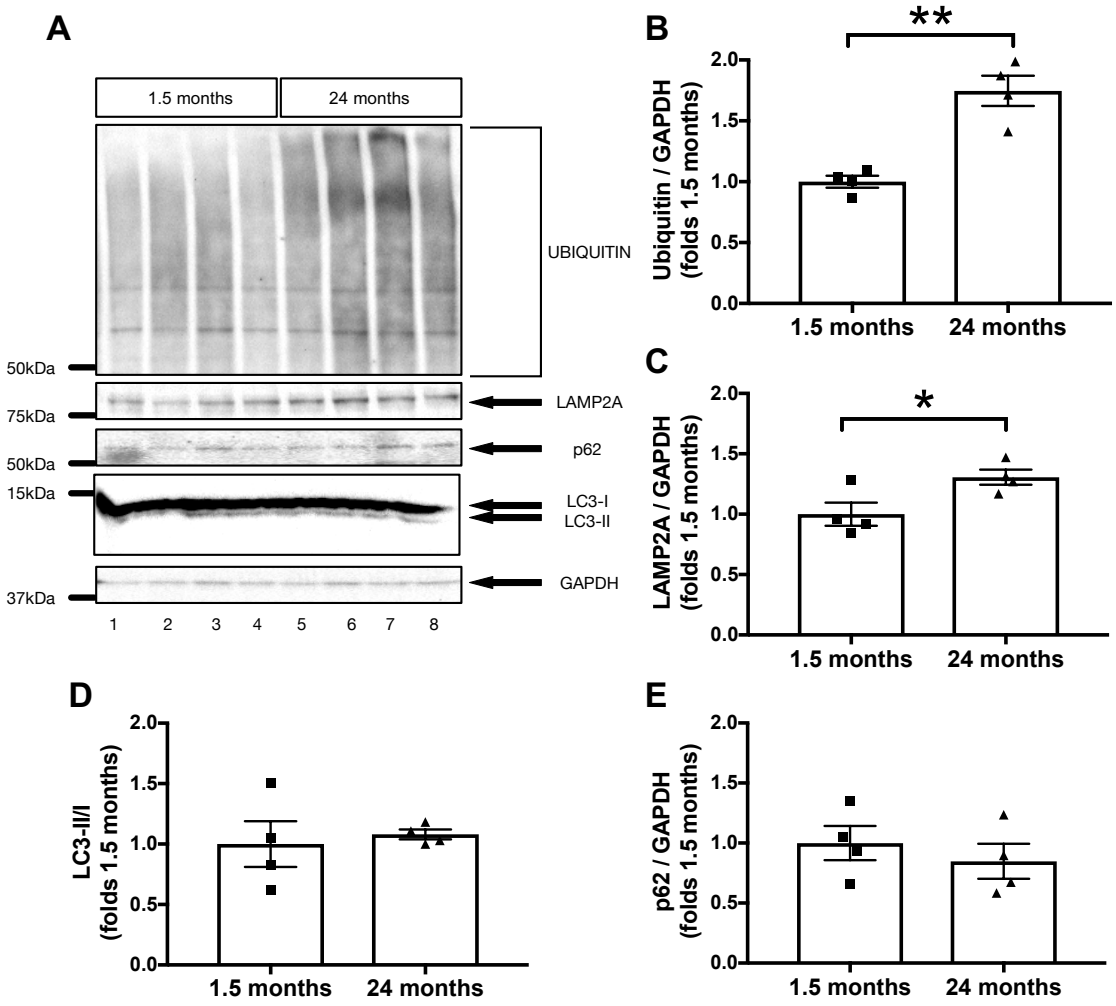

Figure 4.14: Proteolytic impairments in the ageing WT FVB mouse brain. Levels of ubiquitin (A, B), LAMP2A (A, C), LC3-II/I (A, D), and p62 (A, E) were measured in whole-brain lysates of young (1.5 months) and aged (24 months) WT FVB mice. The optical density of ubiquitin, LAMP2A, LC3-II/I, and SQSTM/p62 bands was normalized to GAPDH and expressed as folds of 1.5-month-old animals (n = 4, * = p<0.05, ** = p<0.01, unpaired t-test). Data are presented as mean ± SEM. Data generated by Oeystein Brekk.

4.3.7 α-synuclein species in brains of aged FVB/N wildtype mice

To assess if there is a possible involvement of or effect on α-synuclein protein in the age-dependent changes in lipid homeostasis, whole-brain lysates of young and aged FVB/N mice were probed for α-synuclein protein (**Figure 4.15**). Interestingly, a significant decrease in α-synuclein monomers in the brains of 24-months old wildtype mice in comparison to 1.5-months old wildtype animals was found (**Figure 4.15A, B**, 51.9%, p=0.0194). Furthermore, a concomitant appearance and significant increase in an uncharacterised α-synuclein species (≈28kDa - roughly corresponding to an α-synuclein dimer (2x14kDa)) was found in the brains of old mice (**Figure 4.15A, C**, 60.2-fold increase, p=0.0124).

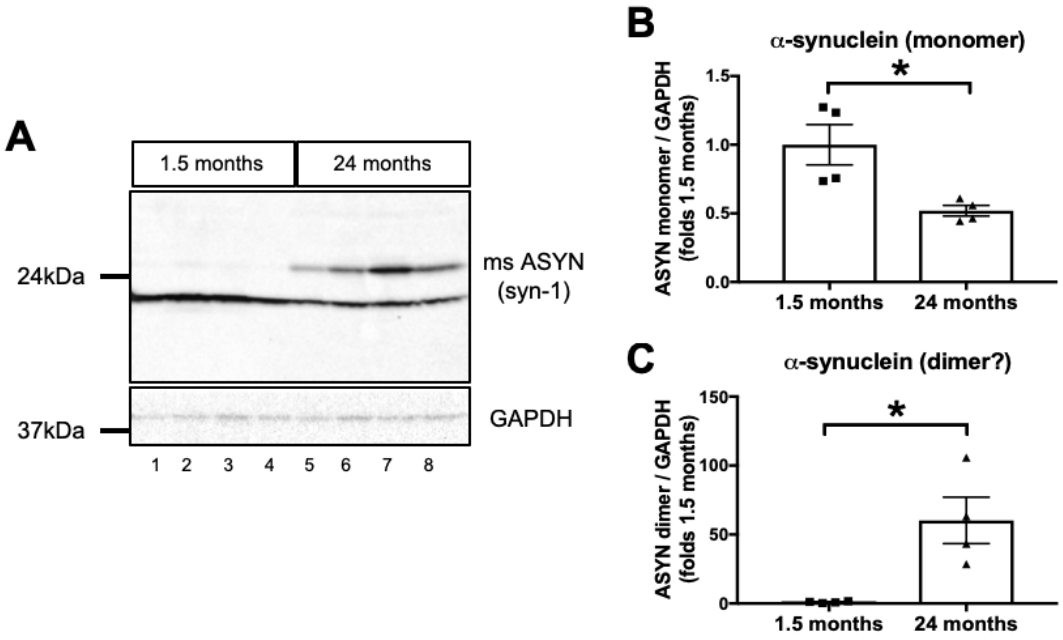

Figure 4.15: Levels of α-synuclein forms in the ageing WT FVB mouse brain. Levels of monomeric α-synuclein (A, B), and a larger α-synuclein form (A, C) were measured in whole-brain lysates of young (1.5 months) and aged (24 months) WT FVB mice. The optical density of α-synuclein bands was normalized to GAPDH and expressed as folds of 1.5-month-old animals (n=4, * = p<0.05, unpaired t-test). Data are presented as mean ± SEM. Data provided by Oeystein Brekk.

4.3.8 Dopaminergic neurons and microglia in BALB/c wildtype brain during ageing

We were interested to assess if loss of dopaminergic neurons or increased inflammation could be observed in normal brain ageing. For this, we performed immunohistochemistry of brains from a young wildtype mouse (2-months old, female) and an old wildtype mouse (21-months old, female) and stained these brains for tyrosine hydroxylase (TH) as a marker for dopaminergic neurons and CD68 as a marker for activated microglia (**Figure 4.16**). There was no obvious loss of dopaminergic neurons in the substantia nigra in wildtype mouse brain with age (**Figure 4.16**). However, there were more activated microglia present in the aged wildtype mouse brain in comparison to the young wildtype mouse brain (**Figure 4.16**).

Next page (in landscape):

Figure 4.16: Ageing leads to increased numbers of activated microglia in the mouse brain. Representative images of brain sections from 2-months and 21-months old wildtype mice (BALB/c background). Sections were stained with antibodies against CD68 (microglia marker, green), tyrosine-hydroxylase (TH, red), and the nuclear counterstain Hoechst (blue). One plane tile scan was used for imaging the whole brain and z-stack tile scan was used for capturing a close-up of the substantia nigra region (indicated by white dotted box). Images were taken by Dr. Elena-Raluca Nicoli (NIH, US).

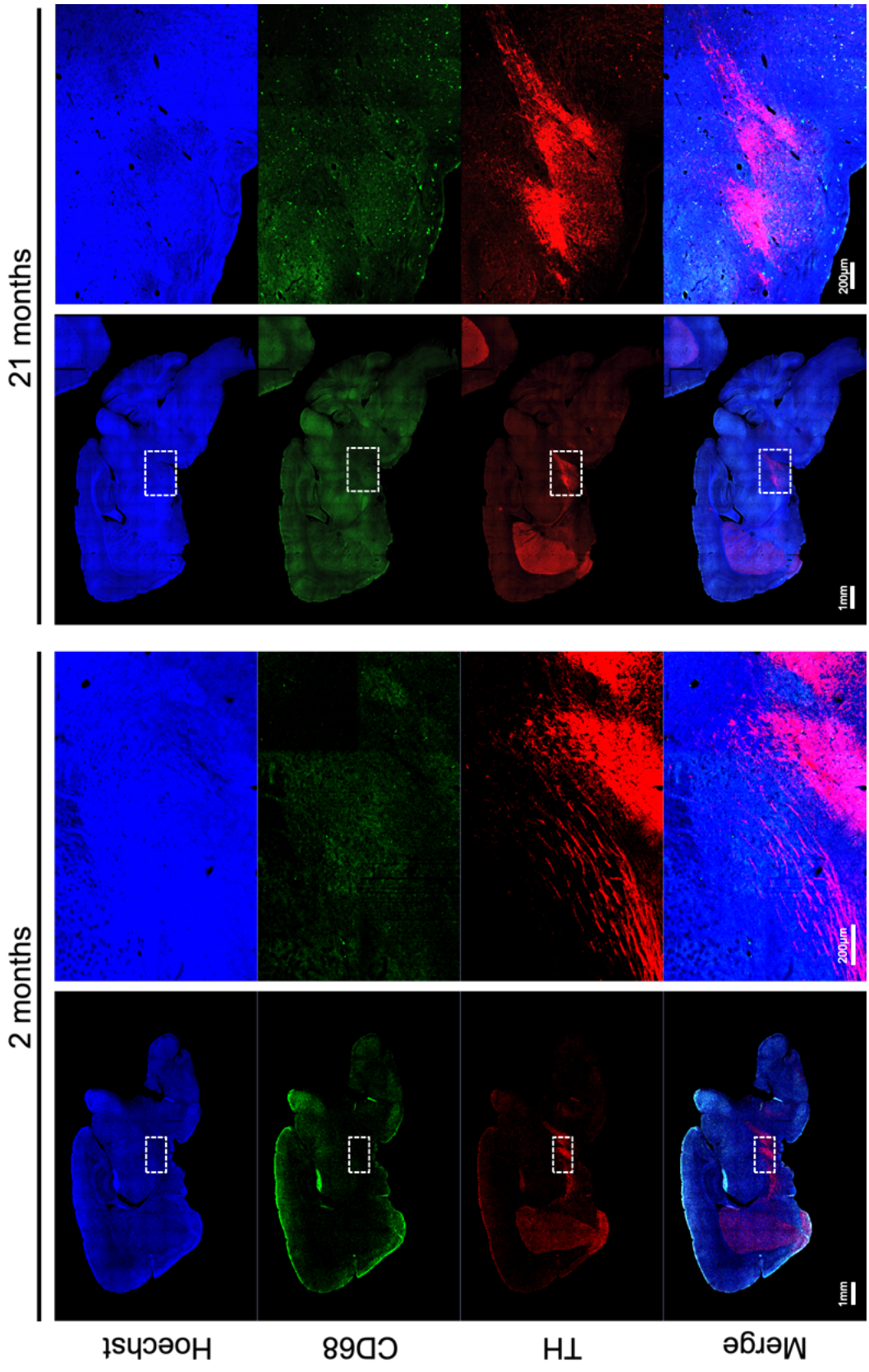
21 months
2 months
Hoechst
CD68
TH
Merge
200µm
1mm
200µm
1mm

4.4 Discussion

Ageing as a significant risk factor for PD

The principal risk factor for developing adult-onset neurodegenerative diseases like PD is ageing [314]. The connection between ageing and genes linked to PD is not well understood, but an interesting question is whether cell biological processes, which are associated with ageing, phenocopy pathophysiological changes that occur in PD. Recently, more studies have focused on this subject and showed a neuropathological resemblance between PD and ageing in human and primate brain. For example, there is selective vulnerability of midbrain substantia nigra (SN) dopamine neurons in both PD and normal ageing [315-320]. The age-dependent reduction of nigral dopamine neurons is conserved between species and in the SN pars compacta of wildtype mice, a reduction of ~10% dopaminergic neurons is observed between 7-25 months of age [321]. It is not known what drives this age-related decline. However, it has become clear that normal ageing in animals and humans, and degeneration of SN dopaminergic neurons in PD, are linked by conserved pathophysiological mechanisms, including lysosomal dysfunction, mitochondrial dysfunction and protein aggregation [318]. Importantly, cellular and molecular hallmarks of brain ageing, especially mitochondrial dysfunction and intracellular accumulation of oxidatively damaged proteins and lipids, clearly demonstrate the importance of effective cellular waste disposal mechanisms, i.e. autophagy-lysosome and proteasome functionality [124, 322].

The association of normal ageing and GSL accumulation, observed here in ageing mice [312], is intriguing for understanding the pathophysiology of age-related diseases and suggests a complex interaction between multiple GSLs, lysosomes, and neurodegeneration. Concerning lysosomal function, genetic and pathological links between the lysosomal storage disorder GD and PD have been well documented [127]. However, recently, the idea of general lysosomal dysfunction, associated with increased risk for PD, has been supported by several links between parkinsonism and/or α-

synucleinopathy and other LSDs [1, 180], including GM1 gangliosidosis [323], Niemann-Pick disease Type C [324], Fabry disease [325] and Krabbe disease [326].

Here, we provide evidence that decreased lysosomal and non-lysosomal GCase activity, GBA and GBA2, and increased lipid load, as observed in brains of sporadic PD patients, also occur in normal ageing in the mouse brain [312].

Changes in GSLs with normal ageing: GlcCer, GlcSph and GBA

Our data show that total GSL levels are progressively increased in the ageing wildtype mouse brain of three different strains, including elevations in levels of GlcSph and GlcCer (**Figures 4.1, 4.2, 4.6-4.10**) [312]. These changes in GSL levels are accompanied by a reduction in the activity of GBA and GBA2 glucocerebrosidases (**Figures 4.11-4.13**) [312]. Thus, we show that ageing mirrors changes to the GBA pathway in the mouse brain, similar to those that occur in genetic (GBA haploinsufficiency) and sporadic (non-GBA) forms of PD. It has been demonstrated that GCase activity is decreased over time in the brain during normal ageing in humans, as well as in sporadic PD [163, 164]. Reduced activity of both GCase and β-galactosidase has also been reported in human neurons from PD patients carrying a *GBA* mutation [147]. One caveat of these studies is that they do not distinguish lysosomal and non-lysosomal forms of glucocerebrosidase. In the present study, lysosomal GBA and non-lysosomal GBA2 activity were carefully measured separately using specific assay conditions for each enzyme. We show for the first time that the non-lysosomal GBA2 is also decreased with normal ageing in murine brain and thus may play a role in PD, like GBA (**Figures 4.11-4.13**) [312]. Future studies will determine possible antecedent cellular mechanisms underlying changes in lysosomal hydrolases in the ageing brain, as well as identify whether specific brain regions relevant to neurodegeneration are affected.

Next, we focused on the lipid substrates of GBA and GBA2, GlcCer and GlcSph. GlcCer is the biosynthetic precursor of all more complex GSLs and the final product of GSL catabolism in the lysosome. GlcCer levels are markedly elevated in the brain in human neuronopathic Gaucher disease (GD) and related experimental GD models [313, 327]. The increase in GlcCer is associated with neuropathological changes in neurons and degeneration [328]. Homozygous GBA deficiency in neuronopathic GD also causes accumulation of GlcSph, which is the deacylated form of GlcCer. Our ageing wildtype mouse data shows that both GlcCer and GlcSph levels in brain were increased in aged mice of three independent wildtype mouse strains (**Figures 4.1, 4.2, 4.7-4.10**) [312]. GlcSph levels have been shown to be directly neurotoxic and are correlated with CNS involvement in GD patients [306, 307]. It was previously shown that accumulation of GlcSph occurs in several brain regions in sporadic PD [164], however, the selective vulnerability of the midbrain dopamine neurons in PD demonstrates that this population of neurons may be particularly vulnerable to GSL accumulation. The elevations of GSLs found in the mouse brain during normal ageing are of course not associated with the same degree of storage and neuronal death observed in neuronopathic GD and other lysosomal storage disorders. Nevertheless, given that the current analyses represent whole-brain homogenates, individual cell types may show greater fold differences. Further studies will determine GSL and enzymatic alterations in young and aged mice in individual brain regions affected in PD and other age-related neurodegenerative disorders.

It is reasonable to expect that modest elevations or reductions of GSLs can already result in multiple pathophysiological consequences and disrupted neuronal function. In their functional roles, GSLs are located in cellular membranes, cluster in lipid rafts, and are involved in synaptogenesis, regulation of nervous signal transduction, and protein cargo sorting [329]. Indeed, many membrane-associated receptors and proteins are influenced by their lipid microenvironment. A moderate accumulation of GSLs and

changes in the relative amounts of GSLs in ageing could have marked physiological effects on these cellular functions. We hypothesize that the increased GSL load associated with ageing of the brain accelerates degenerative processes in vulnerable neurons, such as midbrain dopaminergic neurons, and lowers the threshold for developing PD. Critically, this hypothesis challenges the prevailing view that proteinopathy is the primary cause of PD since lipids and lysosomal changes could precede or exacerbate the protein load and aggregation.

Gangliosides & neuraminidases

Next, we focused on gangliosides in the ageing brain, the pre-dominant, complex GSLs in the CNS of all mammals. Whereas levels of GM1a are increased with age, our present data also show significant reductions in the levels of GD1a, GD1b and GT1b in the ageing brains of three independent mouse strains (**Figures 4.4, 4.7 and 4.9**) [312]. Not all GSLs are necessarily exclusively formed by *de novo* biosynthesis as they recycle and can be remodelled by neuraminidases. Indeed, our data demonstrates that neuraminidase activity is increased in aged mice (**Figures 4.11-4.13**), and this may account for the observed age-related increase in GM1a and concomitant reduction in GD1a, GD1b and GT1b through sequential removal of sialic acid residues (schematic shown in **Figure 4.17**) [312]. Similarly, it was demonstrated that genetic deficiency of neuraminidases 3 and 4 in mice causes a reduction in levels of GM1a [330]. Our findings on altered ganglioside levels with ageing are consistent with earlier reports describing similar patterns of changes both in ageing mouse brain [310], and in a mouse model of accelerated senescence [311]. Reductions in GM1a, GD1a, GD1b and GT1b have been reported in the frontal and temporal cortices of patients with Alzheimer's disease, another age-associated disease, compared to the same area of control patients [308]. Furthermore, previous reports have indicated alterations in levels of several complex gangliosides in multiple brain regions of the human brain during normal ageing, including

reduced GM1a and GD1a [308, 309]. Our current data indicate disrupted balance in GSL composition in ageing and is therefore potentially relevant for determining underlying disease mechanisms not only in PD but also in several age-related neurodegenerative disorders.

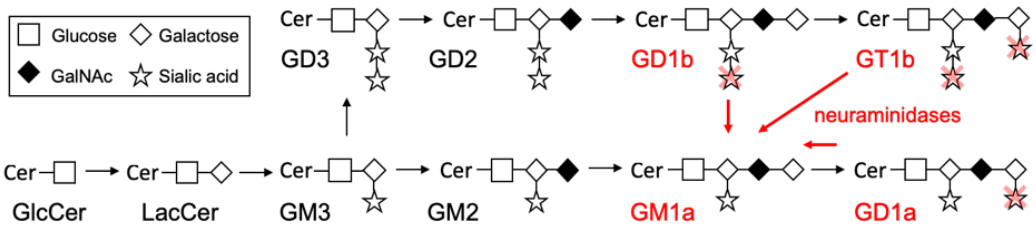

Figure 4.17: Schematic showing the remodelling of gangliosides via neuraminidases. Gangliosides GD1a, GD1b and GT1b can be remodelled to become GM1a through the sequential removal of sialic acid residues by the action of neuraminidases.

In adult-onset GM1 gangliosidosis, which is caused by β-galactosidase deficiency and is characterised by accumulation of the ganglioside GM1a in the CNS, patients present with generalised dystonia associated with akinetic-rigid parkinsonism [323]. We show that β-galactosidase activity in brains of aged wildtype mice is decreased (**Figures 4.11-4.13**) and GM1a levels are increased in normal ageing in mice (**Figures 4.4, 4.7 and 4.9**) [312]. It has been shown that GM1a levels are increased in lipid rafts in synaptosomes in aged animals [331] and, interestingly, nigrostriatal degeneration is thought to occur in a retrograde manner with synaptic terminals affected first in early PD [332]. Links between GM1a and the dopaminergic system also suggest that a loss of GM1a is associated with PD-like pathophysiological changes [156, 161]. GM1a is involved in signalling of the neurotrophic factor, GDNF [157], and elevated levels of GM1a, as we observed with normal murine ageing, could represent an age-related compensatory mechanism to enhance neurotrophic activity. Remarkably, pharmacological supplementation of PD patients with GM1a has been shown to have beneficial effects on clinical motor and neuropsychological functions in a 5-year study [249]. In addition to having essential functions in membrane lipid rafts [333], GM1a is

enriched in myelin [334] and the GM1a increase observed in the ageing mouse brain may also reflect age-related changes in myelin structures.

Lysosomes and α-synuclein

As already mentioned, there are many reports showing that lysosomal and proteasomal degradation is impaired in neurons during ageing, as demonstrated by intracellular accumulation of autophagosomes with undegraded cargo and polyubiquitinated proteins [104, 335]. In this study, we demonstrate a significant increase in ubiquitin protein and a significant increase in LAMP2A protein in aged FVB/N mouse brain, supporting the occurrence of defective or less-efficient proteasomal and lysosomal degradation in the ageing mouse brain (**Figure 4.14**) [312]. The cellular processes altered by pathologically increased GSLs can provide further clues for pathophysiological mechanisms in age-related neurodegenerative disease. Interestingly, there is considerable evidence for an association between GSL metabolism and α-synuclein, a key pathogenic protein in PD [148, 153, 170, 176, 313]. It was previously demonstrated that modulating the activity of lysosomal GBA in rodents causes inverse changes in α-synuclein accumulation: Reducing GBA activity (with a concomitant elevation of GlcCer and GlcSph) increases α-synuclein high molecular weight (HMW) species and aggregation, whereas elevation of GBA through gene delivery reduces α-synucleinopathy and protects dopamine neurons from degeneration in the rodent substantia nigra [170, 313]. Furthermore, it has been shown that oligomeric α-synuclein levels also increased with age in the brain of cynomolgus monkeys, which was accompanied by a decrease in GCase activity [336]. Intriguingly, it is further important to note that α-synuclein is a ganglioside-binding protein that starts to form fibrils in the absence of the ganglioside GM1a [159, 160]. A recent report demonstrates that Lewy bodies and Lewy neurites, which contain α-synuclein and are pathological hallmarks of PD, are also enriched in lipids, membrane fragments and distorted organelles [337]. Thus, alterations in the homeostasis of the GBA and GSL

metabolic pathways may precede or be part of abnormal α-synuclein handling in PD. In the current study, a significant reduction in 14kDa α-synuclein was observed in aged mouse brain, but a prominent increase in an α-synuclein species at ~28kDa was identified in aged animals (**Figure 4.15**) [312]. This 28-kDa α-synuclein species may represent an α-synuclein dimeric species or a post-translationally altered α-synuclein species. An increased α-synuclein dimer/monomer ratio has previously been reported in erythrocytes from patients with Gaucher disease, and erythrocytes from control patients in normal ageing [338], and was positively correlated with lipid levels, including GlcCer, in erythrocytes from GD patients [339]. Increased levels of lipids may directly enhance the formation of dimers and toxic oligomeric forms of α-synuclein, and directly contribute to α-synuclein associated toxicity. Future experiments will determine the temporal sequence of events regarding lipidopathy and proteinopathy. However, we hypothesize that lipid abnormalities may precede or exacerbate protein abnormalities and our data provide new evidence for the link between age-related GSL changes and known pathophysiological changes in PD.

Dopaminergic neurons and microglia

We were interested to see if loss of dopaminergic neurons or increased inflammation are taking place in normal mouse brain ageing. With respect to the vulnerable substantia nigra dopamine neurons, it has previously been demonstrated that nigral dopamine neurons are progressively lost during normal ageing in humans, with a 7-10% reduction per decade [315-317, 319, 320, 340]. This age-dependent reduction of nigral dopamine neurons is conserved between species. In the substantia nigra pars compacta of wildtype mice, a reduction of ~10% is observed between 7 and 25 months of age [321]. Furthermore, DA neurons from aged mice (25-30 months of age) exhibit electrophysiological changes suggestive of reduced functional capacity [341]. In agreement with the published studies, we observed no dramatic loss of dopaminergic

neurons in wildtype mouse brain with age (**Figure 4.16**). This confirms that the observed changes in GSLs are not based on neuronal loss of dopaminergic neurons.

However, we observed more activated microglia in the aged wildtype mouse brain in comparison to young wildtype mouse brain (**Figure 4.16**). Microglia are the dynamic innate immune effector cells of the CNS and monitor the well-being of the brain [342, 343]. In response to damage or injury, microglia transform into an active phagocytic state, expressing high levels of CD68, and attempt phagocytosis of damaged cells and debris to combat further neurological damage [343-345]. Our observation of increased activated microglia in the aged mouse brain agrees with multiple studies [343, 346-348]. It is possible that the increased presence of activated microglia is due to the higher demand of their clearance function during ageing, e.g. for the degradation of myelin [348]. The higher activation of microglia in the ageing mouse brain might also be a result of the observed increased GSL load and increased levels of α-synuclein, leading to neuronal stress. Interestingly, it has been shown that microglia get activated by gangliosides, so the increase in activated microglia might also be due to the observed increase in GM1a levels [349, 350]. One could speculate whether the increased number of primed microglia/macrophages could plausibly affect the changes in GSLs we observe in the ageing mouse brain. The GSL profile of microglia is not known. However, we know from studies in our group that murine RAW macrophages contain equally high amounts of GM1a and GD1a. In the ageing mouse brain, we see an increase in GM1a, but a decrease in GD1a. If we assume that the GSL expression of mouse microglia is similar to that of RAW macrophages, microglia do not seem to play a major factor in the GSL expression of the whole brain, as we would expect to also see an increase in GD1a ganglioside in our data. In addition, the effect of ageing on the number of microglia is controversial, but the general consensus is that the total number of microglia in the brain stays stable during healthy ageing, with just increased transitioning of microglia into a primed state with age [343, 351-353]. It would be interesting to know if activated

microglia have a different pattern of GSL expression to dormant microglia. In healthy rodents, microglia make up 5–12% of all CNS-specific cells [351, 354], thus there are probably not enough microglia to affect levels of gangliosides through the whole brain.

Clinical relevance for PD

The cellular processes affected by altered levels of GSLs, e.g. lysosomal function, can provide mechanistic clues for treatment and prevention of age-related neurodegenerative disease. For example, storage of the potentially neurotoxic lipids GlcCer and GlcSph could be targeted by effective interference in relevant enzymatic pathways. This could be achieved by either using gene delivery to increase the hydrolysis of lipid substrates, using small molecules to decrease GSL biosynthesis (substrate reduction therapy) or pharmacological chaperones, which facilitate transport of lysosomal hydrolases to the lysosomal compartment. Indeed, such strategies are already successfully in use or are being developed clinically for several lysosomal storage disorders [38, 355, 356]. Furthermore, direct supplementation of neuroprotective gangliosides might also be a treatment option for neurodegenerative diseases. For decades, the neurotrophic ganglioside GM1a has already been of special interest for treating neurological PD-like conditions in mice and non-human primates [157, 161, 357-360]. Intriguingly, pharmacological supplementation of PD patients with GM1a has already been shown to have beneficial effects on clinical motor and neuropsychological functions in a 5-year study [249].

Importantly, age-related changes in some GSLs appear to be conserved between mice and humans and resemble the changes observed in sporadic PD [312]. This may allow the identification of rational treatments for age-related neurodegenerative disorders with the aim to normalise altered patterns of GSL expression.

5 Glycosphingolipids in PD mouse models

5.1 Introduction

5.1.1 Genetic risk factors for PD: SNCA and LRRK2

Parkinson's disease (PD) is characterised by the degeneration and loss of dopaminergic neurons within the substantia nigra of the midbrain, which is important for the control of motor function in the basal ganglia. Only 5-10% of PD cases have been linked to a genetic, heritable cause, whereas 90% of PD cases are sporadic [117]. Though rare, genetic forms of PD can provide clues to mechanisms underlying the neuropathology of PD. Six genes have been proposed to cause autosomal dominant forms of PD, amongst them are *SNCA* and *LRRK2* [116].

SNCA (or P*ARK1*) encodes α-synuclein, an abundant, cytosolic 140 amino acid-long protein, which is mainly found in pre-synaptic terminals of neurons [361]. Not surprisingly, α-synuclein is most highly expressed in the CNS and peripheral nerves (The Human Protein Atlas, www.proteinatlas.org). Mouse and human α-synuclein proteins share 95% amino acid identity (www.ncbi.nlm.nih.gov/homologene). The soluble α-synuclein protein is intrinsically unfolded, but upon binding to membranes it adopts a more stable, α-helical structure [362]. The precise function of α-synuclein within the CNS is not known. It probably has a role in pre-synaptic stability or plasticity, synaptic vesicle dynamics, neurotransmitter release, dopamine metabolism, and/or intracellular trafficking (e.g. of membranes or lipids) [361, 363, 364]. Three missense mutations in the α-synuclein gene (A53T, A30P and E46K) are associated with rare familial forms of PD [365-367]. Furthermore, genetic studies have shown that the multiplication (duplication or triplication) of the gene encoding wildtype α-synuclein is sufficient to cause PD, suggesting that the level of α-synuclein expression is a critical determinant of PD onset or progression [368-371]. Finally, genome-wide association studies have shown that *SNCA* is also linked to sporadic PD [372]. Amino acid substitutions due to

missense mutations or increased protein expression due to gene locus multiplications, amongst other modifying factors, render α-synuclein prone to aggregation. Then, α-synuclein acquires neurotoxic properties in which soluble α-synuclein monomers initially form oligomers, then progressively combine to eventually form large, insoluble α-synuclein aggregates, as found in Lewy bodies in PD [361, 373].

LRRK2 (or P*ARK8*) encodes the leucine-rich repeat kinase 2 (LRRK2), a large multidomain protein (286 kDa), involved in multiple cellular processes. Interestingly, contrary to α-synuclein, LRRK2 is highest expressed in kidneys and lungs, but less in brain or other peripheral organs (The Human Protein Atlas, www.proteinatlas.org). Mouse and human LRRK2 proteins share 87% amino acid identity (www.ncbi.nlm.nih.gov/homologene). LRRK2 contains, amongst others, a leucine-rich repeat (LRR) domain, a serine-threonine kinase domain, and a GTPase domain, thus displaying two enzymatic functions. The protein may also function as a scaffold protein due to its several protein-protein interaction domains. The precise function of the LRRK2 protein remains unknown, but it seems to play a role in neurite outgrowth, synaptic morphogenesis, vesicle or membrane trafficking and/or autophagy, as well as in the innate immune system [374-378]. LRRK2 mutations are one of the most frequent causes of genetic PD, as they are found in 5-6% of familial PD cases and around 1-2% of sporadic PD cases worldwide [374, 379]. Several disease-causing *LRRK2* mutations have been identified, all mostly clustered within the catalytic domains of the protein [379, 380]. The most common LRRK2 mutation in PD patients is the G2019S mutation, a point mutation in the kinase domain, which leads to a hyperactivation of the kinase with increased phosphorylation of its substrates and increased autophosphorylation [374, 381]. The second most common mutation is the R1441C mutation, a mutation in the GTPase domain, which leads to GTPase dysfunction and destabilisation [382, 383].

5.1.2 Mouse models of PD

An essential step in research and drug discovery is the generation of animal models of the disease and the subsequent testing of drug candidates in these models. There is plenty of choice for mouse models for PD, especially for α-synuclein [299, 384, 385]. These models can for example be based on the expression of either mutated or wildtype forms of α-synuclein and can be driven by a variety of promoters. However, most models only recapitulate some, but not all aspects of PD, and thus often lack specific neuropathological and/or behavioural features of PD [299]. For example, almost all studies failed to find significant loss of DA neurons in the nigrostriatal system in these genetic models. Thus, just to recapitulate genetic alterations, which are found in PD patients, in mouse models, seems to be insufficient to reproduce the neuropathological features of PD [299]. Nevertheless, most of these mouse models are still useful to provide clues to the mechanisms underlying the neuropathology of PD.

5.1.2.1 α-synuclein overexpressing (ASO) mouse model

To date, various α-synuclein transgenic mice have been developed. No significant nigrostriatal degeneration has been found in the majority, but, in some of these mice, decreased striatal levels of TH or DA and behavioural impairments were found, indicating that the accumulation of α-synuclein can significantly alter the function of DA neurons [299]. Here, we used transgenic mice overexpressing human wildtype α-synuclein under the murine *THY1* promoter, Thy-1 expression being most abundant in CNS and peripheral nerves [386, 387]. This mouse model mimics multiplication mutations in familial PD, as well as overexpression of the nonmutated protein encountered in sporadic PD. The α-synuclein overexpressing (ASO) mouse model reproduces many features of PD, including α-synuclein pathology, progressive changes in dopamine release and striatal dopamine content, and deficits in motor functions [387]. In ASO mice, human α-synuclein protein accumulates in synapses and neurons

throughout the brain, including the thalamus, basal ganglia, substantia nigra, and brainstem [386]. Both mRNA measurements in SN dopaminergic neurons and immunohistochemical detection of human α-synuclein in the SN indicate that ASO mice express the transgenic protein in dopaminergic neurons of the SN pars compacta [387]. Interestingly, high expression of *THY1* also occurs in the cerebral cortex and hippocampus (The Human Protein Atlas, www.proteinatlas.org). Nevertheless, ASO mice only express moderate levels of human α-synuclein in neurons (2-5-fold increased expression) and the human α-synuclein is transported normally to synaptic terminals [387]. A-synuclein is present in insoluble protein aggregates in PD patients [118]. Accordingly, α-synuclein aggregates are present in the substantia nigra of ASO mice from 5 months of age and increase in size and number in older mice. Beyond 14 months of age, mortality increases in ASO mice, thus ASO mice generally have a reduced lifespan compared to wildtypes [387]. ASO mice exhibit a progressive loss of striatal dopamine, with normal levels of dopamine and TH being present at 8-12 months of age, but a loss of around 40% of striatal dopamine by 14 months of age, accompanied by a more moderate loss of TH of around 20% [388]. Importantly, ASO mice do not show any reduction in the number of TH-positive dopaminergic neurons [387]. Thus, the model lacks a cardinal feature of PD. Nevertheless, ASO mice show progressive PD-like motor deficits. In humans, the loss of dopamine in the striatum, the brain region involved in movement control, leads to akinesia, rigidity, and tremor [116]. At 14 months of age, ASO mice show decreased locomotion in the open field and a slowness in sensory motor tests [387]. With increasing age, progressively more severe deficits are evident. Interestingly, deficits in fine motor skills between can be observed already at 4-5 months of age [387].

5.1.2.2 LRRK2(R1441G) mouse model

Next, we used the LRRK2(R1441G) mouse model [389]. These mice express the mutant form of human leucine-rich repeat kinase 2 LRRK2(R1441G) driven by the human LRRK2 promoter on a bacterial artificial chromosome (BAC) transgene. The mutation R1441G is a common missense mutation in large family lineages with nearly complete penetrance [380, 390]. In the LRRK2(R1441G) mouse, mutant LRRK2 is approximately five- to ten-fold higher expressed in cortex, cerebellum, striatum and ventral midbrain than the endogenous mouse LRRK2 [389]. In the original publication, LRRK2(R1441G) mice showed significant hypokinesia by 10-12 moths of age [389]. However, in response to numerous reports questioning the hypokinetic motor deficits of this strain, the Jackson Laboratory as well as the Michael J. Fox Foundation (MJFF) initiated longitudinal phenotyping studies comparing wildtype and LRRK2(R1441G) mice. To date, both institutions have been unable to validate the hypokinetic motor deficits at 12 months of age reported for this strain. Accordingly, our collaborators only see a very subtle motor and cognitive phenotype with high age and no reduced lifespan in LRRK2(R1441G) mice (personal communication, Prof. Penelope Hallett, Harvard). Nevertheless, LRRK2(R1441G) mice exhibit multiple late-onset and progressive characteristics of PD, including progressive dopaminergic neuron dysfunction, axonal injury pathology, and hyperphosphorylated tau [389]. For example, a significant reduction of extracellular dopamine in LRRK2(R1441G) mice, due to reduced dopamine release, was reported in the original study [389]. The MJFF study also noted significant differences in striatal content of neurotransmitters when comparing LRRK2(R1441G) mice to controls at eight months of age. Importantly, dopaminergic neurons in the substantia nigra pars compacta were normal in number and anatomical organization, but smaller cell body size and less dendrites [389]. Thus, this model also lacks the cardinal feature of dopaminergic neuron degeneration of PD. Nevertheless, LRRK2(R1441G) mice recapitulate some features of

PD and may be useful to study the dominant toxic effects of mutant LRRK2(R1441G) expression.

5.1.2.3 LRRK2 KO and LRRK2(G2019S) KI mouse models

Finally, we used LRRK2 knock-out (KO) and LRRK2 knock-in (KI, LRRK2(G2019S)) mice affecting the murine *LRRK2* gene described by [375]. The G2019S mutation is the most common LRRK2 mutation and is located in the kinase domain, increasing LRRK2 kinase activity and toxicity [374, 391-394]. To distinguish LRRK2 kinase effects from potential scaffolding functions of LRRK2, mice lacking LRRK2 completely (knock-out, KO) were generated [375]. LRRK2 KO mice showed an early-onset (age 6 weeks), marked increase in number and size of secondary lysosomes in kidney proximal tubule cells and lamellar bodies in lung type II cells [375]. LRRK2 KI (LRRK2(G2019S)) mice expressing the kinase-enhancing pathogenic mutation showed none of the LRRK2 protein level and histopathological changes observed in KO mice [375]. Importantly, no major neurodegeneration, changes in striatal DA content or overt motor deficits were observed, even at nearly 2 years of age [375] (personal communication, Prof. Carsten Wagner, Zürich). However, following more detailed experiments, it was reported that LRRK2(G2019S) KI mice displayed an age-dependent, progressive dysfunction of dopamine transporters, along with elevated levels of Serine129-phosphorylated α-synuclein at striatal dopaminergic terminals [395]. Consequently, the LRRK2(G2019S) KI model has been proposed to be used as a pre-symptomatic PD model [395]. Also, these mouse models may be useful to further study aspects of peripheral LRRK2 biology like kidney and lung pathology in LRRK2 mutant mice, with possible implications for PD.

In this chapter, we were interested whether alterations in GSL homeostasis and lysosomal hydrolase activities, as seen in ageing and in PD patients, could be detected

in PD mouse models. This could be important for investigating and understanding processes involved in PD pathology.

The aims of this experimental chapter are therefore:

- To determine levels of GlcCer and GlcSph in the ageing brain of ASO, LRRK2(R1441G), LRRK2 KO and LRRK2(G2019S) KI mice.
- To analyse levels of gangliosides in the ageing brain of ASO, LRRK2(R1441G), LRRK2 KO and LRRK2(G2019S) KI mice.
- To assess various lysosomal hydrolase activities in the ageing brain of ASO, LRRK2(R1441G), LRRK2 KO and LRRK2(G2019S) KI mice.
- To evaluate peripheral impairments in the liver and kidney of LRRK2 KO and LRRK2(G2019S) KI mice.

5.2 Materials and Methods

5.2.1 Animals

Brain tissues from α-synuclein overexpressing (ASO) mice and LRRK2(R1441G) mice were provided by Prof. Penelope Hallett, Neuroregeneration Research Institute, McLean Hospital, Harvard. All animal procedures in Harvard were performed in accordance with the guidelines of the National Institute of Health and were approved by the Institutional Animal Care and Use Committee (IACUC) at McLean Hospital, Harvard Medical School. Tissues from LRRK2 knock-out (KO) and LRRK2 knock-in (KI, LRRK2(G2019S)) mice were provided by Prof. Carsten Wagner, Institute of Physiology, University of Zürich. Experiments in Zürich were carried out in accordance with the authorization guidelines of the Swiss federal and cantonal veterinary offices for the care and use of laboratory animals. The study was approved by the local Veterinary Authority (Kantonales Veterinäramt Zürich). Animals were housed according to standard conditions, in a dark/light cycle of 12 hours, with *ad libitum* access to food and water.

In this study, transgenic mice overexpressing human wildtype α-synuclein under the murine *THY1* promoter were used [386, 387]. Wildtype (WT) male mice (BDF1 strain, Charles River Laboratories, Wilmington, USA) were bred with female mice hemizygous for α-synuclein overexpression (ASO mice, mixed C57BL/6-DBA/2 background). Mice were maintained on a mixed BDF1/C57BL/6-DBA/2 background. Male wildtype mice at 3-4 months (n=6) and 17-18 months (n=7) and age-matched male ASO mice at 3-4 months (n=6) and 17-18 months (n=4) of age were used in this study.

Furthermore, LRRK2(R1441G) mice on the FVB/N background from The Jackson Laboratory were used (JAX stock #009604) [389]. These mice express the mutant form of human leucine-rich repeat kinase 2 LRRK2(R1441G) driven by the human LRRK2 promoter on a bacterial artificial chromosome (BAC) transgene. Male and female FVB/N

wildtype mice at 3 months of age (n=6) and 24 months of age (n=4), as well as 24-month-old LRRK2(R1441G) mice (n=3) were used in this study.

Finally, we used LRRK2 knock-out (KO) and LRRK2 knock-in (KI, LRRK2(G2019S)) mice affecting the murine *LRRK2* gene described by [375]. These strains were mostly in the C57BL/6J background (targeted BALB/C embryonic stem cells were injected into C57Bl/6J host blastocysts and later backcrossed to C57BL/6J). Non-transgenic, wildtype mice from heterozygous breeding served as control. Mice were all littermates, male and about 70-80 days old (roughly 2.5 months). Six to seven animals per genotype were used.

Mice were terminally anesthetised by intraperitoneal injection of sodium pentobarbital (130 mg/kg) and intracardially perfused with heparinised saline. Tissues were rapidly dissected and stored at -80°C or immediately homogenised in water using a handheld Ultraturax T25 probe homogeniser (IKA, Germany) and aliquoted before being stored at -80°C.

5.2.2 Glycosphingolipids (NP-HPLC)

GlcCer and downstream GSLs were analysed as previously described in **Chapters 2.2.6 and 3.2.7**.

5.2.3 Sphingosine and glucosylsphingosine (RP-HPLC)

As detailed in **Chapter 3.2.8**.

5.2.4 Cholesterol

As detailed in **Chapter 4.2.5**.

5.2.5 Lysosomal hydrolase activity assays

As detailed in **Chapter 3.2.6**.

5.2.6 Statistical analysis

All statistical analyses were performed with GraphPad Prism 7.0 (GraphPad, San Diego, CA). Unpaired student's *t*-test was used to compare two groups, one-way ANOVA was used to compare three groups and two-way ANOVA was used to compare more than three groups.

5.3 Results

5.3.1 GSLs are not altered in the brain of ASO mice

To investigate if levels of GSLs are altered in PD mouse models, we first analysed GSLs in brains of young (3-4 months of age) and aged (17-18 months of age) α-synuclein overexpressing (ASO) mice (n=4-6 per age group) compared to age-matched BDF1 wildtype mice (n=6-7 per age group).

First, we were interested in studying the levels of glucosylceramide (GlcCer) and lactosylceramide (LacCer), both precursors in the GSL biosynthetic pathway. There was no difference in GlcCer and LacCer levels in whole-brain homogenates of young and old ASO mice compared to age-matched wildtype BDF1 mice (**Figure 5.1**). Nevertheless, comparable increases in GlcCer and LacCer were seen during ageing in brains of both mutant and wildtype mice (**Figure 5.1**, GlcCer: p=0.0024 for WT, p=0.0167 for ASO; LacCer: p=0.0093 for WT), as already described for ageing BDF1 wildtype mice in **Chapter 4**. Next, levels of complex gangliosides were measured with NP-HPLC. The major GSLs found in the mammalian nervous system are GM1a, GD1a, GD1b and GT1b. There were no differences in GM1a, GD1a, GD1b and GT1b levels in whole-brain homogenates of young and old ASO mice compared to age-matched wildtype BDF1 mice (**Figure 5.2A-D**). Nevertheless, comparable increases in GM1a and decreases in GD1a, GD1b and GT1b levels were seen during ageing in brains of both mutant and wildtype mice (**Figure 5.2**, GM1a: p=0.0003 for WT, p=0.0004 for ASO; GD1a: p=0.0484 for WT; p=0.0393 for ASO; GT1b: p=0.0838 for WT; p=0.0369 for ASO), as already described for ageing BDF1 wildtype mice in **Chapter 4**. Accordingly, the total level of brain GSLs increased with ageing in both wildtype and ASO mice, but there was no difference between both strains (**Figure 5.2E**, p=0.0018 for WT; p=0.0149 for ASO).

Next, we were interested in studying the levels of sphingosine (Sph), sphinganine (SphA) and glucosylsphingosine (GlcSph) in the brain of ASO mice using RP-HPLC. A slight, but significant increase in C18-Sph was observed in the brains of 17-18-month-old ASO

mice compared to age-matched wildtype mice (**Figure 5.3A**, p=0.0440). However, no difference in SphA or C18-GlcSph levels in whole-brain homogenates of young and old ASO mice compared to age-matched wildtype BDF1 mice was found (**Figure 5.3B, C**). Nevertheless, comparable increases in C18-GlcSph and decreases in SphA levels were seen during ageing in brains of both mutant and wildtype mice (**Figure 5.3**, SphA: p=0.0097 for WT; p=0.0242 for ASO; GlcSph: p=0.0256 for WT; p=0.0024 for ASO), as already described in **Chapter 4** for ageing wildtype mice. To test whether cholesterol is involved in PD, cholesterol levels were measured in brain homogenates from young (3-4 months) and old (17-18 months) ASO mice and age-matched wildtype BDF1 mice using the Amplex Red kit. A slight, but significant decrease in total brain cholesterol levels was detected in young ASO mice compared to age-matched wildtype mice, but was not detected in old mice (**Figure 5.3D**, p=0.0365). In summary, no obvious alterations in GSL levels were uncovered in whole-brain homogenates of ASO mice compared to wildtype BDF1 mice.

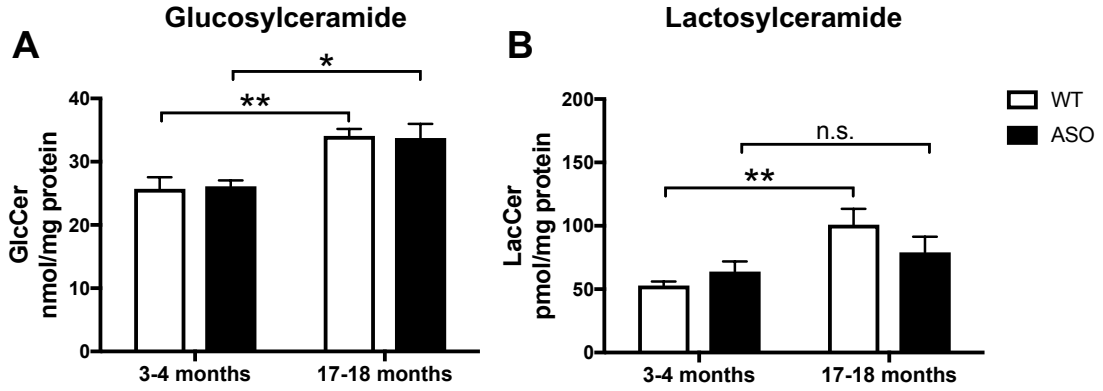

Figure 5.1: No difference in GlcCer and LacCer levels between brains of young and aged WT and ASO mice. Whole-brain homogenates from WT BDF1 mice at 3-4 months and 17-18 months of age (n=6-7 per group) and from ASO BDF1 mice at 3-4 months and 17-18 months of age (n=4-6 per group) were used to determine GlcCer (A) and LacCer (B) levels using NP-HPLC (* = p<0.05, ** = p<0.01, two-way ANOVA). Data are presented as mean ± SEM.

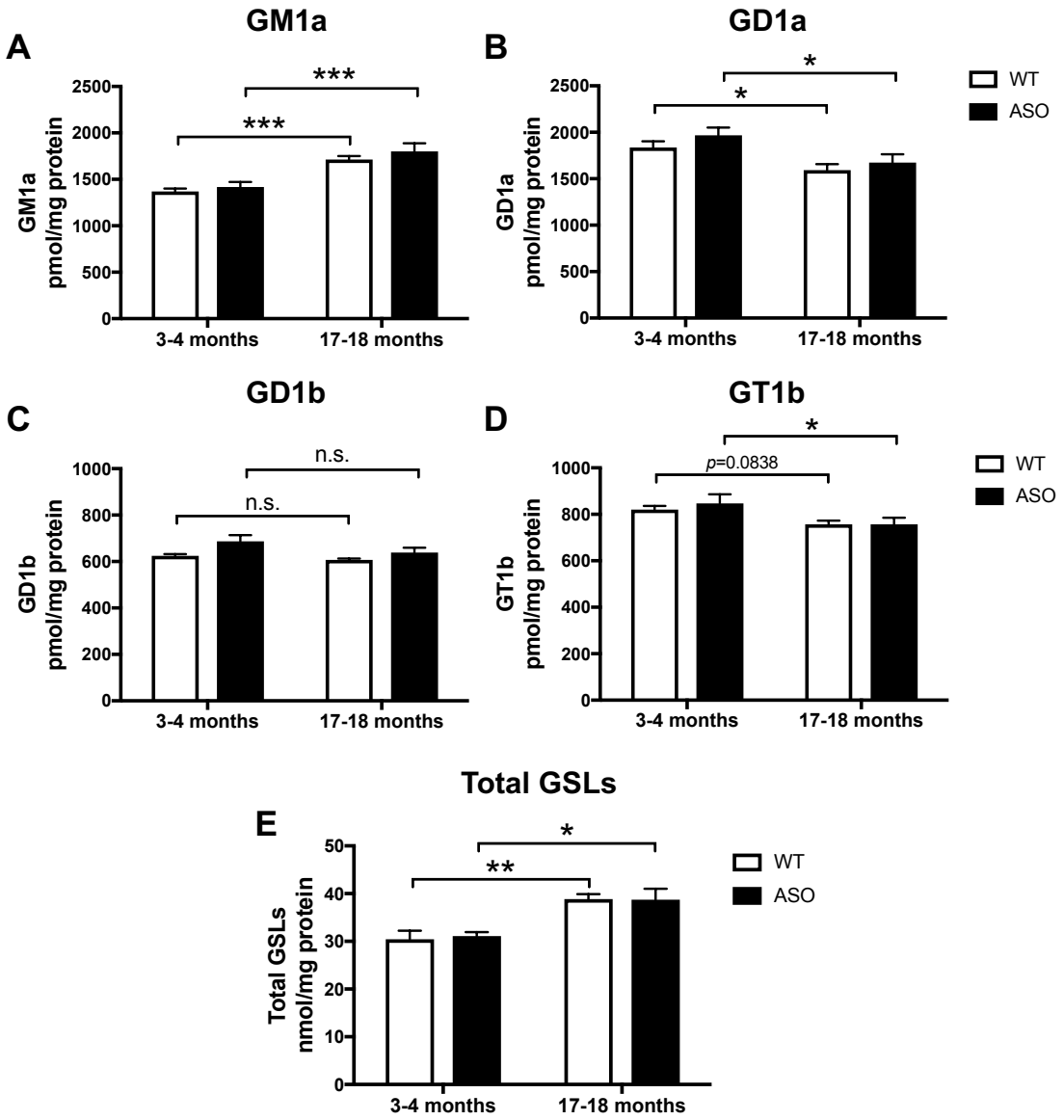

Figure 5.2: No difference in ganglioside and total GSL levels between brains WT and ASO mice. Whole-brain homogenates from WT BDF1 mice at 3-4 months and 17-18 months of age (n=6-7 per group) and from ASO BDF1 mice at 3-4 months and 17-18 months of age (n=4-6 per group) were used to determine GM1a (A), GD1a (B), GD1b (C), GT1b (D) and total GSL (B) levels using NP-HPLC (* = p<0.05, ** = p<0.01, *** = p<0.001, two-way ANOVA). Data are presented as mean ± SEM.

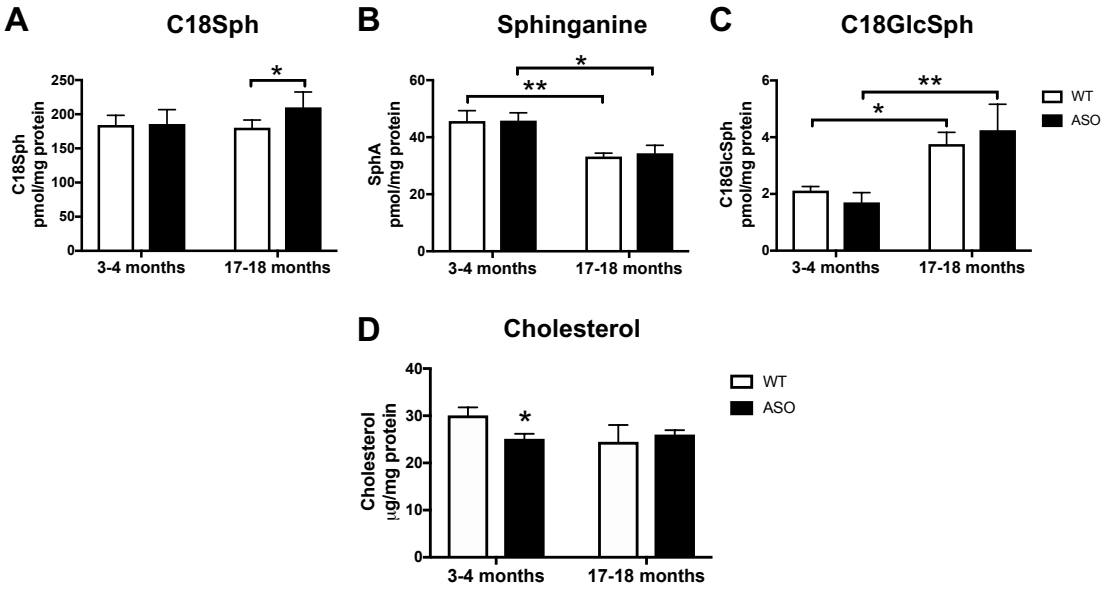

Figure 5.3: Sphingosine, sphinganine, glucosylsphingosine and cholesterol levels in brains of young and aged BDF1 WT and ASO mice. C18-sphingosine (A), sphinganine (B) and C18-glucosylsphingosine (C) levels in whole-brain homogenates of BDF1 WT and ASO mice at 3-4 months and 17-18 months of age (n=4-5 per group) were analysed using RP-HPLC (* = $p<0.05$, ** = $p<0.01$, two-way ANOVA). (D) Comparison of total cholesterol levels in whole-brain homogenates of WT and ASO mice (n=4-5 per group) (* = $p<0.05$, two-way ANOVA). Cholesterol levels were analysed with Amplex Red kit. Data are presented as mean ± SEM.

5.3.2 Altered lysosomal hydrolase activities in murine ASO brains

Levels of GSLs can be modulated by the activity of several lysosomal hydrolases. For example, as previously discussed in **Chapter 4**, the observed increase in GlcCer and GlcSph levels in the ageing mouse brain could be due to a decrease in the activity of their degrading enzymes, β-glucosidases GBA and GBA2. Consequently, the activities of various lysosomal hydrolases were assayed in whole-brain homogenates of 3-4-month and 17-18-month old ASO and age-matched WT mice (n=4-5 per group). Activities of lysosomal β-glucosidase (GBA) and non-lysosomal β-glucosidase (GBA2) were measured independently. A significant decrease in GBA β-glucosidase activity was observed in brain homogenates of old ASO and wildtype mice compared to young ASO and wildtype mice (**Figure 5.4A**, $p=0.0001$ for WT, $p=0.0067$ for ASO). However, there was no difference between ASO and wildtype mice at both ages (**Figure 5.4A**).

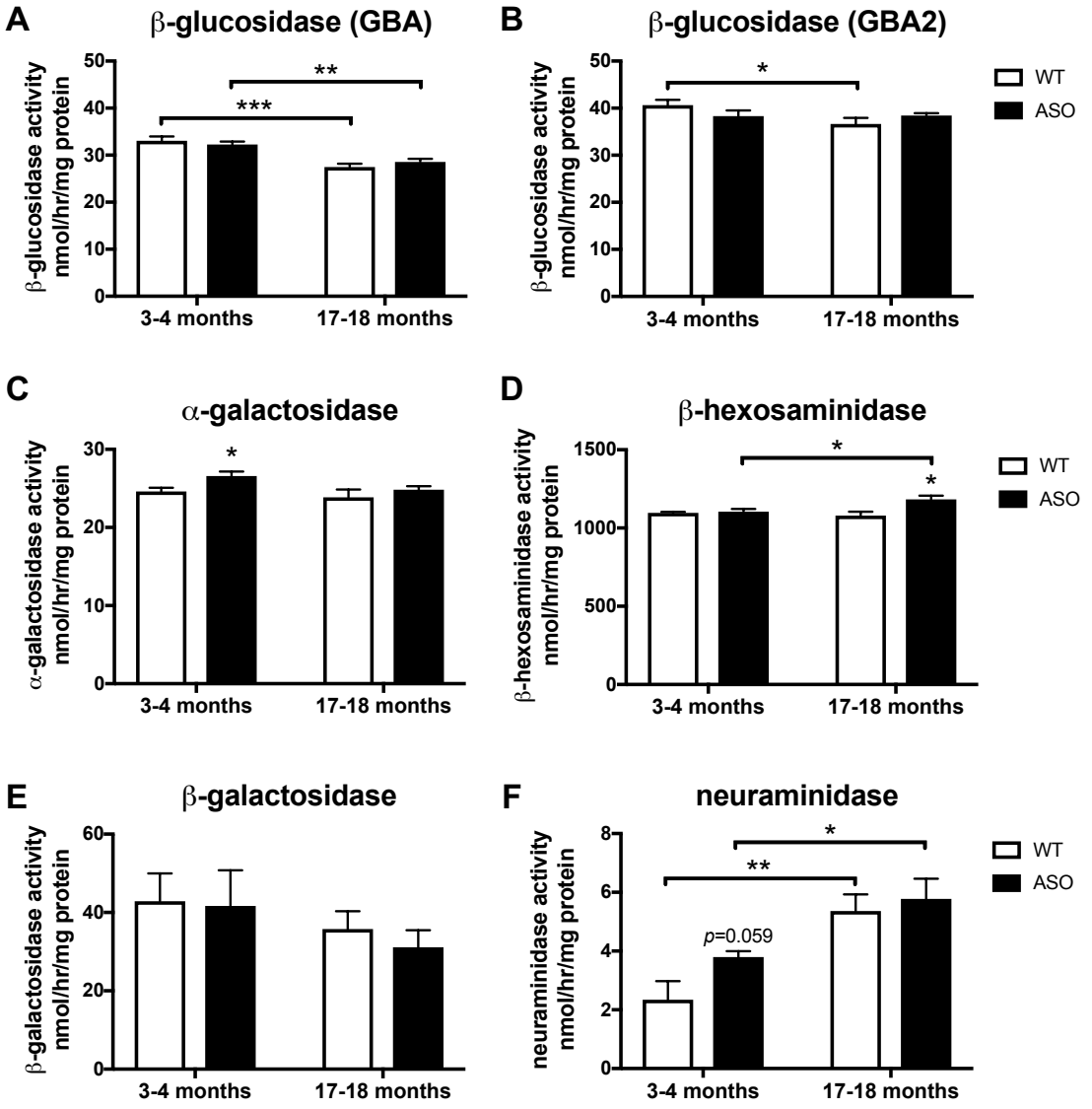

Figure 5.4: Slightly increased α-galactosidase, β-hexosaminidase and neuraminidase activities in brains of ASO mice. Lysosomal hydrolase activities were measured in whole-brain homogenates of 3-4 and 17-18 months old BDF1 WT and ASO mice (n=4-5 per group) using artificial 4-MU-substrates. Lysosomal β-glucosidase activity is defined as GBA, and non-lysosomal β-glucosidase as GBA2. Data are presented as mean ± SEM (* = p<0.05, * = p<0.05, ** = p<0.01, *** = p<0.001, two-way ANOVA).

In addition, no difference in GBA2 β-glucosidase activity was observed in brain homogenates of young and aged ASO mice compared to age-matched WT BDF1 mice (**Figure 5.4B**). Interestingly, there was a significant increase in α-galactosidase activity in brain of young ASO mice compared to young wildtype mice (**Figure 5.4C**, p=0.0316). Furthermore, a significant increase in β-hexosaminidase activity in brains of aged ASO mice compared to aged wildtype mice was detected (**Figure 5.4D**, p=0.0225). Although

not significant, a slightly more decreased β-galactosidase activity in whole-brain homogenates of 17-18 months old ASO mice compared to age-matched wildtype mice was observed (**Figure 5.4E**). In addition, neuraminidase activity in whole-brain homogenates was found to be increased already in young ASO mice compared to young wildtype mice (**Figure 5.4F**, p=0.0598), and was further increased in ASO mice with age (**Figure 5.4F**, p=0.0021 for WT, p=0.0480 for ASO), as already reported for aged BDF1 wildtype mice in **Chapter 4**.

In summary, minor but significant alterations in α-galactosidase, β-hexosaminidase, β-galactosidase and neuraminidase activities were found in whole-brain homogenates of ASO mice compared to wildtype BDF1 mice.

5.3.3 GSLs are not altered in the aged brain of LRRK2(R1441G) mice

To investigate if altered GSL levels might be detectable in another PD mouse model, we analysed the GSLs in brains of aged FVB LRRK2(R1441G) mice (24-month-old) and compared our findings to young (3-month-old) as well as age-matched (24-month-old) FVB wildtype mice. Mutations in leucine-rich repeat kinase 2 (LRRK2) pose a significant genetic risk for developing familial and sporadic PD and cause dominantly inherited, late-onset PD [390].

There was no difference in GlcCer and ganglioside levels in whole-brain homogenates between 24-month-old wildtype FVB mice and 24-month-old LRRK2(R1441G) mice (**Figure 5.5**). However, as already reported for ageing FVB wildtype mice in **Chapter 4**, ageing induced a significant increase in levels of brain GlcCer and GM1a, together with significant decreases in levels of complex gangliosides GD1a, GD1b and GT1b in aged mice (**Figure 5.5**, GlcCer: p=0.0003 for WT, p=0.0002 for LRRK2; GM1a: p<0.0001 for both WT and LRRK2; GD1a: p=0.0008 for WT, p=0.0062 for LRRK2; GD1b: p=0.0087 for WT, p=0.0077 for LRRK2; GT1b: p=0.0001 for both WT and LRRK2).

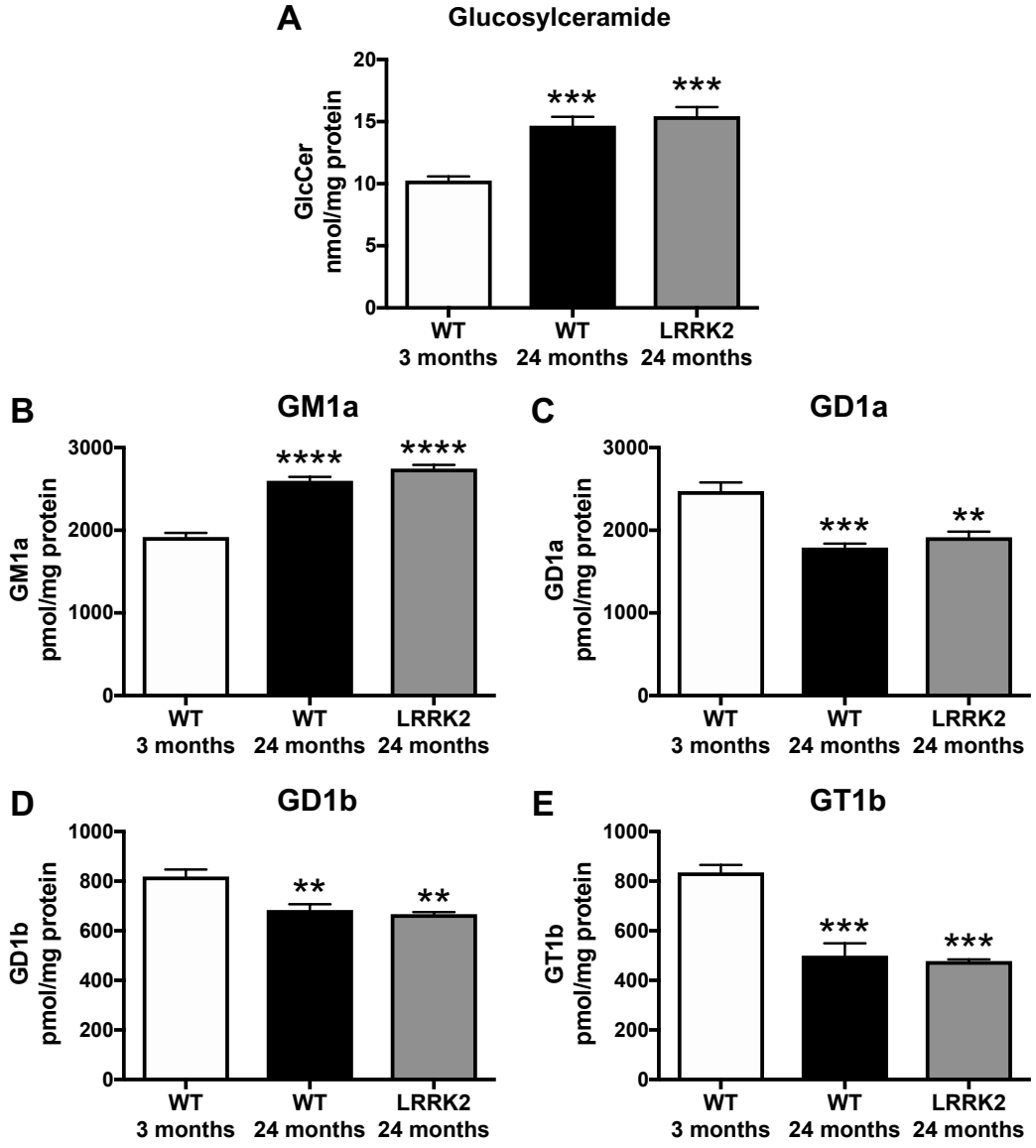

Figure 5.5: No difference in GSL levels between brains of aged FVB WT and LRRK2(R1441G) mice. GlcCer (A), GM1a (B), GD1a (C), GD1b (D) and GT1b (E) levels in whole-brain homogenates of FVB WT and LRRK2(R1441G) mice at 3 months and 24 months of age (n=3-6 per group) were analysed using NP-HPLC (** = p<0.01, *** = p<0.001, **** = p<0.0001, one-way ANOVA). Data are presented as mean ± SEM.

Next, we were interested in studying levels of sphingosine, sphinganine and glucosylsphingosine (GlcSph) in the brain of aged LRRK2(R1441G) mice using RP-HPLC. No difference in C18-sphingosine, sphinganine or C18-GlcSph levels in whole-brain homogenates of 24-month-old LRRK2(R1441G) mice compared to age-matched wildtype FVB mice was found (**Figure 5.6A-C**). Nevertheless, comparable increases in C18-GlcSph and decreases in sphinganine levels during ageing were seen in brains of

both mutant and wildtype mice, as already described in **Chapter 4** for ageing FVB wildtype mice (**Figure 5.6**, SphA: p=0.0044 for WT, p=0.0244 for LRRK2; GlcSph: p=0.0048 for WT, p=0.0032 for LRRK2). To test if cholesterol is altered in this mouse model, cholesterol levels were measured in brain homogenates of 24-month-old LRRK2(R1441G) mice and age-matched wildtype FVB mice using the Amplex Red kit. A slight, but non-significant increase in total brain cholesterol levels was detected in aged LRRK2(R1441G) mice compared to age-matched, 24-month-old FVB wildtype mice (**Figure 5.6D**, p=0.0527).

In summary, no alterations in GSL levels were found in whole-brain homogenates of LRRK2(R1441G) mice at 24 months of age compared to age-matched wildtype FVB mice.

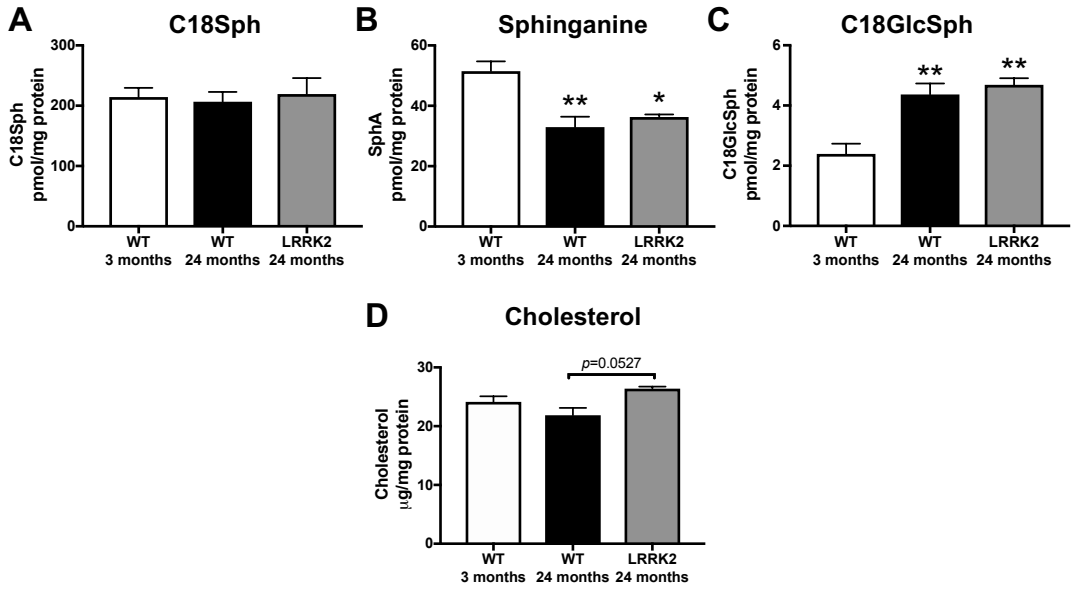

Figure 5.6: No difference in sphingosine, sphinganine, glucosylsphingosine and cholesterol levels between brains of aged FVB WT and LRRK2(R1441G) mice. C18-sphingosine (A), sphinganine (B) and C18-glucosylsphingosine (C) levels in whole-brain homogenates of FVB WT and LRRK2(R1441G) mice at 3 months and 24 months of age (n=3-6 per group) were analysed using RP-HPLC (* = p<0.05, ** = p<0.01, one-way ANOVA). (D) Comparison of total cholesterol levels in whole-brain homogenates of WT and LRRK2 mice (n=3-6 per group, one-way ANOVA) determined with Amplex Red kit. Data are presented as mean ± SEM.

5.3.4 Reduced glucocerebrosidase and increased neuraminidase activities in brains of aged LRRK2(R1441G) and wildtype mice

The levels of GSLs can be modulated by the activity of several lysosomal hydrolases. Thus, we measured the activities of various lysosomal hydrolases using 4-MU assays in whole-brain homogenates of 24-months old LRRK2(R1441G) mice and compared them to 3-months old and 24-months old FVB wildtype mice (n=3-4 per group).

There were no differences in GBA β-glucosidase, GBA2 β-glucosidase, α-galactosidase, β-hexosaminidase, β-galactosidase and neuraminidase activities between brain homogenates of aged LRRK2(R1441G) and aged FVB wildtype mice (**Figure 5.7**). However, as in ageing wildtype FVB mice, significant decreases in GBA β-glucosidase, GBA2 β-glucosidase and β-galactosidase activities and a significant increase in neuraminidase activity were observed in brain homogenates of 24-month old LRRK2(R1441G) mice compared to 3-month old WT FVB mice (**Figure 5.7**, GBA: p=0.0003 for WT, p=0.0011 for LRRK2; GBA2: p=0.045 for WT, p=0.0342 for LRRK2; β-gal: p=0.0374 for WT, p=0.0251 for LRRK2; neuraminidase: p=0.0304 for WT, p=0.0163 for LRRK2).

To summarise, a decrease in both GBA and GBA2 β-glucosidase activities and a decrease in β-galactosidase activity, together with an increase in neuraminidase activity take place in the murine LRRK2(R1441G) brain with normal ageing. However, these age-dependent changes are the same in wildtype FVB brain. Thus, no differences in hydrolase activities were found in whole-brain homogenates of aged LRRK2(R1441G) mice when compared with age-matched wildtype FVB mice.

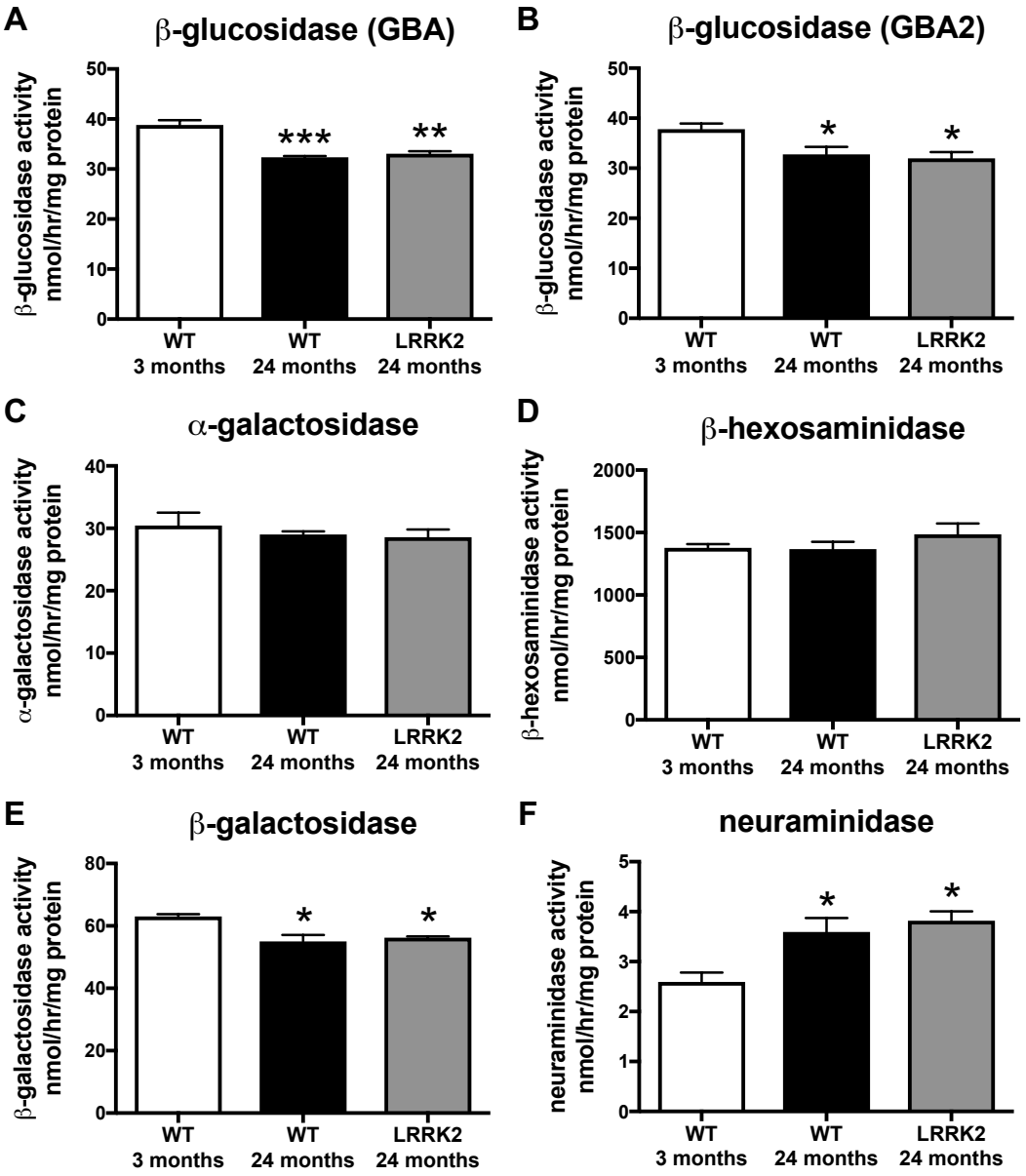

Figure 5.7: Reduced GBA, GBA2 and β-galactosidase activities and increased neuraminidase activity in the brain of aged LRRK2(R1441G) mice, comparable to aged WT mice. Lysosomal hydrolase activities were measured in whole-brain homogenates of 3- and 24-month-old FVB WT mice and 24-month-old FVB ASO mice using artificial 4-MU-substrates. Lysosomal β-glucosidase activity is defined as GBA, and non-lysosomal β-glucosidase as GBA2. Data are presented as mean ± SEM (n=3-4 per age, * = $p<0.05$, ** = $p<0.01$, *** = $p<0.001$, one-way ANOVA).

5.3.5 Elevated GlcCer levels and increased neuraminidase activity in brain of LRRK2(G2019S) KI mice, but not in LRRK2 KO mice

To further investigate if altered GSL levels might be evident in a different PD mouse model, GSLs in brains of roughly 2.5 months old LRRK2(G2019S) KI mice, LRRK2 KO mice and age-matched wildtype mice (n=6-7 per group) were analysed. The G2019S mutation is the most common LRRK2 mutation and is located in the kinase domain, increasing LRRK2 kinase activity and toxicity [374, 391-394]. To distinguish LRRK2 kinase effects from potential scaffolding functions of LRRK2, mice lacking LRRK2 completely (knock-out, KO) were also generated [375].

First, we were interested in determining levels of glucosylceramide (GlcCer) and lactosylceramide (LacCer), both precursors in the GSL biosynthetic pathway. Interestingly, a significant increase in GlcCer levels in whole-brain homogenates of LRRK2(G2019S) KI mice compared to wildtype mice was found, but not in LRRK2 KO mice (**Figure 5.8A**, 24.66% increase, p=0.0396). No differences in LacCer levels in brains of LRRK2(G2019S) KI and LRRK2 KO mice were found compared to age-matched wildtype mice (**Figure 5.8B**). Next, levels of the major GSLs found in the mammalian nervous system, the complex gangliosides GM1a, GD1a, GD1b and GT1b, were analysed using NP-HPLC. No differences in GM1a, GD1a, GD1b and GT1b levels in brains of LRRK2(G2019S) KI and LRRK2 KO mice were found compared to age-matched wildtype mice (**Figure 5.8 C-F**). Next, we were interested in analysing levels of sphingosine, sphinganine and glucosylsphingosine (GlcSph) in the brains of LRRK2(G2019S) KI and LRRK2 KO mice using RP-HPLC. No differences in C18-sphingosine, sphinganine or C18-GlcSph levels in whole-brain homogenates of LRRK2(G2019S) KI and LRRK2 KO compared to age-matched wildtype mice were found (**Figure 5.9**). Then, we analysed the activities of various lysosomal hydrolases in whole-brain homogenates of LRRK2(G2019S) KI and LRRK2 KO mice. No alterations in GBA β-glucosidase, GBA2 β-glucosidase, α-galactosidase, β-hexosaminidase and β-

galactosidase activities in brain homogenates of LRRK2(G2019S) KI and LRRK2 KO mice compared to wildtype mice were discovered (**Figure 5.10**). However, a significant increase in brain neuraminidase activity in LRRK2(G2019S) KI mice compared to age-matched wildtype mice was found (**Figure 5.10F**, 47.5% increase, p=0.0149).

In summary, knock-out of LRRK2 does not alter GSL levels or lysosomal hydrolase activities in the murine brain. However, knock-in of the mutant LRRK2(G2019S) leads to elevated GlcCer levels and increased neuraminidase activity in the brain of KI mice.

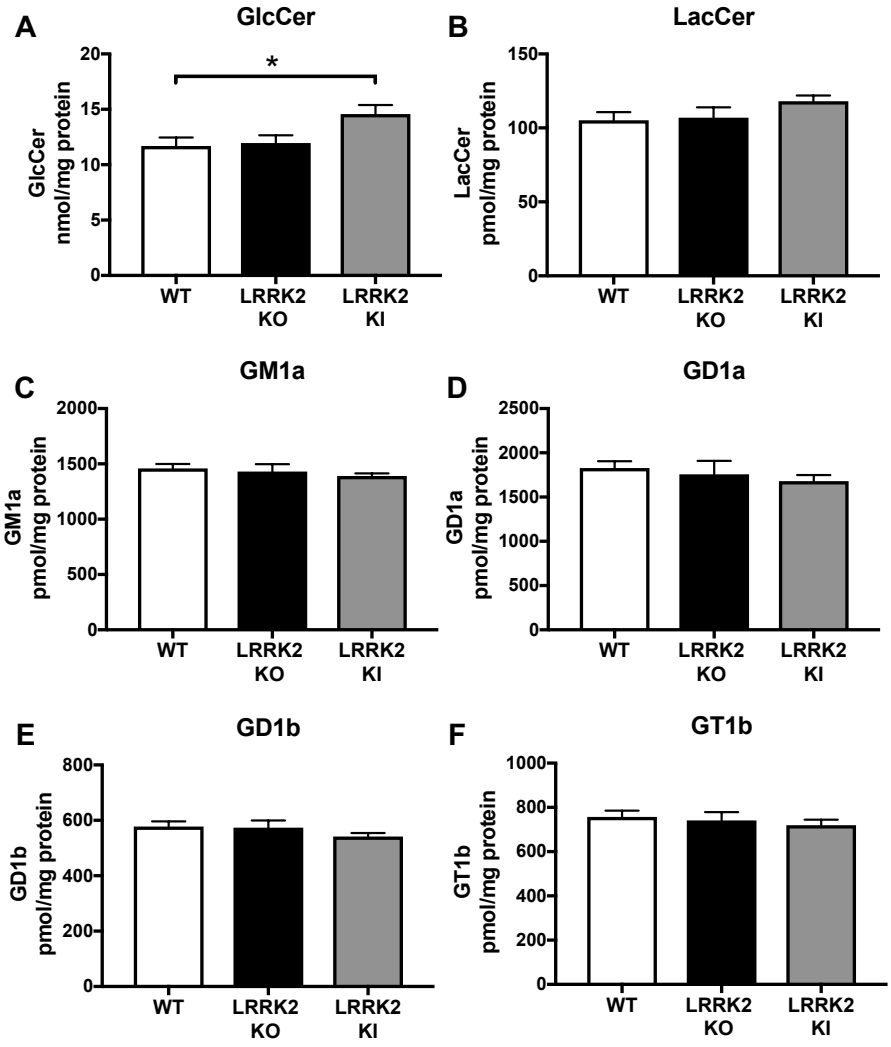

Figure 5.8: Increase in GlcCer in brains of LRRK2(G2019S) KI mice, but no difference in LacCer and ganglioside levels between brains of WT and LRRK2 mice. Whole-brain homogenates from WT, LRRK2 KO, and LRRK2(G2019S) KI mice (n=6-7 per group) were used to determine GlcCer (A), LacCer (B), GM1a (C), GD1a (D), GD1b (E) and GT1b (F) levels using NP-HPLC (* = p<0.05, one-way ANOVA). Data are presented as mean ± SEM.

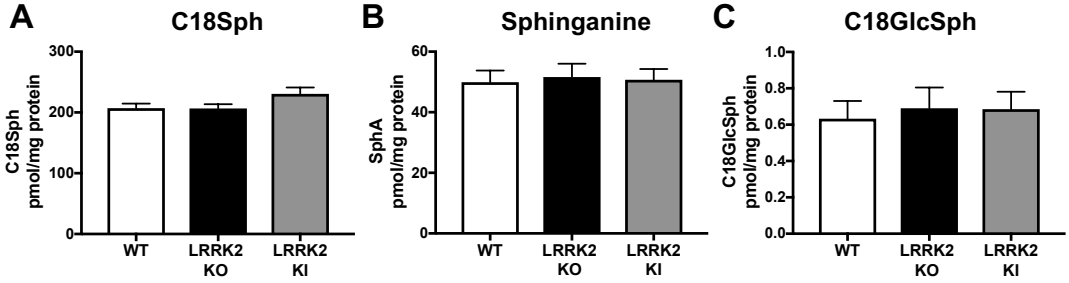

Figure 5.9: No difference in sphingosine, sphinganine and glucosylsphingosine levels between brains of WT, LRRK2 KO and LRRK2(G2019S) KI mice. C18-sphingosine (A), sphinganine (B) and C18-glucosylsphingosine (C) levels in whole-brain homogenates of WT, LRRK2 KO and LRRK2(G2019S) KI mice were analysed using RP-HPLC (n=6-7 per group, not significant, one-way ANOVA). Data are presented as mean ± SEM.

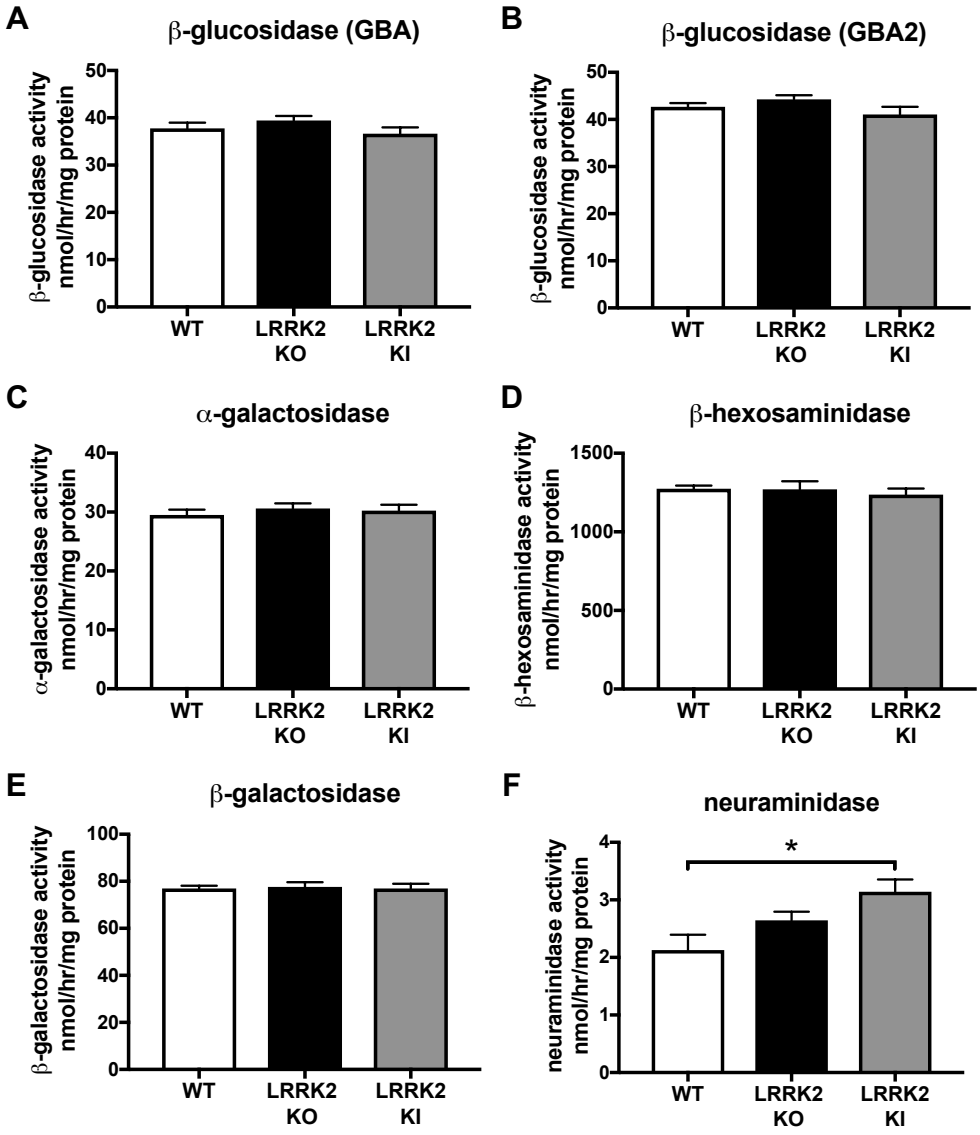

Figure 5.10: Increased neuraminidase activity in brain of LRRK2(G2019S) KI mice. Lysosomal hydrolase activities were measured in whole-brain homogenates of WT, LRRK2 KO and LRRK2(G2019S) KI mice using artificial 4-MU-substrates (n=6-7 per group, * = p<0.05, one-way ANOVA). Data are presented as mean ± SEM.

5.3.6 Increased lysosomal hydrolase activities in the liver of LRRK2(G2019S) KI mice, but not in LRRK2 KO mice

LRRK2 is most highly expressed in peripheral organs and less in brain (The Human Protein Atlas, www.proteinatlas.org). Thus, we wanted to evaluate possible peripheral impairments due to knock-out of LRRK2 or knock-in of the mutant LRRK2(G2019S). For this, we analysed GSL levels and activities of lysosomal hydrolases in liver tissue of LRRK2 KO and LRRK2(G2019S) KI mice in comparison to age-matched wildtype mice (n=6-7 per group).

There was no difference in GlcCer and LacCer levels in liver tissue of LRRK2 KO and LRRK2(G2019S) KI mice in comparison to age-matched wildtype mice (**Figure 5.11A, B**). Next, the main GSLs in murine liver tissue, GM2Gc and GM3Gc, were quantified. No alterations in GM2Gc and GM3Gc levels in liver tissue of LRRK2 KO and LRRK2(G2019S) KI mice compared to wildtype mice were found (**Figure 5.11C, D**). Furthermore, we did not detect any significant changes in the levels of C18-sphingosine and sphinganine in livers of LRRK2 KO and LRRK2(G2019S) KI mice compared to wildtype mice (**Figure 5.12**). However, analysis of various lysosomal hydrolase activities revealed several significant changes in livers from LRRK2(G2019S) KI mice: A significant increase in GBA β-glucosidase, α-galactosidase and β-galactosidase activities was seen in livers of LRRK2(G2019S) KI mice compared to LRRK2 KO and wildtype mice (**Figure 5.13A, C, E**; GBA: 16.9% increase, p=0.0444; α-gal: 31.9% increase, p=0.0225; β-gal:14.4% increase, p=0.0240). However, no differences in GBA2 β-glucosidase, β-hexosaminidase and neuraminidase activities were found in liver of either LRRK2(G2019S) KI or LRRK2 KO mice (**Figure 5.13B, D, F**).

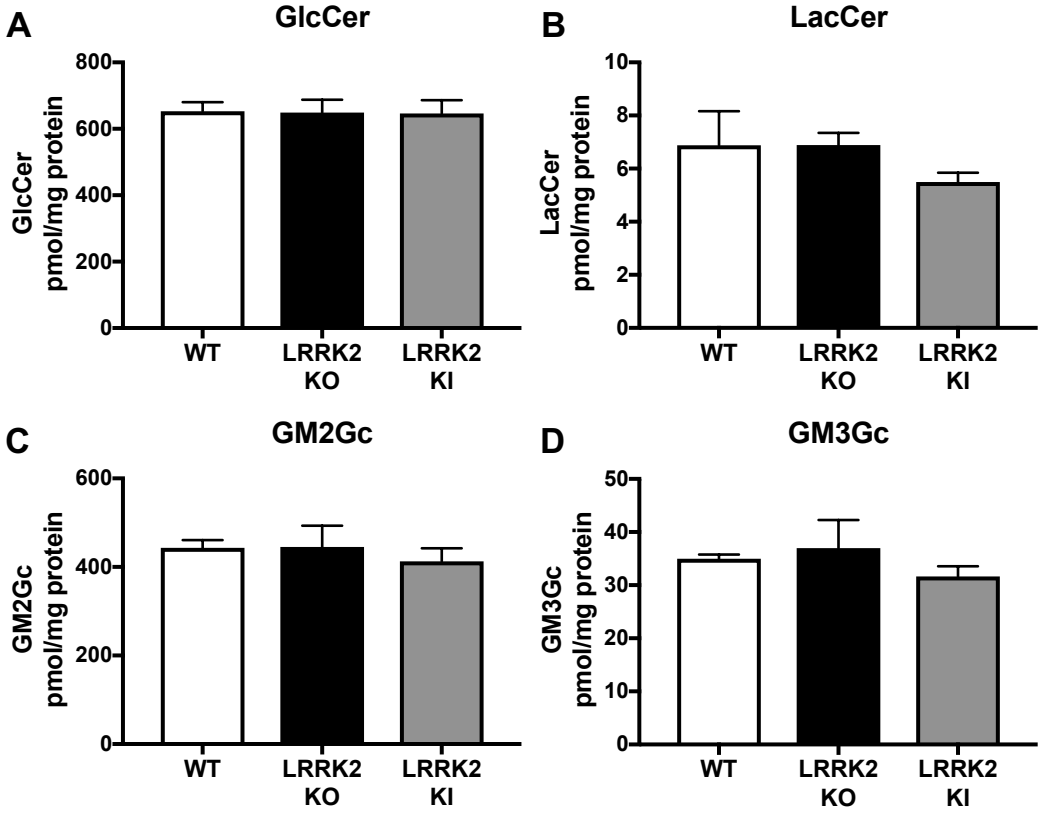

Figure 5.11: Similar levels of GSLs in livers of WT, LRRK2 KO and LRRK2(G2019S) KI mice. Liver homogenates from WT, LRRK2 KO, and LRRK2(G2019S) KI mice (n=6-7 per group) were used to determine GlcCer (A), LacCer (B), GM2Gc (C), and GM3Gc (D), levels using NP-HPLC (not significant, one-way ANOVA). Data are presented as mean ± SEM.

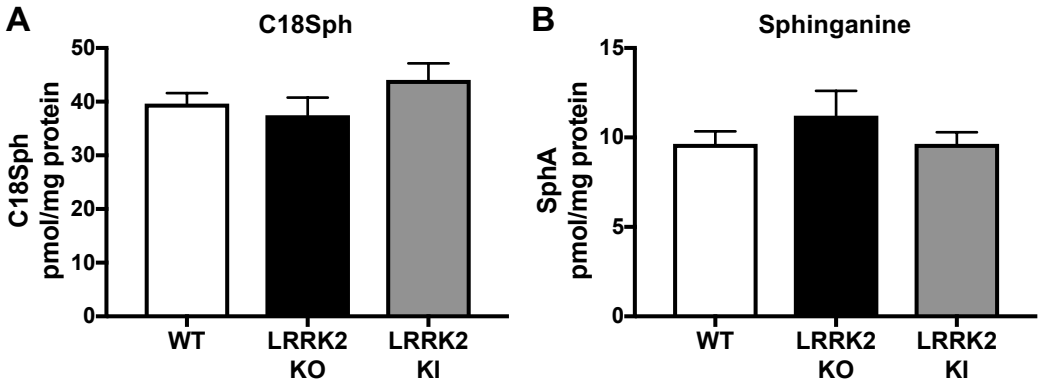

Figure 5.12: No difference in sphingosine and sphinganine levels in livers of WT, LRRK2 KO and LRRK2(G2019S) KI mice. C18-sphingosine (A) and sphinganine (B) levels in liver homogenates of WT, LRRK2 KO and LRRK2(G2019S) KI mice mice were analysed using RP-HPLC (n=6-7 per group, not significant, one-way ANOVA). Data are presented as mean ± SEM.

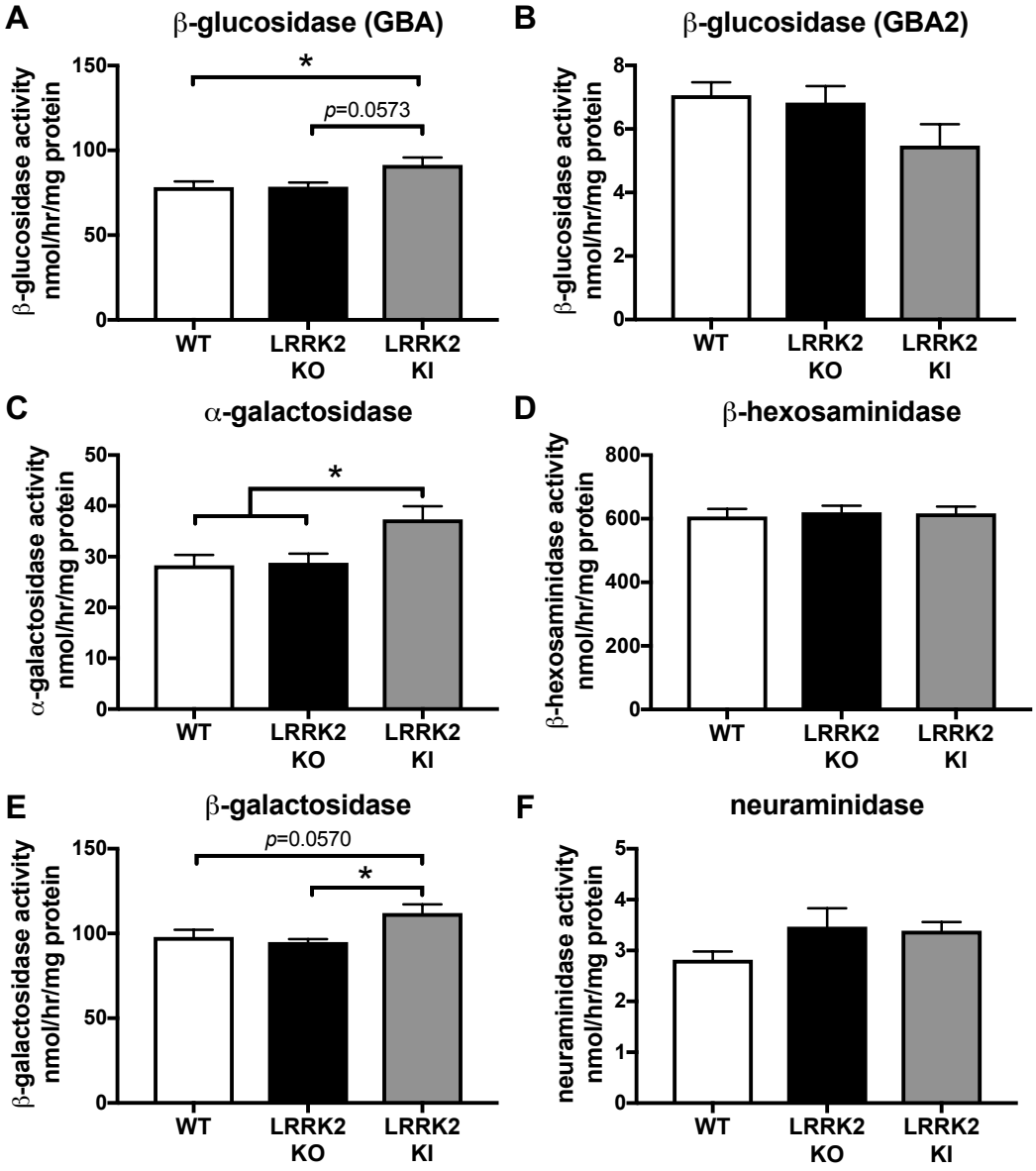

Figure 5.13: Increased GBA and α-galactosidase activity in liver of LRRK2(G2019S) KI mice. Lysosomal hydrolase activities were measured in liver homogenates of WT, LRRK2 KO and LRRK2(G2019S) KI mice using artificial 4-MU-substrates (n=6-7 per group, * = $p<0.05$, one-way ANOVA). Data are presented as mean ± SEM.

5.3.7 Accumulation of GSLs and increased lysosomal hydrolase activities in kidneys of LRRK2 KO mice

LRRK2 is most highly expressed in kidneys and lungs (The Human Protein Atlas, www.proteinatlas.org). Thus, we wanted to evaluate possible kidney impairments owing to knock-out of LRRK2 or knock-in of the mutant LRRK2(G2019S). For this, we analysed GSL levels and activities of lysosomal hydrolases in kidneys of LRRK2 KO and LRRK2(G2019S) KI mice compared to age-matched wildtype mice (n=6-7 per group).

There was no difference in GlcCer levels in kidneys of LRRK2 KO and LRRK2(G2019S) KI mice in comparison to age-matched wildtype mice (**Figure 5.14A**). However, there was a trend for increased LacCer levels in kidneys of LRRK2 KO compared to age-matched wildtype mice and LRRK2(G2019S) KI mice (**Figure 5.14B**, 128.97% of wildtype, p=0.068). Next, the principal neutral GSLs in murine kidney tissue, Gb3 and Gb4, were quantified with NP-HPLC. Intriguingly, significant increases in both Gb3 and Gb4 levels in kidneys of LRRK2 KO mice were found compared to wildtype as well as LRRK2(G2019S) KI mice (**Figure 5.14C, D**; Gb3: p=0.0023 and p=0.0013, respectively; 225.9% of wildtype mice; Gb4: p=0.0175 and p=0.0082, respectively; 133.4% of wildtype mice). In accordance, the total GSL level (sum of LacCer, Gb3 and Gb4, together with minor GSLs GM3, GM2, GA2, and GA1) in kidneys of LRRK2 KO mice was significantly increased to 172.2% of wildtype kidney (**Figure 5.14E**, p=0.0005). In addition, kidneys of LRRK2(G2019S), LRRK2 KO and wildtype mice were weighed before homogenisation for biochemistry analyses. This revealed a significant increase in LRRK2 KO kidney weight compared to wildtype kidneys (**Figure 5.14F**, 36.26% increase, p<0.0001), whereas kidneys of LRRK2 KI mice weighed the same as wildtype kidneys.

Next, we were interested in studying levels of sphingosine and sphinganine in kidneys from LRRK2(G2019S) KI and LRRK2 KO mice using RP-HPLC. We discovered a significant increase in the levels of C18-sphingosine and sphinganine in kidneys of

LRRK2 KO mice compared to wildtype and LRRK2(G2019S) KI mice (**Figure 5.15**, Sph: $p<0.0001$, 219.2% of wildtype; SphA: $p=0.075$, 131.7% of wildtype).

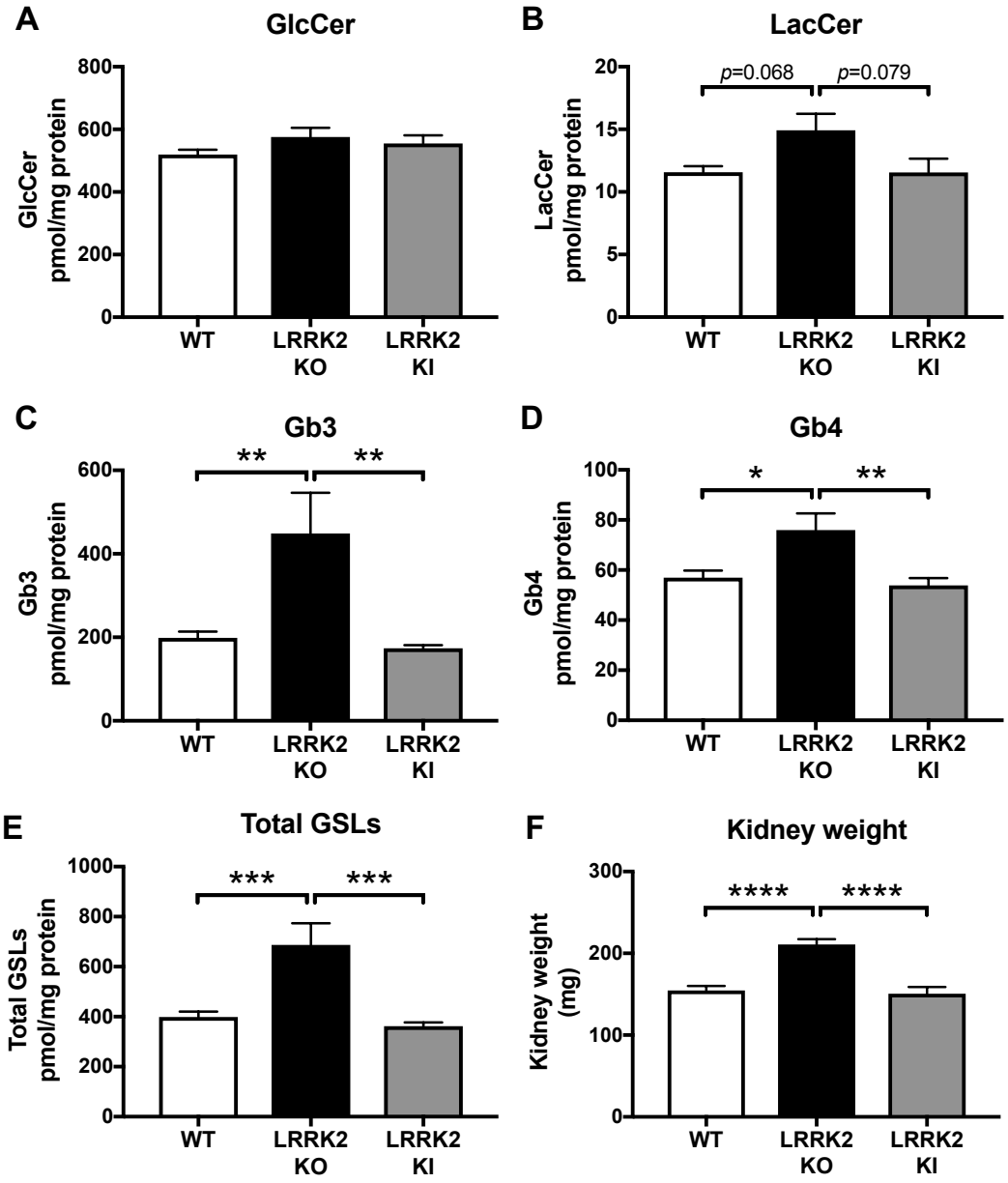

Figure 5.14: Increase in weight and main GSLs, Gb3 and Gb4, in kidneys of LRRK2 KO mice. Kidney homogenates from WT, LRRK2 KO, and LRRK2(G2019S) KI mice (n=6-7 per group) were used to determine GlcCer (A), LacCer (B), Gb3 (C), Gb4 (D), and total GSL (E) levels using NP-HPLC (* = $p<0.05$, ** = $p<0.01$, *** = $p<0.001$, **** = $p<0.0001$, one-way ANOVA). Data are presented as mean ± SEM.

Importantly, analysis of various lysosomal hydrolase activities revealed significant increases in all studied hydrolases in kidney of LRRK2 KO mice: A significant increase in GBA β-glucosidase and GBA2 β-glucosidase was measured in kidneys of LRRK2 KO mice compared to LRRK2(G2019S) KI and wildtype mice (**Figure 5.16A, B**; GBA: $p<0.0001$, 171.6% of wildtype; GBA2: $p=0.0487$ compared to wildtype, 14.0% increase). Furthermore, α-galactosidase, β-hexosaminidase, β-galactosidase and neuraminidase activities were all significantly elevated in LRRK2 KO kidney compared to kidneys of age-matched LRRK2 KI and wildtype mice (**Figure 5.16C-F**; α-gal: $p<0.0001$, 171.8% of wildtype; β-hex: $p=0.0026$ compared to wildtype, 17.2% increase; β-gal: $p<0.0001$, 143.4% of wildtype; neuraminidase: $p<0.0001$, 209.8% of wildtype).

In summary, major changes in GSLs and lysosomal hydrolases were found in LRRK2 KO kidney: GSL levels were significantly increased and lysosomal hydrolase activities were greatly upregulated in kidneys of LRRK2 KO mice compared to age-matched wildtype mice. No differences in LRRK2(G2019S) KI kidneys were found.

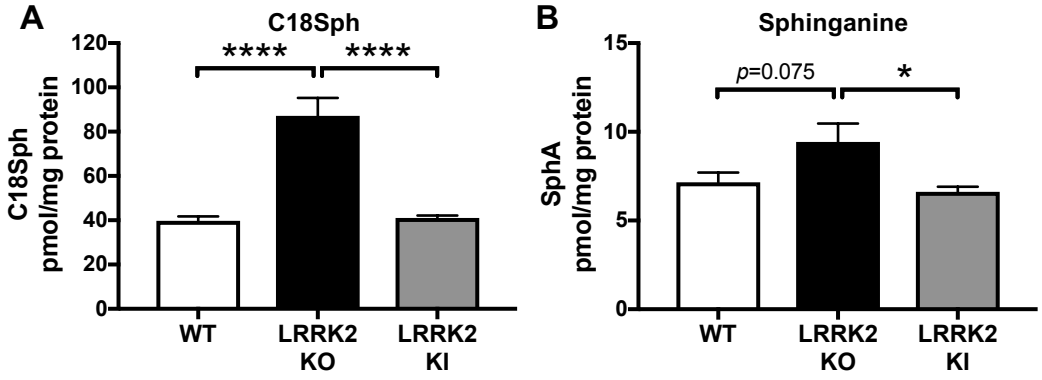

Figure 5.15: Sphingosine and sphinganine levels are increased in kidneys of LRRK2 KO mice. C18-sphingosine (A) and sphinganine (B) levels in kidney homogenates of WT, LRRK2 KO and LRRK2(G2019S) KI mice were analysed using RP-HPLC (n=6-7 per group, * = $p<0.05$, **** = $p<0.0001$, one-way ANOVA). Data are presented as mean ± SEM.

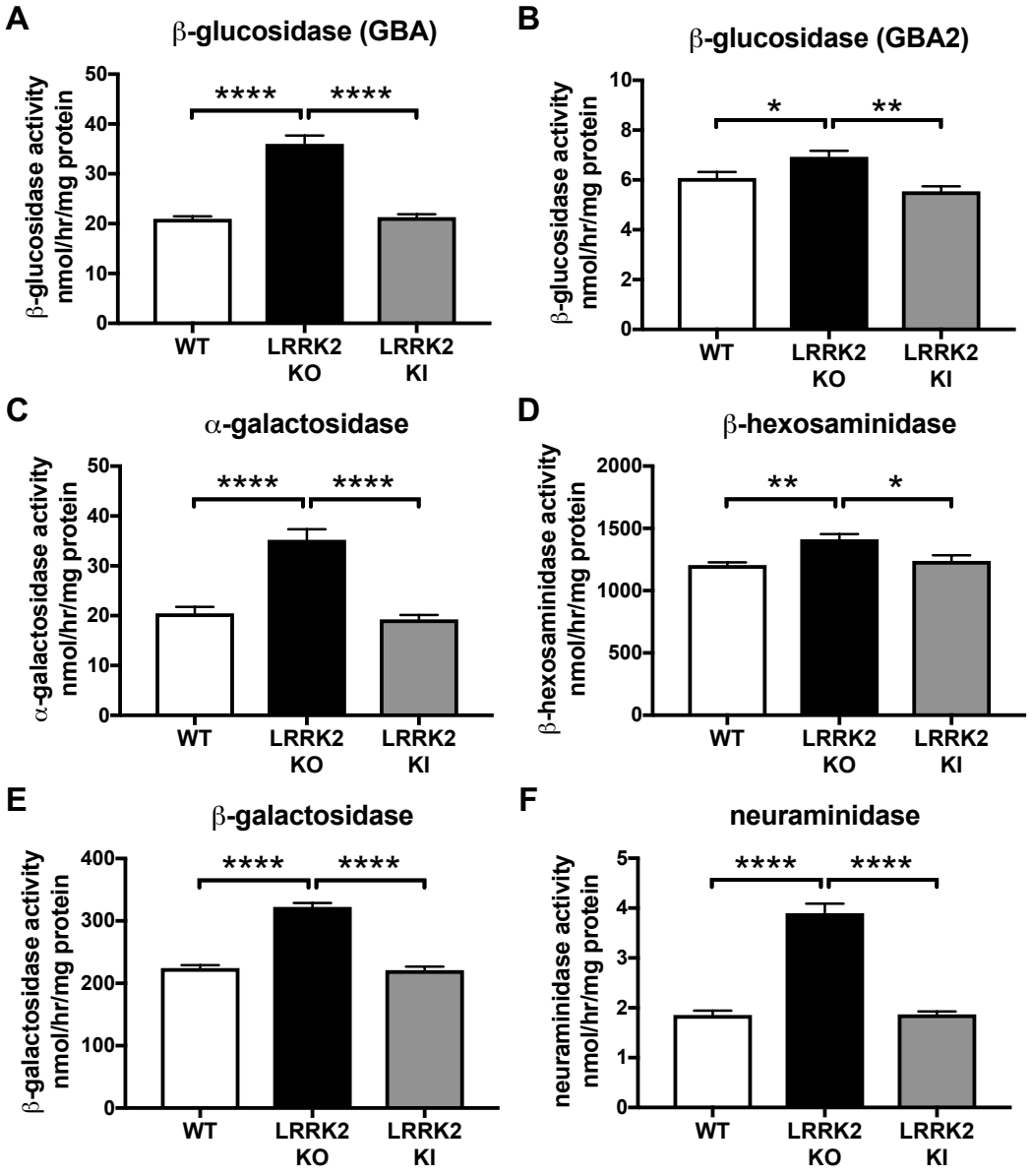

Figure 5.16: Significantly increased hydrolase activities in kidney of LRRK2 KO mice. Lysosomal hydrolase activities were measured in kidney homogenates of WT, LRRK2 KO and LRRK2(G2019S) KI mice using artificial 4-MU-substrates (n=6-7 per group, * = $p<0.05$, ** = $p<0.01$, *** = $p<0.001$, **** = $p<0.0001$, one-way ANOVA). Data are presented as mean ± SEM.

5.4 Discussion

Here, levels of GSLs and activities of various lysosomal hydrolases were analysed in three different PD mouse models. The PD mouse models we used were the human α-synuclein overexpressing (ASO) mouse model, the LRRK2(R1441G) mouse model (expressing the R1441G mutant form of the human LRRK2 protein), and the LRRK2(G2019S) KI mouse model, affecting the murine *LRRK2* gene. Furthermore, tissues from a LRRK2 knock-out (KO) mouse model were also analysed.

ASO: Differences between mouse and man

We analysed brains of 3-4 months old, pre-symptomatic and 17-18 months old, symptomatic ASO mice. α-synuclein aggregates are present in the substantia nigra of ASO mice from 5 months of age and increase in size and number in older mice [387]. ASO mice exhibit a progressive loss of striatal dopamine, with loss of around 40% of striatal dopamine by 14 months of age [388]. Importantly, ASO mice do not show any reduction in the number of TH-positive dopaminergic neurons [387]. Thus, the model lacks a cardinal feature of PD.

First, we found that GSL levels in the brain of α-synuclein overexpressing (ASO) mice are not altered (**Figures 5.1, 5.2 and 5.3**). This confirms the recently published findings of unaltered GlcSph and GlcCer levels in ASO brain compared to age-matched wildtype brain [396]. However, we discovered several altered lysosomal hydrolase activities in whole-brain homogenates of ASO mice, hinting at changes in lysosomal function in ASO mice (**Figure 5.4**). For example, increased β-hexosaminidase activity and decreased β-galactosidase activity were found in brains of aged, 17-18-months old mice compared to age-matched WT mice. This could point to increased overall lysosomal function as β-hexosaminidase is an abundant protein in lysosomes. Furthermore, the ganglioside GM1a is essential for myelination, neuritogenesis, synaptogenesis and signalling of the neurotrophic factor GDNF [42, 43, 157]. Downregulation of its degrading enzyme, β-

galactosidase, could represent an age- and PD-related compensatory mechanism to enhance neurotrophic activity. In addition, GSLs can be remodelled by neuraminidases. It is interesting to note that an increase in GM1a can also be achieved by sequential removal of sialic acid residues from GD1a, GD1b and GT1b by neuraminidases. Consequently, the observed increase in neuraminidase activity in brains of young ASO mice could point to a possible compensatory mechanism to maintain neuronal health despite α-synuclein overexpression already at young age. Importantly, a link between increased α-synuclein accumulation and decreased GCase activity in the context of PD has been demonstrated by several lines of evidence [145, 148, 149, 185, 397]. However, it has already been shown, and we here further confirm, that ASO mice modelling α-synucleinopathy do not show altered GCase (combined GBA and GBA2) activity compared to age-matched wildtype mice [396, 398, 399]. This may be due to the only modest, 2-5-fold overexpression of α-synuclein, as higher levels of expression may be needed for effects on GCase activity [387].

Efforts to model PD in mice by overexpression of wildtype α-synuclein or expression of mutant human α-synuclein have mostly resulted in models lacking neurodegeneration in the substantia nigra. This points to important, fundamental differences between mouse and man. For example, dopaminergic neurons are entirely spared in an α-synuclein A53T transgenic mouse model [400], maybe because the murine α-synuclein protein naturally has a threonine at position 53 [401, 402]. Interestingly, wildtype mouse α-synuclein aggregates more rapidly than human wildtype or A53T α-synuclein *in vitro*, but aged mice still do not spontaneously develop α-synuclein inclusions or PD-like disorders [401, 402]. It is possible that mice have evolved protective mechanisms against α-synuclein aggregation, such as an enhanced ability to maintain α-synuclein in a stable lipid- or protein-bound state, and that these mechanisms may counteract efforts to initiate disease by transgenic α-synuclein expression [401]. Importantly, focusing on dopaminergic neurons, it was suggested that altered calcium and dopamine metabolism

may contribute to species-specific differences between human and mouse neurons [162]. Burbulla *et al.* reported that mitochondrial oxidant stress lead to accumulation of oxidized dopamine, resulting in lysosomal dysfunction and α-synuclein accumulation, in dopaminergic neurons derived from sporadic and familial PD patients [162]. However, this was not observed in dopaminergic neurons of a PD mouse model. As a possible explanation, Burbulla *et al.* found that human control dopaminergic neurons already display elevated, roughly doubled dopamine levels compared to mouse wildtype dopaminergic neurons, suggesting a difference in dopamine metabolism between species [162]. Dopamine can either be converted into non-toxic downstream metabolites or form toxic, reactive oxidized dopamine species. Thus, an increased basal level of dopamine may render human neurons especially vulnerable to the development of oxidized dopamine species [162]. Furthermore, control human neurons showed both increased protein amounts and activity of calcineurin, a phosphatase critical for calcium signalling, suggesting that alterations in calcium homeostasis may also contribute to inter-species differences in dopaminergic neurons [162]. Consequently, increasing dopamine synthesis or increasing α-synuclein levels in mouse PD dopaminergic neurons recapitulated the pathological phenotypes observed in PD human neurons [162]. Similarly, dopaminergic cell death in mice expressing human A53T mutant α-synuclein, which is lacking under normal conditions, was triggered by raising dopamine levels through targeted expression of human tyrosine hydroxylase in the substantia nigra, inducing accumulation of α-synuclein oligomers, progressive nigrostriatal degeneration and reduced locomotion [401].

In summary, variances in α-synuclein handling, calcium homeostasis and dopamine metabolism in dopaminergic neurons are important inter-species differences between mouse and man, complicating the development of suitable PD mouse models.

LRRK2(R1441G): Doubtful phenotype?

Analysis of whole-brain homogenates of 24-month-old LRRK2(R1441G) mice did not reveal any alterations in GSLs and lysosomal hydrolases compared to age-matched wildtype mice (**Figures 5.5, 5.6 and 5.7**). First of all, this mouse model also lacks the cardinal feature of PD, namely DA neuron degeneration [389]. Importantly, the LRRK2(R1441G) mouse recently became focus of numerous reports questioning the hypokinetic motor deficits of this strain, which has not been validated by MJFF or The Jackson Laboratory to date. Accordingly, our collaborators only see a very subtle motor and cognitive phenotype with high age (personal communication, Prof. Penelope Hallett, Harvard), leading us to study 24-month-old animals. Finally, an important fact, which is true for all studied mouse models, is that the current analyses represent whole-brain homogenates and individual cell types may show differences. Further studies will focus on determining GSL and enzymatic alterations in individual brain regions or cell types affected in PD and other age-related neurodegenerative disorders. Nevertheless, in summary, the LRRK2(R1441G) mouse did not prove to be a valuable PD model for our research area of interest.

LRRK2(G2019S) KI: GlcCer and neuraminidase

In contrast, analysis of whole-brain homogenates of LRRK2(G2019S) KI mice revealed significantly elevated brain GlcCer levels and increased neuraminidase activity compared to age-matched wildtype mice (**Figures 5.8 and 5.10**). Concerning the elevated GlcCer levels in murine LRRK2(G2019S) brain, it was previously shown that accumulation of another lipid substrate of GBA, namely GlcSph, the deacylated form of GlcCer, occurs in several brain regions in sporadic PD [164]. GlcSph has been reported to promote α-synuclein pathology in mutant GBA-associated PD [153]. Furthermore, iPSC-derived dopaminergic neurons from GBA-associated PD patients showed elevated levels of GlcCer [147]. Additional, more detailed studies are needed to determine if

changes in GSLs such as GlcCer do occur in PD patients. Interestingly, brain homogenates of the LRRK2(G2019S) KI model showed increased neuraminidase activity, as was also described for brain tissue of the ASO model (**Figure 5.10**). This points again to a possible compensatory, neuroprotective mechanism in the mouse brain, which uses neuraminidases to maintain beneficial levels of the neurotrophic ganglioside GM1a, needed for neuronal health. This possible mechanism was now observed in two independent PD mouse models as well as in murine brain ageing (**Chapter 4**), which further strengthens the need for more detailed studies into neuraminidases and GM1a in PD.

LRRK2 in the periphery: Important function in the kidney

Concerning the role of LRRK2 in peripheral organs, where its expression is the highest, several interesting findings were made. Firstly, increased lysosomal hydrolase activities were found in the liver of LRRK2(G2019S) KI mice, but not in LRRK2 KO mice (**Figure 5.13**). The increased activities of GBA β-glucosidase, α-galactosidase and β-galactosidase could point to increased lysosomal function in LRRK2(G2019S) livers, however the role of LRRK2 in liver has not been studied in detail to date and needs further investigation.

LRRK2 is most highly expressed in kidneys. Importantly, major changes in GSLs and lysosomal hydrolases were found in LRRK2 KO kidney: GSL levels were significantly increased and all studied lysosomal hydrolase activities were greatly upregulated in kidneys of LRRK2 KO mice compared to age-matched wildtype mice (**Figures 5.14, 5.15 and 5.16**). This points to a significant role of LRRK2 in kidney physiology, as the complete knock-out of LRRK2 seems to cause a lysosomal dysfunction phenotype in kidney. The functions of LRRK2 in kidney are rather unknown. However, several studies with LRRK2 KO mice and LRRK2 KO rats provide clear evidence of abnormal kidney phenotypes in these animals. For example, increased kidney weight, dark kidney

pigmentation due to the occurrence of lipofuscin droplets, accumulation of ubiquitinated proteins and accumulation of lysosomes was shown, suggesting a specific role of LRRK2 in the kidney for the function of the lysosome/autophagy pathway [375, 403-405]. It was reported that the LRRK2 KO mouse model used in this study showed a marked increase in number and size of secondary lysosomes in kidney proximal tubule cells at 6 weeks of age, preceding the darkening of the kidneys and the deposition of lipofuscin [375]. We confirmed an increased weight of LRRK2 KO kidneys at 2.5 months of age (**Figure 5.14**), and our results further support the notion of lysosomal dysfunction in LRRK2 KO kidneys. We described an accumulation of GSLs, like Gb3, Gb4 and sphingosine, in kidneys of 2.5 months old animals. These lipids might be a possible source or component of the described lipofuscin, developing over time. Lipofuscin aggregates consist of highly oxidized and crosslinked proteins, lipids and carbohydrates, which are no longer properly degraded by lysosomes [406]. The accumulation of Gb3 in LRRK2 KO kidneys resembles the Gb3 accumulation found in Fabry disease, although lipid storage is higher in Fabry disease. Fabry disease is caused by homozygous mutations in the enzyme α-galactosidase, a lysosomal hydrolase responsible for the degradation of the lipid Gb3 [407, 408]. It is possible that the observed accumulation of lipids in LRRK2 KO kidneys takes place in a cellular compartment where these lipids are not accessible for their degrading enzymes, leading to a compensatory upregulation of those lysosomal enzymes and lysosomes in general. It is also conceivable that an accumulation of lipids, as we observed, can disturb normal lysosomal function when occurring inside lysosomes, overwhelming the autophagy machinery and leading to the reported accumulation of secondary lysosomes. For future work, it would be interesting to determine the localisation of Gb3 and other lipids, like sphingosine, in murine LRRK2 KO kidney. Interestingly, it was reported that LAMP1 as well as the lysosomal enzymes cathepsin B and prosaposin were increased in LRRK2 KO rat kidney [409], indicating an upregulation of the lysosomal pathways and supporting our findings of increased

lysosomal enzyme activities. Furthermore, proteomics of LRRK2 KO rat kidneys compared to wildtype kidneys showed a remarkable enrichment of proteins associated with lysosomal storage diseases, further implicating a role for LRRK2 in lysosomal function in renal cells [409]. Further investigations into the potential causes for the observed lipid storage and elevated lysosomal enzyme activities in kidneys devoid of LRRK2 should be undertaken and might further elucidate the vital role of LRRK2 in kidneys.

Surprisingly, it was reported that the kidney function in LRRK2 KO animals is not drastically altered despite the reported morphological and histopathological changes [375, 404]. Nevertheless, because of our findings and previous reports demonstrating abnormal lung and kidney pathology in LRRK2 KO animal models [375, 405], the development of LRRK2 kinase inhibitors as a treatment for PD should be viewed with cautious optimism. A complete inhibition of LRRK2 should be avoided, as possible harmful side effects in peripheral tissues of PD patients might be found.

PD mouse models: Useful?

Despite the significant contribution of PD animal models to our understanding of PD, none of these models truthfully reproduce the human condition [299]. Critically, all PD animal models lack a significant degeneration of dopaminergic neurons in the substantia nigra, the major pathology of human PD. In my opinion, this remains a major limitation of these models. Nevertheless, transgenic PD models offer insights into the causes of PD pathogenesis and allow the discovery of common biochemical pathways, such as lysosomal dysfunction, in different genetic models [299]. However, another problem is the inconsistency in the reported phenotypes in genetic PD mouse models. In this study, this was the case for the LRRK2(R1441G) mouse model, which did not display hypokinetic motor deficit, although previously described in the original publication [389]. It is also troubling that genetic models with the same mutations, but generated in different

laboratories, show inconsistent phenotypes [299]. These discrepancies might be related to artefacts due to the generation of these models (e.g. insertion of the transgene) or to differences in the genetic background (e.g. different mouse strains). In conclusion, it seems advisable to use more than one disease model to confirm theories and results. Finally, and most importantly, there are inherent differences between human and murine dopaminergic neuron vulnerability, amongst others due to distinctive dopamine metabolism and calcium homeostasis [162]. This emphasizes the value of studies with human neurons or human post-mortem tissues to identify pathways and targets for therapies in PD [162]. In my opinion, this should be more focused on in the current drug discovery process, rather than animal models.

In summary, it seems unlikely that a single genetic model of PD will ever fully replicate the complexity of the human disease. But future, more 'humane' models could be based on combining genetic mutations with further modulations, like exposure to neurotoxins or increasing dopamine levels, in order to 'humanise' animal models to be able to study the progressive neuropathology of PD more accurately.

6 Glycosphingolipids in human PD tissue

6.1 Introduction

6.1.1 Affected brain regions in PD

Parkinson's disease (PD) is characterised by an impaired nigrostriatal pathway in the midbrain. The nigrostriatal pathway is one of the major dopaminergic pathways in the brain and is crucial for movement control and involved in cognitive and emotional response. The nigrostriatal pathway connects the substantia nigra (SN) pars compacta with the dorsal striatum. The SN is a basal ganglia structure located in the midbrain. Many of the effects of the SN are mediated through the striatum via dopaminergic input in the nigrostriatal pathway. The dorsal striatum, which is also a basal ganglia structure, is comprised of the caudate nucleus and putamen. The putamen (or striatum) transmits received motor signals to the thalamus, which then further relays the motor signals to the cerebral motor cortex. Importantly, inputs and outputs of the putamen are interconnected to the SN. Loss of dopamine neurons in the SN is one of the main pathological features of PD. Thus, the cause of PD can be seen as a loss of dopaminergic innervation to the dorsal striatum. Furthermore, SN neurons do not directly stimulate movement, but instead play an indirect role by regulating the more direct role of the striatum and thus contribute to fine motor control. SN inputs influence both the direct (facilitation of wanted movements) and indirect (prevention of unwanted movements) pathways of movement. Accordingly, the loss of dopaminergic neurons in the SN, and hence the loss of this fine motor control, leads to the classic motor symptoms in PD, including tremors, rigidity, and gait dysfunction.

Dopaminergic (DA) neurons have an unusual, distinctive physiological phenotype [292, 410]: Firstly, they are comparatively few in number and their cell bodies are confined to few relatively small brain areas [411, 412]. However, DA neurons have an enormous axonal field, with long axons (mean axonal length of a typical SN DA neuron has been

estimated to be 470 mm) and many neurites and synapses (around 370,000 synapses per axon) projecting to many other brain areas [292, 413, 414]. Secondly, DA neurons have an autonomous pace-making activity, generating action potentials regularly, even in the absence of synaptic input. This pace-making is achieved through engagement of ion channels called L-type Ca^{2+} channels that allow Ca^{2+} to enter the cell [292]. The constant influx of calcium comes with an obvious metabolic cost to SN DA neurons and leads to elevated intracellular Ca^{2+} concentrations, which can eventually become cytotoxic [292, 410]. Lastly, but not to be underestimated, DA neurons have to produce the neurotransmitter dopamine, which is synthesized from its precursor L-DOPA. Dopamine can become neurotoxic in high quantities, as oxidation of cytosolic dopamine and its metabolites readily occurs, leading to the production of cytotoxic free radicals, possibly damaging proteins, lipids and nucleic acids [292, 410]. Nevertheless, Levodopa, a pure form of the precursor L-DOPA, is the most widely used treatment for PD. In summary, dopaminergic neurons have to deal with a substantial metabolic load, which makes these neurons especially prone to 'multiple hits' at different cellular levels and might render them selectively vulnerable [292, 410].

Interestingly, dopamine has recently gained new attention in the PD research field. Dopamine has been shown to interact with α-synuclein and induce soluble α-synuclein oligomers, leading to nigrostriatal degeneration [401]. Furthermore, dopamine oxidation was shown to mediate mitochondrial and lysosomal dysfunction in PD [162]. Consequently, possible neurotoxic properties of dopamine might indeed play an important role in the specific neuropathology in PD.

6.1.2 Risk factors for PD: *GBA* and further LSD genes

The importance of normal lysosomal function for the health of neurons is clearly illustrated by the pathology associated with LSDs. Defects in many different, unique aspects of lysosomal function commonly result in a relentless neurodegenerative clinical

course, with neurons being particularly vulnerable to disruption in lysosomal function [415]. The most extensively researched area to date is the link between Gaucher disease (GD) and PD [127, 132, 134, 152, 416]. Importantly, in a major multicentre study, heterozygote carriers of *GBA* mutations, with a 30-50% reduction in GBA activity, have been shown to be at highest risk for developing PD [127].

With mutations in a lysosomal enzyme suddenly being the highest known genetic risk factor for developing PD, the GBA and LSD research field has gained a lot of attention from PD researchers. For example, it has been reported that GBA activity is reduced in human brain tissue, e.g. SN, putamen and cerebellum, from PD-GBA patients, as expected in heterozygote GBA mutation carriers [163]. Surprisingly, GBA activity was also found to be reduced in the same brain regions in sporadic PD patients, not carrying any GBA mutations, suggesting a broader role for the lysosome in PD [163-165]. Importantly, it was reported that GBA activity progressively declines even with healthy ageing in SN and putamen of controls and eventually becomes comparable to the lower GBA activity found in PD patients [164].

Besides lysosomal β-glucocerebrosidase GBA, there is also a non-lysosomal glucocerebrosidase, called GBA2. GBA2 is a membrane-associated protein at the cytoplasmic site of the ER and Golgi [47]. Unfortunately, GBA2 is currently largely overlooked in the PD research community, although GBA2 seems to be important for brain function and motor coordination [417]. Moreover, most publications do not reliably distinguish GBA and GBA2 activities, thus actually measuring a combined GBA+GBA2 glucocerebrosidase activity. GBA2 is highly expressed in brain, testis, and liver, which accumulate cytosolic GlcCer in a GBA2 knockout mouse model [49]. Recently, it has been proposed that GBA2 depends on GBA, but not *vice versa*: It has been shown that a reduction in GBA activity leads to GlcSph and sphingosine accumulation, which then bind to and inhibit GBA2 [284]. Further studies are needed to determine how GBA2 may also be involved in PD.

Besides the link between GBA/GD and PD, there have been several reports linking other LSDs, e.g. Fabry disease and Niemann Pick disease type C, with PD [178, 179, 418, 419]. In 2017, a major study reinforced this notion, stating that there is an excessive burden of LSD gene variants in PD patients [180]. For example, besides *GBA*, variants in 54 LSD genes were found, including *GLA* (α-galactosidase, mutated in Fabry disease), *HEXB* (β-hexosaminidase, mutated in Sandhoff disease), *GLB1* (β-galactosidase, mutated in GM1-gangliosidosis) and *NEU1* (neuraminidase 1, mutated in sialidosis) [180].

6.1.3 GlcCer, GlcSph and gangliosides in PD

In GD, significantly reduced lysosomal GBA activity causes storage of its substrates, glucosylceramide (GlcCer) and glucosylsphingosine (GlcSph). Several reports already suggested a connection between PD and altered GSL homeostasis. GlcCer was shown to directly influence amyloid formation of α-synuclein by stabilising soluble oligomeric intermediates in a lysosome-like environment, which in turn lead to further depletion of lysosomal GBA activity, ending in a self-propagating positive feedback loop resulting in neurodegeneration [148]. Further studies have supported a link between the lipids GlcCer and GlcSph with α-synuclein [153-155]. For example, both GlcSph and GlcCer have been reported to promote the formation of oligomeric α-synuclein species and thus to mediate neuropathology in GBA-associated PD [153, 154].

Concerning changes in GlcCer and GlcSph levels in human tissue, iPSC-derived dopaminergic neurons from GBA-associated PD patients showed elevated levels of GlcCer [147]. Interestingly, it has also been shown that lipid changes even occur in sporadic PD patients [164, 420]. For example, accumulation of GlcSph was reported in several brain regions, e.g. substantia nigra, from sporadic PD patients [164]. However, other reports have stated that levels of GlcCer and GlcSph do not increase in either GBA-associated PD or sporadic PD in putamen, cerebellum and temporal cortex [166,

167]. Further studies are needed to determine if these GSLs accumulate in PD, as analysis of different brain regions might already explain these reported discrepancies.

To further substantiate dysregulation of lipids in PD, it was reported that mice lacking major brain gangliosides, in particular GM1a, develop Parkinsonism [421]. Gangliosides are complex GSLs, which are the most abundant GSLs in the CNS in all mammals and are essential for brain development and function [40, 202]. The ganglioside GM1a has gained special interest as it is essential for neuritogenesis, synaptogenesis and signalling of the neurotrophic factor GDNF [42, 43, 157]. Interestingly, a reduction in GM1a levels has been described in SN and occipital cortex from PD patients [156-158].

In summary, additional and more detailed studies are needed to determine the degree to which specific changes in GSL metabolism or even lipid accumulation are a common feature of PD. Furthermore, additional studies are needed to analyse the role of more-complex gangliosides in PD in more in detail.

Research over the past decade has revealed several links between PD and LSDs associated with lysosomal dysfunction and altered glycosphingolipid homeostasis. Thus, we were interested whether alterations in brain GSL homeostasis and changes in lysosomal hydrolase activities occur in human tissues from ageing control subjects and sporadic PD patients. These studies are important for shedding light on processes involved in ageing and the neuropathology of PD.

The aims of this experimental chapter are therefore:

- To assess various lysosomal hydrolase activities, e.g. GBA and GBA2, in substantia nigra of control subjects and PD patients.
- To determine if substrate accumulation, i.e. GlcCer and GlcSph, takes place in substantia nigra of control subjects and PD patients.

- To analyse levels of gangliosides in substantia nigra of control subjects and PD patients.
- To evaluate whether changes in lysosomal hydrolase activities and GSL levels can be found in other tissues, i.e. putamen and spinal cord, of control subjects and PD patients.

Most of the data in this experimental chapter are part of a submitted manuscript (Huebecker *et al.*, 2019).

6.2 Materials and Methods

6.2.1 Patients

Frozen post-mortem brain tissue from neurologically unaffected patients (healthy control subjects) and sporadic PD patients was provided by the Harvard Brain Tissue Resource Centre (HBTRC; McLean Hospital, Belmont, MA), the Parkinson's UK Brain Bank (PDUK; Imperial College London, UK) and the Oxford Brain Bank (OBB; Oxford, UK). All PD cases met a pathological diagnosis of PD made by the brain banks, which was based on the extent of neuronal (pigment) loss in the substantia nigra and Braak staging. Research was performed under the HBTRC's ethical approval from the Institutional Review Board (2015P002028/MGH) and under the PDUK Brain Bank's and the OBB's Research Ethics Committee approval (REC08/MRE09/31+5 and REC15/SC/0639, respectively).

From the HBTRC, post-mortem substantia nigra (SN) tissue from healthy subject controls (n=20) and PD patients (n=18), which were closely matched for age, sex, and post-mortem interval, were provided (**Table 6.1**). The brain tissue was sequenced for GBA mutations (the GBA pseudogene was also considered) at Beckman Coulter Genomics (Danvers, MA). Four PD patients were found to be GBA mutation carriers (L444P, V294M and twice E326K). PD patients with GBA mutation were not removed from further analysis as no statistically significant differences were observed to sporadic PD cases (data not shown). However, for the reader's convenience, PD patients, who were identified as GBA mutation carriers, are coloured in grey, to be distinguishable from sporadic PD patients coloured in black. The PDUK Brain Bank provided a second, independent cohort of post-mortem SN tissue from healthy control subjects (n=5) and age-matched PD patients (n=20) (**Table 6.2**). A third cohort of post-mortem SN tissue from control subjects in their 50s (n=7), control subjects in their 80s (n=13) and PD patients in their 80s (n=12) was provided by the Oxford Brain Bank (OBB, **Table 6.3**). Furthermore, frozen post-mortem putamen tissue from the same control subjects

(50s, n=7; 80s, n=13) and sporadic PD patients (80s, n=12) was provided by the OBB (**Table 6.3**). In addition, frozen post-mortem lumbar spinal cord (SpC) tissue from healthy control subjects and sporadic PD patients was provided by the PDUK Brain Bank and the OBB. Both cohorts were combined and processed together to increase n-numbers. SpC tissue from control subjects in their 50s (n=5), control subjects in their 80s (n=10) and PD patients in their 80s (n=22) were used for analysis (**Table 6.4**). Tissues were rapidly homogenised in PBS using a handheld Ultraturax T25 probe homogeniser (IKA, Germany) and aliquoted before being stored at -80°C.

Table 6.1: PD and control case information from substantia nigra received from the HBTRC. PMI = post-mortem interval. Data summarised as mean ± SD.

	Control subjects (70s cohort)	Control subjects (80s cohort)	PD subjects (70s cohort)	PD subjects (80s cohort)
Cohort size	10	10	10	8
Female (%)	20.0	50.0	10.0	37.5
Male (%)	80.0	50.0	90.0	62.5
Age (years)	71.2 ± 2.9	81.6 ± 4.8	71.0 ± 3.3	81.9 ± 3.9
PMI (hours)	23.0 ± 4.6	22.7 ± 6.5	16.3 ± 6.4	17.1 ± 6.0

Table 6.2: PD and control case information from substantia nigra received from the PDUK Brain Bank. PMI = post-mortem interval. Data summarised as mean ± SD.

	Control subjects	PD subjects
Cohort size	5	20
Female (%)	20	20
Male (%)	80	80
Age (years)	83.4 ± 9.5	77.6 ± 6.9
PMI (hours)	15.4 ± 6.9	15.9 ± 5.2

Table 6.3: PD and control case information from substantia nigra and putamen received from the OBB. PMI = post-mortem interval. Data summarised as mean ± SD.

	Control subjects (50s cohort)	Control subjects (80s cohort)	PD subjects
Cohort size	7	13	12
Female (%)	28.6	30.8	16.7
Male (%)	71.4	69.2	83.3
Age (years)	46.7 ± 7.8	81.4 ± 6.9	80.0 ± 8.1
PMI (hours)	N/A	N/A	N/A

Table 6.4: PD and control case information from spinal cord received from the PDUK Brain Bank and the OBB. PMI = post-mortem interval. Data summarised as mean ± SD.

	Control subjects (50s cohort)	Control subjects (80s cohort)	PD subjects
Cohort size	5	10	22
Female (%)	20.0	36.4	22.7
Male (%)	80.0	63.6	77.3
Age (years)	46.8 ± 9.0	81.7 ± 10.5	78.1 ± 6.4
PMI (hours)	N/A	N/A	N/A

6.2.1.1 Acknowledgements

We would like to express our gratitude to the brain banks for their service. We would like to thank the Harvard Brain Tissue Resource Centre (McLean Hospital, Belmont, MA, US) for providing human tissue samples. Tissue samples and associated clinical and neuropathological data were also supplied by the Parkinson's UK Brain Bank (Imperial College London, UK), funded by Parkinson's UK, a charity registered in England and Wales (258197) and in Scotland (SC037554). We further acknowledge the Oxford Brain Bank (Oxford, UK), supported by the Medical Research Council (MRC), the NIHR Oxford Biomedical Research Centre and the Brains for Dementia Research programme, jointly funded by Alzheimer's Research UK and the Alzheimer's Society. Lastly, I would like to thank the patients and their families for deciding to donate to these brain banks. Without their incredible commitment, my research would have not been possible.

6.2.2 Glycosphingolipids (NP-HPLC)

GlcCer and downstream GSLs were analysed as previously described in **Chapters 2.2.6 and 3.2.7**.

6.2.3 Sphingosine and glucosylsphingosine (RP-HPLC)

As detailed in **Chapter 3.2.8**.

6.2.4 Cholesterol

As detailed in **Chapter 4.2.5**.

6.2.5 Lysosomal hydrolase activity assays

As detailed in **Chapter 3.2.6**.

6.2.6 Statistical analysis

All statistical analyses were performed with GraphPad Prism 7.0 (GraphPad, San Diego, CA). Unpaired student's *t*-test was used to compare two groups, one-way ANOVA was used to compare three groups and two-way ANOVA was used to compare more than three groups. Correlations were analysed with Pearson correlation analysis.

6.3 Results

6.3.1 GBA and GBA2 activities progressively decline in substantia nigra with normal ageing and are further decreased in PD

To investigate if activities of the β-glucosidases GBA and GBA2 are altered in ageing or PD, GBA and GBA2 activities were assayed in substantia nigra (SN) from healthy control subjects and PD patients. These tissues were provided by the Harvard Brain Tissue Resource Centre (HBTRC). Patients and controls were divided into those in their 7th or 8th decades of life, termed here the 70s and 80s cohorts (n=10 per condition and n=5 per age group). PD patients, which were identified as GBA mutation carriers, are coloured in grey, to be distinguishable from sporadic PD patients coloured in black.

GBA activity in substantia nigra was significantly, negatively correlated with the age of control subjects (r=-0.7806, p=0.0077) and PD patients (r=-0.6375, p=0.0474) (**Figure 6.1A**). GBA activity in the substantia nigra of 80s-cohort control subjects was significantly reduced to 80.5% of the GBA activity in the 70s control cohort (**Figure 6.1B**, p=0.0091). The activity of GBA in SN of PD patients was significantly reduced by 34.2% in the 70s-cohort and 26.0% in the 80s-cohort compared to the respective controls (**Figure 6.1B**, p<0.0001 and p=0.0052, respectively).

GBA2 activity in substantia nigra had a trend towards a negative correlation with the age of control subjects (r=-0.5641, p=0.0894), but not with the age of PD patients (r=-0.1832, p=0.6124) (**Figure 6.1C**). There was a trend towards a reduction in GBA2 activity in SN of 80s-cohort control subjects compared to 70s-cohort control subjects (**Figure 6.1D**, p=0.057, 20.6% reduction). A significant decrease in GBA2 activity was seen in SN of 70s-cohort PD patients (p=0.0001, 42.6% reduction) and of 80s-cohort PD patients (p=0.0371, 27.9% reduction) compared to age-matched controls (**Figure 6.1D**).

In summary, both lysosomal GBA and non-lysosomal GBA2 activities in the substantia nigra are negatively correlated with ageing in control subjects and are significantly reduced in PD patients compared to age-matched control subjects.

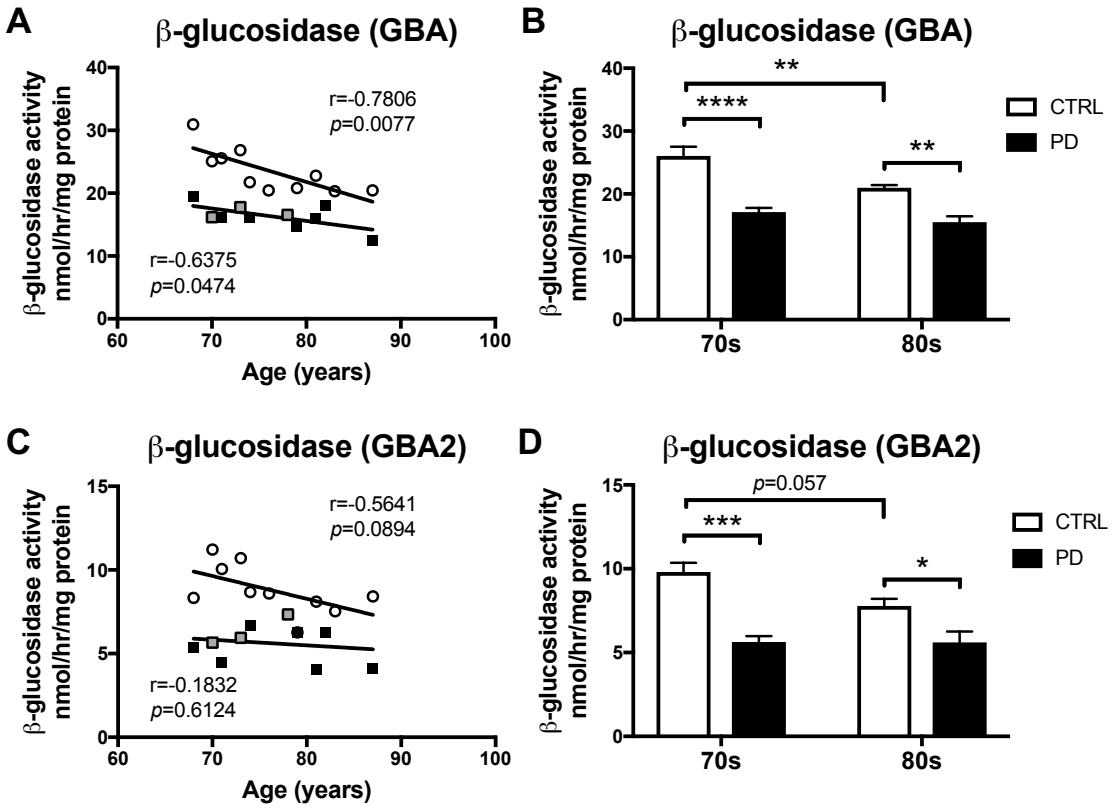

Figure 6.1: Reduced GBA and GBA2 activities in substantia nigra of PD patients and with normal ageing. GBA and GBA2 β-glucosidase activities were measured using artificial 4-MU-substrate and the inhibitor NB-DGJ. Activity of GBA (A, B) and GBA2 (C, D) were determined in substantia nigra homogenates from control subjects and PD patients. Data were analysed using Pearson correlation analysis (A, C) (n=10 per group) and 2-way ANOVA (B, D) (n=5 per cohort; * = $p<0.05$, ** = $p<0.01$, *** = $p<0.001$, **** = $p<0.0001$). Bar graphs are presented as mean ± SEM.

6.3.2 Reduced activity of various lysosomal hydrolases in substantia nigra of PD patients

Mutations in multiple lysosomal hydrolases were recently identified as risk factors for PD [180]. Consequently, additional lysosomal hydrolases, including α-galactosidase, β-hexosaminidase, β-galactosidase and neuraminidase, were assayed in substantia nigra

from control subjects and PD patients (n=10 per condition and n=5 per age group, provided by HBTRC).

Substantia nigra α-galactosidase activity had a trend towards a negative correlation with increasing age of control subjects (r=-0.5208, *p*=0.1227), but less so in PD patients (r=-0.2055, *p*=0.5690) (**Figure 6.2A**). A significant reduction in α-galactosidase activity was however observed in SN of 70s-cohort PD patients (*p*<0.0001, 59.2% reduction) and 80s-cohort PD patients (*p*=0.0004, 55.9% reduction) compared to age-matched controls (**Figure 6.2B**). Consequently, we analysed levels of Gb3, the principle GSL substrate for α-galactosidase. We did not observe any change in Gb3 levels in the substantia nigra of PD patients compared to control subjects (**Figure 6.3A, B**).

β-hexosaminidase activity was significantly, negatively correlated with the age of PD patients (r=-0.7297, *p*=0.0166), but not in control subjects (r=-0.1137, *p*=0.7546) (**Figure 6.2C**). A significant reduction in β-hexosaminidase activity was observed in the 80s-cohort PD patients compared to 80s-cohort control subjects (**Figure 6.2D**, *p*=0.0095, 30.7% reduction).

Substantia nigra β-galactosidase activity was significantly, negatively correlated with the age of control subjects (r=-0.6644, *p*=0.0361), and had a negative correlation with the age of PD patients (r=-0.5299, *p*=0.1151) (**Figure 6.2E**). The activity of β-galactosidase in SN of 70s-cohort PD patients was significantly reduced to 70.7% of β-galactosidase activity of age-matched control subjects (**Figure 6.2F**, *p*=0.0192). Furthermore, there was a trend to reduced activity in PD patients when comparing β-galactosidase activities of both 80s-cohorts (**Figure 6.2F**, *p*=0.064, 27.8% reduction).

Neuraminidase activity in substantia nigra of control subjects and PD patients was not significantly correlated with age (**Figure 6.2G**, r=-0.0572, *p*=0.8751 for CTRL, r=-0.3854, *p*=0.2714 for PD). However, strongly decreased neuraminidase activity was observed in SN of 70s-cohort PD patients compared to 70s-cohort control subjects (**Figure 6.2H**, *p*=0.052, 41.7% reduction), but did not reach statistical significance. Importantly, the

activity of neuraminidase in SN of the 80s-cohort PD patients was significantly reduced to 52.4% of activity in SN of age-matched control subjects (**Figure 6.2H**, *p*=0.0161).

In summary, all lysosomal hydrolases assayed, e.g. α-galactosidase and neuraminidase, had significantly reduced activities in the substantia nigra of PD patients compared to age-matched control subjects.

6.3.3 Accumulation of GlcCer in substantia nigra of PD patients

Next, we were interested in studying the levels of glucosylceramide (GlcCer), one of the substrates for the β-glucosidases GBA and GBA2, and lactosylceramide (LacCer), sequential precursors of all the more complex GSLs in the biosynthetic pathway. Levels of GlcCer and LacCer were measured in substantia nigra from PD patients (n=18) and age-matched controls (n=20, provided by HBTRC) by NP-HPLC. For the reader's convenience, PD patients, which were identified as GBA mutation carriers, are coloured in grey, to be distinguishable from sporadic PD patients coloured in black.

GlcCer levels were significantly, positively correlated with increasing age in substantia nigra of PD patients (r=0.7118, *p*=0.0008), but not in control subjects (r=0.0085, *p*=0.9716) (**Figure 6.4A**). In the 70s-cohort PD patients, GlcCer levels in substantia nigra were increased to 137.1% of age-matched control subjects, but did not reach statistical significance (**Figure 6.4B**, *p*=0.055). In substantia nigra of 80s-cohort PD patients, GlcCer levels were significantly increased to 174.0% of 80s-cohort control subjects (**Figure 6.4B**, *p*=0.0002). Exemplary NP-HPLC traces of GlcCer from substantia nigra of 80s-cohort control subjects and PD patients are shown in **Figure 6.5A**.

For LacCer, there was no significant correlation with age in substantia nigra of control subjects and PD patients (**Figure 6.4C**; r=0.0142, *p*=0.9528 for CTRL; r=-0.2419, *p*=0.3335 for PD). Furthermore, there were no significant changes observed when comparing substantia nigra LacCer levels between control and PD cohorts at different ages (**Figure 6.4D**).

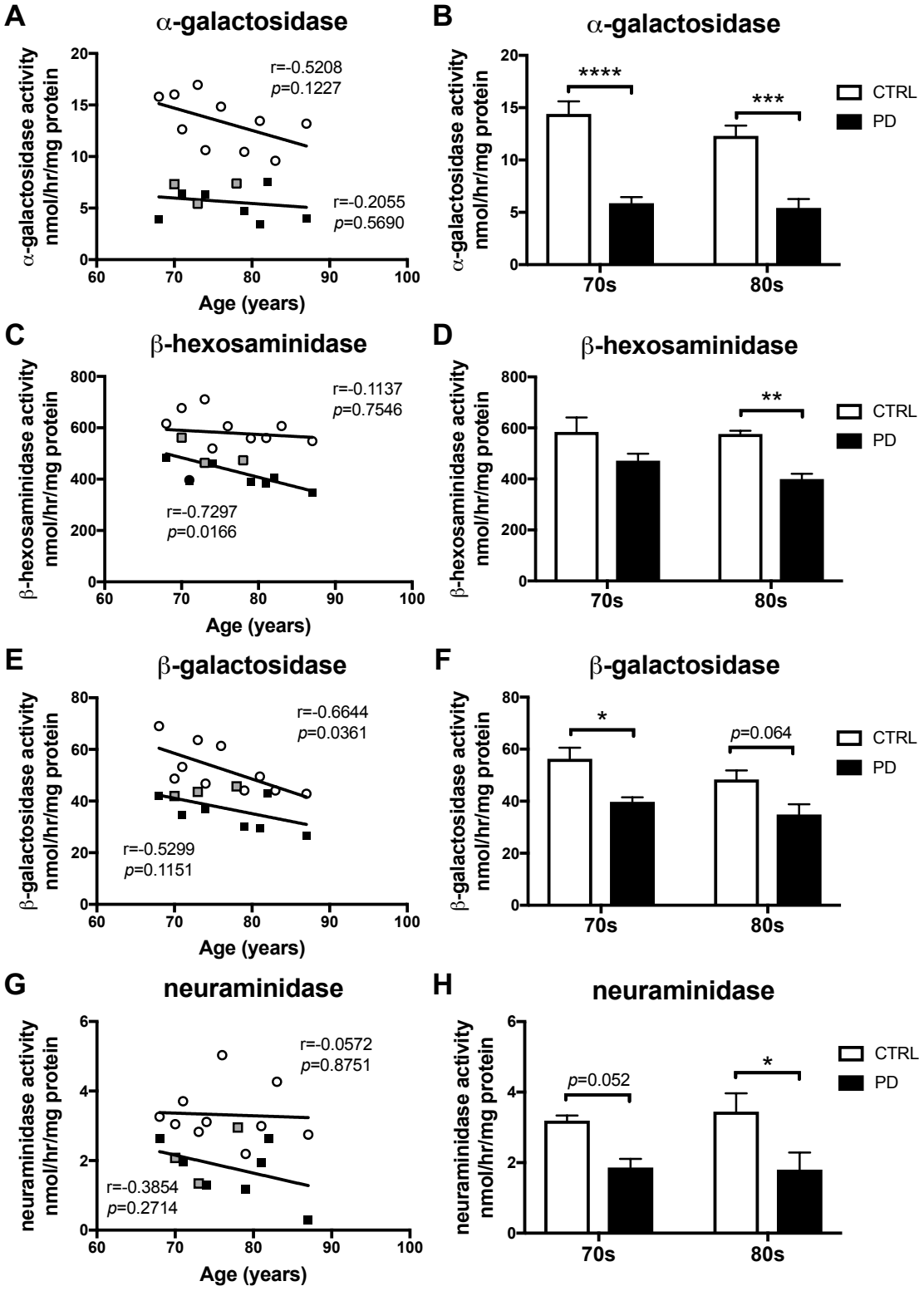

Figure 6.2: Reduced lysosomal hydrolase activities in substantia nigra of PD patients. Lysosomal hydrolase activities were measured using artificial 4-MU-substrates. Activity of α-galactosidase (A, B), β-hexosaminidase (C, D), β-galactosidase (E, F) and neuraminidase (G, H) were determined in the substantia nigra homogenates from control subjects and PD patients. Data were analysed using Pearson correlation analysis (A, C, E, G) (n=10 per group) and 2-way ANOVA (B, D, F, H) (n=5 per cohort; * = $p<0.05$, ** = $p<0.01$, *** = $p<0.001$, **** = $p<0.0001$). Bar graphs are presented as mean ± SEM.

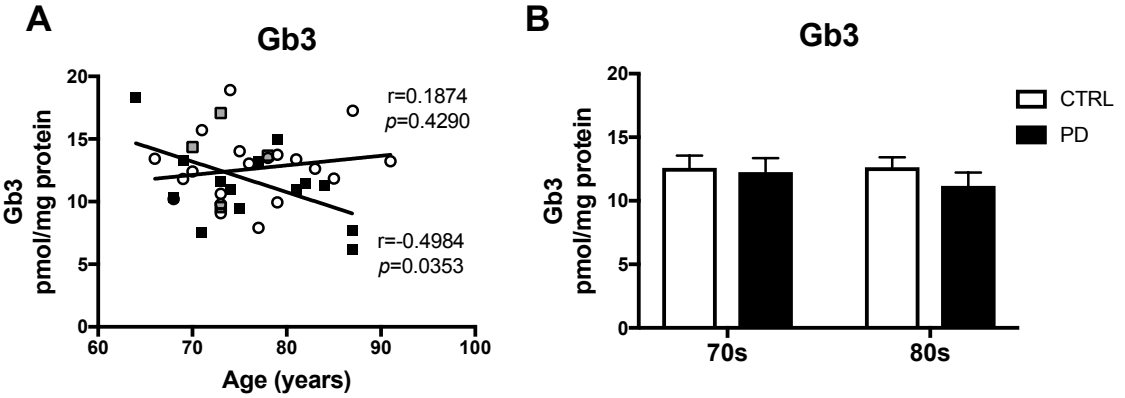

Figure 6.3: No change in Gb3 levels in substantia nigra of PD patients. (A) Substantia nigra homogenates from control subjects (n=20) and PD patients (n=18) were used to determine Gb3 levels with NP-HPLC. Data were analysed using Pearson correlation analysis. (B) Comparison of Gb3 levels in 70s-cohorts and 80s-cohorts of control subjects and PD patients (n=8-10 per cohort). Bar graphs are presented as mean ± SEM.

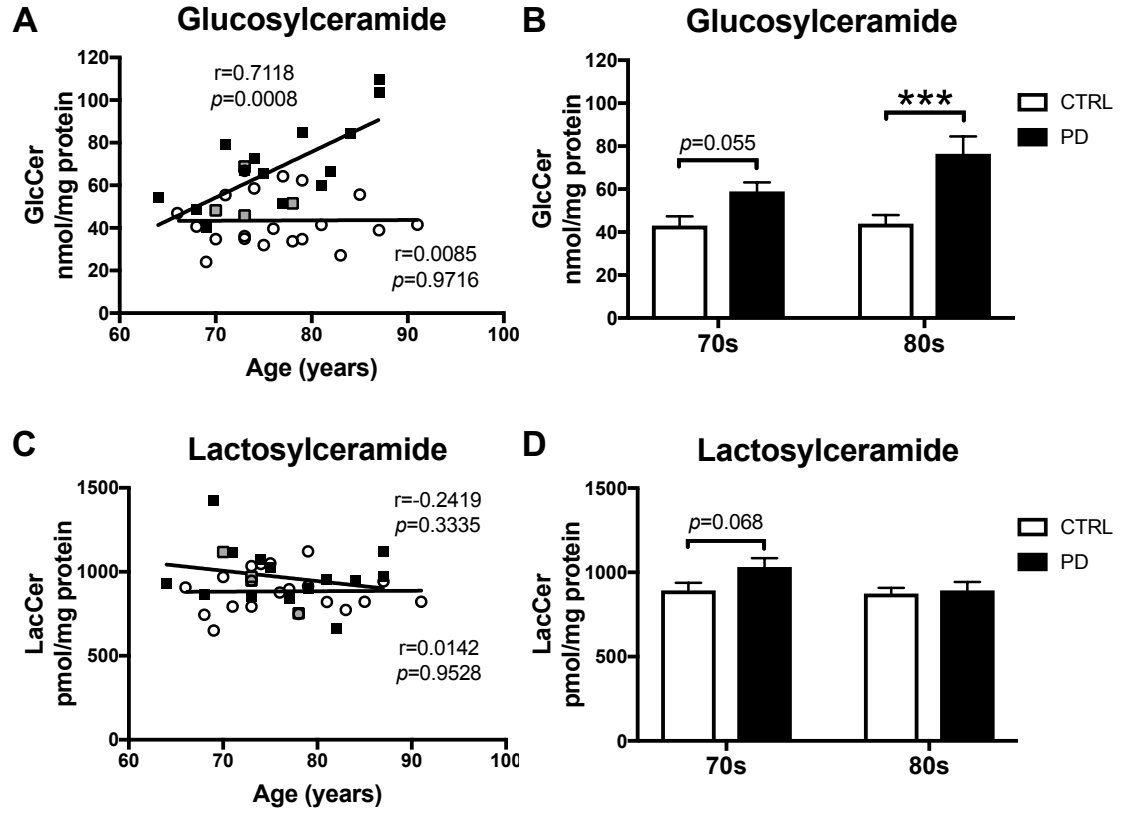

Figure 6.4: Glucosylceramide levels are increased in substantia nigra of PD patients. (A) Substantia nigra homogenates from control subjects (n=20) and PD patients (n=18) were used to determine glucosylceramide (GlcCer) levels with NP-HPLC. Data were analysed using Pearson correlation analysis. (B) Comparison of GlcCer levels in 70s-cohorts and 80s-cohorts of control subjects and PD patients (n=8-10 per cohort, *** = $p<0.001$, 2-way ANOVA). (C) Substantia nigra homogenates from control subjects and PD patients were used to determine lactosylceramide (LacCer) levels with NP-HPLC. Data were analysed using Pearson correlation analysis (C), and 2-way ANOVA (D) (n=8-10 per cohort). Bar graphs are presented as mean ± SEM.

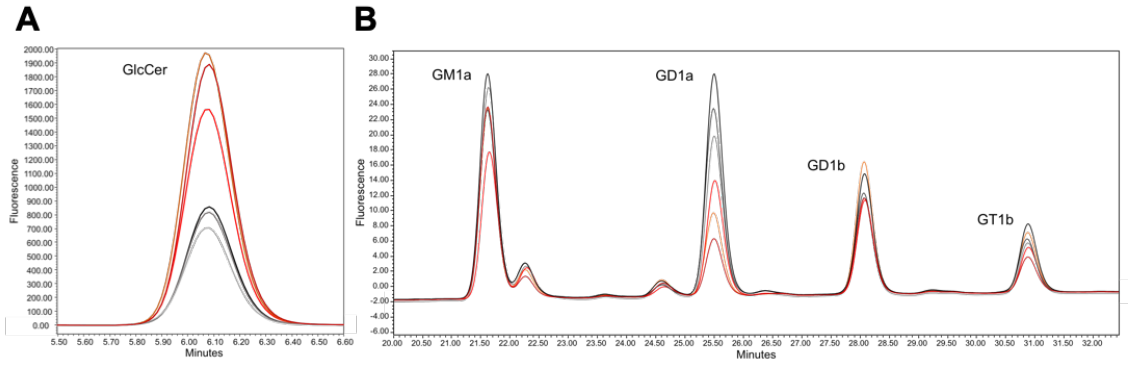

Figure 6.5: HPLC traces of glucosylceramide and gangliosides GM1a, GD1a, GD1b and GT1b from substantia nigra homogenates of control subjects and PD patients. Exemplary HPLC traces of (A) GlcCer and (B) gangliosides of 80s-cohort control subjects are shown in grey and 80s-cohort PD patients are shown in red (n=3).

6.3.4 Accumulation of GlcSph in substantia nigra of PD patients

Next, levels of glucosylsphingosine (GlcSph), another substrate for GBA and GBA2, as well as levels of sphingosine (Sph) and sphinganine (SphA) were quantified in substantia nigra of PD patients and age-matched controls (n=10 per condition and n=5 per age group) using RP-HPLC.

In 70s-cohort PD patients, GlcSph levels in substantia nigra were increased to 164.4% of age-matched control subjects, but did not reach statistical significance (**Figure 6.6A**, p=0.055). In substantia nigra of 80s-cohort PD patients, GlcSph levels were significantly increased to 215.9% of the 80s-cohort control subjects (**Figure 6.6A**, p=0.0049). Furthermore, both Sph and SphA levels were significantly increased in substantia nigra of 70s-cohort PD patients in comparison to levels in age-matched control subjects (**Figure 6.6B, C**; Sph: p=0.0295, 86.2%; SphA: p=0.0447, 87.5%).

To assess whether cholesterol is involved in ageing or PD, cholesterol levels were measured in substantia nigra tissues of PD patients and age-matched controls (n=10 per condition and n=5 per age group) using Amplex Red assay. No differences in cholesterol levels were seen (**Figure 6.7**).

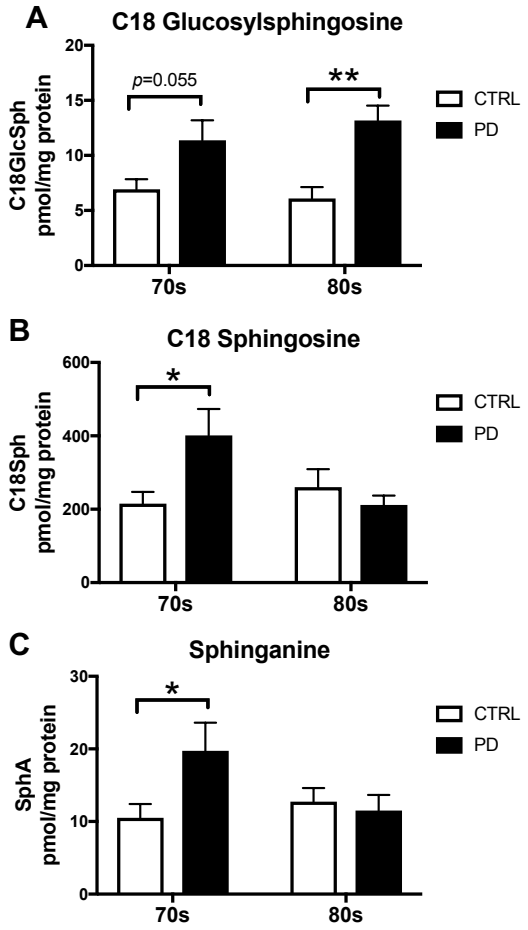

Figure 6.6: Glucosylsphingosine levels are increased in substantia nigra of PD patients. Substantia nigra homogenates from control subjects and PD patients were used to determine glucosylsphingosine (GlcSph), sphingosine (Sph) and sphinganine (SphA) levels with RP-HPLC. (A) GlcSph, (B) Sph and (C) GlcSph levels in SN of 70s-cohorts and 80s-cohorts of control subjects and PD patients (n=5 per cohort, * = $p<0.05$, ** = $p<0.01$, 2-way ANOVA). Data are presented as mean ± SEM.

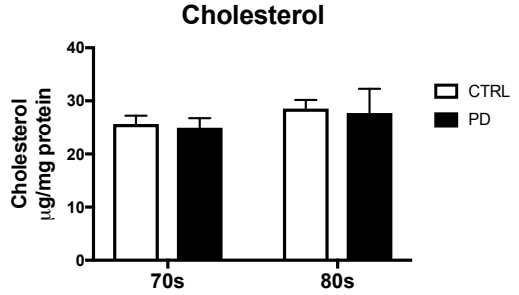

Figure 6.7: Substantia nigra cholesterol levels are not changed with normal ageing or PD. Comparison of total cholesterol levels in substantia nigra homogenates from control subjects and PD patients of both 70s-cohorts and 80s-cohorts. Cholesterol levels were analysed with Amplex Red kit. Data are presented as mean ± SEM.

6.3.5 Loss of gangliosides GM1a, GD1a, GD1b and GT1b in substantia nigra with normal ageing and further in PD

Levels of the more-complex gangliosides, GM1a, GD1a, GD1b and GT1b, were quantified in substantia nigra from PD patients (n=18) and age-matched controls (n=20) by NP-HPLC (provided by HBTRC).

GM1a levels were significantly, negatively correlated with increasing age in substantia nigra of both control subjects and PD patients (**Figure 6.8A**; r=-0.4795, *p*=0.0324 for CTRL; r=-0.5659, *p*=0.0144 for PD). A significant decrease in GM1a levels was observed in SN of 70s-cohort PD patients compared to age-matched control subjects (**Figure 6.8B**, *p*=0.0233, 21.8% reduction), but was not significant anymore when comparing 80s-cohorts. Furthermore, a negative correlation with age in GD1a substantia nigra levels of both control subjects and PD patients was found (**Figure 6.8C**; r=-0.3886, *p*=0.1002 for CTRL; r=-0.3850, *p*=0.1146 for PD). Similar to GM1a, a significant decrease in GD1a levels was observed in SN of 70s-cohort PD patients compared to 70s-cohort control subjects (**Figure 6.8D,** *p*=0.0414, 38.7% reduction). GD1b and GT1b levels in substantia nigra of PD patients were both negatively correlated with age, but not in substantia nigra of control subjects (**Figure 6.8E, G**; GD1b: r=-0.0489, *p*=0.8376 for CTRL and r=-0.5422, *p*=0.0201 for PD; GT1b: r=0.0468, *p*=0.8445 for CTRL and r=-0.3676, *p*=0.1334 for PD). GD1b levels in substantia nigra of PD patients of both age cohorts were significantly reduced compared to substantia nigra of age-matched control subjects (**Figure 6.8F**; 70s: *p*=0.0478, 16.5%; 80s: *p*=0.0232, 21.0%). Similarly, a decrease in GT1b levels in substantia nigra of PD patients in both age cohorts was observed in comparison to age-matched controls (**Figure 6.8H**, 70s: *p*=0.068, 23.3%, 80s: *p*=0.0415, 26.9%). Exemplary NP-HPLC traces of GM1a, GD1a, GD1b and GT1b from substantia nigra of 80s-cohort control subjects and PD patients are shown in **Figure 6.5B**.

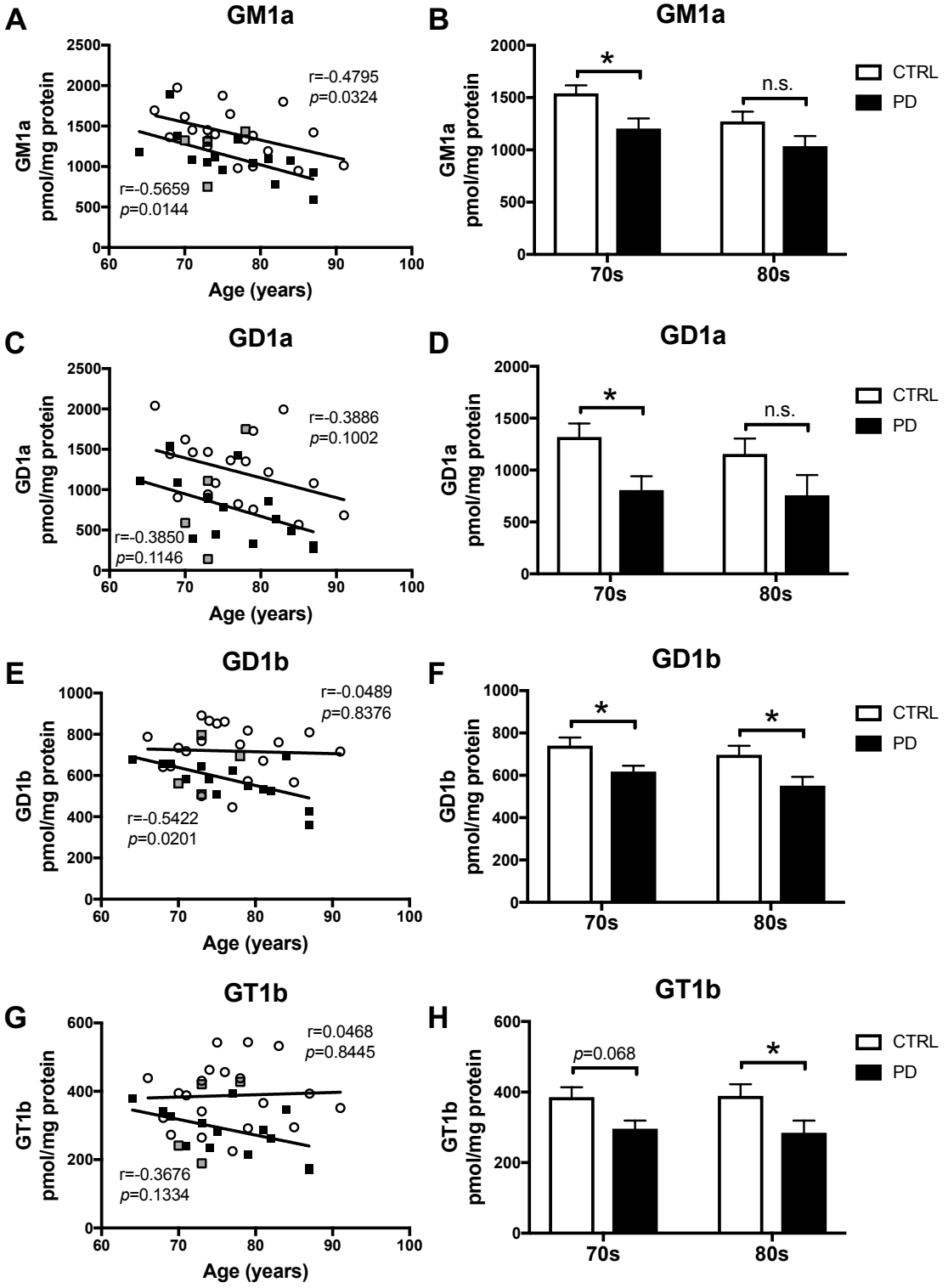

Figure 6.8: Loss of gangliosides in the substantia nigra of PD patients and with normal ageing. Levels of GM1a (A, B), GD1a (C, D), GD1b (E, F) and GT1b (G, H) were determined in substantia nigra homogenates from control subjects and PD patients with NP-HPLC. Data were analysed using Pearson correlation analysis (A, C, E, G) (n=18-20 per group) and 2-way ANOVA (B, D, F, H) (n=8-10 per cohort; * = $p<0.05$). Bar graphs are presented as mean ± SEM.

In summary, both GM1a and GD1a levels in the substantia nigra are negatively correlated with ageing in control subjects. Importantly, ganglioside levels are further, significantly reduced in substantia nigra of PD patients compared to age-matched control subjects.

6.3.6 Increase in total GSLs, due to GlcCer, but loss of more complex gangliosides in substantia nigra of PD patients

To assess whether total brain glycosphingolipid (GSL) load in substantia nigra changes with healthy ageing or with PD, GlcCer, LacCer and ganglioside levels were summed and termed total GSLs. Total GSL levels in substantia nigra of PD patients were significantly correlated with age (r=0.7198, *p*=0.0008), but not in the substantia nigra of control subjects (r=-0.0168, *p*=0.9438) (**Figure 6.9A**). In 70s-cohort PD patients, total GSL levels in the substantia nigra were increased to 131.1% of age-matched control subjects, but did not reach statistical significance (**Figure 6.9B**, *p*=0.065). In substantia nigra of 80s-cohort PD patients, total GSL levels were significantly increased to 165.5% of 80s-cohort control subjects (**Figure 6.9B**, *p*=0.0002).

As the total amount of GSLs is mostly influenced by the highly abundant GlcCer, we also calculated the levels of more-complex gangliosides alone, by summing GM1a, GD1a, GD1b and GT1b. Ganglioside levels in substantia nigra of PD patients were significantly, negatively correlated with age (r=-0.4897, *p*=0.0392), and also negatively correlated in substantia nigra of control subjects (r=-0.3610, *p*=0.1179) (**Figure 6.9C**). In substantia nigra of 70s-cohort PD patients, ganglioside levels were significantly decreased to 71.3% of age-matched control subjects (**Figure 6.9D**, *p*=0.0091). In substantia nigra of 80s-cohort PD patients, ganglioside levels were decreased to 75.0% of 80s-cohort control subjects, trending towards statistical significance (**Figure 6.9D**, *p*=0.078).

In summary, total lipid load is increased in SN of PD patients, due to high amounts of GlcCer, whereas levels of more complex gangliosides, e.g. GM1a, are significantly decreased in SN of PD patients compared to age-matched controls.

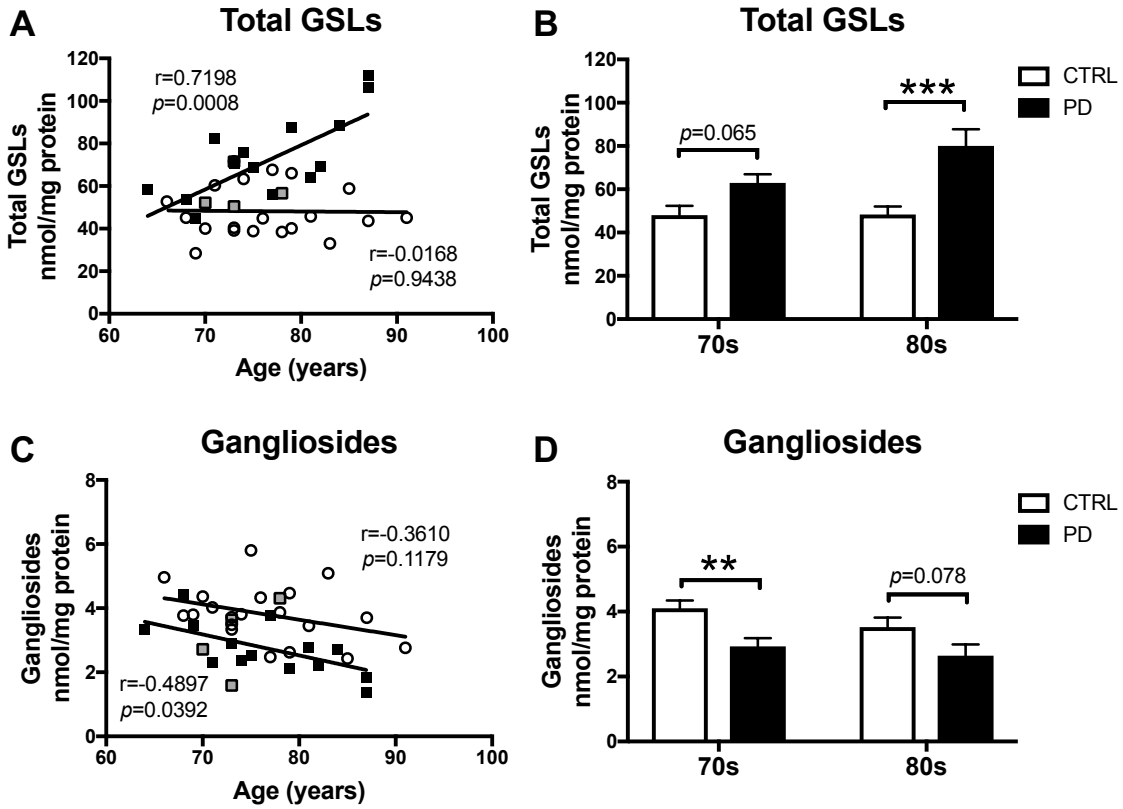

Figure 6.9: Increase in glycosphingolipid load, but reduction in gangliosides, in substantia nigra of PD patients. (A) Pearson correlation analysis of the sum of GlcCer + LacCer + GM1a + GD1a + GD1b + GT1b levels in substantia nigra homogenates from control subjects (n=20) and PD patients (n=18) shows that PD is associated with increased load of GSLs with age. (B) Comparison of total GSL levels in 70s-cohorts vs. 80s-cohorts of control subjects and PD patients (n=8-10 per cohort). (C) Pearson correlation analysis of the sum of GM1a + GD1a + GD1b + GT1b levels in substantia nigra homogenates from control subjects (n=20) and PD patients (n=18). (B) Comparison of ganglioside levels in 70s-cohorts vs. 80s-cohorts of control subjects and PD patients (n=8-10 per cohort). Bar graphs were analysed using 2-way ANOVA (** = $p<0.01$, *** = $p<0.001$). Bar graphs are presented as mean ± SEM.

6.3.7 Increase in GlcCer and decrease in gangliosides in substantia nigra from a second PD patient cohort

We sought to confirm the results obtained with the substantia nigra tissues from PD patients and control subjects provided by the HBTRC (Mc Lean Hospital, Belmont, MA). For this, we analysed GSLs in a second, independent cohort of post-mortem SN tissue from healthy control subjects (n=5) and age-matched PD patients (n=20) in their 80s provided by the Parkinson's UK Brain Bank (PDUK; Imperial College London, UK).

GlcCer levels were significantly increased in the substantia nigra of PD patients compared to control subjects (**Figure 6.10A**, p=0.0358, 45.0% increase). There were no significant changes in substantia nigra LacCer levels observed when comparing PD patients and control subjects (**Figure 6.10B**). A significant decrease in GM1a levels was observed in SN of PD patients compared to age-matched control subjects (**Figure 6.10C**, p=0.0115, 25.7% reduction). Furthermore, a decrease in GD1a levels was found in SN of PD patients compared to controls (**Figure 6.10D**, p=0.055, 47.4% reduction). In addition, gangliosides GD1b and GT1b were both significantly reduced in SN of PD patients in comparison to control subjects (**Figure 6.10E, F**; GD1b: p=0.0142, 30.6% reduction; GT1b: p=0.0138, 34.3% reduction). Consequently, in substantia nigra of PD patients, ganglioside levels (sum of GM1a, GD1a, GD1b and GT1b) were significantly decreased to 67.2% of age-matched control subjects (**Figure 6.10G**, p=0.0052). However, total GSL levels (sum of GlcCer, LacCer and gangliosides; mostly influenced by the highly abundant GlcCer) were significantly increased in substantia nigra of PD patients to 139.1% of control subjects (**Figure 6.10H**, p=0.0404).

In summary, we confirmed previous SN results and demonstrate a significant increase in glucosylceramide and decrease in gangliosides in substantia nigra from a second, independent cohort of PD patients compared to age-matched control subjects.

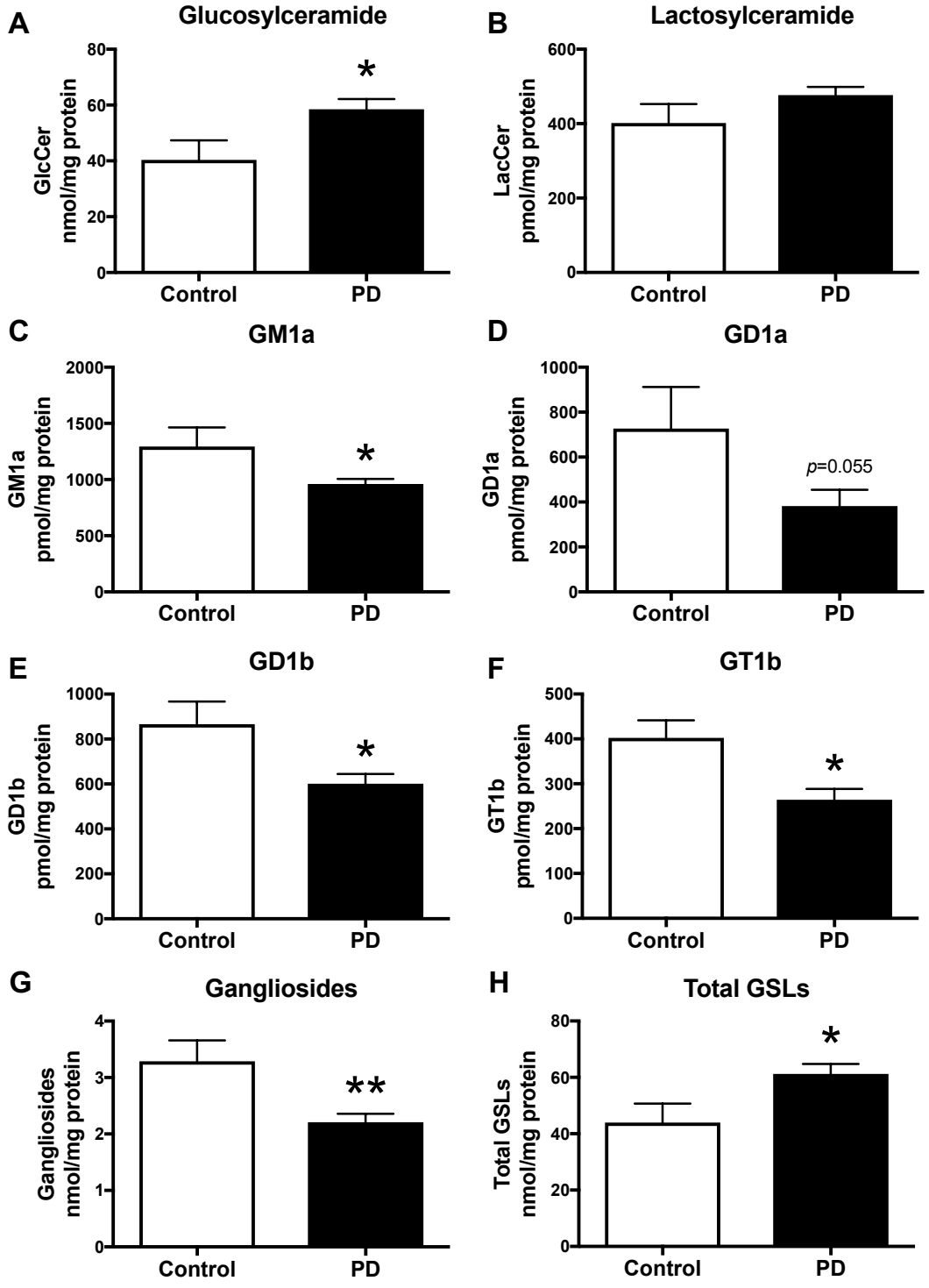

Figure 6.10: Increase in GlcCer levels and loss of gangliosides in substantia nigra from a second cohort of PD patients. Substantia nigra from control subjects (n=5) and PD patients (n=20) were used to determine GlcCer (A), LacCer (B) GM1a (C), GD1a (D), GD1b (E) and GT1b (F) levels with NP-HPLC (* = $p<0.05$, unpaired t-test). (G) Comparison of total ganglioside levels (sum of GM1a, GD1a, GD1b and GT1b) in substantia nigra from control subjects and PD patients (** = $p<0.01$, unpaired t-test). (H) Total GSL levels (sum of GlcCer + LacCer + GM1a + GD1a + GD1b + GT1b levels) in substantia nigra from control subjects and PD patients (* = $p<0.05$, unpaired t-test). Data are presented as mean ± SEM.

6.3.8 Reduced activity of various lysosomal hydrolases, including GBA, in substantia nigra from a second PD patient cohort

To confirm previous hydrolase results obtained with substantia nigra tissues from the HBTRC, we analysed hydrolase activities in a second, independent cohort of post-mortem SN tissue from healthy control subjects in their 80s (n=5) and age-matched PD patients (n=9, provided by PDUK, Imperial College London, UK).

GBA activity in substantia nigra of PD patients was significantly reduced to 79.1% of GBA activity in control subjects (**Figure 6.11A**, p=0.0146). Furthermore, a decrease in GBA2 activity was seen in SN of PD patients compared to control subjects (**Figure 6.11B**, p=0.1061, 17.9% reduction). A significant reduction in α-galactosidase activity was observed in SN of PD patients compared to age-matched control subjects (**Figure 6.11C**, p=0.0103, 28.4% reduction). Additionally, a significant reduction in β-hexosaminidase activity was detected in SN of PD patients compared to SN of control subjects (**Figure 6.11D**, p=0.0047, 23.1% reduction). The activity of β-galactosidase in substantia nigra of PD patients was significantly reduced to 77.3% of β-galactosidase activity of age-matched control subjects (**Figure 6.11E**, p=0.0159). Finally, the activity of neuraminidase in substantia nigra of PD patients was significantly reduced to 54.0% of activity in SN of age-matched controls (**Figure 6.11F**, p=0.0150).

In summary, confirming previous SN results, all lysosomal hydrolases assayed, e.g. GBA, α-galactosidase and neuraminidase, displayed significantly reduced activities in the substantia nigra of PD patients compared to age-matched control subjects.

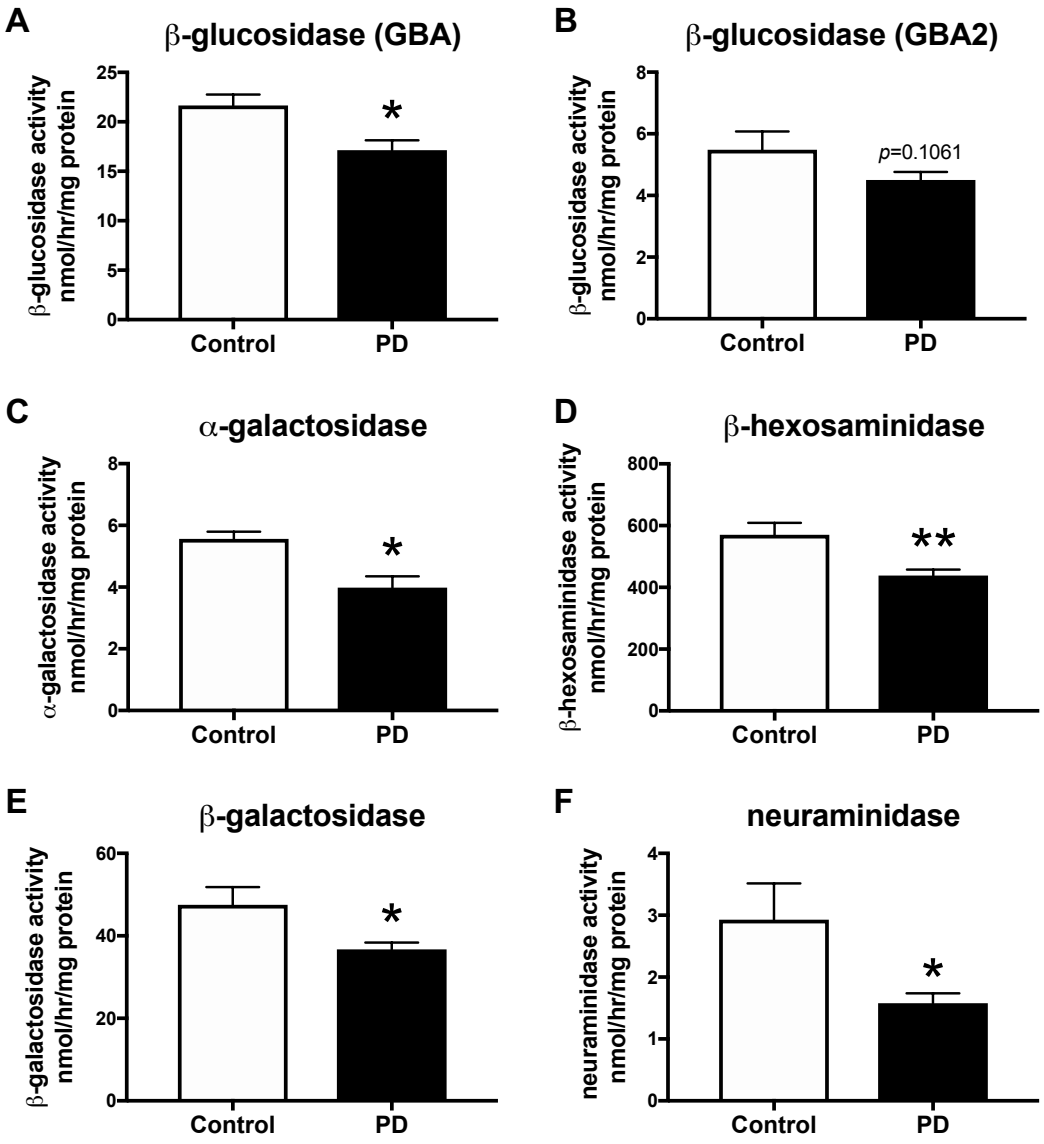

Figure 6.11: Reduced lysosomal hydrolase activities in substantia nigra of a second cohort of PD patients. Lysosomal hydrolase activities were measured using artificial 4-MU-substrates. Activity of GBA (A), GBA2 (B), α-galactosidase (C), β-hexosaminidase (C), β-galactosidase (E) and neuraminidase (F) were determined in the substantia nigra homogenates from age-matched control subjects (n=5) and PD patients (n=9). Data were analysed using unpaired t-test (* = $p<0.05$, ** = $p<0.01$). Data are presented as mean ± SEM.

6.3.9 GSLs in substantia nigra during ageing and in PD in a third cohort of patients

To further confirm previous substantia nigra results and in an attempt to focus more on the effect of ageing, we analysed GSLs in a third, independent cohort of post-mortem SN tissue from control subjects in their 50s (n=7), control subjects in their 80s (n=13)

and PD patients in their 80s (n=12) provided by the Oxford Brain Bank (OBB; Oxford, UK).

GlcCer levels were not changed with age in substantia nigra of control cohorts, but were slightly increased in the substantia nigra of PD patients compared to age-matched 80s control subjects (**Figure 6.12A**, *p*=0.4719, 17.2% increase). There were no significant changes in substantia nigra LacCer levels observed when comparing PD patients and control subjects of both age groups (**Figure 6.12B**). Interestingly, a decrease in GM1a levels in SN of 80s control subjects compared to 50s control subjects was found, although not significant (**Figure 6.12C**, *p*=0.1353, 21.9% reduction). In addition, a significant decrease in GM1a levels was observed in SN of PD patients compared to 50s control subjects (**Figure 6.12C**, *p*=0.0199, 33.1% reduction). Furthermore, a decrease in GD1a levels in SN of 80s control subjects compared to 50s control subjects was found and was trending towards statistical significance (**Figure 6.12D**, *p*=0.0806, 35.8% reduction). Also, a significant decrease in GD1a levels was observed in SN of PD patients compared to 50s control subjects (**Figure 6.12D**, *p*=0.0169, 48.5% reduction). With regard to the levels of gangliosides GD1b and GT1b, no significant changes were found in SN of 80s control subjects or of PD patients compared to 50s control subjects (**Figure 6.12E, F**). Nevertheless, in substantia nigra of PD patients and 80s control subjects, ganglioside levels (sum of GM1a, GD1a, GD1b and GT1b) were decreased to 77.4% and 67.1% of levels found in SN of 50s control subjects, respectively (**Figure 6.12G**, *p*=0.0844 for 80s CTRL, *p*=0.0010 for PD). However, total GSL levels (sum of GlcCer, LacCer and gangliosides; mostly influenced by the highly abundant GlcCer) were not changed in substantia nigra of PD patients and both control cohorts (**Figure 6.12H**).

In summary, these observations support previous SN results and demonstrate a decrease in ganglioside levels in SN with healthy ageing and further reductions in substantia nigra with PD.

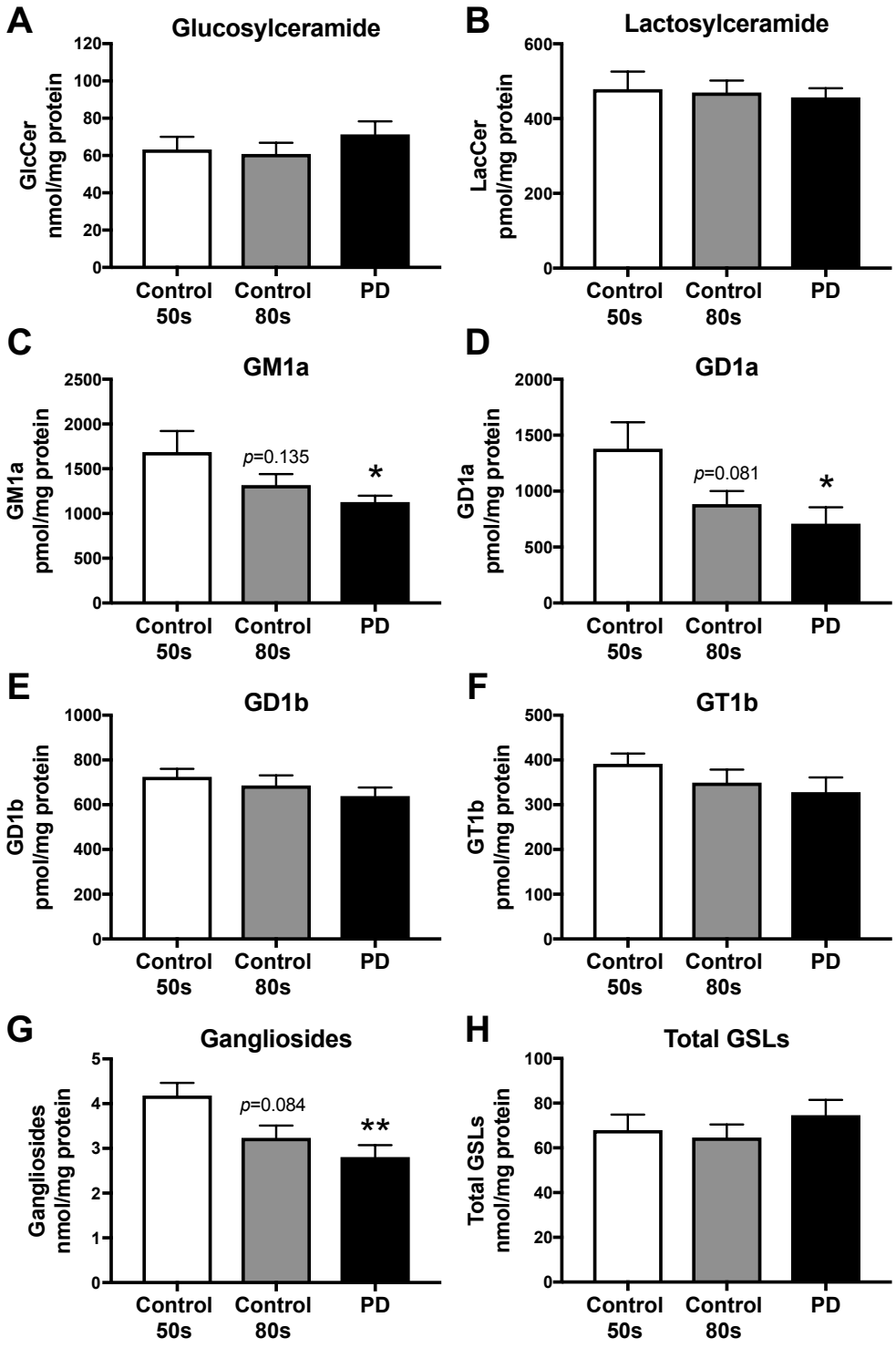

Figure 6.12: Reduced gangliosides in substantia nigra with normal ageing and in a third cohort of PD patients. Substantia nigra homogenates from 50s control subjects (n=7), 80s control subjects (n=13) and 80s PD patients (n=12) were used to determine GlcCer (A), LacCer (B), GM1a (C), GD1a (D), GD1b (E) and GT1b (F) levels with NP-HPLC. (G) Comparison of total ganglioside levels (sum of GM1a, GD1a, GD1b and GT1b) in substantia nigra from 50s control subjects, 80s control subjects and PD patients. (H) Total GSL levels (sum of GlcCer + LacCer + GM1a + GD1a + GD1b + GT1b) in substantia nigra from 50s control subjects, 80s control subjects and PD patients. Data were analysed using one-way ANOVA (* = $p<0.05$, ** = $p<0.01$) and are presented as mean ± SEM.

6.3.10 Changes in GSL levels and hydrolase activities in putamen during ageing and in PD

Next, we wanted to evaluate if changes in lysosomal hydrolase activities and GSL levels can also be found in other CNS tissues related to PD, i.e. the putamen, which is connected to the SN via the nigrostriatal pathway. For this, we used post-mortem putamen tissue from control subjects in their 50s (n=7), control subjects in their 80s (n=13) and PD patients in their 80s (n=12) provided by the Oxford Brain Bank (OBB; Oxford, UK).

GlcCer levels were not changed with age in putamen of control cohorts, but were increased in the putamen of PD patients by 40.6% in comparison to levels observed in age-matched 80s control subjects (**Figure 6.13A**, p=0.4068). There were no significant changes in putamen LacCer levels when comparing control subjects of both age groups, but a slight increase in LacCer levels in putamen of PD patients in comparison to age-matched 80s control subjects (**Figure 6.13B**, p=0.5899, 20.6% increase). Interestingly, a significant decrease in GM1a levels in putamen of 80s control subjects compared to younger 50s control subjects was found (**Figure 6.13C**, p=0.0351, 21.7% reduction). Furthermore, a higher, significant decrease in GM1a levels was observed in putamen of PD patients compared to 50s control subjects (**Figure 6.13C**, p=0.0011, 34.3% reduction). Likewise, a decrease in GD1a levels in putamen of 80s control subjects compared to 50s control subjects was found and was trending towards statistical significance (**Figure 6.13D**, p=0.0970, 25.9% reduction). In addition, a significant decrease in GD1a levels was observed in putamen from PD patients compared to 50s control subjects as well as in comparison to 80s control subjects (**Figure 6.13D**; 50s: p=0.0003, 55.6% reduction; 80s: p=0.0221, 40.2% reduction). Concerning levels of gangliosides GD1b and GT1b, no significant changes were found in putamen of 80s control subjects or of PD patients compared to 50s control subjects (**Figure 6.13E, F**). Nevertheless, in putamen of PD patients and 80s control subjects, ganglioside levels

(sum of GM1a, GD1a, GD1b and GT1b) were decreased to 84.4% and 67.7% of levels found in putamen of 50s control subjects, respectively (**Figure 6.13G**, p=0.2619 for 80s CTRL, p=0.0009 for PD). However, total GSL levels (sum of GlcCer, LacCer and gangliosides; mostly influenced by the highly abundant GlcCer) were not changed in putamen of PD patients and both control cohorts (**Figure 6.13H**).

In summary, these observations support previous results obtained with SN tissue and demonstrate that an increase in GlcCer as well as a decrease in ganglioside levels with healthy ageing and more severe with PD also occurs in the putamen.

Next, we analysed various lysosomal hydrolase activities in putamen samples provided by the OBB. Regarding the activity of GBA, no significant changes were found in putamen of 80s control subjects or of PD patients in comparison to 50s control subjects (**Figure 6.14A**). However, a decrease in non-lysosomal GBA2 activity was seen in putamen of 80s control subjects and more strongly in PD patients compared to 50s control subjects (**Figure 6.14B**; 80s: p=0.0902, 31.1% reduction; PD: p=0.0232, 41.0% reduction). No significant changes were observed in either α-galactosidase, β-hexosaminidase, β-galactosidase or neuraminidase activities in putamen of aged control subjects or PD patients (**Figure 6.14C-F**). However, neuraminidase activity in putamen of 80s control subjects as well as PD patients was reduced to 75.5% and 74.2% of activity in putamen of 50s control subjects, respectively (**Figure 6.14F**; 80s: p=0.1384; PD: p=0.1142).

In summary, and in accordance with previous SN results, GBA2 β-glucosidase and neuraminidase displayed reduced activities in the putamen of aged controls and PD patients in comparison to younger control subjects.

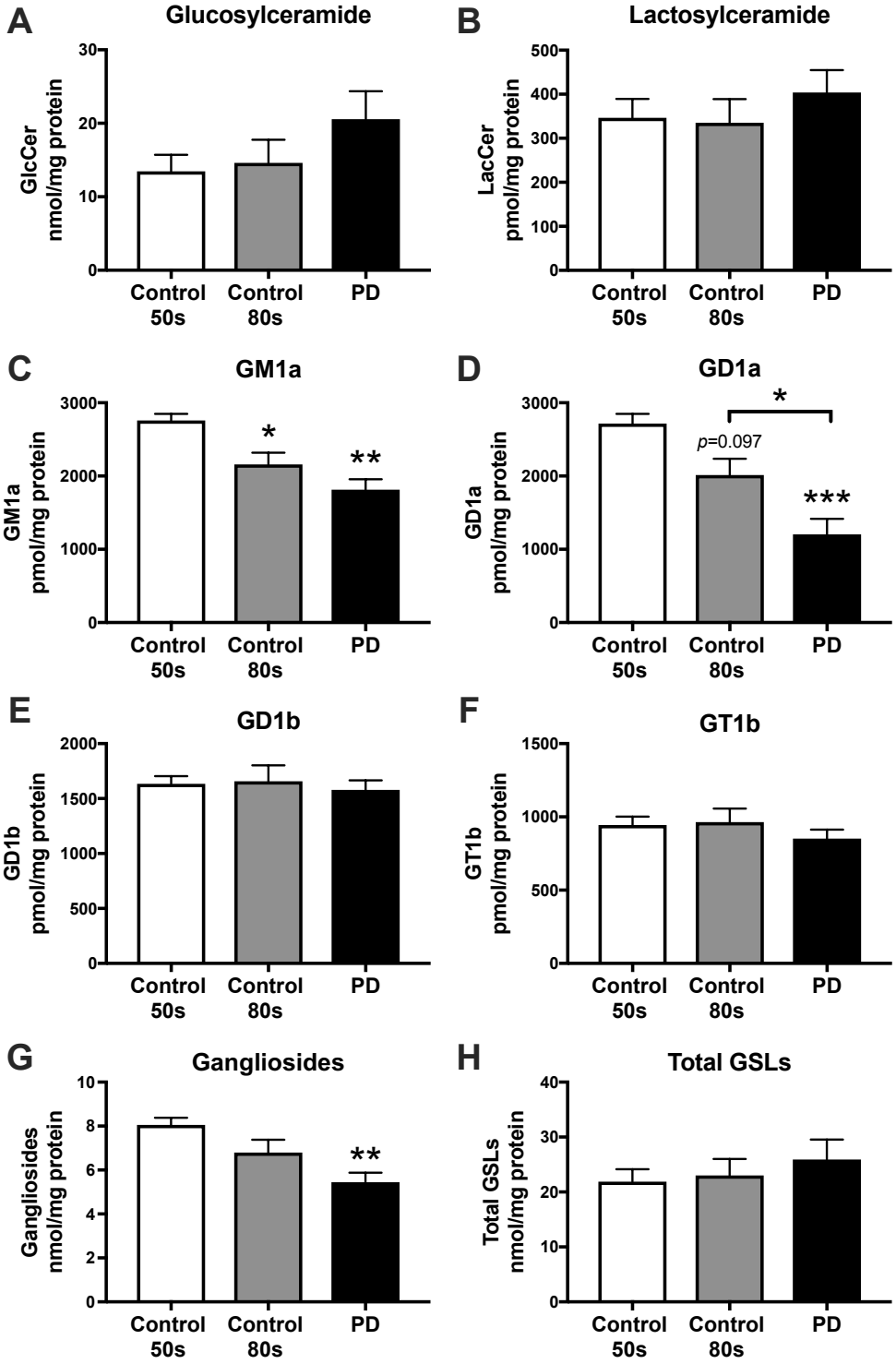

Figure 6.13: Increased GlcCer and LacCer levels in putamen from PD patients and loss of gangliosides GM1a and GD1a in putamen with normal ageing and with PD. Putamen homogenates from 50s control subjects (n=7), 80s control subjects (n=13) and 80s PD patients (n=12) were used to determine GlcCer (A), LacCer (B), GM1a (C), GD1a (D), GD1b (E) and GT1b (F) levels with NP-HPLC. (G) Comparison of total ganglioside levels (sum of GM1a, GD1a, GD1b and GT1b) in putamen from 50s control subjects, 80s control subjects and PD patients. (H) Total GSL levels (sum of GlcCer + LacCer + GM1a + GD1a + GD1b + GT1b) in substantia nigra from 50s control subjects, 80s control subjects and PD patients. Data were analysed using one-way ANOVA (* = $p<0.05$, ** = $p<0.01$, *** = $p<0.001$) and are presented as mean ± SEM.

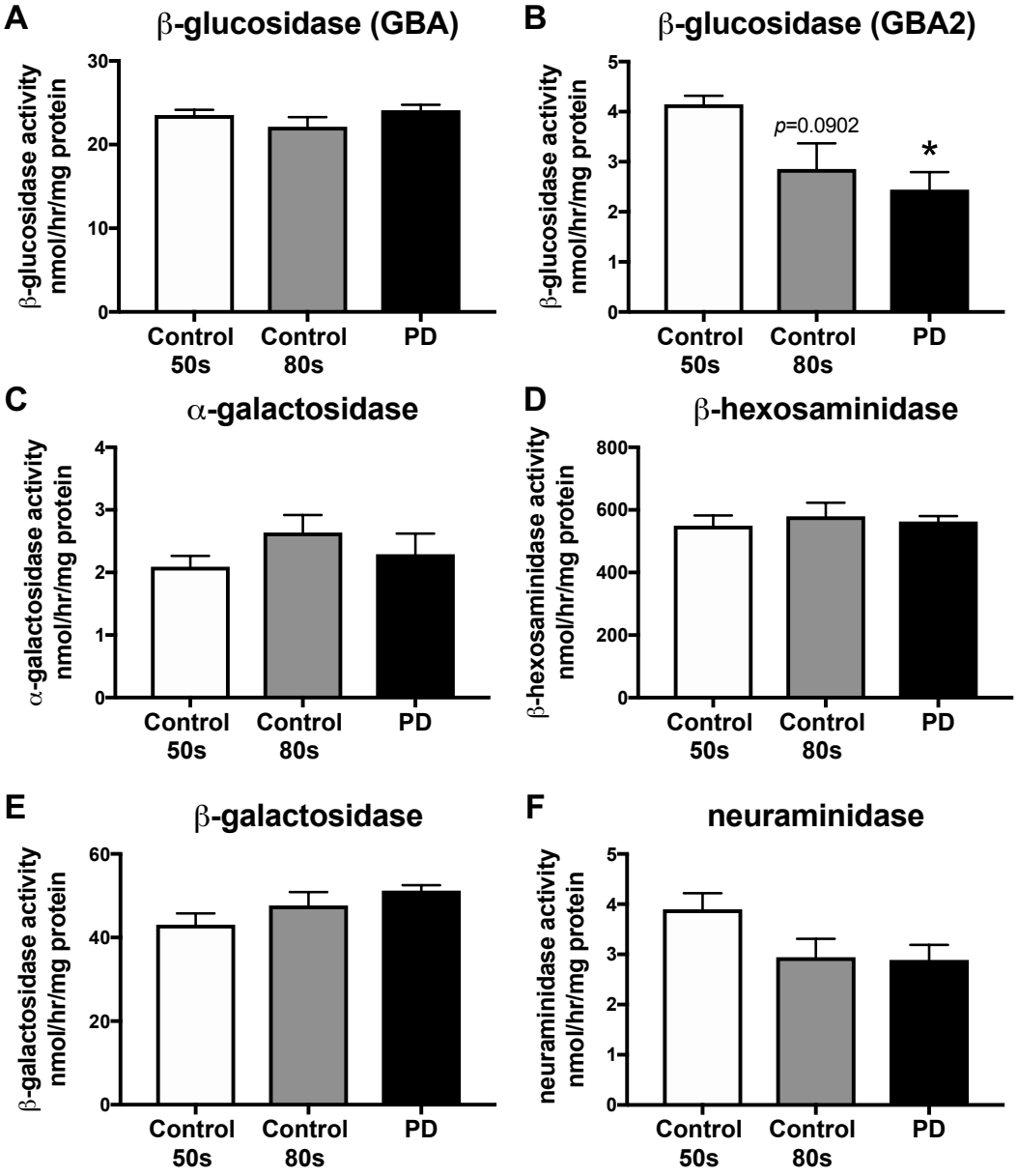

Figure 6.14: Reduced GBA2 and neuraminidase activities in putamen in normal ageing and in PD patients. Lysosomal hydrolase activities were measured using artificial 4-MU-substrates. Activity of GBA (A), GBA2 (B), α-galactosidase (C), β-hexosaminidase (C), β-galactosidase (E) and neuraminidase (F) were determined in putamen homogenates from 50s control subjects (n=6), 80s control subjects (n=6) and PD patients (n=6). Data were analysed using one-way ANOVA (* = $p<0.05$). Data are presented as mean ± SEM.

6.3.11 GSL levels in spinal cord during ageing and in PD

Next, we wanted to assess if changes in GSL levels occur in another CNS compartment, i.e. spinal cord. For this, we used post-mortem spinal cord tissue from control subjects

in their 50s (n=5), control subjects in their 80s (n=10) and PD patients in their 80s (n=22) provided by PDUK (Imperial College London, UK) and OBB (Oxford, UK).

The pattern of spinal cord GSLs is slightly different to the usual GSL pattern in brain tissue. Spinal cord features large peaks of the lipids GM3 and GD3 in roughly equal amounts to the gangliosides GM1a and GD1b, but still shows most prominent levels of GlcCer and LacCer and slightly lower levels in GD1a and GT1b in comparison to brain tissue. GlcCer levels as well as LacCer levels were not changed with age in spinal cord of control cohorts and in PD patients (**Figure 6.15A, B**). Interestingly, GM3 levels were significantly elevated in spinal cord of 80s control subjects as well as of PD patients compared to 50s control subjects (**Figure 6.15C**; 80s: p=0.0004, 49.9% increase; PD: p=0.0007, 42.2% increase). However, there were no changes in GD3 levels in spinal cord of the different cohorts (**Figure 6.15D**).

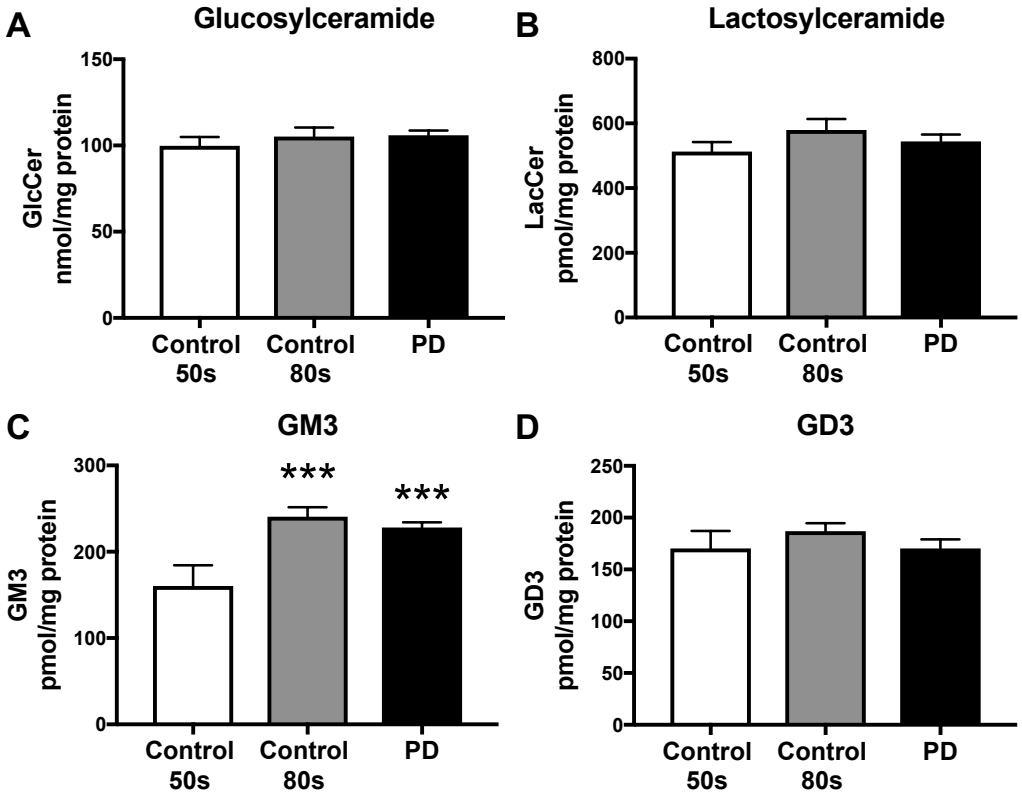

Figure 6.15: No changes in glucosylceramide or lactosylceramide levels, but increase in GM3 levels, in spinal cord with normal ageing and in PD. Spinal cord homogenates from 50s control subjects (n=5), 80s control subjects (n=10) and 80s PD patients (n=22) were used to determine GlcCer (A), LacCer (B), GM3 (C) and GD3 (D) levels with NP-HPLC (*** = p<0.001, one-way ANOVA). Data are presented as mean ± SEM.

No significant changes were found in spinal cord of 80s control subjects or of PD patients in comparison to spinal cord of 50s control subjects concerning levels of GM1a, GD1a, GD1b or GT1b (**Figure 6.16A-D**). Consequently, in spinal cord of PD patients and 80s control subjects, ganglioside levels (sum of GM1a, GD1a, GD1b and GT1b) were unchanged compared to 50s control subjects (**Figure 6.16E**). Also, total GSL levels (sum of GlcCer, LacCer and gangliosides; mostly influenced by the highly abundant GlcCer) were not changed in spinal cord of PD patients and both control cohorts (**Figure 6.16F**).

In summary, these results demonstrate that GSL changes observed in substantia nigra and putamen tissue do not occur in spinal cord tissue either in healthy ageing or with PD.

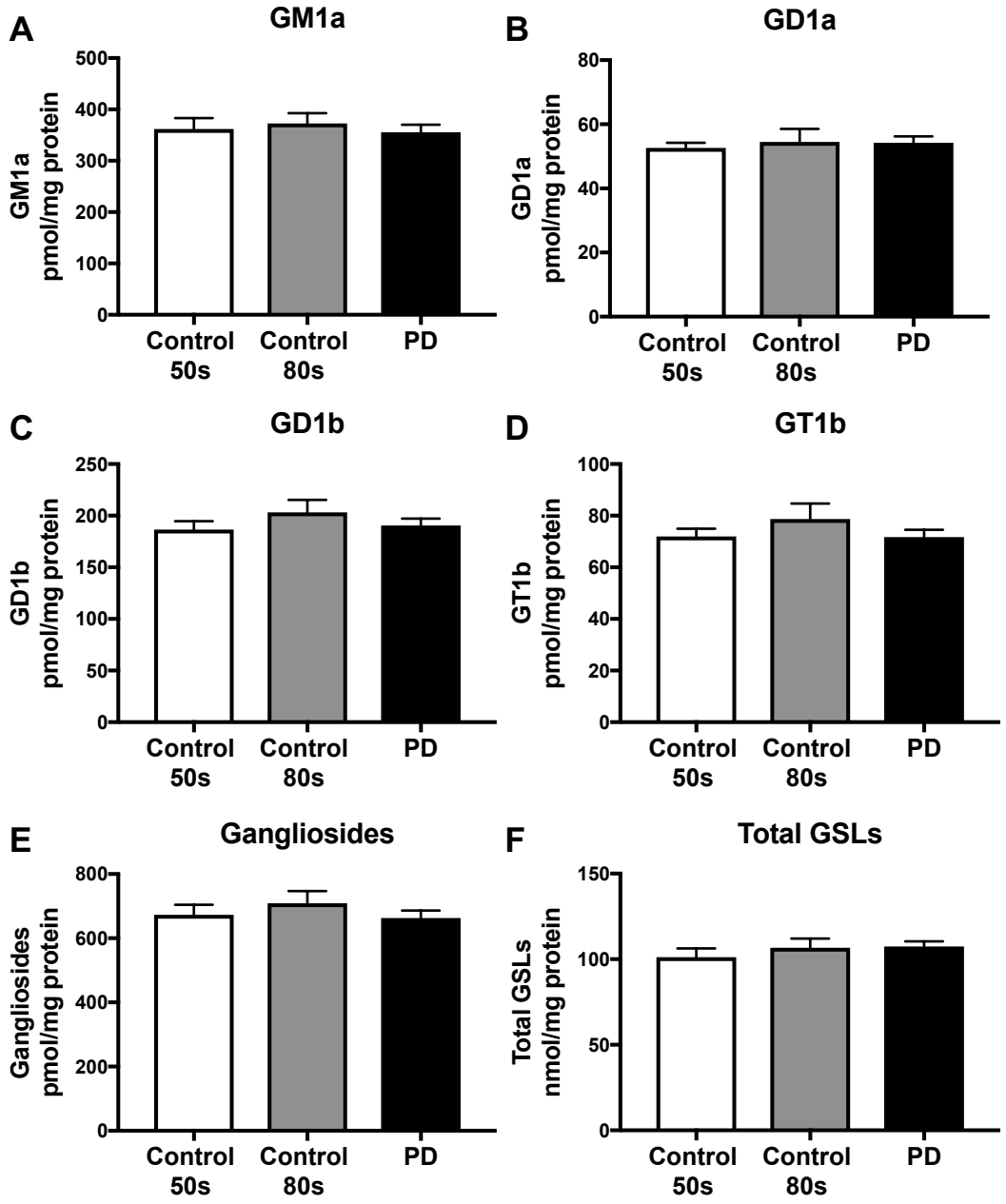

Figure 6.16: No changes in ganglioside levels or total GSL load in spinal cord with normal ageing or with PD. Spinal cord homogenates from 50s control subjects (n=5), 80s control subjects (n=10) and 80s PD patients (n=22) were used to determine GM1a (A), GD1a (B), GD1b (C) and GT1b (D) levels with NP-HPLC (not significant, one-way ANOVA). (E) Comparison of total ganglioside levels (sum of GM1a, GD1a, GD1b and GT1b). (F) Total GSL levels (sum of GlcCer + LacCer + GM1a + GD1a + GD1b + GT1b) in spinal cord from 50s control subjects, 80s control subjects and PD patients. Data are presented as mean ± SEM.

6.4 Discussion

In this chapter, levels of GSLs and activities of lysosomal hydrolases were analysed in human post-mortem tissues, including SN, putamen and SpC. Tissues were provided by the Harvard Brain Tissue Resource Centre (HBTRC; Mc Lean Hospital, Belmont, MA), the Parkinson's UK Brain Bank (PDUK; Imperial College London, UK) and the Oxford Brain Bank (OBB; Oxford, UK).

Sporadic PD versus genetic PD

Substantia nigra from control subjects (n=20) and PD patients (n=18) provided by the HBTRC were sequenced for GBA mutations. Four PD cases (22% of PD patients) were identified as having mutations in GBA. PD patients with GBA mutations were not removed from further analysis as no statistically significant differences were observed relative to sporadic PD cases (data not shown). Another reason to keep PD-GBA patients together with other PD patients is that, based on our current knowledge, the majority of PD patients (around 60%) might carry at least one putative damaging variant in a LSD gene, and some (around 20%) even carry multiple damaged alleles [180]. It is therefore highly likely that several of our here analysed PD patients are carriers for mutations in other LSD genes other than *GBA*. Consequently, the definition of 'sporadic' PD may need to be reconsidered in general and the conventional way of separating sporadic from genetic carriers may in the end turn out to be not entirely invalid.

Reduced GBA activity, but also reduced GBA2 activity with ageing and PD

Nearly 10 years ago, mutations in *GBA* were confirmed as the most common genetic risk factor for developing PD [127]. Subsequent studies demonstrated a decrease in GBA activity in various brain regions from PD patients with a mutation in the *GBA* gene (GBA-PD) and also in brain tissue from sporadic PD patients, not carrying a GBA

mutation [163-165]. For example, GBA activity was significantly decreased in the substantia nigra, putamen, cerebellum, and hippocampus of sporadic PD brains [163, 164]. Furthermore, it was reported that GBA activity progressively declined in normal ageing in healthy controls [164]. However, none of these studies distinguished between lysosomal GBA and non-lysosomal GBA2 activity and thus measured a mixture of GBA+GBA2 activity in their assays.

Here, we carefully distinguished GBA and GBA2 activities, using the inhibitor *N*B-DGJ and specific assay buffers at different pH values. We confirm previously published findings [163, 164] and show that GBA activity in substantia nigra is negatively correlated with age in control subjects and is significantly reduced in sporadic PD patients compared to age-matched controls (**Figure 6.1**). In addition, we confirm a significant reduction in GBA activity in an independent, second cohort of SN from PD patients compared to controls (**Figure 6.11**). Nevertheless, we did not find a difference in GBA activity in putamen comparing PD patients and control subjects in their 80s (**Figure 6.14**). This is in accordance with a published study, which reports no significant change in GBA activity in putamen from sporadic PD patients compared to controls [163]. Interestingly, this could point to a selective vulnerability of SN dopaminergic neurons to reduced GBA activity. However, as only one cohort of putamen tissues was available, results should be confirmed in an independent set of PD tissues. Importantly, we found for the first time that GBA2 activity gradually declines in the substantia nigra of control subjects with age and is further significantly reduced in PD patients compared to age-matched controls (**Figure 6.1**). In addition, we confirm a reduction in GBA2 activity in an independent, second cohort of SN tissue from PD patients compared to control subjects, although not significant (**Figure 6.11**). Furthermore, we show that GBA2 activity also declines in putamen tissue from control subjects during healthy ageing and is further reduced in PD patients (**Figure 6.14**). Interestingly, it has been reported that GBA2 activity depends on GBA activity, but not vice versa [284]. This may explain the observed

reduction in GBA2 activity in SN from PD patients with reduced GBA activity, but not in putamen tissue without reduced GBA activity. The role of GBA2 in substantia nigra and putamen in PD needs to be further explored, but these results suggest a possible involvement of other hydrolases in PD, in addition to GBA.

Substrate accumulation in SN and putamen of PD patients

It has remained unclear whether GlcCer or GlcSph levels are elevated in PD, as a consequence of the observed reduction in GBA (and GBA2) activity. In human studies, on the one hand, analysis of putamen, cerebellum and temporal cortex samples from PD-GBA patients and sporadic PD patients showed no evidence for significant accumulation of GlcCer and GlcSph [166, 167]. Nevertheless, a trend for increased GlcCer levels was seen with increased PD severity [167]. On the other hand, significant GlcSph accumulation was detected in substantia nigra and hippocampus of sporadic PD patients [164]. In addition, psychosine (galactosylsphingosine, GalSph) levels of the cerebral cortex were found to be slightly elevated in PD brain compared to healthy controls, but did not reach statistical significance [422].

Here, using sensitive and quantitative NP-HPLC analysis, we found a significant increase in GlcCer levels in the substantia nigra of two independent cohorts of PD patients compared to age-matched controls, as well as a significant correlation between age and GlcCer levels in the substantia nigra of PD patients (**Figures 6.4 and 6.10**). Furthermore, we found a significant increase in GlcSph levels in the same substantia nigra of PD patients compared to age-matched control subjects, as well as significant increases in sphingosine and sphinganine (**Figure 6.6**). However, in a third cohort of SN tissue, the observed increase in GlcCer levels in SN of 80s PD patients compared to age-matched controls did not reach statistical significance (**Figure 6.12**). These results eventually may eventually be seen as a cautionary tale about the importance of good tissue quality, sufficient numbers of patients and analysis of several cohorts as good

practice. Importantly, although statistically not significant, we also show an increase in GlcCer levels in putamen from PD patients compared to control subjects (**Figure 6.13**). These data support previously published findings of increased GlcSph in substantia nigra of sporadic PD patients [164], but are in contrast to other published studies reporting no changes in GlcSph or GlcCer levels in PD [166, 167]. The discrepancies between published work might be due to low numbers of analysed patients, different analytical methods and/or most importantly analysis of different brain regions, which are not necessarily affected in PD (e.g. temporal cortex), rather than substantia nigra.

Recently, a model has been proposed in which GlcSph accumulates before GlcCer in murine GBA-PD brains [153], which is in agreement with our human SN data on 70s versus 80s cohorts PD subjects (**Figures 6.4 and 6.6**). Interestingly, GlcCer can be alternatively processed to GlcSph via lysosomal acid ceramidase, which can then exit the lysosome [44-46]. Thus, there may be crosstalk between GlcCer and GlcSph levels. Furthermore, it is important to note that several studies have shown that GSLs, especially GlcCer and GlcSph, interact with α-synuclein and promote the formation of assembly-state oligomeric α-synuclein species [148, 153-155]. This indicates a possible pathological role of the observed lipid accumulation in human SN in PD through interaction with α-synuclein.

We recently reported a significant increase in GlcCer and GlcSph levels in mouse brain during healthy ageing from 1.5 months to 24 months of age, which we suggested might lower the threshold for developing PD [312]. However, in this study, increases in GlcCer and GlcSph levels were not observed in human brain tissues from control subjects during ageing. There could be several reasons for this discrepancy. Firstly, there may be basic differences in brain ageing in different species. Secondly, there may be variation in GSLs in other brain regions, not analysed in the present study, e.g. the cortex or the cerebellum. Thirdly, in the HBTRC cohort, only comparison of 70s and 80s control subjects was possible, which is not covering a very broad age range. On the other hand,

SN and putamen tissue from control subjects from the OBB in their 50s and 80s also did not show differences in GlcCer levels, but only low n-numbers from younger control subjects were available and the age range is still not large (PD risk is already increased from 50 years of age). In summary, more detailed studies are needed with the sole focus of analysing GSLs in human brain ageing.

Altered lysosomal enzyme activities in PD

Last year, a major study reported that there is an excessive burden of putatively damaging variants of lysosomal storage disorder genes in PD [180]. This prompted us to investigate the activity of multiple lysosomal hydrolases in substantia nigra and putamen tissues of PD patients and age-matched controls.

We found significantly reduced lysosomal α-galactosidase activity in substantia nigra of PD patients compared to age-matched control subjects (**Figure 6.2**). In addition, we confirmed a reduction in α-galactosidase activity in an independent, second cohort of SN tissue from PD patients compared to control subjects (**Figure 6.11**). These results agree with a previously published study showing a decrease in α-galactosidase activity and protein levels in temporal cortex in late-stage PD [423]. α-galactosidase activity was also found to be lower in dried blood spots and in leukocytes of PD patients compared to controls [424, 425]. In addition, we analysed levels of Gb3, the principle GSL substrate of α-galactosidase. We did not see any change in Gb3 levels in substantia nigra of PD patients compared to controls (**Figure 6.3**). This confirms a previous study reporting that Gb3 levels were not significantly different between temporal cortex of control and PD cases [423]. Interestingly, a link between α-galactosidase and PD is supported by several lines of evidence. Firstly, pathological accumulation of α-synuclein, concomitant with disruption of autophagy-lysosome markers, has been reported in α-galactosidase A-deficient (Fabry) mouse brains [426]. Furthermore, numerous Fabry patients have been diagnosed with symptoms of Parkinsonism, suggesting an increased risk of

developing PD in individuals with *GLA* mutations [180, 325, 427, 428]. Thus, deficiency of the lysosomal enzyme α-galactosidase in PD brain might be associated with the pathological accumulation of α-synuclein. However, the physiological role of α-galactosidase in brain tissue still has to be determined, as we did not observe any related Gb3 substrate accumulation. However, Gb3 is only expressed at very low levels in the brain. In the Fabry murine brain, Gb3 is only stored in selected cells of the piriform cortex (Platt lab, unpublished data). It is possible that the residual enzyme activity may be sufficient to prevent substrate accumulation, but might not be sufficient for other cellular functions.

In the present study, we also found a significant decrease in β-galactosidase and β-hexosaminidase activities in substantia nigra of two independent cohorts of PD patients compared to age-matched control subjects (**Figures 6.2 and 6.11**). Supporting our results, reduced β-galactosidase and β-hexosaminidase activities have been reported in CSF of PD patients compared to control subjects in several studies [147, 305, 429]. Interestingly, accumulation of α-synuclein was found in brains of both β-hexosaminidase deficient Sandhoff mice and Sandhoff patients [430, 431]. Also, some patients with adult-onset GM1-gangliosidosis (deficiency in β-galactosidase) have been found to display akinetic-rigid parkinsonism [323, 432, 433]. Mutations in *GLB1* and *HEXB* were recently confirmed as LSD gene variants in PD cases [180]. These findings further support an important role of the lysosome in PD.

Finally, we report for the first time a significant decrease in neuraminidase activity in the substantia nigra of two independent cohorts of PD patients compared to age-matched control subjects (**Figures 6.2 and 6.11**). Furthermore, although statistically not significant, we also show a decrease in neuraminidase activity in putamen from 80s PD patients and age-matched control subjects compared to younger 50s control subjects (**Figure 6.14**). Besides lysosomal degradation of gangliosides, neuraminidases can also remodel gangliosides in the outer leaflet of the plasma membrane [330, 434]. For this,

neuraminidases can sequentially remove sialic acid residues from GD1a, GD1b and GT1b, subsequently leading to an increase in GM1a levels. Indeed, genetic deficiency of neuraminidases 3 and 4 in mice causes a reduction in levels of GM1a [330]. We recently observed an increase in neuraminidase activity in mouse brain during normal ageing and proposed that this might reflect the observed increase in GM1a and concomitant reduction in GD1a, GD1b and GT1b levels, which could be protective for DA neurons [312]. In contrast, in human substantia nigra from PD patients, we here observe a significant decrease in neuraminidase activity, which might be reflective of the observed decrease in GM1a levels. In general, these results suggest that mice might have a compensatory, neuroprotective mechanism based on increasing neuraminidase activity and subsequent increased GM1a brain expression with age, which is not effective or present in the human brain. Interestingly, this seems to resemble the mechanism by which a mouse model of Tay-Sachs disease (β-hexosaminidase A deficiency, GM2 gangliosidosis) is able to escape the human disease (via degradation of GM2 to GA2 via murine neuraminidases) in contrast to the human population [435]. In summary, neuraminidases could be an interesting therapeutic target for PD.

Loss of gangliosides in human SN with ageing is more prominent in PD

Gangliosides are the most abundant GSLs in the CNS in all mammals and are essential for brain development and function [23, 40, 41]. For example, the ganglioside GM1a is a neurotrophic and neuroprotective factor, critical for neuritogenesis, synaptogenesis, and myelination [42, 43, 157]. In this study, we have shown that GM1a and GD1a levels of substantia nigra are negatively correlated with ageing in control subjects from two independent cohorts (**Figures 6.8 and 6.12**). Interestingly, a reduction in GM1a and GD1a levels was also found in putamen in control subjects with increasing age (**Figure 6.13**). Supporting our results, previous reports have indicated changes in levels of several complex gangliosides, including a progressive decline in GM1a and GD1a

levels, in multiple regions of the human brain during ageing [308, 309, 436]. Moreover, we demonstrate that levels of all main gangliosides (GM1a, GD1a, GD1b and GT1b) are negatively correlated with ageing in substantia nigra in PD subjects and ganglioside levels are significantly reduced in the substantia nigra of PD patients compared to age-matched control subjects (**Figure 6.8**). Importantly, we confirm a significant decrease in ganglioside levels in two additional, independent cohorts of SN tissue from PD patients compared to control subjects, as well as in a cohort of putamen tissue from PD patients (**Figures 6.10, 6.12 and 6.13**). In agreement with our data, a reduction in GM1a levels in the substantia nigra of PD subjects, and reductions in GM1a, GD1a, GD1b and GT1b levels in the occipital cortex of PD subjects have previously been described, using immunohistochemical staining or thin-layer chromatography [156, 157]. Interestingly, in the substantia nigra of PD patients, GM1a staining with cholera toxin was diminished near α-synuclein aggregates and neurons with reduced levels of tyrosine hydroxylase [156]. In addition, a recent study showed reductions in GM1a, GD1a, GD1b and GT1b in the substantia nigra in a smaller cohort of PD patients using thin-layer chromatography [158]. To support these findings, a significant decrease in gene expression of key biosynthetic enzymes involved in synthesis of GM1a/GD1b (*B3GALT4*) and GD1a/GT1b (*ST3GAL2*) was reported in residual neuromelanin-containing cells in the SN of PD patients compared to age-matched controls [437].

Ganglioside metabolism, especially GM1a, and its role in PD was recently reviewed [161]. There are two important aspects of GM1a biology with regard to ageing and PD: Its function as an α-synuclein binding partner in the plasma membrane and its role in neurotrophic signalling. Firstly, α-synuclein is a ganglioside-binding protein, which adopts a more stable, α-helical structure when bound to membranes, but starts to form fibrils in the absence of GM1a ganglioside [159, 160]. Secondly, GM1a is crucial for efficient signalling of the growth factor glial cell-derived neurotrophic factor (GDNF) [157]. It has been proposed that even a modest decline in GM1a ganglioside levels might

inhibit this trophic support in dopaminergic neurons [161]. Mice deficient in the ability to synthesize a-series gangliosides (genetic deletion of *B4GALNT1*, encoding GM2 synthase), specifically GM1a, develop parkinsonism, including the loss of TH-positive cells, lower striatal dopamine levels, an accumulation of α-synuclein aggregates and impaired motor function [421]. GM2 synthase deficiency in humans results in severe spastic paraplegia [39], which may reflect a more central role for gangliosides in myelinated neurons in humans compared to mice. Intriguingly, treatment with exogenous GM1a has been reported to be beneficial in multiple preclinical models of PD [358-360, 438, 439] and in PD patients [249, 440, 441]. Furthermore, deletion of GD3 synthase, which leads to an increase in GM1a ganglioside, was neuroprotective in a preclinical PD model [442].

In summary, it is interesting to speculate whether the observed depletion of GM1a ganglioside in human substantia nigra during ageing, and to a greater extent in PD patients, might contribute to the development of PD, rather than accumulation of the protein α-synuclein.

No changes in GSLs in spinal cord in PD

In this study, we also requested spinal cord (SpC) of control patients and PD patients and analysed GSL levels in these tissues. The spinal cord is not involved in the major neuropathology in PD, however, as the natural input/output structure of the brain from/to the periphery, the spinal cord is vital for the processing and the performance of motor functions. Interestingly, spinal cord function has been reported to be affected by ageing [443]. For example, perturbed cholesterol homeostasis was found in SpC of ageing rats [443]. Furthermore, a recent study has shown that spinal cord injury is associated with a subsequent increased risk of developing PD [444]. In addition, SpC stimulation is under investigation as a treatment of PD [445, 446]. Importantly, SpC stimulation was reported to alleviate motor deficits in a primate model of PD [447] and has already been shown

to improve gait function in PD patients in several pilot studies [448, 449]. Concerning LSDs, disease pathology was surprisingly found to start in the SpC in Batten disease (PPT1-deficient form, a neuronal ceroid lipofuscinosis (NCL)) (personal communication, Prof. Jonathan Cooper). Consequently, we wanted to look at the SpC of PD patients to not miss possible clues to pathogenesis in PD.

Here, we report no changes in levels of GlcCer, LacCer or more complex gangliosides GM1a, GD1a, GD1b or GT1b in human SpC during ageing or in PD (**Figures 6.15 and 6.16**). This is in contrast to results obtained with human substantia nigra or putamen tissue from PD patients. However, we show significantly increased levels of GM3, the precursor of more complex a-series and b-series gangliosides, in SpC of aged control subjects and PD patients compared to SpC of younger control subjects (**Figure 6.15**). These results support the general notion that SpC is not involved in the major neuropathology in PD. Nevertheless, changes in levels of specific GSLs, i.e. increased GM3 levels, might occur during ageing and the role of these changes in e.g. neurodegenerative diseases or spinal cord injury need to be further investigated.

Therapeutic options for PD

Modulation of GSL levels and/or lysosomal enzyme activities might offer a novel approach to treat late-onset neurodegenerative disorders, like PD.

For example, the possibility of enzyme replacement therapy (ERT) for GBA has already been exploited. The first *in vivo* proof-of-concept experiment for increasing GBA activity as a therapeutic strategy to prevent synucleinopathy was provided by Sardi and co-workers in 2011 using a GD mouse model [168]. Further studies have shown that AAV-mediated expression of GBA reduced α-synucleinopathy in mutant α-synuclein (A53T) mice [169] and protected SN dopamine neurons from PD-like degeneration by preventing α-synucleinopathy in two PD rodent models [170]. ERT might also be an option for other lysosomal enzymes, like α-galactosidase or β-hexosaminidase, as we

here show that their activity is significantly reduced in SN of PD patients and mutations were recently identified as risk factors for PD [180].

In addition, treatment with glucosylceramide synthase (GCS) inhibitors to reduce the lipid load in neurons (substrate reduction therapy) [38], is under investigation for PD [175-177]. Interestingly, a clinical trial to assess the safety and efficacy of ibiglustat, a GCS inhibitor, is currently ongoing with GBA-PD patients (NCT02906020). It is important to keep in mind that the potential beneficial effects of GlcCer biosynthesis inhibitors, which lead to a reduction in levels of all GSLs, may be partly offset by depletion of the more-complex gangliosides, i.e. neurotrophic GM1a.

Finally, treatment with exogenous GM1a or with neuraminidases might prove to be beneficial for PD. The ability of GM1a to partially counteract the effects of damage to the dopaminergic system in MPTP-toxin mouse models of PD was first described in the 1980s [359, 438]. Intriguingly, treatment with exogenous GM1a has been reported to be beneficial in several preclinical models of PD, including non-human primates [358-360, 438, 439]. Importantly, a randomized double-blind placebo control trial and a subsequent long-term open extension study reported that systemic administration of GM1a improved functional outcomes in PD patients [249, 441]. Another approach to increase GM1a levels in the brain is via enzymatic conversion of polysialo-gangliosides (GD1a, GD1b and GT1b) to GM1a using neuraminidases. Intraventricular neuraminidase administration, leading to the expected change in ganglioside expression with a significant increase in GM1 levels, has been shown to partially protect against loss of dopaminergic neurons in MPTP-treated mice, similar to systemic GM1a administration [450]. This might be an interesting option for PD patients, as we here show for the first time that neuraminidase activity is significantly reduced in SN of PD patients

In summary, there are several options how activities of lysosomal enzymes and levels of GSLs could be modulated to exert beneficial effects in PD.

7 Glycosphingolipid biomarkers for PD

7.1 Introduction

7.1.1 Biomarkers for PD: Serum and CSF studies

All current therapeutic interventions in PD have limited benefits for disease progression. This is mostly because neuronal damage likely has progressed over an estimated period of 5-15 years and lead to loss of around 50-70% of SN DA neurons before symptoms start to emerge [451]. Thus, there is an urgent need to find early diagnostic biomarkers. Besides intervention at disease onset, finding novel biomarkers for PD is also crucial for monitoring disease progression, evaluating the effectiveness of therapies and patient stratification for clinical trials. However, there is no accepted definitive biomarker for PD yet [451, 452]. Ideal biomarkers are measurable in easily obtainable body fluids, e.g. urine or serum [453]. However, cerebrospinal fluid (CSF) could also be used. Furthermore, it is possible to include patients who are at risk of developing PD in biomarker studies, e.g. patients diagnosed with rapid eye movement (REM) sleep behaviour disorder (RBD). RBD is a parasomnia which involves acting out dreams and abnormal movements during REM sleep stage. It was reported that RBD patients have an 80-90% risk of conversion to a synucleinopathy disorder (e.g. PD or dementia with Lewy bodies) over 14 years from the time of RBD diagnosis [454-456]. Interestingly, single-nucleotide polymorphisms in the *SCARB2* gene, encoding the lysosomal integral membrane protein 2 (LIMP-2), an important receptor for trafficking GBA to the lysosome, were significantly associated with RBD [457].

Research over the past decade has revealed several links between PD and lysosomal storage disorders, associated with lysosomal dysfunction and altered GSL homeostasis. Thus, we were interested whether changes in GSL levels could be found in CSF and/or serum from PD patients compared to control subjects. These studies may identify novel

lipid-related biomarkers in PD patients for clinical monitoring and patient stratification for clinical trials.

The aim of this experimental chapter is therefore:

- To analyse GSLs in cerebrospinal fluid and serum samples from control subjects and PD patients in the search for possible lipid biomarkers.

Most of the data in this experimental chapter are part of a submitted manuscript (Huebecker *et al.*, 2019).

7.2 Materials and Methods

7.2.1 Patients

Post-mortem CSF from control subjects and sporadic PD patients was provided by the PDUK Brain Bank and the OBB. Both cohorts were combined and processed together to increase n-numbers. CSF from control subjects (n=15) and PD patients (n=27) were used for analysis (**Table 7.1**). Research was performed under the PDUK Brain Bank's and the OBB's Research Ethics Committee approval (REC08/MRE09/31+5 and REC15/SC/0639, respectively).

Ante-mortem CSF and serum samples from control subjects and PD patients were provided by the Oxford Parkinson's Disease Centre (OPDC; Oxford, UK). Ante-mortem CSF of control subjects (n=15) and age-matched PD subjects (n=28) was used for GSL analysis (**Table 7.2**). Furthermore, serum samples from patients at risk of developing PD (prodromal PD phase), diagnosed with REM sleep behaviour disorder (RBD), were provided. Serum of control subjects (n=15), PD patients (n=30) and RBD patients (n=30) were used for GSL analysis (**Table 7.2**). Research was performed under the OPDC's Research Ethics Committee approval (REC16/SC/0108).

Table 7.1: PD and control case information from post-mortem CSF received from the PDUK Brain Bank and the OBB. Data summarised as mean ± SD.

	Control subjects	PD subjects
Cohort size	15	27
Female (%)	26.7	18.5
Male (%)	73.3	81.5
Age (years)	80.0 ± 9.8	79.0 ± 7.7

Table 7.2: PD, RBD and control case information from ante-mortem CSF and serum received from the OPDC. RBD = REM sleep behaviour disorder. Data shown as mean ± SD.

	Control subjects	PD subjects	RBD subjects
Cohort size	15	30	30
Female (%)	50.0	50.0	13.3
Male (%)	50.0	50.0	86.7
Age (years)	65.7 ± 8.4	63.8 ± 9.9	64.4 ± 11.6

7.2.1.1 Acknowledgements

CSF samples were supplied by the Parkinson's UK Brain Bank (Imperial College London, UK), funded by Parkinson's UK, a charity registered in England and Wales (258197) and in Scotland (SC037554). We further acknowledge the Oxford Brain Bank (Oxford, UK), supported by the Medical Research Council (MRC), the NIHR Oxford Biomedical Research Centre and the Brains for Dementia Research programme, jointly funded by Alzheimer's Research UK and the Alzheimer's Society. We also acknowledge the Oxford Parkinson's Disease Centre (Oxford, UK), funded by Parkinson's UK, a charity registered in England and Wales (258197) and in Scotland (SC037554).

7.2.2 Glycosphingolipids (NP-HPLC)

GlcCer and downstream GSLs were analysed as previously described in **Chapters 2.2.6 and 3.2.7.**

7.2.3 Statistical analysis

All statistical analyses were performed with GraphPad Prism 7.0 (GraphPad, San Diego, CA). Unpaired student's *t*-test was used to compare two groups, one-way ANOVA was used to compare three groups and two-way ANOVA was used to compare more than three groups. Correlations were analysed with Pearson correlation analysis.

7.3 Results

7.3.1 Method development for GSLs in CSF and serum

The aim of this chapter was to analyse GSLs in cerebrospinal fluid (CSF) and serum samples from control subjects and PD patients in the search for possible GSL biomarkers. For this, we first tested what volumes of serum and CSF are needed to reliably measure GSLs with rEGCase digestion on the one hand and GlcCer with Cerezyme digestion on the other hand. Serum from one control subject (provided by Dr. David Priestman) and CSF from one control subject (provided by Parkinson's UK Brain Bank) were used in increasing amounts to test the GSL and GlcCer assays. For serum various amounts between 5µl and 100µl were used and for CSF various amounts between 5µl and 200µl were used.

First, total GSL levels in serum and CSF samples were quantified using NP-HPLC (n=1-2 per quantity of fluid). As expected, with increasing amounts of serum and CSF, increasing amounts of total GSLs were detected in a linear fashion (**Figure 7.1A, B**). Interestingly, serum contains 5-6-fold higher levels of GSLs compared to CSF (**Figure 7.1C**). Importantly, the amount of GSLs measured in various quantities of both body fluids follows a linear function with roughly a doubling in GSL levels when doubling the amount of analysed fluids (indicated with ideal doubling standard curves in grey, **Figure 7.1D**). Thus, GSL measurements using rEGCase digestion can be used for robust GSL analysis in serum and CSF, even with low quantities of either fluid. In further experiments, 50µl serum and 75µl CSF were used for GSL analysis.

Next, GlcCer levels in serum and CSF samples were quantified using NP-HPLC (n=1-2 per quantity of fluid). With increasing amounts of serum, increasing amounts of GlcCer were measured, however only in a linear fashion with dampened slope (**Figure 7.2A**). Compared to an ideal doubling standard curve for GlcCer levels, 50µl or 100µl serum already seemed to overwhelm the GlcCer digestion via Cerezyme (**Figure 7.2D**). Furthermore, unexpectedly, there was nearly no increase in the measured amounts of

GlcCer with increasing amounts CSF, pointing to a possible inhibition of Cerezyme used for GlcCer digestion (**Figure 7.2B**). Consequently, higher levels of GlcCer were measured in serum compared to CSF (**Figure 7.2C**) and GlcCer may only be analysed using Cerezyme in low quantities of serum (**Figure 7.2D**). In further experiments, 25µl serum and 25µl CSF were used for GlcCer analysis with Cerezyme.

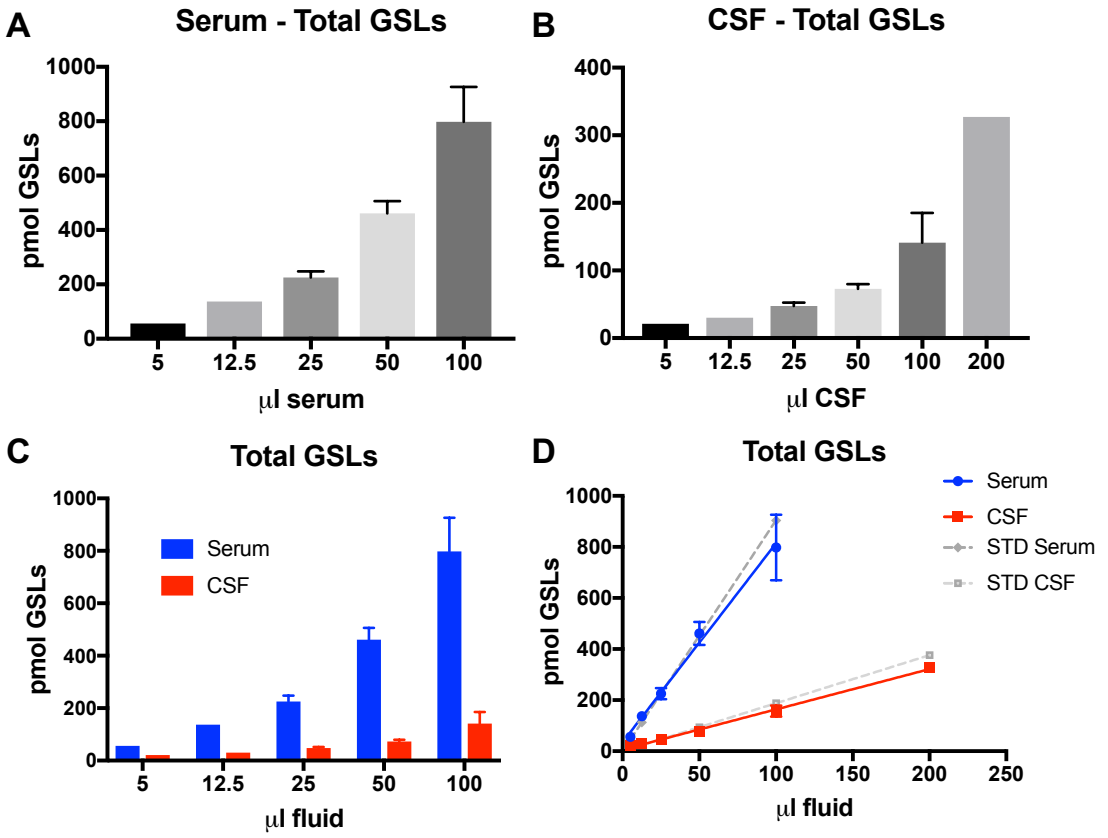

Figure 7.1: Method development for the quantification of glycosphingolipids in human serum and CSF samples using rEGCase digestion. Levels of total GSLs were measured in different quantities of serum and CSF using NP-HPLC after digestion with rEGCase (n=1-2 per quantity of fluid). (A) Increasing levels of total GSLs with increasing amounts of serum. (B) Increasing levels of total GSLs with increasing amounts of CSF. (C) Comparison of total GSL levels measured in serum and CSF. (D) Linear regression of GSL levels with increasing amounts of serum and CSF. Ideal standard (STD) curves are shown in grey. Data are presented as mean ± SD.

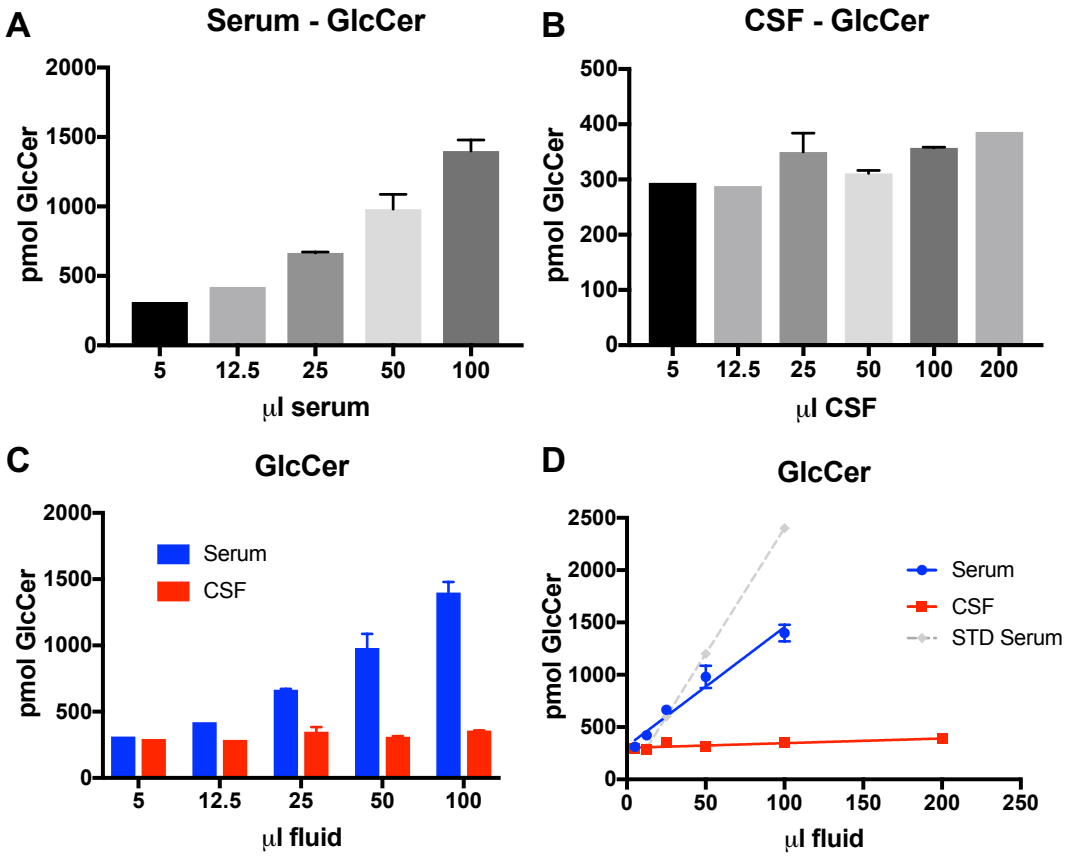

Figure 7.2: Method development for the quantification of glucosylceramide in human serum and CSF samples using Cerezyme digestion. (A-D) Levels of GlcCer were measured in different quantities of serum and CSF using NP-HPLC after digestion with Cerezyme (n=1-2 per quantity of fluid). (A) Increasing levels of GlcCer with increasing amounts of serum. (B) No change in GlcCer levels with increasing amounts of CSF. (C) Comparison of GlcCer levels measured in serum and CSF. (D) Linear regression of GlcCer levels with increasing amounts of serum and CSF. Ideal standard (STD) curve for serum is shown in grey. Data are presented as mean ± SD.

7.3.2 GSL biomarkers in CSF of PD patients

Our aim was to analyse GSLs in CSF from control subjects and PD patients in the search for possible GSL biomarkers. For this, we received a cohort of post-mortem CSF and a cohort of ante-mortem CSF. Post-mortem CSF from control subjects in their 80s (n=15) and sporadic PD patients in their 80s (n=27) was provided by the PDUK Brain Bank (Imperial College London, UK) and the OBB (Oxford, UK). Ante-mortem CSF samples from control subjects (n=15, average age of 64 years) and age-matched PD subjects (n=28, average age of 66 years) were provided by the OPDC (Oxford, UK).

The pattern of GSLs in CSF is different and more complex than the GSL pattern in brain tissue. Moreover, we found differences between the GSL expression patterns in ante-mortem CSF and post-mortem CSF samples. Ante-mortem CSF displays a large LacCer peak and GA2 peak (o-series), with prominent peaks of GM2, GM1a, GD1a, GD1b and GT1b (a-series & b-series), but rather small peaks of GM3 and GD3 (precursors of a-series and b-series). In contrast, post-mortem CSF features a large peak of the lipid GM3 (precursor of a-series), with still prominent peaks of LacCer, GD3, GM1a, GD1a, GD1b and GT1b (a-series and b-series), but low levels of GA2 (o-series) and GM2.

First, we measured the levels of GlcCer and LacCer, sequential precursors in the GSL biosynthetic pathway, in post-mortem CSF samples. No differences in GlcCer levels or LacCer levels were detected in post-mortem CSF of PD patients in comparison to control subjects (**Figure 7.3A, B**). Next, we focused on downstream gangliosides GM3 and GM2 (a-series), GD3 (b-series) and GA2 (o-series), with GM3 being the highest expressed GSL. Interestingly, a significant decrease in GM3 levels and a significant increase in GM2 levels was found in post-mortem CSF of PD patients compared to controls (**Figure 7.3C, D**; GM3: p=0.0055, 47.6% reduction; GM2: p=0.0165, 43.3% increase). A non-significant increase in GA2 levels was observed in CSF of PD patients compared to age-matched control subjects (**Figure 7.3E**, p=0.0590, 11.7% increase). No change in GD3 levels was observed in post-mortem CSF of PD patients in comparison to controls (**Figure 7.3F**). Then, we analysed levels of more complex gangliosides of the a-series and b-series, GM1a, GD1a, GD1b and GT1b. Levels of all these four gangliosides were not significantly different in post-mortem CSF from PD patients in comparison to CSF from control subjects (**Figure 7.4A-D**). Consequently, in CSF of PD patients, ganglioside levels (sum of GM1a, GD1a, GD1b and GT1b) were not changed in comparison to age-matched control subjects (**Figure 7.4E**).

In summary, no changes in GlcCer, LacCer or more-complex gangliosides were detected in post-mortem CSF of PD patients in comparison to control subjects, but significant changes in a-series gangliosides GM3 and GM2 were found.

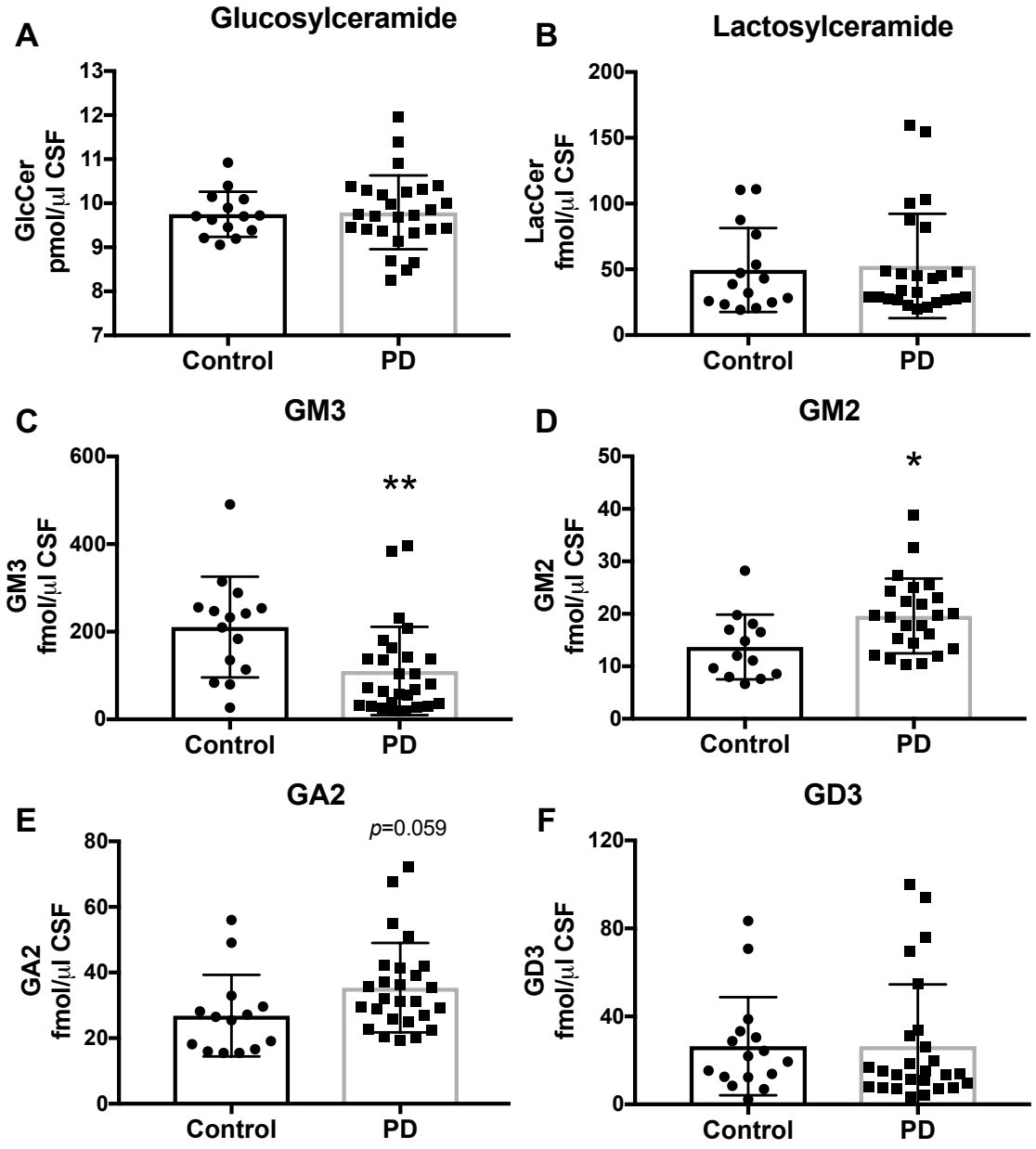

Figure 7.3: Significant decrease in GM3 and increase in GM2 levels in post-mortem CSF of PD patients. Post-mortem CSF from control subjects (n=15) and age-matched PD patients (n=27) was used to determine GlcCer (A), LacCer (B), GM3 (C), GM2 (D) GA2 (E), and GD3 (F) levels with NP-HPLC (* = $p<0.05$, ** = $p<0.01$, unpaired t-test). Data are presented as mean ± SD.

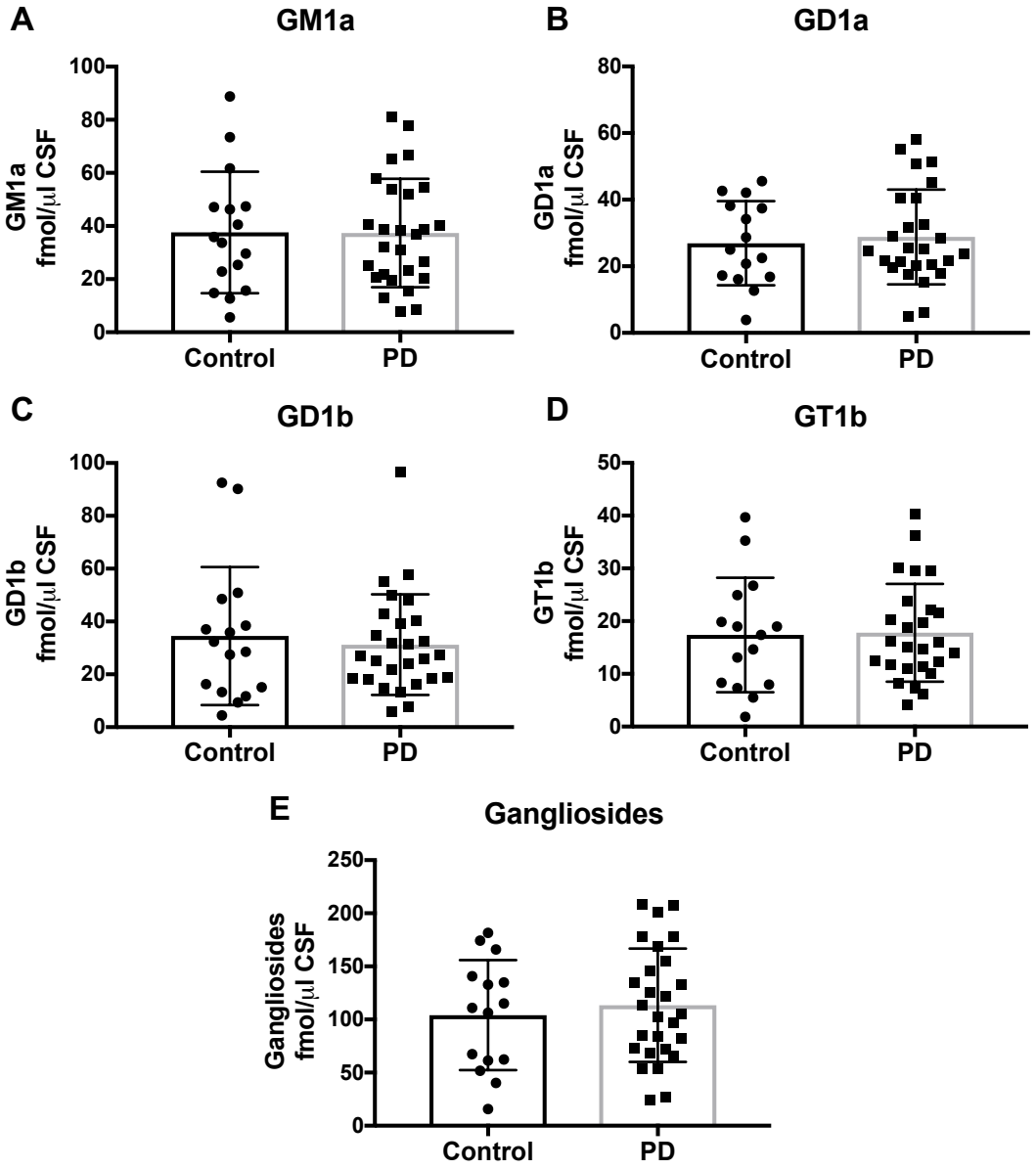

Figure 7.4: No changes in ganglioside levels in post-mortem CSF of PD patients. Post-mortem CSF from control subjects (n=15) and age-matched PD patients (n=27) was used to determine GM1a (A), GD1a (B) GD1b (C), and GT1b (D) levels with NP-HPLC. (E) Comparison of total ganglioside levels (sum of GM1a, GD1a, GD1b and GT1b) in post-mortem CSF from control subjects and PD patients. Data are presented as mean ± SD.

To expand our investigation, we analysed ante-mortem CSF samples from PD patients and age-matched control subjects and first measured the levels of GlcCer. First, no significant differences in GlcCer levels in ante-mortem CSF of PD patients were detected in comparison to CSF of control subjects (**Figure 7.5A**). However, a larger spread of PD patients was observed in comparison to control subjects (**Figure 7.5A**). Thus, we plotted

the histogram of the relative frequency of GlcCer levels documented for control subjects and PD patients and saw two subpopulations in the PD cohort (**Figure 7.5B**). When splitting these subpopulations into two PD cohorts, the following results were obtained: GlcCer levels were significantly increased in ante-mortem CSF of PD cohort 1 (n=21) compared to control subjects (**Figure 7.5C**, p=0.0221, 6.7% increase). Consequently, GlcCer levels in ante-mortem CSF from PD cohort 2 (n=7) were significantly reduced in comparison to control subjects using both digestion methods (**Figure 7.5C**, p<0.0001, 24.5% reduction). No significant correlation of GlcCer levels in ante-mortem CSF with age was found in all three cohorts, but interestingly linear regression of PD cohort 1

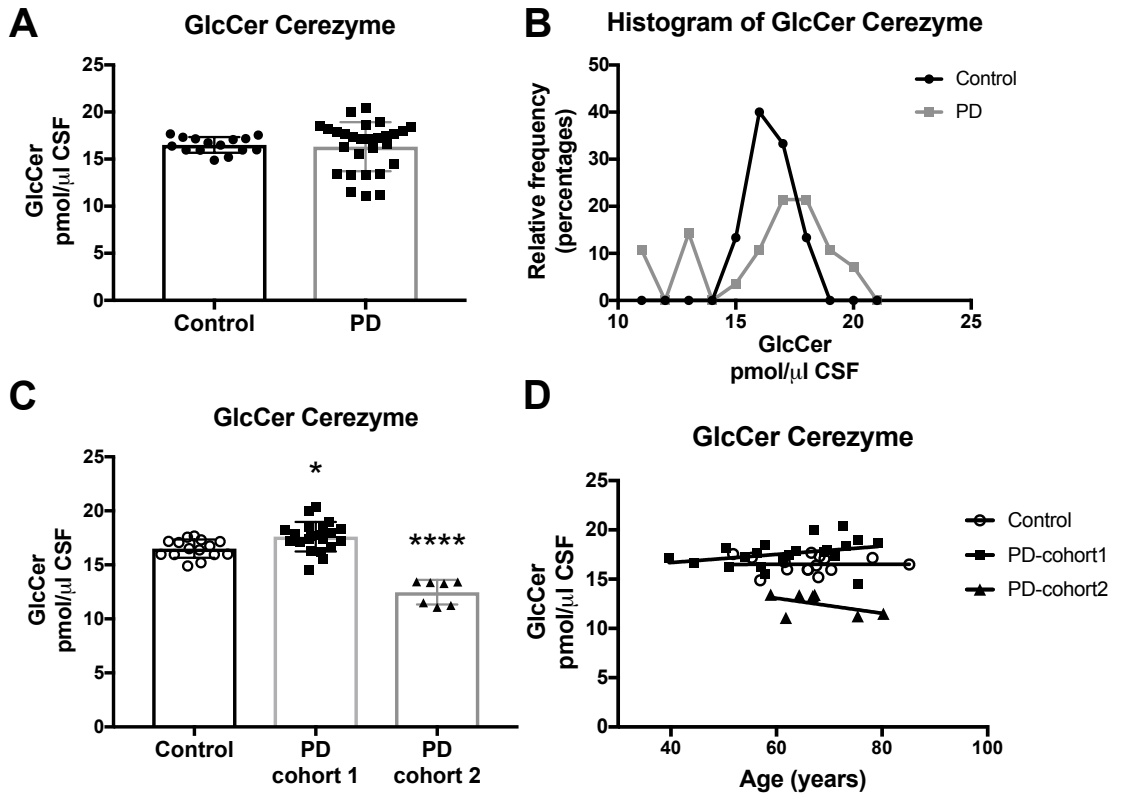

Figure 7.5: Glucosylceramide levels in ante-mortem CSF of PD patients reveal two subpopulations in PD cohort. GlcCer levels in ante-mortem CSF from control subjects (n=15) and age-matched PD patients (n=28) were determined after digestion with Cerezyme using NP-HPLC. (A) GlcCer levels were not significantly different in CSF of PD patients compared to control subjects. (B) Histogram of the relative frequency of GlcCer levels documented for CSF from control subjects and PD patients reveals two subpopulations in PD cohort. (C) Significant changes in GlcCer levels in CSF from both PD cohorts (n=21 and n=7) compared to CSF from control subjects (n=15) (* = p<0.05, **** = p<0.0001, one-way ANOVA). (D) Linear regression analysis of GlcCer levels in ante-mortem CSF from control subjects (n=15) and both PD cohorts (n=21 and n=7, respectively). Bar graphs are presented as mean ± SD.

showed a positive slope, whereas PD cohort 2 displayed a negative slope (**Figure 7.5D**). In summary, two subpopulations were found in the PD cohort, which displayed significantly altered GlcCer levels in CSF compared to the control cohort.

Next, we focused on downstream GSLs LacCer, GA2 (o-series), GM3 and GM2 (a-series) and GD3 (b-series), with LacCer and GA2 as the highest expressed GSLs. Interestingly, LacCer levels in ante-mortem CSF of PD patients were significantly increased in comparison to age-matched control subjects (**Figure 7.6A**, p=0.0003, 21.8% increase). There were no changes detected in GA2 levels in CSF of PD patients compared to control subjects (**Figure 7.6B**). However, a significant increase in GM3 levels and a significant decrease in GM2 levels was found in ante-mortem CSF of PD patients compared to controls (**Figure 7.6C, D**; GM3: p=0.0438, 40.2% increase; GM2: p=0.0455, 22.6% reduction). Furthermore, a significant decrease in GD3 levels was observed in CSF of PD patients compared to age-matched control subjects (**Figure 7.6E**, p=0.0160, 33.0% reduction). Then, we analysed levels of more complex gangliosides of the a-series and b-series, GM1a, GD1a, GD1b and GT1b. A statistically non-significant decrease in GM1a levels was observed in ante-mortem CSF of PD patients compared to age-matched control subjects (**Figure 7.7A**, p=0.1603, 17.4% reduction). However, a significant decrease in GD1a levels was found in CSF of PD patients compared to controls (**Figure 7.7B**, p=0.0038, 37.6% reduction). In addition, gangliosides GD1b and GT1b were both significantly reduced in ante-mortem CSF of PD patients in comparison to control subjects (**Figure 7.7C, D**; GD1b: p=0.0009, 41.6% reduction; GT1b: p=0.0002, 51.3% reduction). Consequently, in ante-mortem CSF of PD patients, ganglioside levels (sum of GM1a, GD1a, GD1b and GT1b) were significantly decreased to 61.4% of age-matched control subjects (**Figure 7.7E**, p=0.0015).

In summary, LacCer and GM3 levels are increased in ante-mortem CSF of PD patients, whereas GM2, GD3 and more-complex gangliosides GM1a, GD1a, GD1b and GT1b are significantly decreased compared to control subjects. Regarding the loss of

gangliosides, these results are comparable to the results obtained with SN and putamen tissue from PD patients (**Chapter 6**).

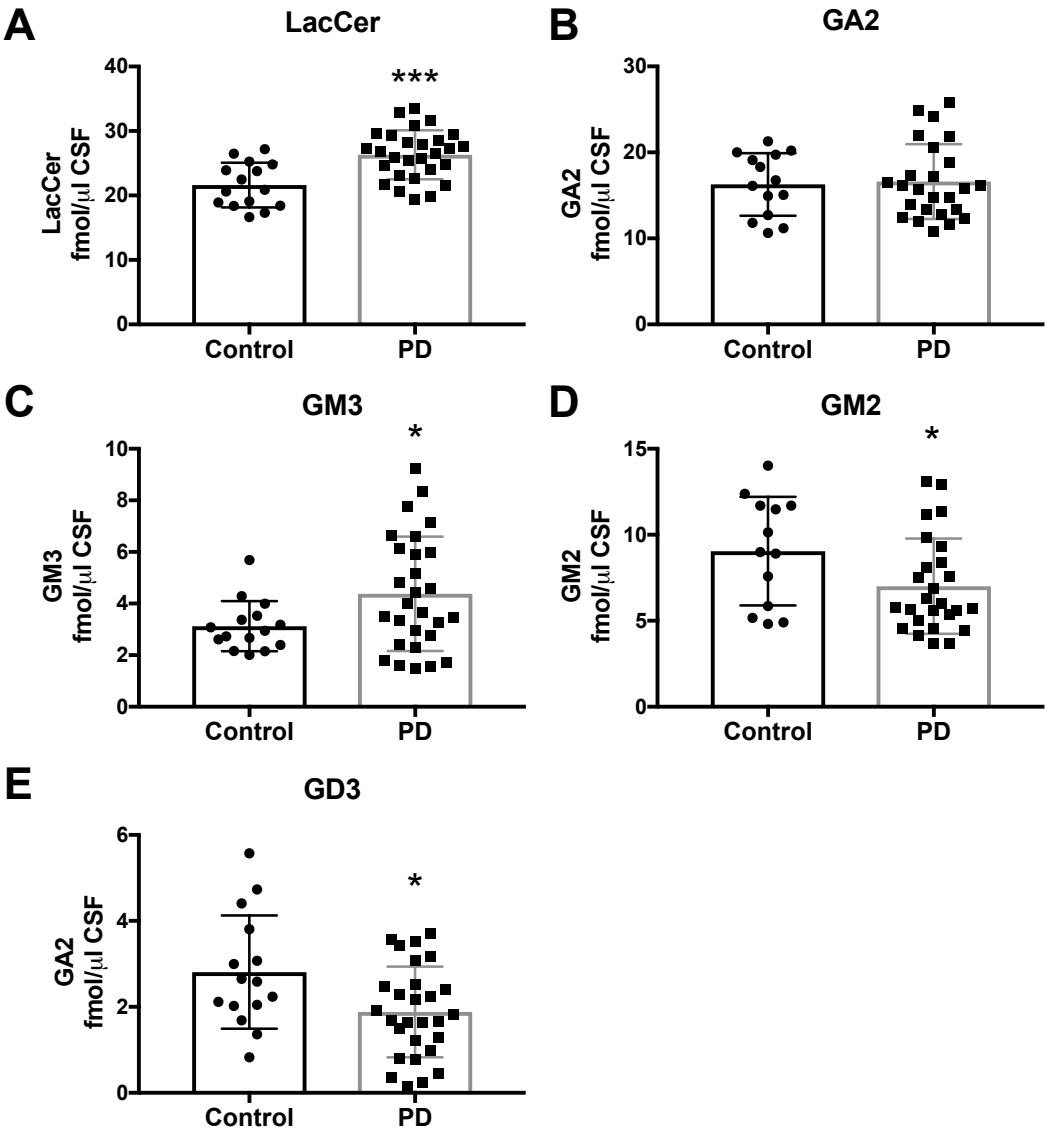

Figure 7.6: Significant increase in LacCer and GM3 levels, but significant decrease in GM2 and GD3 levels, in ante-mortem CSF of PD patients. Ante-mortem CSF from control subjects (n=15) and age-matched PD patients (n=28) was used to determine LacCer (A), GA2 (B), GM3 (C), GM2 (D), and GD3 (E) levels with NP-HPLC (* = p<0.05, *** = p<0.001, unpaired t-test). Data are presented as mean ± SD.

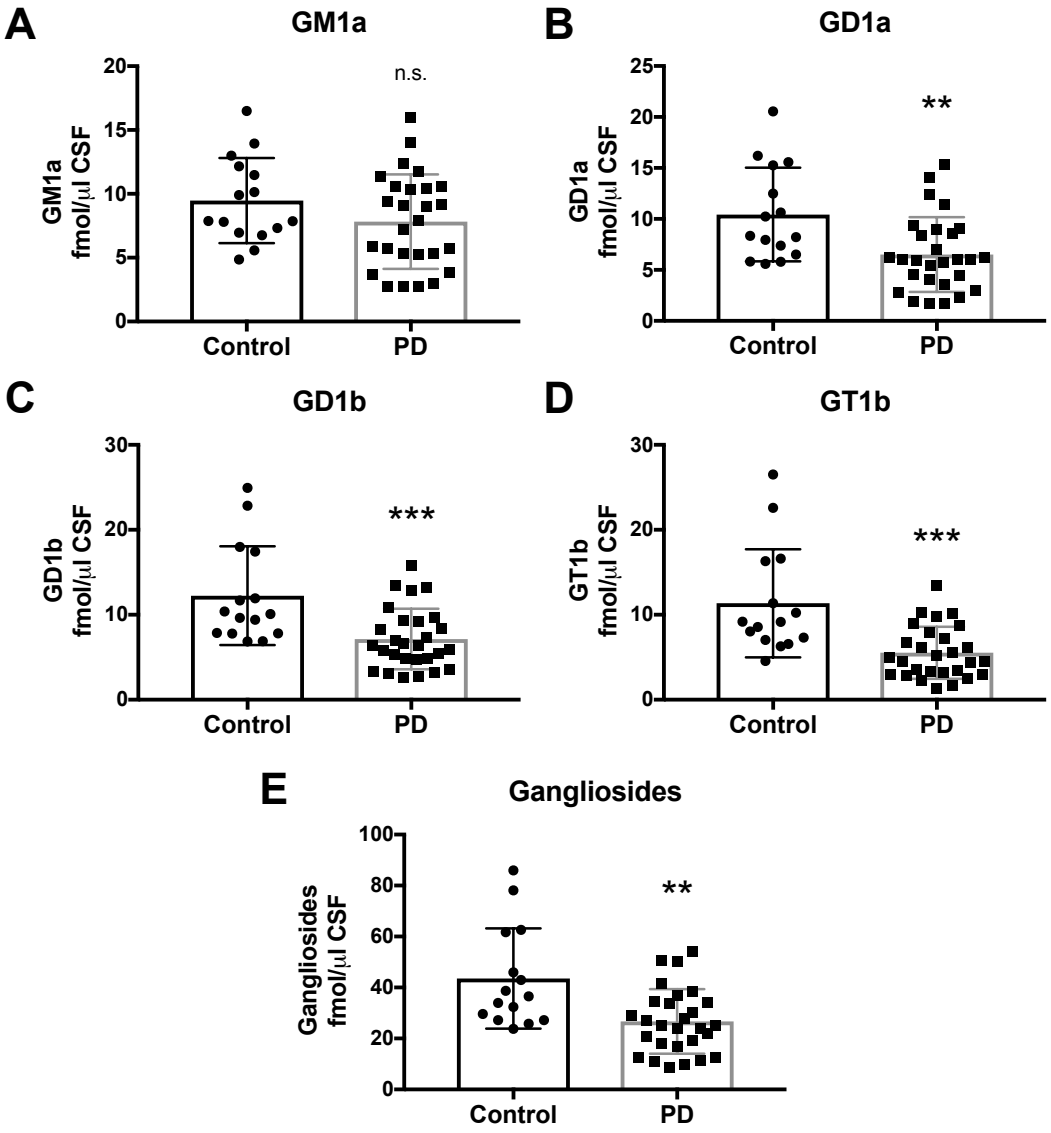

Figure 7.7: Significant reduction in ganglioside levels in ante-mortem CSF of PD patients. Ante-mortem CSF from control subjects (n=15) and age-matched PD patients (n=28) was used to determine GM1a (A), GD1a (B), GD1b (C), and GT1b (D) levels with NP-HPLC (** = p<0.01, *** = p<0.001, unpaired t-test). (E) Total ganglioside levels (sum of GM1a, GD1a, GD1b and GT1b) in ante-mortem CSF from control subjects and PD patients (** = p<0.01, unpaired t-test). Data are presented as mean ± SD.

7.3.3 GSL biomarkers in serum of PD patients and RBD patients

Next, we analysed GSLs in serum from control subjects and PD patients in the search for possible GSL biomarkers. For this, we received ante-mortem serum samples from control subjects (n=16, average age of 64 years) and age-matched PD subjects (n=30, average age of 66 years) from the OPDC (Oxford, UK). The pattern of GSLs in serum is unique: Serum features a major peak of the lipid GM3 (a precursor for a-series

gangliosides), with still prominent peaks of LacCer, Gb3 and Gb4 (globo-series), and low levels of GM2, GM1a, and GD1a (a-series).

First, we measured the levels of GlcCer and LacCer in serum samples from PD patients and control subjects. No differences in GlcCer and LacCer levels in serum of PD patients were detected in comparison to control subjects (**Figure 7.8A, B**). Next, we focused on downstream gangliosides Gb3 and Gb4 from the globo-series and GM3 and GM2 from the a-series, with GM3 being the highest expressed GSL. No changes in Gb3 or Gb4 levels were observed in serum of PD patients in comparison to control subjects (**Figure 7.8C, D**). Interestingly, no significant change in GM3 levels, but a trend towards a reduction in GM2 levels was found in ante-mortem serum of PD patients compared to controls (**Figure 7.8E, F**; GM3: p=0.1989, 8.3% reduction; GM2: p=0.0727, 15.3% decrease). Then, we analysed levels of more complex gangliosides of the a-series, GM1a, and GD1a. Levels of GM1a as well as GD1a were significantly reduced in serum from PD patients in comparison to serum from age-matched control subjects (**Figure 7.8G, H**; GM1a: p=0.0020, 22.6% reduction; GD1a: p=0.0006, 19.8% decrease).

In summary, no changes in GlcCer, LacCer or globo-series gangliosides were detected in ante-mortem serum of PD patients in comparison to control subjects, but significantly reduced levels of complex a-series gangliosides GM1a and GD1a were found. Concerning the reduction in gangliosides, these results reflect the results obtained with SN and putamen tissue (**Chapter 6**), as well as ante-mortem CSF of PD patients.

Additionally, for GSL analysis, we received serum samples from patients at risk of developing PD (prodromal PD phase), diagnosed with REM sleep behaviour disorder (RBD, n=30), from the OPDC. No difference in GlcCer levels, but a reduction in LacCer levels in serum of RBD patients was detected in comparison to serum from control subjects and PD patients (**Figure 7.9A, B**, p=0.0340, 14.8% reduction). Furthermore, a significant decrease in Gb3 and Gb4 levels (globo-series) was observed in serum of

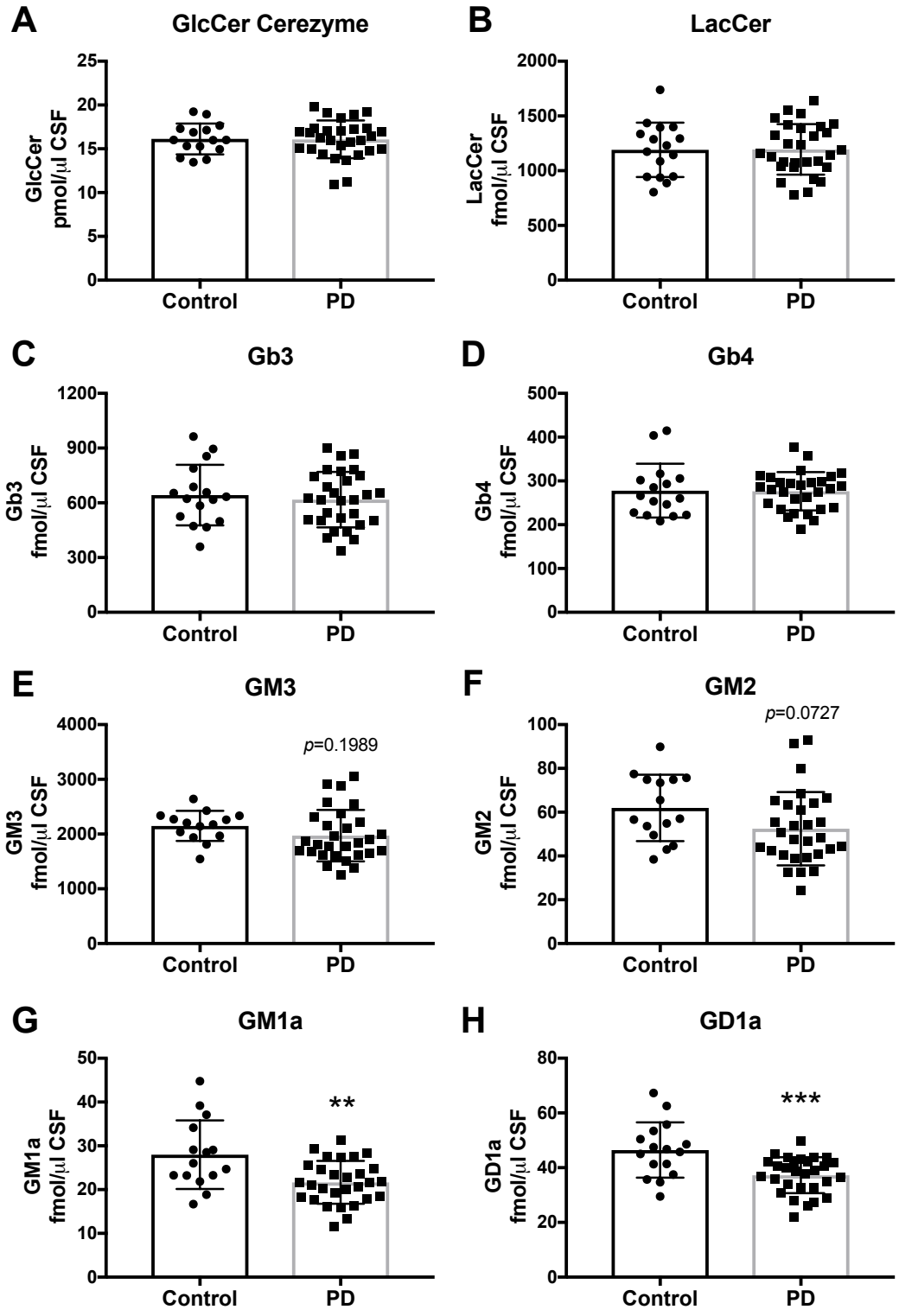

Figure 7.8: Significant reduction in GM1a and GD1a levels in serum from PD patients. Serum samples from control subjects (n=15) and age-matched PD patients (n=30) were used to determine GlcCer (A), LacCer (B), Gb3 (C), Gb4 (D), GM3 (E), GM2 (F), GM1a (G) and GD1a (H) levels with NP-HPLC (** = $p<0.01$, *** = $p<0.001$, unpaired t-test). Data are presented as mean ± SD.

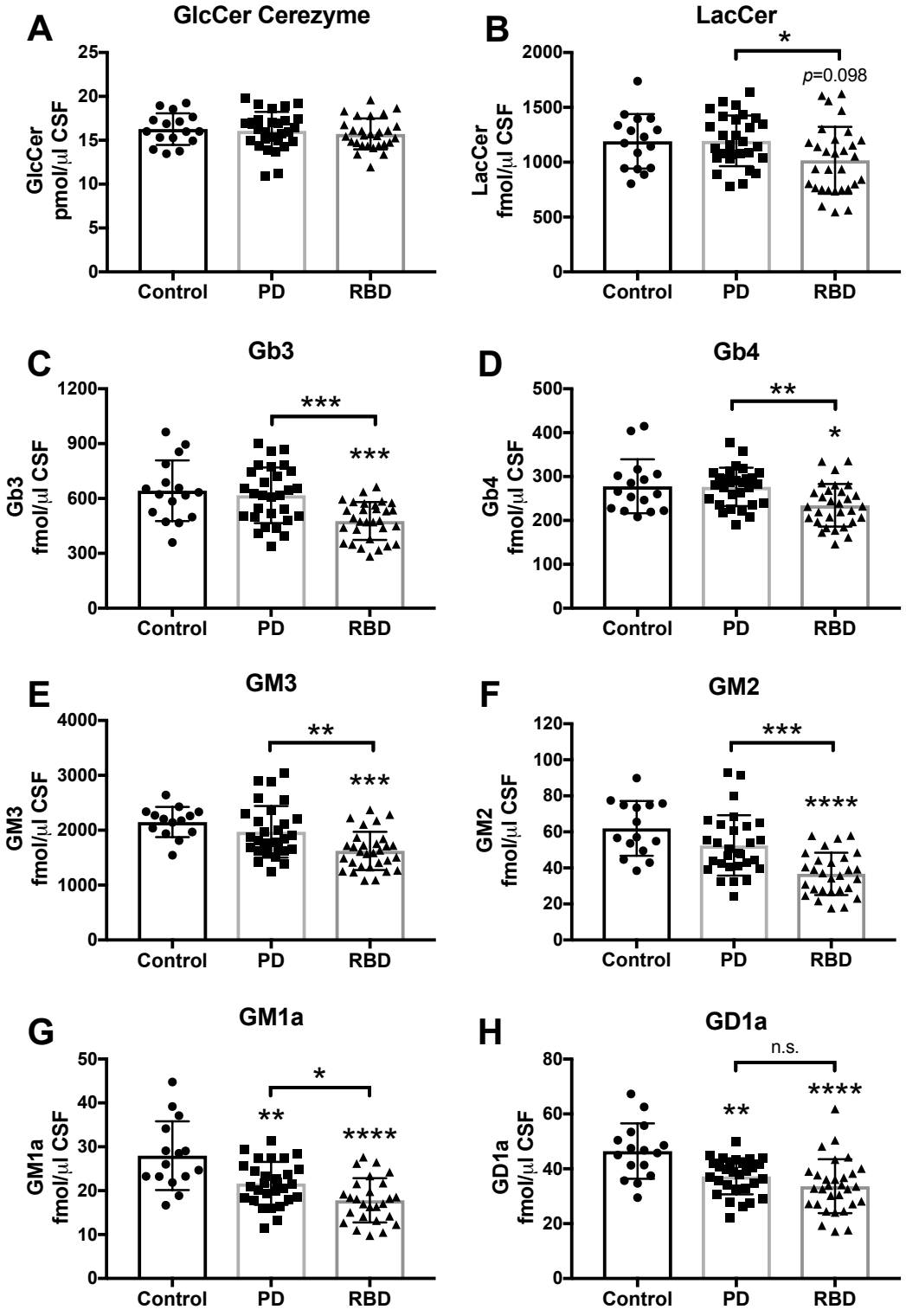

Figure 7.9: Significant reduction in all measured glycosphingolipids, except glucosylceramide, in serum from RBD patients. Levels of GlcCer (A), LacCer (B), Gb3 (C), Gb4 (D), GM3 (E), GM2 (F), GM1a (G) and GD1a (H) were determined in serum samples from control subjects (n=15), PD patients (n=30) and age-matched RBD patients (n=30) with NP-HPLC (* = p<0.05, ** = p<0.01, *** = p<0.001, **** = p<0.0001, one-way ANOVA). Data are presented as mean ± SD.

RBD patients in comparison to control subjects and PD patients (**Figure 7.9C, D**; Gb3: p=0.0007 and 25.8% decrease to controls, p=0.0006 and 22.8% decrease to PD; Gb4: p=0.0176 and 15.6% decrease to controls, p=0.0054 and 15.3% decrease to PD). Interestingly, a significant reduction in GM3 and GM2 levels was found in ante-mortem serum of RBD patients compared to serum samples from controls and PD patients (**Figure 7.9E, F**; GM3: p=0.0003 and 24.4% decrease to controls, p=0.0031 and 17.6% decrease to PD; GM2: p<0.0001 and 40.7% decrease to controls, p=0.0004 and 30.0% decrease to PD). Importantly, levels of GM1a as well as GD1a were significantly reduced in serum from RBD patients in comparison to serum from age-matched control subjects, but less so compared to PD patients (**Figure 7.9G, H**; GM1a: p<0.0001 and 36.4% decrease to controls, p=0.0377 and 17.8% decrease to PD; GD1a: p<0.0001 and 27.6% decrease to controls, p=0.2606 and 9.7% decrease to PD).

In summary, no changes in GlcCer levels were detected in ante-mortem serum from RBD patients compared to serum from control subjects or PD patients, but significantly reduced levels of LacCer, globo-series gangliosides, and all analysed a-series gangliosides were found in serum of RBD patients.

7.4 Discussion

There is an urgent need to find biomarkers for PD. Thus, in this chapter, we analysed levels of GSLs in serum and in post-mortem as well as in ante-mortem CSF from PD patients and age-matched control subjects in the search for possible lipid biomarkers. Several studies have been published showing altered activities of various lysosomal hydrolases in CSF from PD patients. For example, decreased GBA, β-hexosaminidase and β-galactosidase activities have been reported in CSF of PD-GBA patients, but also sporadic PD patients [147, 305, 429]. However, no studies have been published regarding GSLs in CSF of PD patients.

Here, we report similar levels of GlcCer, LacCer and more complex gangliosides GM1a, GD1a, GD1b or GT1b in post-mortem CSF from PD patients compared to CSF from age-matched control subjects (**Figures 7.3 and 7.4**). Nevertheless, we found significant changes in a-series gangliosides, namely decreased GM3 levels and increased GM2 levels, in CSF of PD patients compared to controls (**Figure 7.3**). However, on a cautionary note, the quality of the analysed CSF is crucial for the reliable determination of GSL levels, as e.g. contamination with blood will significantly alter GSL patterns. Thus, heavily blood-contaminated CSF was excluded prior to analysis, but it was not possible to exclude all CSF samples with a potential slight contamination (not clear-coloured). Furthermore, post-mortem intervals (the time taken for brain banks to collect CSF from the deceased patient) ranged from several hours up to a full day. As the CSF is in direct contact with the brain and has been shown to play a major role in the clearance of neuronal and axonal debris and waste [229-231], it is reasonable to assume that GSL levels may well be affected by increased post-mortem intervals. Additionally, it was reported that there are several factors, e.g. storage conditions and freeze-thaw cycles, that influence lysosomal enzyme activities, and thus most likely GSL levels, in human CSF [458]. All these pre-analytical factors need to be taken into consideration for conducting a reliable study. Not surprisingly, we observed many differences in the overall

GSL pattern and thus GSL levels between post-mortem and ante-mortem CSF from control subjects, e.g. increased GM3 and GD3 levels in post-mortem CSF. Thus, we suggest that reliable and meaningful measurements of GSL levels in CSF may only be possible in ante-mortem CSF samples.

The ante-mortem CSF samples provided by the OPDC were of superb quality (gin-clear colour) and well-controlled for accurate storage conditions and minimum number of freeze-thaw cycles. In this cohort, we found significant changes in levels of GlcCer, LacCer, and most gangliosides of the a-series (GM3, GM2, GM1a, GD1a) and b-series (GD3, GD1b, GT1b) in PD patients compared to age-matched controls (**Figures 7.5-7.7**). Importantly, an increase in GlcCer levels and a significant loss in levels of more complex gangliosides GM1a, GD1a, GD1b and GT1b were detected, in accord with our results obtained with substantia nigra or putamen tissue from PD patients (**Chapter 6**). Consequently, alterations in GlcCer or ganglioside levels in ante-mortem CSF might serve as biomarkers for PD.

Reports about GSLs in plasma or serum of PD patients have highlighted increases in ceramide, monohexosylceramides (GlcCer and GalCer) and LacCer levels in sporadic PD patients compared to controls [420]. Furthermore, it was reported that levels of GM3, the precursor of a-series and b-series gangliosides, were elevated in plasma from sporadic PD cases compared to control subjects [459]. Comparing sporadic PD patients with GBA-associated PD patients, it has been shown that serum of GBA-PD patients displayed higher levels of monohexosylceramides (GlcCer/GalCer), GlcSph and LacCer in polar lipid fractions [460].

Here, we report similar levels of GlcCer, LacCer and globo-series gangliosides Gb3 and Gb4 in serum from PD patients compared to age-matched control subjects (**Figures 7.8**). However, we found significant changes in a-series gangliosides, namely a trend for decreased GM3 and GM2 levels and significantly decreased GM1a and GD1a levels, in the serum of PD patients in comparison to serum from control subjects (**Figure 7.8**).

Some of our results are in contrast with published studies. Firstly, we did not see an increase in either GlcCer nor LacCer levels, as reported by Mielke and co-workers [420]. However, Mielke *et al.* only reported differences of around 5-7% in the levels of these GSLs [420]. Higher numbers of PD patients might be needed to detect such small changes. Furthermore, there are fundamental differences in the methodologies used (LC-MS versus NP-HPLC). For example, as shown in the method development, digestion of GlcCer from serum samples using Cerezyme might not be going to completion (**Figure 7.2**). However, a limitation of the LC-MS methods used in the published studies is the inability to distinguish GlcCer from GalCer species [420, 460]. Unfortunately, Guedes *et al.* only compared sporadic PD patient with PD-GBA patients, but not with control patients, thus not allowing a direct comparison with our results [460]. Finally, we did not observe significant changes in GM3 levels in serum of PD patients, although elevated GM3 levels in sporadic PD patients have been reported [459]. Interestingly, Chan *et al.* used plasma samples, which might have a slightly different GSL composition than serum [459]. Furthermore, no change in GM3 levels in serum from PD-GBA patients was reported [460]. In summary, further studies with higher patient numbers and refined methods are needed to confirm or reject previous results. Nevertheless, importantly, the observed significant loss in levels of more complex gangliosides, i.e. GM1a and GD1a, is in accordance with our results obtained with human substantia nigra and putamen (**Chapter 6**) as well as ante-mortem CSF from PD patients. As a result, reduced ganglioside levels in serum might prove to serve as biomarkers for PD in future studies.

Finally, GSL levels in serum from patients diagnosed with REM sleep behaviour disorder (RBD), who are at significant risk of developing PD, were analysed. We found no changes in GlcCer levels in the serum from RBD patients compared to serum from control subjects or PD patients (**Figure 7.9**). However, we report for the first time significantly reduced levels of LacCer, globo-series gangliosides Gb3 and Gb4, and the

a-series gangliosides (GM3, GM2, GM1a, and GD1a) in the serum of RBD patients (**Figure 7.9**). No published reports of GSL levels in RBD patients were found. It is interesting that RBD patients have lower serum levels of the gangliosides GM1a and GD1a than PD patients. One hypothesis is that fundamental changes in GSL levels in RBD patients might be intrinsic to the disease itself and might predispose these patients to develop PD over time. Supporting this notion, single-nucleotide polymorphisms in the *SCARB2* gene, encoding the lysosomal integral membrane protein 2 (LIMP-2), an important receptor for trafficking GBA to the lysosome, were significantly associated with RBD [457]. Future studies should elucidate a possible role for GSLs in RBD.

In summary, reduced levels of gangliosides, e.g. GM1a and GD1a, in serum and CSF might be useful biomarkers for PD. However, it is important to note that GSL levels cannot be used alone for diagnostic purposes, but need to be combined with other markers to have diagnostic value. Nevertheless, they could be useful biomarkers for monitoring disease progression, patient stratification for clinical trials or determining the effect of therapies.

8 Conclusion and Future Directions

In conclusion, the work presented in this thesis supports the link between rare early-onset neurodegenerative diseases (LSDs) and more common late-onset neurodegenerative diseases (PD and ALS). Lysosomal dysfunction is a known shared feature of these neurodegenerative disorders, but we have also found evidence of glycosphingolipid (GSL) dysregulation in PD and in ALS.

GSLs in ALS

In this thesis, we provide evidence that GSL metabolism is altered during denervation, in an ALS mouse model, and in ALS patients (**Chapter 2**). Denervation in wildtype mice resulted in increased muscle glucosylceramide synthase (GCS) expression together with significant increases in levels of GlcCer and downstream GSLs (GM3 and GM2) [115]. We saw the same pattern of altered GSL expression and increased GCS expression in muscle of symptomatic SOD1(G86R) mice. Inhibition of GCS after denervation resulted in disturbed neuromuscular junctions and delayed motor function recovery [115]. This suggests that GCS and GSLs are part of a vital, physiological and protective, but late, response to neurodegeneration.

We further show that pharmacological modulation of GSL levels, especially GlcCer and downstream ganglioside GM1a, could be a therapeutic approach for ALS, as we report for the first time a beneficial effect of a GCase inhibitor in an ALS mouse model [211]. Partial inhibition of GCase activity in early-symptomatic SOD1(G86R) mice with CBE resulted in increased levels of GlcCer and more complex GSLs, and subsequently preserved neuromuscular junction integrity and motor functions (**Chapter 2**). Interestingly, CBE treatment *in vitro* had major effects on neuronal GSLs (GM1a, GD1a), but to a lesser extent on predominantly muscular GSLs (GM3), suggesting the positive effect of CBE may be the consequence of action at the neuronal level. Accordingly, the increase in GM1a observed in spinal cord of symptomatic SOD1 mice may serve to

counteract pathological processes. Complex gangliosides, like the neurotrophic GM1a, reside in lipid rafts, which are key for the stability of cell-cell interactions in neuromuscular junctions and are important for the clustering of signalling receptors e.g. the acetylcholine receptor [238-240]. Importantly, we show that altered ganglioside expression is also evident in CSF of ALS patients and correlates with disease severity.

In future studies, once clear targets are identified, GSL-modifying compounds could be suitable therapeutic candidates for ALS patients. Loss of GM1a has been reported in PD and subcutaneous administration of purified GM1a stabilised disease progression and reduced motor symptoms in PD patients [156, 248, 249]. Thus, administration of GM1a may also be a treatment option for ALS.

Human PD fibroblasts

Here, we focused for the first time on lysosomal phenotypes in sporadic PD fibroblasts. We observed that a subset of sporadic PD fibroblasts phenocopied several characteristics of lysosomal dysfunction associated with GBA mutations (**Chapter 3**). Our major finding was that these sporadic PD fibroblasts phenocopied PD-GBA patient-derived cells in their GBA activity and showed an approximately 50% reduction in GBA activity compared to controls. Thus, focussing on GBA enzyme activity, a sub-classification of sporadic PD patients was possible, underling common mechanisms in sporadic PD cases, but also demonstrating the heterogeneity of sporadic PD patients. These data may have potential implications as biomarkers for recruiting patients for clinical trials, as not all sporadic PD cases may respond the same way to novel treatments aiming at improving GBA activity (e.g. ambroxol). In conclusion, fibroblasts are useful tools to investigate cellular biochemical changes associated with PD that might predispose to neurodegeneration. However, keeping their non-neuronal nature in mind, differences in expression of lysosomal enzymes and thus GSL metabolism as well

as the missing expression of dopamine might highlight that iPSC-derived dopaminergic neurons have several advantages.

For future experiments, it is key to investigate lysosomal, ER and global cytosolic calcium levels in our fibroblast cohort, as calcium dysregulation has been strongly implicated in PD, with dopaminergic neurons being especially vulnerable to alterations in calcium homeostasis [147, 267, 290-295]. Furthermore, having discovered several characteristics of lysosomal dysfunction in sporadic PD fibroblasts, it would be interesting to perform whole genome sequencing of these fibroblast lines, with a focus on all lysosomal genes, as a significantly increased burden of LSD gene variants was found in association with increased risk for PD [180].

GSLs and lysosomal hydrolases in ageing and PD

Ageing is the major non-genetic risk factor for adult-onset neurodegenerative diseases such as PD. We show that levels of GSLs and activities of lysosomal hydrolases, relevant to PD, are altered in the ageing brain of wildtype mice of three different strains (**Chapter 4**). For example, GBA and GBA2 activities are reduced, while their GSL substrates GlcCer and GlcSph progressively accumulate with age. Importantly, confirming previously published reports, we also found reduced GBA activity in post-mortem human substantia nigra with ageing and to a greater extent in PD (**Chapter 6**). One major caveat of the published studies is that they do not distinguish lysosomal and non-lysosomal forms of glucocerebrosidase. In the present thesis, we carefully distinguished lysosomal GBA from non-lysosomal GBA2 activities using the inhibitor *N*B-DGJ and specific assay buffers for each enzyme. Importantly, we show for the first time that non-lysosomal GBA2 activity also gradually declines with age and is further significantly reduced in substantia nigra and putamen in sporadic PD and thus may play a role in PD, as does GBA. It had remained unclear whether GlcCer or GlcSph levels are elevated in PD, as a consequence of the observed reduction in GBA (and GBA2)

activity. Here, using sensitive and quantitative NP-HPLC analysis, we report a significant increase in GlcCer levels in the substantia nigra of two independent cohorts of PD patients compared to age-matched controls, as well as a significant correlation between age and GlcCer levels in the substantia nigra of PD patients (**Chapter 6**). On a cautionary note, we also obtained results showing no significant changes in GlcCer levels in a third cohort of substantia nigra. Besides the general difficulties in obtaining human brain tissue for research, post-mortem delay will affect the quality of tissues and if sampling is not rigorously performed (e.g. not exactly the same brain region sampled) the interpretation of results can be difficult or even misleading [126].

In general, we hypothesize that the increased GSL load (GlcCer and GlcSph) associated with ageing of the brain accelerates degenerative processes in vulnerable neurons, such as midbrain dopaminergic neurons, and lowers the threshold for developing PD (**Figure 8.1**). Critically, this hypothesis challenges the prevailing view that proteinopathy is the primary cause of PD since lipid and lysosomal changes could precede or exacerbate the protein load and promote aggregation. Nevertheless, the elevations of GSLs found in brain during normal ageing or in PD are of course not associated with the same degree of storage and neuronal death observed in neuronopathic GD and other LSDs. Thus, I would not go as far and call PD a lysosomal storage disorder, as other researchers have recently been tempted to suggest [461].

We further show that changes in some complex brain GSLs appear to be conserved between mice and humans during ageing and resemble the changes observed in sporadic PD. However, there is one major difference between mouse and man. Levels of the ganglioside GM1a increase with age in the murine brain, whereas they decrease in the human substantia nigra and putamen (**Chapters 4 and 6**). Importantly, loss of gangliosides in human substantia nigra and putamen is even more prominent in sporadic PD patients (**Figure 8.1**). There are two important aspects of GM1a biology with regard to ageing and PD: Its function as an α-synuclein binding partner in the plasma membrane

and its role in neurotrophic signalling (as discussed in detail in **Chapter 6.4**). Our working hypothesis is that mice might have a compensatory, neuroprotective mechanism based on increasing neuraminidase activity allowing the remodelling of complex gangliosides to increase brain expression of the neurotrophic ganglioside GM1a with age (**Figure 4.17**), which is not effective or present in the human brain. This suggest the mouse is an inappropriate species to use to model PD for this fundamental biochemical reason. Interestingly, this is also the mechanism by which a mouse model of Tay-Sachs disease (β-hexosaminidase A deficiency, GM2 gangliosidosis) is able to escape the human disease (via degradation of GM2 to GA2 via murine neuraminidases) in contrast to the human population [435]. Supporting this hypothesis, in human substantia nigra from PD patients, we here observed a significant decrease in neuraminidase activity, which might be reflective of the observed decrease in GM1a levels. In summary, neuraminidases and GM1a could be interesting therapeutic targets for PD. Interestingly, subcutaneous administration of purified GM1a has already been in clinical trial for PD and stabilised disease progression and reduced motor symptoms in PD patients [248, 249].

Finally, it has begun to emerge that additional LSDs might also be associated with PD. Most importantly, a major study reported an excessive burden of mutant LSD gene variants in PD [180]. Accordingly, we found, in two independent cohorts of human post-mortem substantia nigra, that sporadic PD is associated with significant deficiencies in multiple lysosomal hydrolases (e.g. α-galactosidase and β-hexosaminidase), in addition to reduced GBA and GBA2 activities. Thus, enzyme replacement therapy might also be an option for other lysosomal enzymes, like β-hexosaminidase. In future studies, funded by the Michael J Fox Foundation, we will investigate β-hexosaminidase as a therapeutic target for PD, through AAV-mediated delivery of β-hexosaminidase in a PD-related rat model of α-synucleinopathy.

Taken together, the findings in this thesis demonstrate that not only diminished GBA activity may lower the threshold for developing PD, but reduced activities of other

lysosomal hydrolases, substrate accumulation, and reduced levels of gangliosides likely contribute to an increased risk of developing PD and related disorders with age.

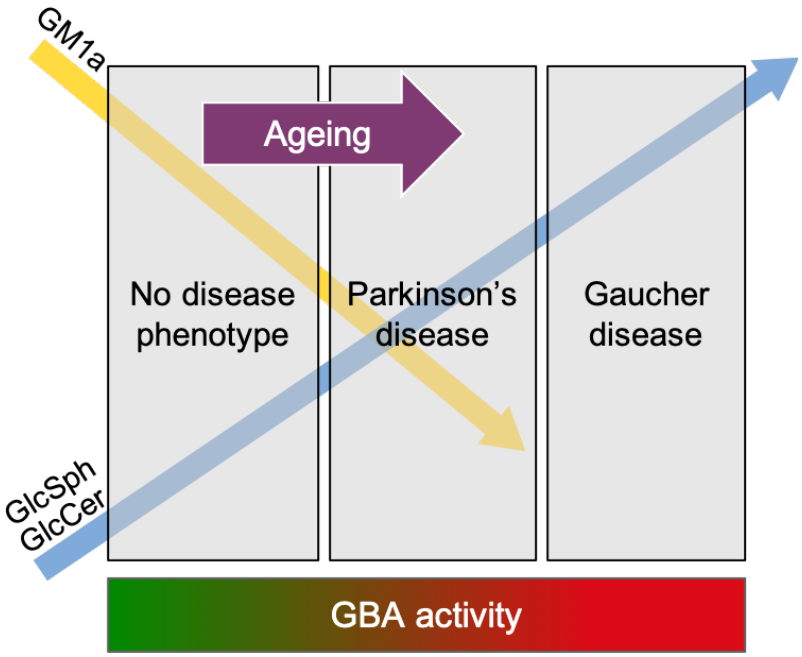

Figure 8.1: Do different levels of GBA activity or its substrates GlcCer/GlcSph cause different diseases in humans? Gaucher disease is caused by homozygous GBA mutations leading to major reductions in GBA enzyme activity and accumulation of its substrates GlcCer and GlcSph. In the case of sporadic PD patients (or GBA-heterozygote carrier PD patients), GBA activity is significantly reduced in the brain. GBA activity also gradually decreases in the brain during normal ageing to levels that mirror GBA haploinsufficiency. The reduction in GBA activity and subsequent accumulation of its substrates presumably contribute to an increased risk for PD in all humans with age. Furthermore, more complex GSLs, such as the neurotrophic ganglioside GM1a, gradually decrease in the brain during normal ageing and to a higher extent in PD patients, possibly also contributing to an increased risk for PD.

PD mouse models

In contrast, we did not observe obvious changes in brain GSL homeostasis and lysosomal hydrolase activities of three different PD mouse models, questioning their usefulness as models for PD (**Chapter 5**). However, brains of young α-synuclein overexpressing (ASO) mice as well as LRRK2(G2019S)KI mice showed increased neuraminidase activity. This points again to a possible compensatory mechanism in the mouse brain, which uses neuraminidases to maintain beneficial levels of the

neurotrophic ganglioside GM1a, needed for neuronal health. This possible mechanism was now observed in two independent PD mouse models as well as in murine brain ageing (**Chapter 4**), which further strengthens the need for more detailed studies into neuraminidases and GM1a in PD.

In conclusion, there are fundamental differences between mouse and man, which seem to undermine the utility of mice in PD research. It seems to be likely that mice have evolved protective mechanisms against α-synuclein aggregation, such as an enhanced ability to maintain α-synuclein in a stable lipid-bound state, and that these mechanisms may counteract efforts to initiate disease by transgenic α-synuclein expression [401]. Furthermore, as discussed in detail in **Chapter 5**, it was suggested that differences in calcium homeostasis and in basal dopamine levels may contribute to species-specific differences in vulnerability of human and mouse dopaminergic neurons [162]. In general, this emphasizes the value of studies with human neurons or human post-mortem tissues to identify pathways and targets for therapies in PD, rather than animal models.

Biomarkers for PD

In this thesis, we report reduced levels of gangliosides, e.g. GM1a and GD1a, in CSF and serum from PD patients, which might be useful as biomarkers for PD (**Chapter 7**). There is a general consensus that not one single biomarker will faithfully reflect the complex pathology of PD, but rather a combination of clinical, imaging and biochemical measures will be needed [452]. Consequently, GSL levels cannot be used alone for diagnostic purposes, but need to be combined with other markers to have diagnostic value. Nevertheless, they could be useful biomarkers for monitoring disease progression, patient stratification for clinical trials or determining the effect of therapies.

Furthermore, on a cautionary note, we have demonstrated that the quality of the analysed CSF is crucial for the reliable determination of GSL levels, as e.g. contamination with blood will significantly alter GSL patterns. Thus, we suggest that

reliable and meaningful measurements of GSL levels in CSF may only be possible in ante-mortem CSF samples.

Therapies for PD

Lastly, there are several ways in which activities of lysosomal enzymes and levels of GSLs could be modulated to exert beneficial effects in PD (**Chapters 1.3.1.2 and 1.3.3.1**). Importantly, already existing therapies for LSDs could be repurposed for potential application in PD and some are already in clinical trial. For example. pharmacological modulation of GBA activity with the small-molecule GBA chaperone ambroxol is currently in clinical trial for GBA-associated and sporadic PD (NCT02941822). Furthermore, substrate reduction therapy to reduce the lipid load is a putative therapeutic approach for PD and treatment with the brain-penetrant GCS inhibitor ibiglustat is currently in clinical trial for GBA-associated PD (NCT02906020). Importantly, in future studies, we will analyse levels of GSLs in CSF and serum from PD patients currently participating in the ambroxol clinical trial in London (NCT02941822) and will determine if ambroxol has the desired effects on GSL expression in these patients.

Bibliography

1. Platt, F.M., B. Boland, and A.C. van der Spoel, *The cell biology of disease: lysosomal storage disorders: the cellular impact of lysosomal dysfunction.* J Cell Biol, 2012. **199**(5): p. 723-34.
2. Ballabio, A., *The awesome lysosome.* EMBO Mol Med, 2016. **8**(2): p. 73-6.
3. Settembre, C., et al., *Signals from the lysosome: a control centre for cellular clearance and energy metabolism.* Nat Rev Mol Cell Biol, 2013. **14**(5): p. 283-96.
4. Saftig, P. and J. Klumperman, *Lysosome biogenesis and lysosomal membrane proteins: trafficking meets function.* Nat Rev Mol Cell Biol, 2009. **10**(9): p. 623-35.
5. Settembre, C. and A. Ballabio, *Lysosome: regulator of lipid degradation pathways.* Trends Cell Biol, 2014. **24**(12): p. 743-50.
6. Medina, D.L. and A. Ballabio, *Lysosomal calcium regulates autophagy.* Autophagy, 2015. **11**(6): p. 970-1.
7. Sardiello, M., et al., *A gene network regulating lysosomal biogenesis and function.* Science, 2009. **325**(5939): p. 473-7.
8. Platt, F.M., et al., *Lysosomal storage diseases.* Nat Rev Dis Primers, 2018. **4**(1): p. 27.
9. Martini-Stoica, H., et al., *The Autophagy-Lysosomal Pathway in Neurodegeneration: A TFEB Perspective.* Trends Neurosci, 2016. **39**(4): p. 221-234.
10. Saftig, P. and A. Haas, *Turn up the lysosome.* Nat Cell Biol, 2016. **18**(10): p. 1025-7.
11. Schwake, M., B. Schroder, and P. Saftig, *Lysosomal membrane proteins and their central role in physiology.* Traffic, 2013. **14**(7): p. 739-48.
12. Futerman, A.H. and G. van Meer, *The cell biology of lysosomal storage disorders.* Nat Rev Mol Cell Biol, 2004. **5**(7): p. 554-65.
13. Braulke, T. and J.S. Bonifacino, *Sorting of lysosomal proteins.* Biochim Biophys Acta, 2009. **1793**(4): p. 605-14.
14. Dittmer, F., et al., *Alternative mechanisms for trafficking of lysosomal enzymes in mannose 6-phosphate receptor-deficient mice are cell type-specific.* J Cell Sci, 1999. **112 (Pt 10)**: p. 1591-7.
15. Gonzalez, A., et al., *Lysosomal integral membrane protein-2: a new player in lysosome-related pathology.* Mol Genet Metab, 2014. **111**(2): p. 84-91.
16. Appelqvist, H., et al., *The lysosome: from waste bag to potential therapeutic target.* J Mol Cell Biol, 2013. **5**(4): p. 214-26.

17. Sano, R., et al., *GM1-ganglioside accumulation at the mitochondria-associated ER membranes links ER stress to Ca(2+)-dependent mitochondrial apoptosis.* Mol Cell, 2009. **36**(3): p. 500-11.
18. Butters, T.D., R.A. Dwek, and F.M. Platt, *Inhibition of glycosphingolipid biosynthesis: application to lysosomal storage disorders.* Chem Rev, 2000. **100**(12): p. 4683-96.
19. Sandhoff, K. and T. Kolter, *Biosynthesis and degradation of mammalian glycosphingolipids.* Philos Trans R Soc Lond B Biol Sci, 2003. **358**(1433): p. 847-61.
20. Wennekes, T., et al., *Glycosphingolipids--nature, function, and pharmacological modulation.* Angew Chem Int Ed Engl, 2009. **48**(47): p. 8848-69.
21. Larsson, E.A., et al., *Synthesis of reference standards to enable single cell metabolomic studies of tetramethylrhodamine-labeled ganglioside GM1.* Carbohydr Res, 2007. **342**(3-4): p. 482-9.
22. D'Angelo, G., et al., *Glycosphingolipids: synthesis and functions.* FEBS J, 2013. **280**(24): p. 6338-53.
23. Sandhoff, R. and K. Sandhoff, *Emerging concepts of ganglioside metabolism.* FEBS Lett, 2018. **592**(23): p. 3835-3864.
24. Hannun, Y.A. and L.M. Obeid, *Sphingolipids and their metabolism in physiology and disease.* Nat Rev Mol Cell Biol, 2018. **19**(3): p. 175-191.
25. Walden, C.M., et al., *Accumulation of glucosylceramide in murine testis, caused by inhibition of beta-glucosidase 2: implications for spermatogenesis.* J Biol Chem, 2007. **282**(45): p. 32655-64.
26. D'Angelo, G., et al., *Glycosphingolipid synthesis requires FAPP2 transfer of glucosylceramide.* Nature, 2007. **449**(7158): p. 62-7.
27. Aureli, M., et al., *The glycosphingolipid hydrolases in the central nervous system.* Mol Neurobiol, 2014. **50**(1): p. 76-87.
28. Aureli, M., et al., *Remodeling of sphingolipids by plasma membrane associated enzymes.* Neurochem Res, 2011. **36**(9): p. 1636-44.
29. Yamashita, T., et al., *A vital role for glycosphingolipid synthesis during development and differentiation.* Proc Natl Acad Sci U S A, 1999. **96**(16): p. 9142-7.
30. Schnaar, R.L. and T. Kinoshita, *Glycosphingolipids*, in *Essentials of Glycobiology*, rd, et al., Editors. 2015: Cold Spring Harbor (NY). p. 125-135.

31. Paget, C., et al., *Activation of invariant NKT cells by toll-like receptor 9-stimulated dendritic cells requires type I interferon and charged glycosphingolipids.* Immunity, 2007. **27**(4): p. 597-609.
32. Jennemann, R., et al., *Cell-specific deletion of glucosylceramide synthase in brain leads to severe neural defects after birth.* Proc Natl Acad Sci U S A, 2005. **102**(35): p. 12459-64.
33. Ramkumar, S., et al., *Induction of HIV-1 resistance: cell susceptibility to infection is an inverse function of globotriaosyl ceramide levels.* Glycobiology, 2009. **19**(1): p. 76-82.
34. Modrak, D.E., D.V. Gold, and D.M. Goldenberg, *Sphingolipid targets in cancer therapy.* Mol Cancer Ther, 2006. **5**(2): p. 200-8.
35. Zhang, T., et al., *The Role of Glycosphingolipids in Immune Cell Functions.* Front Immunol, 2019. **10**: p. 90.
36. Aerts, J.M., et al., *Glycosphingolipids and insulin resistance.* Adv Exp Med Biol, 2011. **721**: p. 99-119.
37. Dielschneider, R.F., E.S. Henson, and S.B. Gibson, *Lysosomes as Oxidative Targets for Cancer Therapy.* Oxid Med Cell Longev, 2017. **2017**: p. 3749157.
38. Platt, F.M., *Emptying the stores: lysosomal diseases and therapeutic strategies.* Nat Rev Drug Discov, 2018. **17**(2): p. 133-150.
39. Harlalka, G.V., et al., *Mutations in B4GALNT1 (GM2 synthase) underlie a new disorder of ganglioside biosynthesis.* Brain, 2013. **136**(Pt 12): p. 3618-24.
40. Yu, R.K., et al., *Structures, biosynthesis, and functions of gangliosides--an overview.* J Oleo Sci, 2011. **60**(10): p. 537-44.
41. Schnaar, R.L., *Gangliosides of the Vertebrate Nervous System.* J Mol Biol, 2016. **428**(16): p. 3325-3336.
42. Schengrund, C.L., *Gangliosides: glycosphingolipids essential for normal neural development and function.* Trends Biochem Sci, 2015. **40**(7): p. 397-406.
43. Ledeen, R.W. and G. Wu, *The multi-tasked life of GM1 ganglioside, a true factotum of nature.* Trends Biochem Sci, 2015. **40**(7): p. 407-18.
44. Elleder, M., *Glucosylceramide transfer from lysosomes--the missing link in molecular pathology of glucosylceramidase deficiency: a hypothesis based on existing data.* J Inherit Metab Dis, 2006. **29**(6): p. 707-15.
45. Ferraz, M.J., et al., *Lysosomal glycosphingolipid catabolism by acid ceramidase: formation of glycosphingoid bases during deficiency of glycosidases.* FEBS Lett, 2016. **590**(6): p. 716-25.

46. Hein, L.K., et al., *Secondary sphingolipid accumulation in a macrophage model of Gaucher disease.* Mol Genet Metab, 2007. **92**(4): p. 336-45.
47. Körschen, H.G., et al., *The non-lysosomal beta-glucosidase GBA2 is a non-integral membrane-associated protein at the endoplasmic reticulum (ER) and Golgi.* J Biol Chem, 2013. **288**(5): p. 3381-93.
48. Boot, R.G., et al., *Identification of the non-lysosomal glucosylceramidase as beta-glucosidase 2.* J Biol Chem, 2007. **282**(2): p. 1305-12.
49. Yildiz, Y., et al., *Mutation of beta-glucosidase 2 causes glycolipid storage disease and impaired male fertility.* J Clin Invest, 2006. **116**(11): p. 2985-94.
50. Sultana, S., et al., *Lack of enzyme activity in GBA2 mutants associated with hereditary spastic paraplegia/cerebellar ataxia (SPG46).* Biochem Biophys Res Commun, 2015. **465**(1): p. 35-40.
51. Hers, H.G., *Inborn Lysosomal Diseases.* Gastroenterology, 1965. **48**: p. 625-33.
52. Fuller, M., P.J. Meikle, and J.J. Hopwood, *Epidemiology of lysosomal storage diseases: an overview*, in *Fabry Disease: Perspectives from 5 Years of FOS*, A. Mehta, M. Beck, and G. Sunder-Plassmann, Editors. 2006: Oxford.
53. Meikle, P.J., et al., *Prevalence of lysosomal storage disorders.* JAMA, 1999. **281**(3): p. 249-54.
54. Vitner, E.B., F.M. Platt, and A.H. Futerman, *Common and uncommon pathogenic cascades in lysosomal storage diseases.* J Biol Chem, 2010. **285**(27): p. 20423-7.
55. Wraith, J.E., *The clinical presentation of lysosomal storage disorders.* Acta Neurol Taiwan, 2004. **13**(3): p. 101-6.
56. Verity, C.M., et al., *The clinical presentation of mitochondrial diseases in children with progressive intellectual and neurological deterioration: a national, prospective, population-based study.* Dev Med Child Neurol, 2010. **52**(5): p. 434-40.
57. Butters, T.D., R.A. Dwek, and F.M. Platt, *Imino sugar inhibitors for treating the lysosomal glycosphingolipidoses.* Glycobiology, 2005. **15**(10): p. 43R-52R.
58. Aerts, J.M., et al., *Biochemistry of glycosphingolipid storage disorders: implications for therapeutic intervention.* Philos Trans R Soc Lond B Biol Sci, 2003. **358**(1433): p. 905-14.
59. Marques, A.R. and P. Saftig, *Lysosomal storage disorders - challenges, concepts and avenues for therapy: beyond rare diseases.* J Cell Sci, 2019. **132**(2).
60. Vitner, E.B. and A.H. Futerman, *Neuronal forms of Gaucher disease.* Handb Exp Pharmacol, 2013(216): p. 405-19.
61. Platt, F.M., et al., *N-butyldeoxynojirimycin is a novel inhibitor of glycolipid biosynthesis.* J Biol Chem, 1994. **269**(11): p. 8362-5.

62. Lloyd-Evans, E., et al., *Glucosylceramide and glucosylsphingosine modulate calcium mobilization from brain microsomes via different mechanisms.* J Biol Chem, 2003. **278**(26): p. 23594-9.
63. Korkotian, E., et al., *Elevation of intracellular glucosylceramide levels results in an increase in endoplasmic reticulum density and in functional calcium stores in cultured neurons.* J Biol Chem, 1999. **274**(31): p. 21673-8.
64. Wong, K., et al., *Neuropathology provides clues to the pathophysiology of Gaucher disease.* Mol Genet Metab, 2004. **82**(3): p. 192-207.
65. Cox, T., et al., *Novel oral treatment of Gaucher's disease with N-butyldeoxynojirimycin (OGT 918) to decrease substrate biosynthesis.* Lancet, 2000. **355**(9214): p. 1481-5.
66. Platt, F.M. and M. Jeyakumar, *Substrate reduction therapy.* Acta Paediatr Suppl, 2008. **97**(457): p. 88-93.
67. Platt, F.M. and R.H. Lachmann, *Treating lysosomal storage disorders: current practice and future prospects.* Biochim Biophys Acta, 2009. **1793**(4): p. 737-45.
68. Van Patten, S.M., et al., *Effect of mannose chain length on targeting of glucocerebrosidase for enzyme replacement therapy of Gaucher disease.* Glycobiology, 2007. **17**(5): p. 467-78.
69. Mistry, P.K., E.P. Wraight, and T.M. Cox, *Therapeutic delivery of proteins to macrophages: implications for treatment of Gaucher's disease.* Lancet, 1996. **348**(9041): p. 1555-9.
70. Zimran, A., *How I treat Gaucher disease.* Blood, 2011. **118**(6): p. 1463-71.
71. Raas-Rothschild, A., et al., *Glycosphingolipidoses: beyond the enzymatic defect.* Glycoconj J, 2004. **21**(6): p. 295-304.
72. Sands, M.S. and B.L. Davidson, *Gene therapy for lysosomal storage diseases.* Mol Ther, 2006. **13**(5): p. 839-49.
73. Lachmann, R.H. and F.M. Platt, *Substrate reduction therapy for glycosphingolipid storage disorders.* Expert Opin Investig Drugs, 2001. **10**(3): p. 455-66.
74. Aerts, J.M., et al., *Substrate reduction therapy of glycosphingolipid storage disorders.* J Inherit Metab Dis, 2006. **29**(2-3): p. 449-56.
75. Shayman, J.A., *ELIGLUSTAT TARTRATE: Glucosylceramide Synthase Inhibitor Treatment of Type 1 Gaucher Disease.* Drugs Future, 2010. **35**(8): p. 613-620.
76. Belmatoug, N., et al., *Management and monitoring recommendations for the use of eliglustat in adults with type 1 Gaucher disease in Europe.* Eur J Intern Med, 2017. **37**: p. 25-32.

77. Patterson, M.C., et al., *Miglustat for treatment of Niemann-Pick C disease: a randomised controlled study.* Lancet Neurol, 2007. **6**(9): p. 765-72.
78. Lyseng-Williamson, K.A., *Miglustat: a review of its use in Niemann-Pick disease type C.* Drugs, 2014. **74**(1): p. 61-74.
79. Marques, A.R., et al., *Reducing GBA2 Activity Ameliorates Neuropathology in Niemann-Pick Type C Mice.* PLoS One, 2015. **10**(8): p. e0135889.
80. Mistry, P.K., et al., *Glucocerebrosidase 2 gene deletion rescues type 1 Gaucher disease.* Proc Natl Acad Sci U S A, 2014. **111**(13): p. 4934-9.
81. Lachmann, R.H., et al., *Treatment with miglustat reverses the lipid-trafficking defect in Niemann-Pick disease type C.* Neurobiol Dis, 2004. **16**(3): p. 654-8.
82. Parenti, G., *Treating lysosomal storage diseases with pharmacological chaperones: from concept to clinics.* EMBO Mol Med, 2009. **1**(5): p. 268-79.
83. Benito, J.M., J.M. Garcia Fernandez, and C. Ortiz Mellet, *Pharmacological chaperone therapy for Gaucher disease: a patent review.* Expert Opin Ther Pat, 2011. **21**(6): p. 885-903.
84. Hughes, D.A., et al., *Oral pharmacological chaperone migalastat compared with enzyme replacement therapy in Fabry disease: 18-month results from the randomised phase III ATTRACT study.* J Med Genet, 2017. **54**(4): p. 288-296.
85. Aflaki, E., et al., *A New Glucocerebrosidase Chaperone Reduces alpha-Synuclein and Glycolipid Levels in iPSC-Derived Dopaminergic Neurons from Patients with Gaucher Disease and Parkinsonism.* J Neurosci, 2016. **36**(28): p. 7441-52.
86. Hardiman, O., et al., *Amyotrophic lateral sclerosis.* Nat Rev Dis Primers, 2017. **3**: p. 17071.
87. van Es, M.A., et al., *Amyotrophic lateral sclerosis.* Lancet, 2017. **390**(10107): p. 2084-2098.
88. Niccoli, T., L. Partridge, and A.M. Isaacs, *Ageing as a risk factor for ALS/FTD.* Hum Mol Genet, 2017. **26**(R2): p. R105-R113.
89. Alonso, A., et al., *Incidence and lifetime risk of motor neuron disease in the United Kingdom: a population-based study.* Eur J Neurol, 2009. **16**(6): p. 745-51.
90. Logroscino, G., et al., *Incidence of amyotrophic lateral sclerosis in Europe.* J Neurol Neurosurg Psychiatry, 2010. **81**(4): p. 385-90.
91. Al-Chalabi, A., et al., *Analysis of amyotrophic lateral sclerosis as a multistep process: a population-based modelling study.* Lancet Neurol, 2014. **13**(11): p. 1108-1113.
92. Kiernan, M.C., et al., *Amyotrophic lateral sclerosis.* Lancet, 2011. **377**(9769): p. 942-55.

93. Dion, P.A., H. Daoud, and G.A. Rouleau, *Genetics of motor neuron disorders: new insights into pathogenic mechanisms.* Nat Rev Genet, 2009. **10**(11): p. 769-82.
94. Rosen, D.R., et al., *Mutations in Cu/Zn superoxide dismutase gene are associated with familial amyotrophic lateral sclerosis.* Nature, 1993. **362**(6415): p. 59-62.
95. Neumann, M., et al., *Ubiquitinated TDP-43 in frontotemporal lobar degeneration and amyotrophic lateral sclerosis.* Science, 2006. **314**(5796): p. 130-3.
96. Kwiatkowski, T.J., Jr., et al., *Mutations in the FUS/TLS gene on chromosome 16 cause familial amyotrophic lateral sclerosis.* Science, 2009. **323**(5918): p. 1205-8.
97. Laaksovirta, H., et al., *Chromosome 9p21 in amyotrophic lateral sclerosis in Finland: a genome-wide association study.* Lancet Neurol, 2010. **9**(10): p. 978-85.
98. Shatunov, A., et al., *Chromosome 9p21 in sporadic amyotrophic lateral sclerosis in the UK and seven other countries: a genome-wide association study.* Lancet Neurol, 2010. **9**(10): p. 986-94.
99. Smith, E.F., P.J. Shaw, and K.J. De Vos, *The role of mitochondria in amyotrophic lateral sclerosis.* Neurosci Lett, 2017.
100. Taylor, J.P., R.H. Brown, Jr., and D.W. Cleveland, *Decoding ALS: from genes to mechanism.* Nature, 2016. **539**(7628): p. 197-206.
101. Cristofani, R., et al., *Inhibition of retrograde transport modulates misfolded protein accumulation and clearance in motoneuron diseases.* Autophagy, 2017. **13**(8): p. 1280-1303.
102. Li, L., X. Zhang, and W. Le, *Altered macroautophagy in the spinal cord of SOD1 mutant mice.* Autophagy, 2008. **4**(3): p. 290-3.
103. Sasaki, S., *Autophagy in spinal cord motor neurons in sporadic amyotrophic lateral sclerosis.* J Neuropathol Exp Neurol, 2011. **70**(5): p. 349-59.
104. Nixon, R.A., *The role of autophagy in neurodegenerative disease.* Nat Med, 2013. **19**(8): p. 983-97.
105. Wong, E. and A.M. Cuervo, *Autophagy gone awry in neurodegenerative diseases.* Nat Neurosci, 2010. **13**(7): p. 805-11.
106. Lee, J.K., et al., *Role of autophagy in the pathogenesis of amyotrophic lateral sclerosis.* Biochim Biophys Acta, 2015. **1852**(11): p. 2517-24.
107. Chen, S., et al., *Autophagy dysregulation in amyotrophic lateral sclerosis.* Brain Pathol, 2012. **22**(1): p. 110-6.
108. Baker, D.J., et al., *Lysosomal and phagocytic activity is increased in astrocytes during disease progression in the SOD1 (G93A) mouse model of amyotrophic lateral sclerosis.* Front Cell Neurosci, 2015. **9**: p. 410.

109. Xie, Y., et al., *Progressive endolysosomal deficits impair autophagic clearance beginning at early asymptomatic stages in fALS mice.* Autophagy, 2015. **11**(10): p. 1934-6.
110. Zhang, Y., et al., *The C9orf72-interacting protein Smcr8 is a negative regulator of autoimmunity and lysosomal exocytosis.* Genes Dev, 2018. **32**(13-14): p. 929-943.
111. Amick, J. and S.M. Ferguson, *C9orf72: At the intersection of lysosome cell biology and neurodegenerative disease.* Traffic, 2017. **18**(5): p. 267-276.
112. Xie, Y., et al., *Endolysosomal Deficits Augment Mitochondria Pathology in Spinal Motor Neurons of Asymptomatic fALS Mice.* Neuron, 2015. **87**(2): p. 355-70.
113. Dodge, J.C., *Lipid Involvement in Neurodegenerative Diseases of the Motor System: Insights from Lysosomal Storage Diseases.* Front Mol Neurosci, 2017. **10**: p. 356.
114. Dodge, J.C., et al., *Glycosphingolipids are modulators of disease pathogenesis in amyotrophic lateral sclerosis.* Proc Natl Acad Sci U S A, 2015. **112**(26): p. 8100-5.
115. Henriques, A., et al., *Amyotrophic lateral sclerosis and denervation alter sphingolipids and up-regulate glucosylceramide synthase.* Hum Mol Genet, 2015. **24**(25): p. 7390-405.
116. Kalia, L.V. and A.E. Lang, *Parkinson's disease.* Lancet, 2015. **386**(9996): p. 896-912.
117. Poewe, W., et al., *Parkinson disease.* Nat Rev Dis Primers, 2017. **3**: p. 17013.
118. Spillantini, M.G., et al., *Alpha-synuclein in Lewy bodies.* Nature, 1997. **388**(6645): p. 839-40.
119. Braak, H., et al., *Staging of brain pathology related to sporadic Parkinson's disease.* Neurobiol Aging, 2003. **24**(2): p. 197-211.
120. Cuervo, A.M., et al., *Impaired degradation of mutant alpha-synuclein by chaperone-mediated autophagy.* Science, 2004. **305**(5688): p. 1292-5.
121. Dehay, B., et al., *Lysosomal impairment in Parkinson's disease.* Mov Disord, 2013. **28**(6): p. 725-32.
122. Chu, Y., et al., *Alterations in lysosomal and proteasomal markers in Parkinson's disease: relationship to alpha-synuclein inclusions.* Neurobiol Dis, 2009. **35**(3): p. 385-98.
123. Alvarez-Erviti, L., et al., *Chaperone-mediated autophagy markers in Parkinson disease brains.* Arch Neurol, 2010. **67**(12): p. 1464-72.
124. Mattson, M.P. and T.V. Arumugam, *Hallmarks of Brain Aging: Adaptive and Pathological Modification by Metabolic States.* Cell Metab, 2018. **27**(6): p. 1176-1199.

125. Engelender, S. and O. Isacson, *The Threshold Theory for Parkinson's Disease.* Trends Neurosci, 2017. **40**(1): p. 4-14.
126. Toulorge, D., A.H. Schapira, and R. Hajj, *Molecular changes in the postmortem parkinsonian brain.* J Neurochem, 2016. **139 Suppl 1**: p. 27-58.
127. Sidransky, E., et al., *Multicenter analysis of glucocerebrosidase mutations in Parkinson's disease.* N Engl J Med, 2009. **361**(17): p. 1651-61.
128. Schapira, A.H. and E. Tolosa, *Molecular and clinical prodrome of Parkinson disease: implications for treatment.* Nat Rev Neurol, 2010. **6**(6): p. 309-17.
129. Schapira, A.H., K.R. Chaudhuri, and P. Jenner, *Non-motor features of Parkinson disease.* Nat Rev Neurosci, 2017. **18**(7): p. 435-450.
130. Bezard, E., et al., *Relationship between the appearance of symptoms and the level of nigrostriatal degeneration in a progressive 1-methyl-4-phenyl-1,2,3,6-tetrahydropyridine-lesioned macaque model of Parkinson's disease.* J Neurosci, 2001. **21**(17): p. 6853-61.
131. Brownell, A.L., et al., *Combined PET/MRS brain studies show dynamic and long-term physiological changes in a primate model of Parkinson disease.* Nat Med, 1998. **4**(11): p. 1308-12.
132. Neudorfer, O., et al., *Occurrence of Parkinson's syndrome in type I Gaucher disease.* QJM, 1996. **89**(9): p. 691-4.
133. Tayebi, N., et al., *Gaucher disease and parkinsonism: a phenotypic and genotypic characterization.* Mol Genet Metab, 2001. **73**(4): p. 313-21.
134. Tayebi, N., et al., *Gaucher disease with parkinsonian manifestations: does glucocerebrosidase deficiency contribute to a vulnerability to parkinsonism?* Mol Genet Metab, 2003. **79**(2): p. 104-9.
135. Bembi, B., et al., *Gaucher's disease with Parkinson's disease: clinical and pathological aspects.* Neurology, 2003. **61**(1): p. 99-101.
136. Lwin, A., et al., *Glucocerebrosidase mutations in subjects with parkinsonism.* Mol Genet Metab, 2004. **81**(1): p. 70-3.
137. Aharon-Peretz, J., H. Rosenbaum, and R. Gershoni-Baruch, *Mutations in the glucocerebrosidase gene and Parkinson's disease in Ashkenazi Jews.* N Engl J Med, 2004. **351**(19): p. 1972-7.
138. Goker-Alpan, O., et al., *Parkinsonism among Gaucher disease carriers.* J Med Genet, 2004. **41**(12): p. 937-40.
139. Anheim, M., et al., *Penetrance of Parkinson disease in glucocerebrosidase gene mutation carriers.* Neurology, 2012. **78**(6): p. 417-20.

140. Alcalay, R.N., et al., *Comparison of Parkinson risk in Ashkenazi Jewish patients with Gaucher disease and GBA heterozygotes.* JAMA Neurol, 2014. **71**(6): p. 752-7.
141. McNeill, A., et al., *A clinical and family history study of Parkinson's disease in heterozygous glucocerebrosidase mutation carriers.* J Neurol Neurosurg Psychiatry, 2012. **83**(8): p. 853-4.
142. Migdalska-Richards, A. and A.H. Schapira, *The relationship between glucocerebrosidase mutations and Parkinson disease.* J Neurochem, 2016. **139 Suppl 1**: p. 77-90.
143. Neumann, J., et al., *Glucocerebrosidase mutations in clinical and pathologically proven Parkinson's disease.* Brain, 2009. **132**(Pt 7): p. 1783-94.
144. Lesage, S., et al., *Large-scale screening of the Gaucher's disease-related glucocerebrosidase gene in Europeans with Parkinson's disease.* Hum Mol Genet, 2011. **20**(1): p. 202-10.
145. Manning-Bog, A.B., B. Schule, and J.W. Langston, *Alpha-synuclein-glucocerebrosidase interactions in pharmacological Gaucher models: a biological link between Gaucher disease and parkinsonism.* Neurotoxicology, 2009. **30**(6): p. 1127-32.
146. Yap, T.L., et al., *Alpha-synuclein interacts with Glucocerebrosidase providing a molecular link between Parkinson and Gaucher diseases.* J Biol Chem, 2011. **286**(32): p. 28080-8.
147. Schöndorf, D.C., et al., *iPSC-derived neurons from GBA1-associated Parkinson's disease patients show autophagic defects and impaired calcium homeostasis.* Nat Commun, 2014. **5**: p. 4028.
148. Mazzulli, J.R., et al., *Gaucher disease glucocerebrosidase and alpha-synuclein form a bidirectional pathogenic loop in synucleinopathies.* Cell, 2011. **146**(1): p. 37-52.
149. Cullen, V., et al., *Acid beta-glucosidase mutants linked to Gaucher disease, Parkinson disease, and Lewy body dementia alter alpha-synuclein processing.* Ann Neurol, 2011. **69**(6): p. 940-53.
150. Xu, Y.H., et al., *Accumulation and distribution of alpha-synuclein and ubiquitin in the CNS of Gaucher disease mouse models.* Mol Genet Metab, 2011. **102**(4): p. 436-47.
151. Osellame, L.D., et al., *Mitochondria and quality control defects in a mouse model of Gaucher disease--links to Parkinson's disease.* Cell Metab, 2013. **17**(6): p. 941-53.

152. Westbroek, W., A.M. Gustafson, and E. Sidransky, *Exploring the link between glucocerebrosidase mutations and parkinsonism.* Trends Mol Med, 2011. **17**(9): p. 485-93.
153. Taguchi, Y.V., et al., *Glucosylsphingosine promotes alpha-synuclein pathology in mutant GBA-associated Parkinson's disease.* J Neurosci, 2017.
154. Zunke, F., et al., *Reversible Conformational Conversion of alpha-Synuclein into Toxic Assemblies by Glucosylceramide.* Neuron, 2017.
155. Suzuki, M., et al., *Pathological role of lipid interaction with alpha-synuclein in Parkinson's disease.* Neurochem Int, 2018.
156. Wu, G., et al., *Deficiency of ganglioside GM1 correlates with Parkinson's disease in mice and humans.* J Neurosci Res, 2012. **90**(10): p. 1997-2008.
157. Hadaczek, P., et al., *GDNF signaling implemented by GM1 ganglioside; failure in Parkinson's disease and GM1-deficient murine model.* Exp Neurol, 2015. **263**: p. 177-89.
158. Seyfried, T.N., et al., *Sex-Related Abnormalities in Substantia Nigra Lipids in Parkinson's Disease.* ASN Neuro, 2018. **10**: p. 1759091418781889.
159. Martinez, Z., et al., *GM1 specifically interacts with alpha-synuclein and inhibits fibrillation.* Biochemistry, 2007. **46**(7): p. 1868-77.
160. Fantini, J. and N. Yahi, *Molecular basis for the glycosphingolipid-binding specificity of alpha-synuclein: key role of tyrosine 39 in membrane insertion.* J Mol Biol, 2011. **408**(4): p. 654-69.
161. Forsayeth, J. and P. Hadaczek, *Ganglioside Metabolism and Parkinson's Disease.* Front Neurosci, 2018. **12**: p. 45.
162. Burbulla, L.F., et al., *Dopamine oxidation mediates mitochondrial and lysosomal dysfunction in Parkinson's disease.* Science, 2017. **357**(6357): p. 1255-1261.
163. Gegg, M.E., et al., *Glucocerebrosidase deficiency in substantia nigra of parkinson disease brains.* Ann Neurol, 2012. **72**(3): p. 455-63.
164. Rocha, E.M., et al., *Progressive decline of glucocerebrosidase in aging and Parkinson's disease.* Ann Clin Transl Neurol, 2015. **2**(4): p. 433-8.
165. Murphy, K.E., et al., *Reduced glucocerebrosidase is associated with increased alpha-synuclein in sporadic Parkinson's disease.* Brain, 2014. **137**(Pt 3): p. 834-48.
166. Gegg, M.E., et al., *No evidence for substrate accumulation in Parkinson brains with GBA mutations.* Mov Disord, 2015. **30**(8): p. 1085-9.

167. Boutin, M., et al., *Tandem Mass Spectrometry Multiplex Analysis of Glucosylceramide and Galactosylceramide Isoforms in Brain Tissues at Different Stages of Parkinson Disease.* Anal Chem, 2016. **88**(3): p. 1856-63.
168. Sardi, S.P., et al., *CNS expression of glucocerebrosidase corrects alpha-synuclein pathology and memory in a mouse model of Gaucher-related synucleinopathy.* Proc Natl Acad Sci U S A, 2011. **108**(29): p. 12101-6.
169. Sardi, S.P., et al., *Augmenting CNS glucocerebrosidase activity as a therapeutic strategy for parkinsonism and other Gaucher-related synucleinopathies.* Proc Natl Acad Sci U S A, 2013. **110**(9): p. 3537-42.
170. Rocha, E.M., et al., *Glucocerebrosidase gene therapy prevents alpha-synucleinopathy of midbrain dopamine neurons.* Neurobiol Dis, 2015. **82**: p. 495-503.
171. Mazzulli, J.R., et al., *Activation of beta-Glucocerebrosidase Reduces Pathological alpha-Synuclein and Restores Lysosomal Function in Parkinson's Patient Midbrain Neurons.* J Neurosci, 2016. **36**(29): p. 7693-706.
172. Sanchez-Martinez, A., et al., *Parkinson disease-linked GBA mutation effects reversed by molecular chaperones in human cell and fly models.* Sci Rep, 2016. **6**: p. 31380.
173. Migdalska-Richards, A., et al., *Ambroxol effects in glucocerebrosidase and alpha-synuclein transgenic mice.* Ann Neurol, 2016. **80**(5): p. 766-775.
174. Migdalska-Richards, A., et al., *Oral ambroxol increases brain glucocerebrosidase activity in a nonhuman primate.* Synapse, 2017. **71**(7).
175. Sybertz, E. and D. Krainc, *Development of targeted therapies for Parkinson's disease and related synucleinopathies.* J Lipid Res, 2014. **55**(10): p. 1996-2003.
176. Sardi, S.P., et al., *Glucosylceramide synthase inhibition alleviates aberrations in synucleinopathy models.* Proc Natl Acad Sci U S A, 2017. **114**(10): p. 2699-2704.
177. Noelker, C., et al., *Glucocerebrosidase deficiency and mitochondrial impairment in experimental Parkinson disease.* J Neurol Sci, 2015. **356**(1-2): p. 129-36.
178. Shachar, T., et al., *Lysosomal storage disorders and Parkinson's disease: Gaucher disease and beyond.* Mov Disord, 2011. **26**(9): p. 1593-604.
179. Kluenemann, H.H., et al., *Parkinsonism syndrome in heterozygotes for Niemann-Pick C1.* J Neurol Sci, 2013. **335**(1-2): p. 219-20.
180. Robak, L.A., et al., *Excessive burden of lysosomal storage disorder gene variants in Parkinson's disease.* Brain, 2017. **140**(12): p. 3191-3203.
181. Boland, B. and F.M. Platt, *Bridging the age spectrum of neurodegenerative storage diseases.* Best Pract Res Clin Endocrinol Metab, 2015. **29**(2): p. 127-43.

182. Neefjes, J. and R. van der Kant, *Stuck in traffic: an emerging theme in diseases of the nervous system.* Trends Neurosci, 2014. **37**(2): p. 66-76.
183. Nixon, R.A., *Amyloid precursor protein and endosomal-lysosomal dysfunction in Alzheimer's disease: inseparable partners in a multifactorial disease.* FASEB J, 2017. **31**(7): p. 2729-2743.
184. Garcia-Arencibia, M., et al., *Autophagy, a guardian against neurodegeneration.* Semin Cell Dev Biol, 2010. **21**(7): p. 691-8.
185. Blanz, J. and P. Saftig, *Parkinson's disease: acid-glucocerebrosidase activity and alpha-synuclein clearance.* J Neurochem, 2016. **139 Suppl 1**: p. 198-215.
186. Dupuis, L., et al., *Energy metabolism in amyotrophic lateral sclerosis.* Lancet Neurol, 2011. **10**(1): p. 75-82.
187. Schmitt, F., et al., *A plural role for lipids in motor neuron diseases: energy, signaling and structure.* Front Cell Neurosci, 2014. **8**: p. 25.
188. Desport, J.C., et al., *Factors correlated with hypermetabolism in patients with amyotrophic lateral sclerosis.* Am J Clin Nutr, 2001. **74**(3): p. 328-34.
189. Desport, J.C., et al., *Hypermetabolism in ALS: correlations with clinical and paraclinical parameters.* Neurodegener Dis, 2005. **2**(3-4): p. 202-7.
190. Funalot, B., et al., *High metabolic level in patients with familial amyotrophic lateral sclerosis.* Amyotroph Lateral Scler, 2009. **10**(2): p. 113-7.
191. Dupuis, L., et al., *Dyslipidemia is a protective factor in amyotrophic lateral sclerosis.* Neurology, 2008. **70**(13): p. 1004-9.
192. Desport, J.C., et al., *Nutritional status is a prognostic factor for survival in ALS patients.* Neurology, 1999. **53**(5): p. 1059-63.
193. Chio, A., et al., *Prognostic factors in ALS: A critical review.* Amyotroph Lateral Scler, 2009. **10**(5-6): p. 310-23.
194. Jawaid, A., et al., *A decrease in body mass index is associated with faster progression of motor symptoms and shorter survival in ALS.* Amyotroph Lateral Scler, 2010. **11**(6): p. 542-8.
195. Dorst, J., et al., *Patients with elevated triglyceride and cholesterol serum levels have a prolonged survival in amyotrophic lateral sclerosis.* J Neurol, 2011. **258**(4): p. 613-7.
196. Dorst, J., J. Cypionka, and A.C. Ludolph, *High-caloric food supplements in the treatment of amyotrophic lateral sclerosis: a prospective interventional study.* Amyotroph Lateral Scler Frontotemporal Degener, 2013. **14**(7-8): p. 533-6.
197. Dorst, J., et al., *Percutaneous endoscopic gastrostomy in amyotrophic lateral sclerosis: a prospective observational study.* J Neurol, 2015. **262**(4): p. 849-58.

198. Wills, A.M., et al., *Hypercaloric enteral nutrition in patients with amyotrophic lateral sclerosis: a randomised, double-blind, placebo-controlled phase 2 trial.* Lancet, 2014. **383**(9934): p. 2065-2072.
199. Ripps, M.E., et al., *Transgenic mice expressing an altered murine superoxide dismutase gene provide an animal model of amyotrophic lateral sclerosis.* Proc Natl Acad Sci U S A, 1995. **92**(3): p. 689-93.
200. Dupuis, L., et al., *Evidence for defective energy homeostasis in amyotrophic lateral sclerosis: benefit of a high-energy diet in a transgenic mouse model.* Proc Natl Acad Sci U S A, 2004. **101**(30): p. 11159-64.
201. Fergani, A., et al., *Increased peripheral lipid clearance in an animal model of amyotrophic lateral sclerosis.* J Lipid Res, 2007. **48**(7): p. 1571-80.
202. Yu, R.K., Y. Nakatani, and M. Yanagisawa, *The role of glycosphingolipid metabolism in the developing brain.* J Lipid Res, 2009. **50 Suppl**: p. S440-5.
203. Plomp, J.J. and H.J. Willison, *Pathophysiological actions of neuropathy-related anti-ganglioside antibodies at the neuromuscular junction.* J Physiol, 2009. **587**(Pt 16): p. 3979-99.
204. Dupuis, L. and J.P. Loeffler, *Neuromuscular junction destruction during amyotrophic lateral sclerosis: insights from transgenic models.* Curr Opin Pharmacol, 2009. **9**(3): p. 341-6.
205. Cutler, R.G., et al., *Evidence that accumulation of ceramides and cholesterol esters mediates oxidative stress-induced death of motor neurons in amyotrophic lateral sclerosis.* Ann Neurol, 2002. **52**(4): p. 448-57.
206. Blasco, H., et al., *1H-NMR-based metabolomic profiling of CSF in early amyotrophic lateral sclerosis.* PLoS One, 2010. **5**(10): p. e13223.
207. Kumar, A., et al., *Metabolomic analysis of serum by (1) H NMR spectroscopy in amyotrophic lateral sclerosis.* Clin Chim Acta, 2010. **411**(7-8): p. 563-7.
208. Wuolikainen, A., et al., *ALS patients with mutations in the SOD1 gene have an unique metabolomic profile in the cerebrospinal fluid compared with ALS patients without mutations.* Mol Genet Metab, 2012. **105**(3): p. 472-8.
209. Wuolikainen, A., et al., *Disease-related changes in the cerebrospinal fluid metabolome in amyotrophic lateral sclerosis detected by GC/TOFMS.* PLoS One, 2011. **6**(4): p. e17947.
210. Blasco, H., et al., *Metabolomics in cerebrospinal fluid of patients with amyotrophic lateral sclerosis: an untargeted approach via high-resolution mass spectrometry.* J Proteome Res, 2013. **12**(8): p. 3746-54.

211. Henriques, A., et al., *Inhibition of beta-Glucocerebrosidase Activity Preserves Motor Unit Integrity in a Mouse Model of Amyotrophic Lateral Sclerosis.* Sci Rep, 2017. **7**(1): p. 5235.
212. Halter, B., et al., *Oxidative stress in skeletal muscle stimulates early expression of Rad in a mouse model of amyotrophic lateral sclerosis.* Free Radic Biol Med, 2010. **48**(7): p. 915-23.
213. Aerts, J.M., et al., *Pharmacological inhibition of glucosylceramide synthase enhances insulin sensitivity.* Diabetes, 2007. **56**(5): p. 1341-9.
214. Kollewe, K., et al., *ALSFRS-R score and its ratio: a useful predictor for ALS-progression.* J Neurol Sci, 2008. **275**(1-2): p. 69-73.
215. Braun, S., V. Askanas, and W.K. Engel, *Different degradation rates of junctional and extrajunctional acetylcholine receptors of human muscle cultured in monolayer and innervated by fetal rat spinal cord neurons.* Int J Dev Neurosci, 1992. **10**(1): p. 37-44.
216. Braun, S., et al., *Neurotrophins increase motoneurons' ability to innervate skeletal muscle fibers in rat spinal cord--human muscle cocultures.* J Neurol Sci, 1996. **136**(1-2): p. 17-23.
217. Croixmarie, V., et al., *Integrated comparison of drug-related and drug-induced ultra performance liquid chromatography/mass spectrometry metabonomic profiles using human hepatocyte cultures.* Anal Chem, 2009. **81**(15): p. 6061-9.
218. Wishart, D.S., et al., *HMDB: a knowledgebase for the human metabolome.* Nucleic Acids Res, 2009. **37**(Database issue): p. D603-10.
219. Kamburov, A., et al., *ConsensusPathDB: toward a more complete picture of cell biology.* Nucleic Acids Res, 2011. **39**(Database issue): p. D712-7.
220. Kamburov, A., et al., *Integrated pathway-level analysis of transcriptomics and metabolomics data with IMPaLA.* Bioinformatics, 2011. **27**(20): p. 2917-8.
221. Neville, D.C., et al., *Analysis of fluorescently labeled glycosphingolipid-derived oligosaccharides following ceramide glycanase digestion and anthranilic acid labeling.* Anal Biochem, 2004. **331**(2): p. 275-82.
222. Mohan, R., A.P. Tosolini, and R. Morris, *Targeting the motor end plates in the mouse hindlimb gives access to a greater number of spinal cord motor neurons: an approach to maximize retrograde transport.* Neuroscience, 2014. **274**: p. 318-30.
223. Jennemann, R. and H.J. Grone, *Cell-specific in vivo functions of glycosphingolipids: lessons from genetic deletions of enzymes involved in glycosphingolipid synthesis.* Prog Lipid Res, 2013. **52**(2): p. 231-48.

224. Bruni, P. and C. Donati, *Pleiotropic effects of sphingolipids in skeletal muscle.* Cell Mol Life Sci, 2008. **65**(23): p. 3725-36.
225. Stephens, M.C., et al., *The Gaucher mouse: differential action of conduritol B epoxide and reversibility of its effects.* J Neurochem, 1978. **30**(5): p. 1023-7.
226. Kanfer, J.N., et al., *The Gaucher mouse.* Biochem Biophys Res Commun, 1975. **67**(1): p. 85-90.
227. Vardi, A., et al., *Delineating pathological pathways in a chemically induced mouse model of Gaucher disease.* J Pathol, 2016. **239**(4): p. 496-509.
228. Ridley, C.M., et al., *beta-Glucosidase 2 (GBA2) activity and imino sugar pharmacology.* J Biol Chem, 2013. **288**(36): p. 26052-66.
229. Iliff, J.J., et al., *A paravascular pathway facilitates CSF flow through the brain parenchyma and the clearance of interstitial solutes, including amyloid beta.* Sci Transl Med, 2012. **4**(147): p. 147ra111.
230. Simon, M.J. and J.J. Iliff, *Regulation of cerebrospinal fluid (CSF) flow in neurodegenerative, neurovascular and neuroinflammatory disease.* Biochim Biophys Acta, 2016. **1862**(3): p. 442-51.
231. Huizinga, R., et al., *Phagocytosis of neuronal debris by microglia is associated with neuronal damage in multiple sclerosis.* Glia, 2012. **60**(3): p. 422-31.
232. Blennow, K., et al., *Gangliosides in cerebrospinal fluid in 'probable Alzheimer's disease'.* Arch Neurol, 1991. **48**(10): p. 1032-5.
233. Blennow, K., et al., *Differences in cerebrospinal fluid gangliosides between "probable Alzheimer's disease" and normal aging.* Aging (Milano), 1992. **4**(4): p. 301-6.
234. Miyatani, N., et al., *Glycosphingolipids in the cerebrospinal fluid of patients with multiple sclerosis.* Mol Chem Neuropathol, 1990. **13**(3): p. 205-16.
235. Huang, F., et al., *The neuroprotective effects of NGF combined with GM1 on injured spinal cord neurons in vitro.* Brain Res Bull, 2009. **79**(1): p. 85-8.
236. Leake, P.A., et al., *Neurotrophic effects of GM1 ganglioside and electrical stimulation on cochlear spiral ganglion neurons in cats deafened as neonates.* J Comp Neurol, 2007. **501**(6): p. 837-53.
237. Sheikh, K.A., et al., *Mice lacking complex gangliosides develop Wallerian degeneration and myelination defects.* Proc Natl Acad Sci U S A, 1999. **96**(13): p. 7532-7.
238. Susuki, K., et al., *Gangliosides contribute to stability of paranodal junctions and ion channel clusters in myelinated nerve fibers.* Glia, 2007. **55**(7): p. 746-57.

239. Campagna, J.A. and J. Fallon, *Lipid rafts are involved in C95 (4,8) agrin fragment-induced acetylcholine receptor clustering.* Neuroscience, 2006. **138**(1): p. 123-32.
240. Willmann, R., et al., *Cholesterol and lipid microdomains stabilize the postsynapse at the neuromuscular junction.* EMBO J, 2006. **25**(17): p. 4050-60.
241. Pestronk, A., et al., *Serum antibodies to GM1 ganglioside in amyotrophic lateral sclerosis.* Neurology, 1988. **38**(9): p. 1457-61.
242. Pestronk, A., et al., *Patterns of serum IgM antibodies to GM1 and GD1a gangliosides in amyotrophic lateral sclerosis.* Ann Neurol, 1989. **25**(1): p. 98-102.
243. Mizutani, K., et al., *Amyotrophic lateral sclerosis with IgM antibody against gangliosides GM2 and GD2.* Intern Med, 2003. **42**(3): p. 277-80.
244. Kollewe, K., et al., *Anti-ganglioside antibodies in amyotrophic lateral sclerosis revisited.* PLoS One, 2015. **10**(4): p. e0125339.
245. Bradley, W.G., et al., *A double-blind controlled trial of bovine brain gangliosides in amyotrophic lateral sclerosis.* Neurology, 1984. **34**(8): p. 1079-82.
246. Harrington, H., M. Hallett, and H.R. Tyler, *Ganglioside therapy for amyotrophic lateral sclerosis: a double-blind controlled trial.* Neurology, 1984. **34**(8): p. 1083-5.
247. Lacomblez, L., et al., *A double-blind, placebo-controlled trial of high doses of gangliosides in amyotrophic lateral sclerosis.* Neurology, 1989. **39**(12): p. 1635-7.
248. Schneider, J.S., et al., *A randomized, controlled, delayed start trial of GM1 ganglioside in treated Parkinson's disease patients.* J Neurol Sci, 2013. **324**(1-2): p. 140-8.
249. Schneider, J.S., et al., *GM1 ganglioside in Parkinson's disease: Results of a five year open study.* J Neurol Sci, 2010. **292**(1-2): p. 45-51.
250. Blasco, H., et al., *Lipidomics Reveals Cerebrospinal-Fluid Signatures of ALS.* Sci Rep, 2017. **7**(1): p. 17652.
251. Verma, M., E.K. Steer, and C.T. Chu, *ERKed by LRRK2: a cell biological perspective on hereditary and sporadic Parkinson's disease.* Biochim Biophys Acta, 2014. **1842**(8): p. 1273-81.
252. Hallett, P.J., et al., *Long-term health of dopaminergic neuron transplants in Parkinson's disease patients.* Cell Rep, 2014. **7**(6): p. 1755-61.
253. Bender, A., et al., *High levels of mitochondrial DNA deletions in substantia nigra neurons in aging and Parkinson disease.* Nat Genet, 2006. **38**(5): p. 515-7.
254. Hou, X., et al., *Age- and disease-dependent increase of the mitophagy marker phospho-ubiquitin in normal aging and Lewy body disease.* Autophagy, 2018. **14**(8): p. 1404-1418.

255. Ryan, B.J., et al., *Mitochondrial dysfunction and mitophagy in Parkinson's: from familial to sporadic disease.* Trends Biochem Sci, 2015. **40**(4): p. 200-10.
256. Audano, M., A. Schneider, and N. Mitro, *Mitochondria, lysosomes, and dysfunction: their meaning in neurodegeneration.* J Neurochem, 2018. **147**(3): p. 291-309.
257. Plotegher, N. and M.R. Duchen, *Crosstalk between Lysosomes and Mitochondria in Parkinson's Disease.* Front Cell Dev Biol, 2017. **5**: p. 110.
258. Gegg, M.E. and A.H. Schapira, *Mitochondrial dysfunction associated with glucocerebrosidase deficiency.* Neurobiol Dis, 2016. **90**: p. 43-50.
259. Kilpatrick, B.S., et al., *Endoplasmic reticulum and lysosomal Ca(2)(+) stores are remodelled in GBA1-linked Parkinson disease patient fibroblasts.* Cell Calcium, 2016. **59**(1): p. 12-20.
260. Dehay, B., et al., *Pathogenic lysosomal depletion in Parkinson's disease.* J Neurosci, 2010. **30**(37): p. 12535-44.
261. Meredith, G.E., et al., *Lysosomal malfunction accompanies alpha-synuclein aggregation in a progressive mouse model of Parkinson's disease.* Brain Res, 2002. **956**(1): p. 156-65.
262. Kett, L.R. and W.T. Dauer, *Endolysosomal dysfunction in Parkinson's disease: Recent developments and future challenges.* Mov Disord, 2016. **31**(10): p. 1433-1443.
263. Auburger, G., et al., *Primary skin fibroblasts as a model of Parkinson's disease.* Mol Neurobiol, 2012. **46**(1): p. 20-7.
264. Skorvanek, M. and K.P. Bhatia, *The Skin and Parkinson's Disease: Review of Clinical, Diagnostic, and Therapeutic Issues.* Mov Disord Clin Pract, 2017. **4**(1): p. 21-31.
265. Hoepken, H.H., et al., *Parkinson patient fibroblasts show increased alpha-synuclein expression.* Exp Neurol, 2008. **212**(2): p. 307-13.
266. del Hoyo, P., et al., *Oxidative stress in skin fibroblasts cultures from patients with Parkinson's disease.* BMC Neurol, 2010. **10**: p. 95.
267. Hockey, L.N., et al., *Dysregulation of lysosomal morphology by pathogenic LRRK2 is corrected by TPC2 inhibition.* J Cell Sci, 2015. **128**(2): p. 232-8.
268. Ambrosi, G., et al., *Bioenergetic and proteolytic defects in fibroblasts from patients with sporadic Parkinson's disease.* Biochim Biophys Acta, 2014. **1842**(9): p. 1385-94.
269. Smith, G.A., et al., *Fibroblast Biomarkers of Sporadic Parkinson's Disease and LRRK2 Kinase Inhibition.* Mol Neurobiol, 2016. **53**(8): p. 5161-77.

270. McNeill, A., et al., *Ambroxol improves lysosomal biochemistry in glucocerebrosidase mutation-linked Parkinson disease cells.* Brain, 2014. **137**(Pt 5): p. 1481-95.
271. Teves, J.M.Y., et al., *Parkinson's Disease Skin Fibroblasts Display Signature Alterations in Growth, Redox Homeostasis, Mitochondrial Function, and Autophagy.* Front Neurosci, 2017. **11**: p. 737.
272. Garcia-Sanz, P., et al., *N370S-GBA1 mutation causes lysosomal cholesterol accumulation in Parkinson's disease.* Mov Disord, 2017. **32**(10): p. 1409-1422.
273. Fernandes, H.J., et al., *ER Stress and Autophagic Perturbations Lead to Elevated Extracellular alpha-Synuclein in GBA-N370S Parkinson's iPSC-Derived Dopamine Neurons.* Stem Cell Reports, 2016. **6**(3): p. 342-56.
274. Brockmann, K., et al., *GBA-associated PD presents with nonmotor characteristics.* Neurology, 2011. **77**(3): p. 276-80.
275. Lu, F., et al., *Identification of NPC1 as the target of U18666A, an inhibitor of lysosomal cholesterol export and Ebola infection.* Elife, 2015. **4**.
276. Stein, F., et al., *FluoQ: a tool for rapid analysis of multiparameter fluorescence imaging data applied to oscillatory events.* ACS Chem Biol, 2013. **8**(9): p. 1862-8.
277. Uchimoto, T., et al., *Mechanism of apoptosis induced by a lysosomotropic agent, L-Leucyl-L-Leucine methyl ester.* Apoptosis, 1999. **4**(5): p. 357-62.
278. te Vruchte, D., et al., *Relative acidic compartment volume as a lysosomal storage disorder-associated biomarker.* J Clin Invest, 2014. **124**(3): p. 1320-8.
279. Aits, S., et al., *Sensitive detection of lysosomal membrane permeabilization by lysosomal galectin puncta assay.* Autophagy, 2015. **11**(8): p. 1408-24.
280. Zhang, Y., et al., *Alterations in ceramide concentration and pH determine the release of reactive oxygen species by Cftr-deficient macrophages on infection.* J Immunol, 2010. **184**(9): p. 5104-11.
281. Ambrosi, G., et al., *Ambroxol-induced rescue of defective glucocerebrosidase is associated with increased LIMP-2 and saposin C levels in GBA1 mutant Parkinson's disease cells.* Neurobiol Dis, 2015. **82**: p. 235-242.
282. Mazzulli, J.R., et al., *alpha-Synuclein-induced lysosomal dysfunction occurs through disruptions in protein trafficking in human midbrain synucleinopathy models.* Proc Natl Acad Sci U S A, 2016. **113**(7): p. 1931-6.
283. Magalhaes, J., et al., *Autophagic lysosome reformation dysfunction in glucocerebrosidase deficient cells: relevance to Parkinson disease.* Hum Mol Genet, 2016. **25**(16): p. 3432-3445.

284. Schonauer, S., et al., *Identification of a feedback loop involving beta-glucosidase 2 and its product sphingosine sheds light on the molecular mechanisms in Gaucher disease.* J Biol Chem, 2017. **292**(15): p. 6177-6189.
285. Sillence, D.J., et al., *Glucosylceramide modulates membrane traffic along the endocytic pathway.* J Lipid Res, 2002. **43**(11): p. 1837-45.
286. Saito, M. and A. Rosenberg, *The fate of glucosylceramide (glucocerebroside) in genetically impaired (lysosomal beta-glucosidase deficient) Gaucher disease diploid human fibroblasts.* J Biol Chem, 1985. **260**(4): p. 2295-300.
287. Sasagasako, N., et al., *Glucosylceramide and glucosylsphingosine metabolism in cultured fibroblasts deficient in acid beta-glucosidase activity.* J Biochem, 1994. **115**(1): p. 113-9.
288. Haggie, P.M. and A.S. Verkman, *Unimpaired lysosomal acidification in respiratory epithelial cells in cystic fibrosis.* J Biol Chem, 2009. **284**(12): p. 7681-6.
289. Schmid, J.A., et al., *Accumulation of sialic acid in endocytic compartments interferes with the formation of mature lysosomes.* J Biol Chem, 1999. **274**(27): p. 19063-71.
290. Schapira, A.H., *Calcium dysregulation in Parkinson's disease.* Brain, 2013. **136**(Pt 7): p. 2015-6.
291. Korecka, J.A., et al., *Neurite Collapse and Altered ER Ca(2+) Control in Human Parkinson Disease Patient iPSC-Derived Neurons with LRRK2 G2019S Mutation.* Stem Cell Reports, 2019. **12**(1): p. 29-41.
292. Surmeier, D.J., J.N. Guzman, and J. Sanchez-Padilla, *Calcium, cellular aging, and selective neuronal vulnerability in Parkinson's disease.* Cell Calcium, 2010. **47**(2): p. 175-82.
293. Surmeier, D.J., et al., *Calcium and Parkinson's disease.* Biochem Biophys Res Commun, 2017. **483**(4): p. 1013-1019.
294. Hurley, M.J., et al., *Parkinson's disease is associated with altered expression of CaV1 channels and calcium-binding proteins.* Brain, 2013. **136**(Pt 7): p. 2077-97.
295. Zaichick, S.V., K.M. McGrath, and G. Caraveo, *The role of Ca(2+) signaling in Parkinson's disease.* Dis Model Mech, 2017. **10**(5): p. 519-535.
296. Takahashi, Y., et al., *The late endosome/lysosome-anchored p18-mTORC1 pathway controls terminal maturation of lysosomes.* Biochem Biophys Res Commun, 2012. **417**(4): p. 1151-7.
297. Rocha, N., et al., *Cholesterol sensor ORP1L contacts the ER protein VAP to control Rab7-RILP-p150 Glued and late endosome positioning.* J Cell Biol, 2009. **185**(7): p. 1209-25.

298. Akiyama, H., et al., *Cholesterol glucosylation is catalyzed by transglucosylation reaction of beta-glucosidase 1.* Biochem Biophys Res Commun, 2013. **441**(4): p. 838-43.
299. Blesa, J. and S. Przedborski, *Parkinson's disease: animal models and dopaminergic cell vulnerability.* Front Neuroanat, 2014. **8**: p. 155.
300. Childs, B.G., et al., *Cellular senescence in aging and age-related disease: from mechanisms to therapy.* Nat Med, 2015. **21**(12): p. 1424-35.
301. Kraytsberg, Y., et al., *Mitochondrial DNA deletions are abundant and cause functional impairment in aged human substantia nigra neurons.* Nat Genet, 2006. **38**(5): p. 518-20.
302. Nguyen, T.N., B.S. Padman, and M. Lazarou, *Deciphering the Molecular Signals of PINK1/Parkin Mitophagy.* Trends Cell Biol, 2016. **26**(10): p. 733-44.
303. Dutta, S. and P. Sengupta, *Men and mice: Relating their ages.* Life Sci, 2016. **152**: p. 244-8.
304. Alcalay, R.N., et al., *Glucocerebrosidase activity in Parkinson's disease with and without GBA mutations.* Brain, 2015. **138**(9): p. 2648-58.
305. Parnetti, L., et al., *Cerebrospinal fluid beta-glucocerebrosidase activity is reduced in parkinson's disease patients.* Mov Disord, 2017. **32**(10): p. 1423-1431.
306. Schueler, U.H., et al., *Toxicity of glucosylsphingosine (glucopsychosine) to cultured neuronal cells: a model system for assessing neuronal damage in Gaucher disease type 2 and 3.* Neurobiol Dis, 2003. **14**(3): p. 595-601.
307. Orvisky, E., et al., *Glucosylsphingosine accumulation in tissues from patients with Gaucher disease: correlation with phenotype and genotype.* Mol Genet Metab, 2002. **76**(4): p. 262-70.
308. Kracun, I., et al., *Human brain gangliosides in development, aging and disease.* Int J Dev Biol, 1991. **35**(3): p. 289-95.
309. Svennerholm, L., et al., *Membrane lipids of adult human brain: lipid composition of frontal and temporal lobe in subjects of age 20 to 100 years.* J Neurochem, 1994. **63**(5): p. 1802-11.
310. Ohsawa, T., *Changes of mouse brain gangliosides during aging from young adult until senescence.* Mech Ageing Dev, 1989. **50**(2): p. 169-77.
311. Ohsawa, T. and S. Shumiya, *Age-related alteration of brain gangliosides in senescence-accelerated mouse (SAM)-P/8.* Mech Ageing Dev, 1991. **59**(3): p. 263-74.
312. Hallett, P.J., et al., *Glycosphingolipid levels and glucocerebrosidase activity are altered in normal aging of the mouse brain.* Neurobiol Aging, 2018. **67**: p. 189-200.

313. Rocha, E.M., et al., *Sustained Systemic Glucocerebrosidase Inhibition Induces Brain alpha-Synuclein Aggregation, Microglia and Complement C1q Activation in Mice.* Antioxid Redox Signal, 2015. **23**(6): p. 550-64.
314. Niccoli, T. and L. Partridge, *Ageing as a risk factor for disease.* Curr Biol, 2012. **22**(17): p. R741-52.
315. McGeer, P.L., E.G. McGeer, and J.S. Suzuki, *Aging and extrapyramidal function.* Arch. Neurol., 1977. **34**: p. 33-35.
316. Ma, S.Y., et al., *Dopamine transporter-immunoreactive neurons decrease with age in the human substantia nigra.* J Comp Neurol, 1999. **409**(1): p. 25-37.
317. Rodriguez, M., et al., *Parkinson's disease as a result of aging.* Aging Cell, 2015. **14**(3): p. 293-308.
318. Collier, T.J., N.M. Kanaan, and J.H. Kordower, *Ageing as a primary risk factor for Parkinson's disease: evidence from studies of non-human primates.* Nat Rev Neurosci, 2011. **12**(6): p. 359-66.
319. Rudow, G., et al., *Morphometry of the human substantia nigra in ageing and Parkinson's disease.* Acta Neuropathol, 2008. **115**(4): p. 461-70.
320. Cabello, C.R., et al., *Ageing of substantia nigra in humans: cell loss may be compensated by hypertrophy.* Neuropathol Appl Neurobiol, 2002. **28**(4): p. 283-91.
321. Lee, Y.I., et al., *Diaminodiphenyl sulfone-induced parkin ameliorates age-dependent dopaminergic neuronal loss.* Neurobiol Aging, 2016. **41**: p. 1-10.
322. Vilchez, D., I. Saez, and A. Dillin, *The role of protein clearance mechanisms in organismal ageing and age-related diseases.* Nat Commun, 2014. **5**: p. 5659.
323. Roze, E., et al., *Dystonia and parkinsonism in GM1 type 3 gangliosidosis.* Mov Disord, 2005. **20**(10): p. 1366-9.
324. Saito, Y., et al., *Aberrant phosphorylation of alpha-synuclein in human Niemann-Pick type C1 disease.* J Neuropathol Exp Neurol, 2004. **63**(4): p. 323-8.
325. Buechner, S., et al., *Parkinsonism and Anderson Fabry's disease: a case report.* Mov Disord, 2006. **21**(1): p. 103-7.
326. Smith, B.R., et al., *Neuronal inclusions of alpha-synuclein contribute to the pathogenesis of Krabbe disease.* J Pathol, 2014. **232**(5): p. 509-21.
327. Nilsson, O. and L. Svennerholm, *Accumulation of glucosylceramide and glucosylsphingosine (psychosine) in cerebrum and cerebellum in infantile and juvenile Gaucher disease.* J Neurochem, 1982. **39**(3): p. 709-18.

328. Farfel-Becker, T., et al., *Neuronal accumulation of glucosylceramide in a mouse model of neuronopathic Gaucher disease leads to neurodegeneration.* Hum Mol Genet, 2014. **23**(4): p. 843-54.
329. Lingwood, C.A., *Glycosphingolipid functions.* Cold Spring Harb Perspect Biol, 2011. **3**(7).
330. Pan, X., et al., *Neuraminidases 3 and 4 regulate neuronal function by catabolizing brain gangliosides.* FASEB J, 2017.
331. Yamamoto, N., et al., *Age-dependent high-density clustering of GM1 ganglioside at presynaptic neuritic terminals promotes amyloid beta-protein fibrillogenesis.* Biochim Biophys Acta, 2008. **1778**(12): p. 2717-26.
332. Chung, C.Y., et al., *Dynamic changes in presynaptic and axonal transport proteins combined with striatal neuroinflammation precede dopaminergic neuronal loss in a rat model of AAV alpha-synucleinopathy.* J Neurosci, 2009. **29**(11): p. 3365-73.
333. Schnaar, R.L., *Gangliosides of the Vertebrate Nervous System.* J Mol Biol, 2016. **428**(16): p. 3325-36.
334. Heinecke, K.A., et al., *Myelin abnormalities in the optic and sciatic nerves in mice with GM1-gangliosidosis.* ASN Neuro, 2015. **7**(1).
335. Graham, S.H. and H. Liu, *Life and death in the trash heap: The ubiquitin proteasome pathway and UCHL1 in brain aging, neurodegenerative disease and cerebral Ischemia.* Ageing Res Rev, 2017. **34**: p. 30-38.
336. Liu, G., et al., *Increased oligomerization and phosphorylation of alpha-synuclein are associated with decreased activity of glucocerebrosidase and protein phosphatase 2A in aging monkey brains.* Neurobiol Aging, 2015. **36**(9): p. 2649-59.
337. Shahmoradian, S.H., et al., *Lewy pathology in Parkinson's disease consists of a crowded organellar membranous medley.* bioRxiv, 2017.
338. Argyriou, A., et al., *Increased dimerization of alpha-synuclein in erythrocytes in Gaucher disease and aging.* Neurosci Lett, 2012. **528**(2): p. 205-9.
339. Moraitou, M., et al., *alpha-Synuclein dimerization in erythrocytes of Gaucher disease patients: correlation with lipid abnormalities and oxidative stress.* Neurosci Lett, 2016. **613**: p. 1-5.
340. Gibb, W.R. and A.J. Lees, *Anatomy, pigmentation, ventral and dorsal subpopulations of the substantia nigra, and differential cell death in Parkinson's disease.* J Neurol Neurosurg Psychiatry, 1991. **54**(5): p. 388-96.

341. Branch, S.Y., R. Sharma, and M.J. Beckstead, *Aging decreases L-type calcium channel currents and pacemaker firing fidelity in substantia nigra dopamine neurons.* J Neurosci, 2014. **34**(28): p. 9310-8.
342. Fetler, L. and S. Amigorena, *Neuroscience. Brain under surveillance: the microglia patrol.* Science, 2005. **309**(5733): p. 392-3.
343. Norden, D.M. and J.P. Godbout, *Review: microglia of the aged brain: primed to be activated and resistant to regulation.* Neuropathol Appl Neurobiol, 2013. **39**(1): p. 19-34.
344. Kreutzberg, G.W., *Microglia: a sensor for pathological events in the CNS.* Trends Neurosci, 1996. **19**(8): p. 312-8.
345. Stence, N., M. Waite, and M.E. Dailey, *Dynamics of microglial activation: a confocal time-lapse analysis in hippocampal slices.* Glia, 2001. **33**(3): p. 256-66.
346. Mouton, P.R., et al., *Age and gender effects on microglia and astrocyte numbers in brains of mice.* Brain Res, 2002. **956**(1): p. 30-5.
347. Poliani, P.L., et al., *TREM2 sustains microglial expansion during aging and response to demyelination.* J Clin Invest, 2015. **125**(5): p. 2161-70.
348. Safaiyan, S., et al., *Age-related myelin degradation burdens the clearance function of microglia during aging.* Nat Neurosci, 2016. **19**(8): p. 995-8.
349. Park, J.Y., et al., *On the mechanism of internalization of alpha-synuclein into microglia: roles of ganglioside GM1 and lipid raft.* J Neurochem, 2009. **110**(1): p. 400-11.
350. Pyo, H., et al., *Gangliosides activate cultured rat brain microglia.* J Biol Chem, 1999. **274**(49): p. 34584-9.
351. Spittau, B., *Aging Microglia-Phenotypes, Functions and Implications for Age-Related Neurodegenerative Diseases.* Front Aging Neurosci, 2017. **9**: p. 194.
352. Askew, K., et al., *Coupled Proliferation and Apoptosis Maintain the Rapid Turnover of Microglia in the Adult Brain.* Cell Rep, 2017. **18**(2): p. 391-405.
353. VanGuilder, H.D., et al., *Concurrent hippocampal induction of MHC II pathway components and glial activation with advanced aging is not correlated with cognitive impairment.* J Neuroinflammation, 2011. **8**: p. 138.
354. Lawson, L.J., V.H. Perry, and S. Gordon, *Turnover of resident microglia in the normal adult mouse brain.* Neuroscience, 1992. **48**(2): p. 405-15.
355. Cox, T.M., *Innovative treatments for lysosomal diseases.* Best Pract Res Clin Endocrinol Metab, 2015. **29**(2): p. 275-311.
356. Platt, F.M. and M. Jeyakumar, *Substrate reduction therapy.* Acta Paediatr, 2008. **97**(457): p. 88-93.

357. Aureli, M., et al., *GM1 Ganglioside: Past Studies and Future Potential.* Mol Neurobiol, 2016. **53**(3): p. 1824-1842.
358. Lipartiti, M., et al., *Monosialoganglioside GM1 reduces NMDA neurotoxicity in neonatal rat brain.* Exp Neurol, 1991. **113**(3): p. 301-5.
359. Toffano, G., et al., *GM1 ganglioside stimulates the regeneration of dopaminergic neurons in the central nervous system.* Brain Res, 1983. **261**(1): p. 163-6.
360. Schneider, J.S., et al., *Recovery from experimental parkinsonism in primates with GM1 ganglioside treatment.* Science, 1992. **256**(5058): p. 843-6.
361. Vekrellis, K., et al., *Pathological roles of alpha-synuclein in neurological disorders.* Lancet Neurol, 2011. **10**(11): p. 1015-25.
362. Vekrellis, K., H.J. Rideout, and L. Stefanis, *Neurobiology of alpha-synuclein.* Mol Neurobiol, 2004. **30**(1): p. 1-21.
363. Burre, J., *The Synaptic Function of alpha-Synuclein.* J Parkinsons Dis, 2015. **5**(4): p. 699-713.
364. Burre, J., et al., *Alpha-synuclein promotes SNARE-complex assembly in vivo and in vitro.* Science, 2010. **329**(5999): p. 1663-7.
365. Kruger, R., et al., *Ala30Pro mutation in the gene encoding alpha-synuclein in Parkinson's disease.* Nat Genet, 1998. **18**(2): p. 106-8.
366. Polymeropoulos, M.H., et al., *Mutation in the alpha-synuclein gene identified in families with Parkinson's disease.* Science, 1997. **276**(5321): p. 2045-7.
367. Zarranz, J.J., et al., *The new mutation, E46K, of alpha-synuclein causes Parkinson and Lewy body dementia.* Ann Neurol, 2004. **55**(2): p. 164-73.
368. Singleton, A.B., et al., *alpha-Synuclein locus triplication causes Parkinson's disease.* Science, 2003. **302**(5646): p. 841.
369. Miller, D.W., et al., *Alpha-synuclein in blood and brain from familial Parkinson disease with SNCA locus triplication.* Neurology, 2004. **62**(10): p. 1835-8.
370. Ibanez, P., et al., *Causal relation between alpha-synuclein gene duplication and familial Parkinson's disease.* Lancet, 2004. **364**(9440): p. 1169-71.
371. Chartier-Harlin, M.C., et al., *Alpha-synuclein locus duplication as a cause of familial Parkinson's disease.* Lancet, 2004. **364**(9440): p. 1167-9.
372. International Parkinson Disease Genomics, C., et al., *Imputation of sequence variants for identification of genetic risks for Parkinson's disease: a meta-analysis of genome-wide association studies.* Lancet, 2011. **377**(9766): p. 641-9.
373. Kim, C. and S.J. Lee, *Controlling the mass action of alpha-synuclein in Parkinson's disease.* J Neurochem, 2008. **107**(2): p. 303-16.

374. Li, J.Q., L. Tan, and J.T. Yu, *The role of the LRRK2 gene in Parkinsonism.* Mol Neurodegener, 2014. **9**: p. 47.
375. Herzig, M.C., et al., *LRRK2 protein levels are determined by kinase function and are crucial for kidney and lung homeostasis in mice.* Hum Mol Genet, 2011. **20**(21): p. 4209-23.
376. Cookson, M.R., *Cellular effects of LRRK2 mutations.* Biochem Soc Trans, 2012. **40**(5): p. 1070-3.
377. Lee, S., et al., *The synaptic function of LRRK2.* Biochem Soc Trans, 2012. **40**(5): p. 1047-51.
378. Dzamko, N. and G.M. Halliday, *An emerging role for LRRK2 in the immune system.* Biochem Soc Trans, 2012. **40**(5): p. 1134-9.
379. Healy, D.G., et al., *Phenotype, genotype, and worldwide genetic penetrance of LRRK2-associated Parkinson's disease: a case-control study.* Lancet Neurol, 2008. **7**(7): p. 583-90.
380. Paisan-Ruiz, C., et al., *Cloning of the gene containing mutations that cause PARK8-linked Parkinson's disease.* Neuron, 2004. **44**(4): p. 595-600.
381. Luzon-Toro, B., et al., *Mechanistic insight into the dominant mode of the Parkinson's disease-associated G2019S LRRK2 mutation.* Hum Mol Genet, 2007. **16**(17): p. 2031-9.
382. Rudenko, I.N. and M.R. Cookson, *Heterogeneity of leucine-rich repeat kinase 2 mutations: genetics, mechanisms and therapeutic implications.* Neurotherapeutics, 2014. **11**(4): p. 738-50.
383. Li, Y., et al., *The R1441C mutation alters the folding properties of the ROC domain of LRRK2.* Biochim Biophys Acta, 2009. **1792**(12): p. 1194-7.
384. Chesselet, M.F. and F. Richter, *Modelling of Parkinson's disease in mice.* Lancet Neurol, 2011. **10**(12): p. 1108-18.
385. Visanji, N.P., et al., *alpha-Synuclein-Based Animal Models of Parkinson's Disease: Challenges and Opportunities in a New Era.* Trends Neurosci, 2016. **39**(11): p. 750-762.
386. Rockenstein, E., et al., *Differential neuropathological alterations in transgenic mice expressing alpha-synuclein from the platelet-derived growth factor and Thy-1 promoters.* J Neurosci Res, 2002. **68**(5): p. 568-78.
387. Chesselet, M.F., et al., *A progressive mouse model of Parkinson's disease: the Thy1-aSyn ("Line 61") mice.* Neurotherapeutics, 2012. **9**(2): p. 297-314.
388. Lam, H.A., et al., *Elevated tonic extracellular dopamine concentration and altered dopamine modulation of synaptic activity precede dopamine loss in the striatum of*

mice overexpressing human alpha-synuclein. J Neurosci Res, 2011. **89**(7): p. 1091-102.

389. Li, Y., et al., *Mutant LRRK2(R1441G) BAC transgenic mice recapitulate cardinal features of Parkinson's disease.* Nat Neurosci, 2009. **12**(7): p. 826-8.
390. Zimprich, A., et al., *Mutations in LRRK2 cause autosomal-dominant parkinsonism with pleomorphic pathology.* Neuron, 2004. **44**(4): p. 601-7.
391. West, A.B., et al., *Parkinson's disease-associated mutations in leucine-rich repeat kinase 2 augment kinase activity.* Proc Natl Acad Sci U S A, 2005. **102**(46): p. 16842-7.
392. Dusonchet, J., et al., *A rat model of progressive nigral neurodegeneration induced by the Parkinson's disease-associated G2019S mutation in LRRK2.* J Neurosci, 2011. **31**(3): p. 907-12.
393. Smith, W.W., et al., *Kinase activity of mutant LRRK2 mediates neuronal toxicity.* Nat Neurosci, 2006. **9**(10): p. 1231-3.
394. Lee, B.D., et al., *Inhibitors of leucine-rich repeat kinase-2 protect against models of Parkinson's disease.* Nat Med, 2010. **16**(9): p. 998-1000.
395. Longo, F., et al., *Age-dependent dopamine transporter dysfunction and Serine129 phospho-alpha-synuclein overload in G2019S LRRK2 mice.* Acta Neuropathol Commun, 2017. **5**(1): p. 22.
396. Moloney, E.B., et al., *The glycoprotein GPNMB is selectively elevated in the substantia nigra of Parkinson's disease patients and increases after lysosomal stress.* Neurobiol Dis, 2018.
397. Goker-Alpan, O., et al., *Glucocerebrosidase is present in alpha-synuclein inclusions in Lewy body disorders.* Acta Neuropathol, 2010. **120**(5): p. 641-9.
398. Richter, F., et al., *A GCase chaperone improves motor function in a mouse model of synucleinopathy.* Neurotherapeutics, 2014. **11**(4): p. 840-56.
399. Rockenstein, E., et al., *Glucocerebrosidase modulates cognitive and motor activities in murine models of Parkinson's disease.* Hum Mol Genet, 2016. **25**(13): p. 2645-2660.
400. Giasson, B.I., et al., *Neuronal alpha-synucleinopathy with severe movement disorder in mice expressing A53T human alpha-synuclein.* Neuron, 2002. **34**(4): p. 521-33.
401. Mor, D.E., et al., *Dopamine induces soluble alpha-synuclein oligomers and nigrostriatal degeneration.* Nat Neurosci, 2017. **20**(11): p. 1560-1568.

402. Rochet, J.C., K.A. Conway, and P.T. Lansbury, Jr., *Inhibition of fibrillization and accumulation of prefibrillar oligomers in mixtures of human and mouse alpha-synuclein.* Biochemistry, 2000. **39**(35): p. 10619-26.
403. Tong, Y., et al., *Loss of leucine-rich repeat kinase 2 causes impairment of protein degradation pathways, accumulation of alpha-synuclein, and apoptotic cell death in aged mice.* Proc Natl Acad Sci U S A, 2010. **107**(21): p. 9879-84.
404. Ness, D., et al., *Leucine-rich repeat kinase 2 (LRRK2)-deficient rats exhibit renal tubule injury and perturbations in metabolic and immunological homeostasis.* PLoS One, 2013. **8**(6): p. e66164.
405. Baptista, M.A., et al., *Loss of leucine-rich repeat kinase 2 (LRRK2) in rats leads to progressive abnormal phenotypes in peripheral organs.* PLoS One, 2013. **8**(11): p. e80705.
406. Brunk, U.T. and A. Terman, *Lipofuscin: mechanisms of age-related accumulation and influence on cell function.* Free Radic Biol Med, 2002. **33**(5): p. 611-9.
407. Bersano, A., et al., *Neurological features of Fabry disease: clinical, pathophysiological aspects and therapy.* Acta Neurol Scand, 2012. **126**(2): p. 77-97.
408. Germain, D.P., *Fabry disease.* Orphanet J Rare Dis, 2010. **5**: p. 30.
409. Boddu, R., et al., *Leucine-rich repeat kinase 2 deficiency is protective in rhabdomyolysis-induced kidney injury.* Hum Mol Genet, 2015. **24**(14): p. 4078-93.
410. Sulzer, D., *Multiple hit hypotheses for dopamine neuron loss in Parkinson's disease.* Trends Neurosci, 2007. **30**(5): p. 244-50.
411. Bjorklund, A. and S.B. Dunnett, *Dopamine neuron systems in the brain: an update.* Trends Neurosci, 2007. **30**(5): p. 194-202.
412. Roeper, J., *Dissecting the diversity of midbrain dopamine neurons.* Trends Neurosci, 2013. **36**(6): p. 336-42.
413. Matsuda, W., et al., *Single nigrostriatal dopaminergic neurons form widely spread and highly dense axonal arborizations in the neostriatum.* J Neurosci, 2009. **29**(2): p. 444-53.
414. Arbuthnott, G.W. and J. Wickens, *Space, time and dopamine.* Trends Neurosci, 2007. **30**(2): p. 62-9.
415. Platt, F.M., *Sphingolipid lysosomal storage disorders.* Nature, 2014. **510**(7503): p. 68-75.
416. Sidransky, E. and G. Lopez, *The link between the GBA gene and parkinsonism.* Lancet Neurol, 2012. **11**(11): p. 986-98.

417. Woeste, M.A. and D. Wachten, *The Enigmatic Role of GBA2 in Controlling Locomotor Function.* Front Mol Neurosci, 2017. **10**: p. 386.
418. Gan-Or, Z., et al., *The p.L302P mutation in the lysosomal enzyme gene SMPD1 is a risk factor for Parkinson disease.* Neurology, 2013. **80**(17): p. 1606-10.
419. Pchelina, S.N., et al., *Increased plasma oligomeric alpha-synuclein in patients with lysosomal storage diseases.* Neurosci Lett, 2014. **583**: p. 188-93.
420. Mielke, M.M., et al., *Plasma ceramide and glucosylceramide metabolism is altered in sporadic Parkinson's disease and associated with cognitive impairment: a pilot study.* PLoS One, 2013. **8**(9): p. e73094.
421. Wu, G., et al., *Mice lacking major brain gangliosides develop parkinsonism.* Neurochem Res, 2011. **36**(9): p. 1706-14.
422. Marshall, M.S., et al., *Analysis of age-related changes in psychosine metabolism in the human brain.* PLoS One, 2018. **13**(2): p. e0193438.
423. Nelson, M.P., et al., *The lysosomal enzyme alpha-Galactosidase A is deficient in Parkinson's disease brain in association with the pathologic accumulation of alpha-synuclein.* Neurobiol Dis, 2018. **110**: p. 68-81.
424. Alcalay, R.N., et al., *Alpha galactosidase A activity in Parkinson's disease.* Neurobiol Dis, 2018. **112**: p. 85-90.
425. Wu, G., et al., *Decreased activities of lysosomal acid alpha-D-galactosidase A in the leukocytes of sporadic Parkinson's disease.* J Neurol Sci, 2008. **271**(1-2): p. 168-73.
426. Nelson, M.P., et al., *Autophagy-lysosome pathway associated neuropathology and axonal degeneration in the brains of alpha-galactosidase A-deficient mice.* Acta Neuropathol Commun, 2014. **2**: p. 20.
427. Wise, A.H., et al., *Parkinson's disease prevalence in Fabry disease: A survey study.* Mol Genet Metab Rep, 2018. **14**: p. 27-30.
428. Borsini, W., et al., *Anderson-Fabry disease with cerebrovascular complications in two Italian families.* Neurol Sci, 2002. **23**(2): p. 49-53.
429. Balducci, C., et al., *Lysosomal hydrolases in cerebrospinal fluid from subjects with Parkinson's disease.* Mov Disord, 2007. **22**(10): p. 1481-4.
430. Suzuki, K., et al., *Neuronal accumulation of alpha- and beta-synucleins in the brain of a GM2 gangliosidosis mouse model.* Neuroreport, 2003. **14**(4): p. 551-4.
431. Suzuki, K., et al., *Neuronal and glial accumulation of alpha- and beta-synucleins in human lipidoses.* Acta Neuropathol, 2007. **114**(5): p. 481-9.
432. Muthane, U., et al., *Clinical features of adult GM1 gangliosidosis: report of three Indian patients and review of 40 cases.* Mov Disord, 2004. **19**(11): p. 1334-41.

433. Yoshida, K., et al., *GM1 gangliosidosis in adults: clinical and molecular analysis of 16 Japanese patients.* Ann Neurol, 1992. **31**(3): p. 328-32.
434. Fanzani, A., et al., *Implications for the mammalian sialidases in the physiopathology of skeletal muscle.* Skelet Muscle, 2012. **2**(1): p. 23.
435. Sango, K., et al., *Mouse models of Tay-Sachs and Sandhoff diseases differ in neurologic phenotype and ganglioside metabolism.* Nat Genet, 1995. **11**(2): p. 170-6.
436. Segler-Stahl, K., J.C. Webster, and E.G. Brunngraber, *Changes in the concentration and composition of human brain gangliosides with aging.* Gerontology, 1983. **29**(3): p. 161-8.
437. Schneider, J.S., *Altered expression of genes involved in ganglioside biosynthesis in substantia nigra neurons in Parkinson's disease.* PLoS One, 2018. **13**(6): p. e0199189.
438. Schneider, J.S. and A. Yuwiler, *GM1 ganglioside treatment promotes recovery of striatal dopamine concentrations in the mouse model of MPTP-induced parkinsonism.* Exp Neurol, 1989. **105**(2): p. 177-83.
439. Hadjiconstantinou, M., et al., *Administration of GM1 ganglioside restores the dopamine content in striatum after chronic treatment with MPTP.* Neuropharmacology, 1986. **25**(9): p. 1075-7.
440. Schneider, J.S., *GM1 ganglioside in the treatment of Parkinson's disease.* Ann N Y Acad Sci, 1998. **845**: p. 363-73.
441. Schneider, J.S., et al., *Parkinson's disease: improved function with GM1 ganglioside treatment in a randomized placebo-controlled study.* Neurology, 1998. **50**(6): p. 1630-6.
442. Akkhawattanangkul, Y., et al., *Targeted deletion of GD3 synthase protects against MPTP-induced neurodegeneration.* Genes Brain Behav, 2017. **16**(5): p. 522-536.
443. Parkinson, G.M., C.V. Dayas, and D.W. Smith, *Perturbed cholesterol homeostasis in aging spinal cord.* Neurobiol Aging, 2016. **45**: p. 123-135.
444. Yeh, T.S., et al., *Spinal cord injury and Parkinson's disease: a population-based, propensity score-matched, longitudinal follow-up study.* Spinal Cord, 2016. **54**(12): p. 1215-1219.
445. de Andrade, E.M., et al., *Spinal cord stimulation for Parkinson's disease: a systematic review.* Neurosurg Rev, 2016. **39**(1): p. 27-35; discussion 35.
446. Yadav, A.P. and M.A.L. Nicolelis, *Electrical stimulation of the dorsal columns of the spinal cord for Parkinson's disease.* Mov Disord, 2017. **32**(6): p. 820-832.

447. Santana, M.B., et al., *Spinal cord stimulation alleviates motor deficits in a primate model of Parkinson disease.* Neuron, 2014. **84**(4): p. 716-722.
448. Pinto de Souza, C., et al., *Spinal cord stimulation improves gait in patients with Parkinson's disease previously treated with deep brain stimulation.* Mov Disord, 2017. **32**(2): p. 278-282.
449. Samotus, O., A. Parrent, and M. Jog, *Spinal Cord Stimulation Therapy for Gait Dysfunction in Advanced Parkinson's Disease Patients.* Mov Disord, 2018. **33**(5): p. 783-792.
450. Schneider, J.S., et al., *Intraventricular Sialidase Administration Enhances GM1 Ganglioside Expression and Is Partially Neuroprotective in a Mouse Model of Parkinson's Disease.* PLoS One, 2015. **10**(12): p. e0143351.
451. Miller, D.B. and J.P. O'Callaghan, *Biomarkers of Parkinson's disease: present and future.* Metabolism, 2015. **64**(3 Suppl 1): p. S40-6.
452. Schapira, A.H., *Recent developments in biomarkers in Parkinson disease.* Curr Opin Neurol, 2013. **26**(4): p. 395-400.
453. Chahine, L.M., M.B. Stern, and A. Chen-Plotkin, *Blood-based biomarkers for Parkinson's disease.* Parkinsonism Relat Disord, 2014. **20 Suppl 1**: p. S99-103.
454. Iranzo, A., et al., *Neurodegenerative disorder risk in idiopathic REM sleep behavior disorder: study in 174 patients.* PLoS One, 2014. **9**(2): p. e89741.
455. Iranzo, A., et al., *Neurodegenerative disease status and post-mortem pathology in idiopathic rapid-eye-movement sleep behaviour disorder: an observational cohort study.* Lancet Neurol, 2013. **12**(5): p. 443-53.
456. Postuma, R.B., et al., *Parkinson risk in idiopathic REM sleep behavior disorder: preparing for neuroprotective trials.* Neurology, 2015. **84**(11): p. 1104-13.
457. Gan-Or, Z., et al., *Parkinson's Disease Genetic Loci in Rapid Eye Movement Sleep Behavior Disorder.* J Mol Neurosci, 2015. **56**(3): p. 617-22.
458. Persichetti, E., et al., *Factors influencing the measurement of lysosomal enzymes activity in human cerebrospinal fluid.* PLoS One, 2014. **9**(7): p. e101453.
459. Chan, R.B., et al., *Elevated GM3 plasma concentration in idiopathic Parkinson's disease: A lipidomic analysis.* PLoS One, 2017. **12**(2): p. e0172348.
460. Guedes, L.C., et al., *Serum lipid alterations in GBA-associated Parkinson's disease.* Parkinsonism Relat Disord, 2017. **44**: p. 58-65.
461. Klein, A.D. and J.R. Mazzulli, *Is Parkinson's disease a lysosomal disorder?* Brain, 2018. **141**(8): p. 2255-2262.